

AN APPROACH TO THE ORIGIN OF KESİKKÖPRÜ (BALA-ANKARA) IRON DEPOSIT

Bilgin DOĞAN*; Taner ÜNLÜ** and İ. Sönmez SAYILI**

ABSTRACT.- This study discusses the ore geology and origin of the Kesikköprü (Bala- Ankara) iron deposit. The basement composed of gneiss, schist, and quartzites of Paleozoic- Mesozoic Kırşehir massive is overlain by sedimentary and volcanic-volcaniclastic rocks that consist of spilitic basalt, basaltic tuff, diabase dikes, cherty limestone, radiolarite, and mudstone-limestone lenses which are transitional with an ophiolitic melange made of crystallized limestone blocks and ultramafic-mafic rocks in a basin that was formed during the upper Cretaceous time. Rocks of the basin are cut by granitoids such as granite, granodiorite, and porphyries of Maastrichtian-Paleocene age. These units are unconformably covered by Eocene Çayraz formation consisting of sandy, clayey, fossiliferous limestone, Miocene-Pliocene (?) İncik formation composing of siltstone, claystone, anhydrite-gypsum alternations, and sandstones with limestone and fossiliferous limestone blocks, volcanic rocks made of rhyolite and tuffs, Pliocene-Quaternary Kızılırmak formation consisting of gravel, sand and mud deposits, and finally post-tectonic basin sediments of Quaternary alluvium. Possible lithologies for source and country rocks of mineralization are examined under two main groups as ultramafic rocks consisting of crystallized limestone blocks, peridotite, pyroxenite, and serpentinites and mafic rocks consisting of gabbro and diabases while in more detail, they are investigated as serpentinites and mafic rocks subjected to hydrothermal alteration. The association among olivine, pyroxene, and plagioclase minerals is distinctive in field, thin section, and XRD studies. Petrographic works conducted on mafic and ultramafic rocks yield occurrences unique to ultramafic cumulates. Ore samples, in the order of abundance, consist mainly of magnetite and lesser amounts of pyrite, chalcopyrite, chromite, siderite, ankerite, and trace amounts of pentlandite, pyrrhotite, gersdorffite, ilmenite, and sphene. In addition, olivine, pyroxene, tremolite, and actinolite also accompany the ore and calcite and dolomite are also observed in crack and fracture fillings. Geochemical studies performed on the ore samples indicate that granitic fluids have no direct effect in the ore formation. The processes of granitic intrusions associated with hydrothermal convection cell affect the mafic rocks and shape the hydrothermal alteration modes formed by "skarn type minerals" and fels-like textures". Expelling of iron element as a result of serpentinization of ferromagnesian minerals within the ultramafic rocks, such as olivine and pyroxene, is the primary source of iron. Their secondary enrichment by the granitic intrusions indicates another important stage in the formation of Kesikköprü iron deposit. Present study favors the idea that Kesikköprü iron deposit is similar to the Divriği type deposit, in other words, as also stated by previous works, iron was derived directly from the granitic rocks.

INTRODUCTION

This study discusses the formation of Kesikköprü (Bala-Ankara) iron deposit located in the Bala town of the city of Ankara designated in Kırşehir J30 b-3 quadrangle.

The basement in the vicinity of study area comprised by rock assemblages of Kırşehir massive is overlain by the upper Cretaceous ophiolitic complex together with sedimentary and volcanic-volcaniclastic rocks and by a sedimentary cover of Tertiary age.

Some of studies on the lithostratigraphy of the Kırşehir massive and its vicinity are of Ketin (1963), Norman (1972), Çapan and Buket (1975), Göncüoğlu (1977), Tülümen (1980), Erkan (1981), Erkan and Ataman (1981), Seymen (1982), Bayhan (1986), Önen

and Ünan (1988), Erler et al., (1989-1991), and Erler and Bayhan (1995) while some of studies on tectonics are of Bailey and Mc Callien (1950), Egeran and Lahn (1951), Ketin (1955), Seymen (1982), and Akıman et al., (1993). The main studies on the general geology and ore geology of the Kesikköprü area are of Brennich (1960), Kraeff (1962), Boroviczeny (1964a, b, c, d), Yaz and Sözen (1965, 1967), Sözen (1970), Sungurlu (1970), Öztürk et al., (1983), Öztürk and Öztürk (1983), Bayhan (1984), Bilgin et al., (1986), Kara and Dönmez (1990), and Wondemagegnehu (1990).

Iron deposits in the Kesikköprü area have been worked since 1960's. However, the studies could not go in detail on the origin of the ore. Although there are no sufficient information on the origin, considering the its close relation to the crystallized limestones, the idea that mineralization is a metasomatic type was widely

accepted by most of the workers while the type of the country rock is still controversial among the workers. Some of the authors suggest that rocks associated with the mineralization are basic in composition while some set forth granitic rocks and propose a skarn type mineralization with an epigenetic character formed as a result of interaction between limestones and iron-rich solutions derived from granitic rocks.

Source of iron element in the Kesikköprü iron deposit is the fatal importance of the controversy on the origin of mineralization. It is the aim of present study to introduce a new aspect to such controversy.

GEOLOGY OF THE STUDY AREA

Geology of five different fields covering an area of about 225 km² was revised on 1/25.000 scaled geology maps (Fig. 1). Studies in the field no. I were directed to intense sampling and revision of geological maps while works in other fields were carried out by sampling and revision of geological maps based on the setting of stratigraphy. Geology of the areas out of the study fields was taken from the studies of Bilgin et al., (1986) and Dönmez (1990). Field no. I in which Kesikköprü iron deposit is located comprises 100 km² part of the Kırşehir J 30 b1, b2, b3, and b4 quadrangles (Fig. 2).

Within the ophiolitic complex exposing around the study area, are the sedimentary and volcanic-volcaniclastic rocks being transitional with the melange, crystallized limestones, and ultramafic-mafic rocks, all intruded by granitoids and blanketed by a sedimentary cover alternated with volcanic fragments. A total of 300 thin sections was prepared, 250 samples from above mentioned lithologies and 50 from pit samples, for mineralogic-petrographic examinations. In addition, a number of 50 samples was subjected to XRD studies. The results are summarized as follow.

Crystallized limestones

Crystallized limestones are exposed in Kartalkaya ridge and around Bolkardağı northeast of field no. I and in a narrow part of field no. II to the northwest and northeast and southeast sections of field no. V.

Crystallized limestones are composed of gray, yellowish beige, white colored, fractured, thick bedded, sugar-textured, coarsely crystalline carbonaceous rocks alternated with dolomitic levels comprising the topographic heights with no vegetation cover.

Petrographic examinations reveal the presence of medium-coarse to very coarse grained, equigranular recrystallized calcites also showing sutured pressure twinnings accompanied by fine to medium grained, partly euhedral dolomite occurrences.

Crystallized limestones in the area are observed as blocks within the upper Cretaceous ultramafic-mafic rocks and unconformably covered by Pliocene-Quaternary sedimentary rocks. They are intruded by granitic rocks giving rise to formation of skarn occurrences at the contacts.

The age of crystallized limestones, in a broad range, is suggested to be Paleozoic-Mesozoic by previous workers (Öztürk et al., 1983; Bilgin et al., 1986; Kara and Dönmez, 1990).

Ultramafic-mafic rocks

Ultramafic-mafic rocks are exposed south of Kesikköprü plateau, around Bolkardağı and southeast of Kartalkaya ridge in the field no. I, in between Kalemka-mış hill at northwest and Uzunmezarin hill mideast of the field no. II, and central parts of the field no. III along an east-west direction.

Ultramafic-mafic rocks in the field no. I are gray, light gray, greenish, and earth brown colored and composed of pyroxenite, gabbro, and diorite type rocks that are detected to be altered where the color gets lighter while those of field no. II are dark gray, green colored, densely fractured and consist of serpentinite, peridotite, pyroxenite, and gabbro-diorite type rocks with a magnetic susceptibility even determined by a hand magnet. Ultramafic-mafic rocks in the field no. III are light green, green, dark green and black colored, densely fractured and fissured. Magnetic susceptibility is distinctive in places. They comprise serpentinite, peridotite, and pyroxenite around the Set hill while they consist of peridotite and gabbroic type rocks in the vi-

cinity of Hirfanlı dam axle, Karapınar Beli hill, and Hirfanlar village. Ultramafic-mafic rocks are cut by granitic rocks and fractured and subjected to the hydrothermal alteration.

As a result of petrographic examinations, ultramafic rocks are grouped as peridotites (intensely alteration of serpentinites to dunite and lherzolite), pyroxenites (clinopyroxenite, olivine, and websterite), and serpentinites while mafic rocks are grouped as mafic plutonic rocks (gabbro and diorite) and mafic sub-plutonic rocks (diabase and diorite porphyry).

Since it is intruded by granitic rocks, the basement of ultramafic-mafic rocks cannot be observed in the study area. Studies conducted out of the area indicate that the contact between lithologies unique to metamorphic basement of the Kirşehir massive and ultramafic-mafic rocks is tectonic one (Seymen, 1982). The upper contact of ultramafic-mafic rocks in the area is covered with young terrestrial deposits while that out of the study area is blanketed by marine sediments (Bilgin et al., 1986; Kara and Dönmez, 1990).

According to Seymen (1982) and Bayhan (1986), the age of ultramafic-mafic rocks is Jurassic-Campanian while Bilgin et al., (1986) and Kara and Dönmez (1990) suggest upper Cretaceous and Cenomanian-Santonian (?) ages, respectively, for the unit.

Ultramafic-mafic rocks seem to be correlated with the Ankara melange (Bailey and Mc Callien, 1950).

Sedimentary and volcanic-volcaniclastic rocks

Volcanosedimentary rocks in the field no. IV are widely exposed in the area between Pöğrenk, Yenimerdan, Efendiköy, and Kasımağa villages while they are cropped out Salik hill, west of Deve hill, and around the Halıldede in the field no. V.

Sedimentary and volcanic-volcaniclastic rocks appear in beige, white, gray, light gray, greenish, and earth brown colors. In some places, due to the effect of iron-rich fluids and oxidation, red color becomes dominant. Sedimentary rocks with volcanic intercalations show a regular sequence. The unit appears to be a vol-

canosedimentary assemblage consisting of spilitic basalt, basaltic tuff, diabase dikes, cherty limestones, radiolarite and mudstone-limestone band and lenses.

As a result of petrographic examinations, sedimentary and volcanic-volcaniclastic rocks are grouped as basalt, spilitic basalt, radiolarite and pelagic limestone.

Its basement cannot be observed in the area. They are cut by granitic rocks and unconformably covered with young volcanic and sedimentary rocks.

Bilgin et al., (1986) were named the unit as the Kasımağa formation with an age of upper Cretaceous and suggested that Kasımağa village is the type location.

Granitic, rocks

Granitic rocks are found around the Kesikköprü town, east of the Kesikköprü plateau, around the Camıısagır village and Maden hill in the field no. I, north, south, and east of the field no. II, around the Tavşancıl hill north-northeastern part of the field no. III and Ziyaret hill at southwest, and finally northeastern section of the field no. V.

They comprise high elevations and rugged terrains in the area. They appear as fractured and fissured and in white, gray, pink gray, and red colors. In hand samples, they are medium grained and display dark and light color tones but mostly dominated by pink and gray colors. It is partly disintegrated and subjected to arenitization.

As a result of petrographic examinations, granitic rocks are combined into three groups as granite, granodiorite, and granodiorite porphyry which show a compositional change in a narrow range.

Granitic rocks are intruded into crystallized limestones and ultramafic-mafic rock's and intensely altered them. They are unconformably overlain by marine and terrestrial sedimentary rocks of Eocene and Pliocene-Quaternary age.

Considering the radiometric determinations, the ages of some granitic rocks exposing in the region are

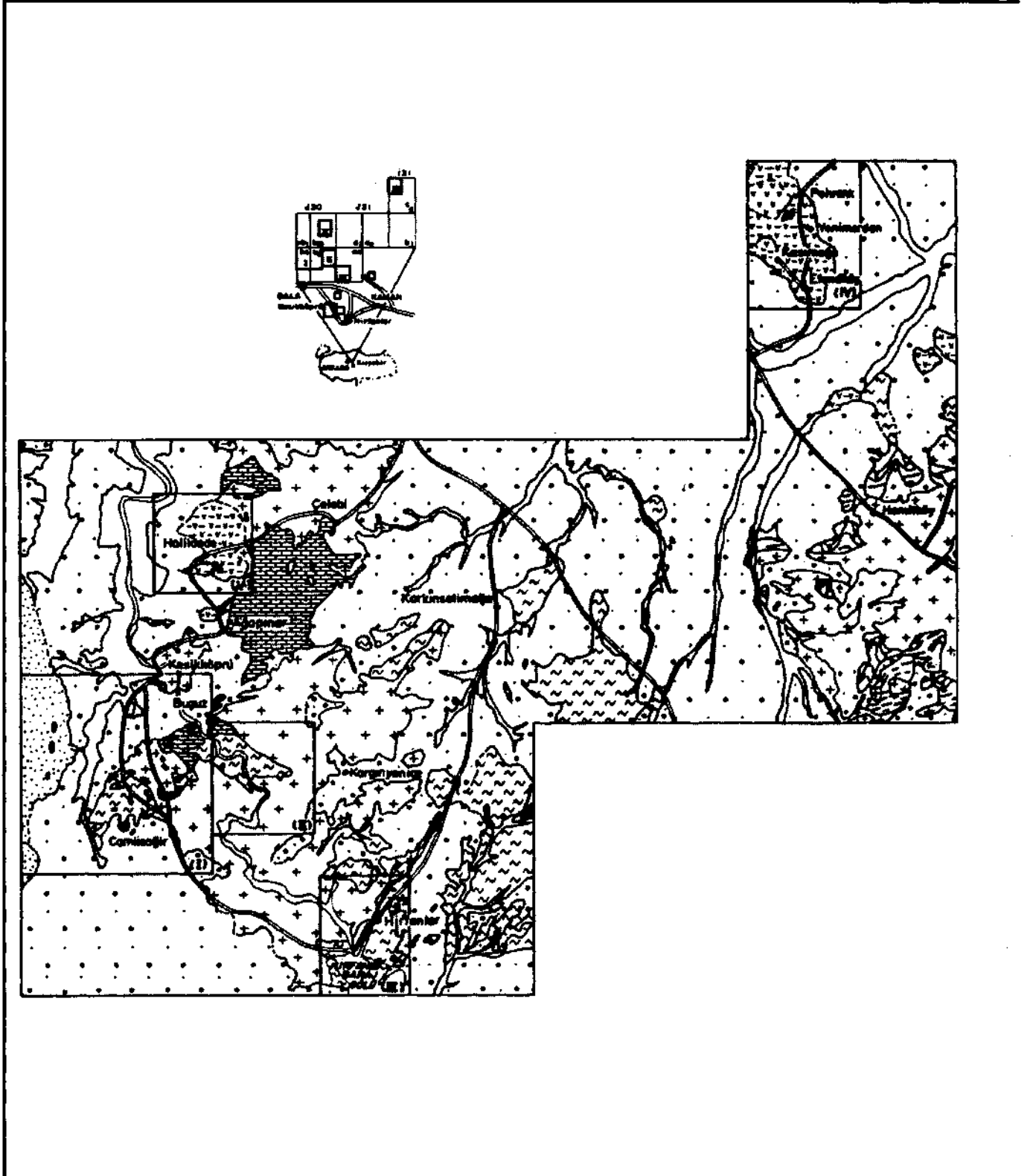


Fig. 1- Geological map of Kesikköprü and surroundings. Fields nos I, II, III, IV and V represent the studied areas (Modified from Doğan, 1996).

Handwritten signature



EXPLANATIONS

Quaternary



Alluvium

Pliocene-Quaternary



Kızılırmak formation
(Gravel, sand, mud deposits)

Miocene-Pliocene (?)



Volcanic rocks
(Rhyolite and tuffs)
İncik formation
(Limestone and fossiliferous limestone
blocks bearing sandstone, siltstone,
claystone, anhydrite, gypsum alternation)

Eocene



Çayroz formation
(Sandy, clayey, fossiliferous limestone)

Maastrichtian-Paleogene



Granitic rocks
(Granite, syenite, monzonite
and porphyries)



Skarn occurrences

Upper Cretaceous



Kosmağa formation
(Spilitic basalt, basaltic tuff, diabase dykes,
cherty limestone, radiolarite, volcanoclastic sequence consisted
of mudstone-limestone bands)
Ophiolitic melange
(Crystalline limestone blocks bearing ultramafic rocks)

Paleozoic-Mesozoic



Metamorphic basement (Kirsehir Massif)
(Gneis, schist, quartzite and marble)

--- Probable formation boundary

~ Formation boundary

~ Unconformity

— Roads

⊕ Active mine

⊖ Closed mine

• Settlement place

0 SCALE 4 km

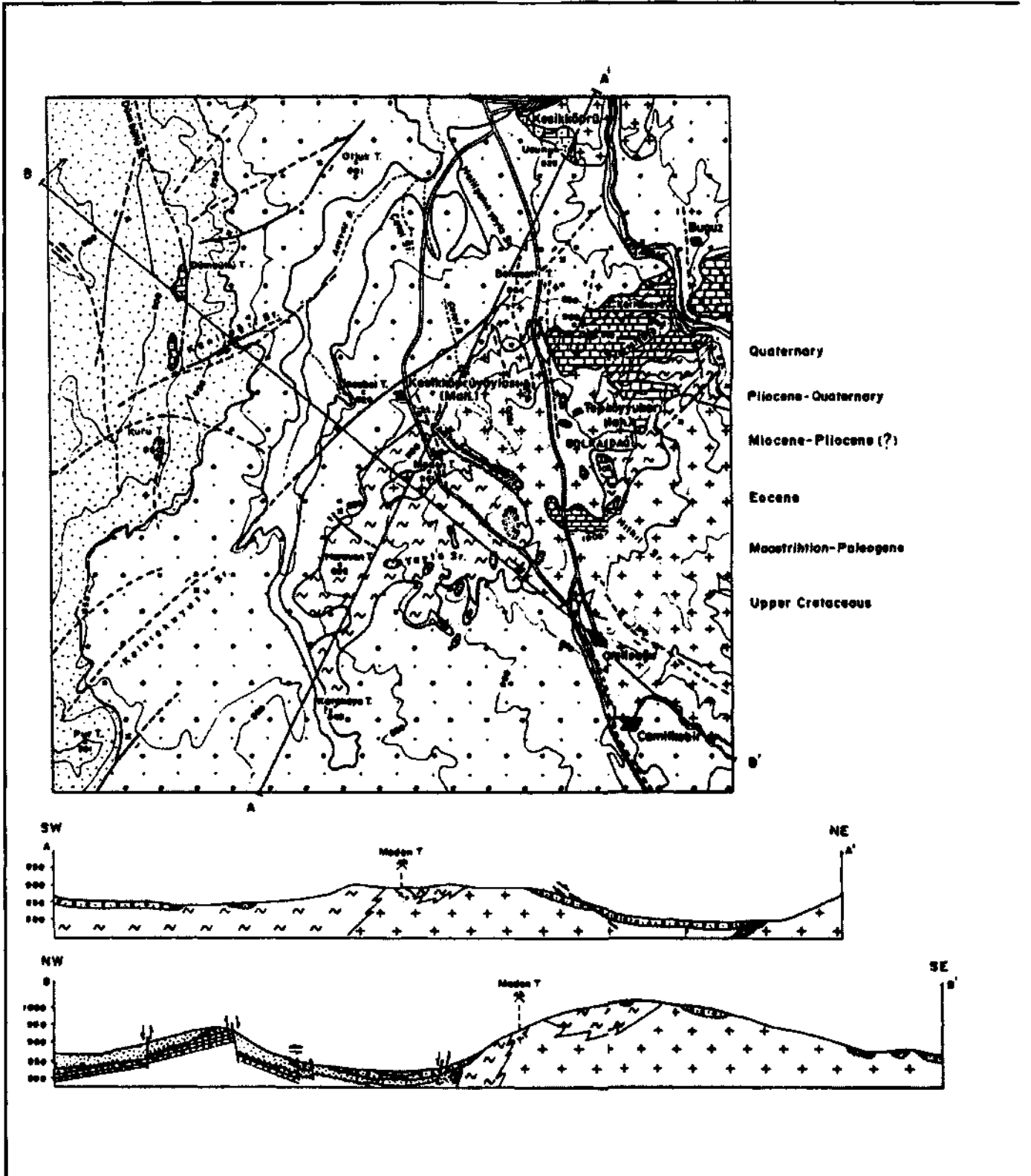
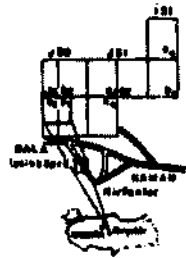





















Fig. 2- Geological map of Field no 1 at Kesikköprü iron deposit (Modified from Doğan, 1996).



EXPLANATIONS

-  Alluvium
-  Kızırmak formation
(Gravel, sand, mud deposits)
-  İncik formation
(Limestone and fossiliferous limestone blocks
bearing sandstone, siltstone, claystone,
anhydrite-gypsum alternation)
-  Coyraz formation
(Sandy, clayey fossiliferous limestone)
-  Kesiköprü granitoid
(Granite, granodiorite
and porphyries)
-  Storm occurrences
-  Ophiolitic melange
(Crystalline limestone blocks
bearing ultramafic rocks)
-  Probable formation boundary
-  Formation boundary
-  Fault probable
-  Fault
-  Unconformity
-  Contour
-  Cross-section line
-  Roads
-  Active mine
-  Projected ore boundary
-  Settlement place
-  Closed mine



proposed to be 54 Ma-Eocene (Ayan, 1963), 71 Ma-upper Cretaceous (Ataman, 1972), and 110 Ma-lower Cretaceous (Güleç, 1994). Based on the observations performed around the study area, different ages were also suggested: Paleocene-Eocene (Öztürk et al., 1983), upper Maastrichtian-Eocene (Bilgin et al., 1986), pre-Maastrichtian or Santonian-Campanian (?) (Kara and Dönmez, 1990). Since granitic rocks are unconformably covered by Eocene units and since they cut the upper Cretaceous units together with consideration of findings of other workers (Bilgin et al., 1986), their age is assigned to be Maastrichtian-Paleocene.

Some of granitic rocks exposing in Central Anatolia are named as Baranadağ massive (Ayan, 1963), Cefalıkdağ granodiorite (Ataman, 1972), Karacaali pluton (Norman, 1972), Üçkapılı granodiorite (Göncüoğlu, 1977), Baranadağ and Buzlukdağ plutons (Seymen, 1982), Çelebi Intrusion (Bayhan, 1986), Ortaköy granitoid (Atabey et al., 1987), and Baranadağ granitoid (Kara and Dönmez, 1990). Since granitic rocks observed in the field no. I have not been named previously and widely exposed around the Kesikköprü town, in the present study, they are called as the Kesikköprü granitoid.

Skarn occurrences

They are found on the contacts of limestone-granitic rocks in the area between Kartalkaya, Bolkaradağı, Maden hill, and Kesikköprü plateau and appear as tightly massive blocks.

As a result of petrographic examinations, fine to medium grained, fels-textured rocks of monomineralic composition were determined, such as epidote-fels, vesuvian-fels, garnet-fels, and diopside-fels consisting of epidote, vesuvian, garnet, and diopside minerals.

Sedimentary rocks

Sedimentary rocks are exposed in wide areas between Dumbullu ridge and Pur hill at north, south, and western parts of the field no. I, a limited area at north-western part of the field no. II, around the Hirfanlı dam lake in the field no. III, south and east of the field no.

IV, south and west of the field no. V, and outside of the study area.

Sedimentary rocks of the Çayraz, İncik, and Kızılırmak formations are cropped out in the field no. I while sedimentary rocks of only the Kızılırmak formation are exposed in the field nos. II, III, IV, and V.

Çayraz formation.- It is exposed in a limited area around the Kesikköprü town in the field no. I.

The unit is composed of reddish beige colored, clayey, sandy, abundantly Nummulites sp.-bearing limestones that are observed as blocks in places.

It unconformably overlies the Kesikköprü granitoid while its upper contact is unconformably overlain by the Kızılırmak formation.

Considering the findings of previous workers (Bilgin et al., 1986), age of the Çayraz formation is accepted to be Eocene.

Lithologies with similar features are also named as Çayraz formation by Schmidt (1960) and Bilgin et al., (1986).

İncik formation.- Sedimentary rocks exposing in the area between Dumbüllü ridge and Pur hill west of the field no. I comprise lacustrine and fluvial facies.

Formation is composed of red, beige, and greenish earth brown colored limestone and alternations of sandstone, siltstone, claystone, and anhydrite-gypsum that also contain fossiliferous limestone blocks of upper Cretaceous-Eocene age.

The basement of the İncik formation in the area could not be detected while its upper contact is unconformably overlain by the Kızılırmak formation.

Considering the findings of previous workers (Bilgin et al., 1986), age of the formation is accepted to be Miocene-Pliocene (?).

Kızılırmak formation.- It is widely cropped out in the field nos. I, IV, and V while it covers a limited area in the field nos. II and III.

Unit is generally observed in beige, grayish beige, greenish earth brown, and earth brown colors. It characterizes loosely cemented slope molasse and fluvial sediment and composed of gravel, sand, and mud accumulations.

Its lower contact is discordant with the Çayraz and İncik formation while its upper contact is discordant with young alluvium deposits.

Based on field observations and findings of previous workers (Bilgin et al., 1986), age of the Kızılırmak formation is believed to be Pliocene-Quaternary.

Volcanic rocks

They are exposed in wide areas between Göztepe and Tütün hill northwest of Kasımağa village and abandoned manganese occurrences in the field no. IV. They are observed to comprise high elevations in the area.

Volcanic rocks are generally beige, white, gray, and light gray in color.

Petrographic examinations indicated that volcanic rocks can be grouped as those intensely silicified in narrow areas, carbonaceous in places, and the ones containing high amount of quartz rhyolite-rhyodacite and tuffs.

Volcanites unconformably cover the volcanosedimentary rocks. Based on the previous works conducted in the region (Akyürek et al., 1984), their age is accepted as Miocene.

Alluvium

It is observed along the Kızılırmak River. They are recent occurrences and composed of the mixture of gravel, sand, silt, and soil comprising the river and valley beds and flat areas. They also contain the material of older units.

It unconformably rests above the Kızılırmak formation and has an age of Quaternary.

RESULTS OF FIELD WORKS

The findings obtained from the field works are given below:

Crystallized limestones that were included to metamorphic basement in previous studies (Öztürk et al., 1983; Bilgin et al., 1986; Kara and Dönmez, 1990) are evaluated as the limestone blocks within the ophiolitic complex (field nos. I and II).

Ultramafic-mafic rocks and such limestone blocks were mapped together as the ophiolitic complex. Karakaya ultramafite (field no. III) described in the study of Seymen (1982) is included to the ophiolitic complex.

Lithologies of field no. I that were included to the Kasımağa formation in previous works (Bilgin et al., 1986) were determined to be the ultramafic-mafic rocks within the ophiolitic complex which were affected from the granitic rocks.

Lithologies of the Kasımağa formation (Bilgin et al., 1986) observed around the Kasımağa village were traced in that area (field no. IV) and based on their lateral and vertical transition with the ophiolitic complex out of the study area (Akyürek et al., 1984), they are believed to be laterally changing to the complex within the area.

Lithologies to be included to the Eocene Çayraz formation were determined in the area (field no. I). Moreover, it is determined in the present study that limestones of the Çayraz formation are technically exposed at the basement of the İncik formation and they are positioned as blocks within the İncik formation (field no. I).

Considering the lateral and vertical transition between Miocene-Pliocene (?) volcanic rocks (field no. IV) and İncik formation out of the study area (Akyürek et al., 1984), they are believed to be laterally transitional within the area.

Detail mapping of lithologies of the Kızılırmak formation that comprises most part of the study area, determining of their relation to the İncik formation, and necessity of differentiation of both formations from each

other are the purposes of present study. It is believed that at least, some part of widely exposing lithologies mapped as Kızılırmak formation may be included to the İncik formation.

BASIN EVOLUTION MODEL

Considering the studies conducted so far, evolution of basin may be schematized as follows:

In the basin evolved during the upper Cretaceous, sedimentary and volcanic- volcanoclastic rocks transitional with the ophiolitic melange were deposited over the basement consisting of lithologies unique to Kırşehir massive of Paleozoic-Mesozoic age. Basement rocks are intruded by Maastrichtian-Paleocene granitoids. They are unconformably covered with Eocene-Quaternary post-tectonic basin deposits.

BRIEF INFORMATION ABOUT THE DEPOSIT

Kesikköprü iron deposit is located 35 km from the southern junction of the Ankara-Kaman highway at 100th km.

There are a total of 8 deposits and occurrences in the region. Of these, Madentepe I, Madentepe II, and Suluocak deposits are presently operated in field no. I while Büyükocak, Adilocak, Kartalkaya I, Kartalkaya II, and Camiisagır pits are already abandoned. Due to their exploitability and having similar features with other occurrences, well samples and samples collected from Madentepe I, Madentepe II, and Suluocak pits will be examined in detail.

The mineralization in the Kesikköprü iron deposit and occurrences is observed as lenses of different sizes (- 100 x 20 x 10 m) around or at the contacts between crystallized limestone, ultramafic-mafic rocks, and granitic rocks. Ore minerals are magnetite and lesser amount of hematite, limonite and trace amounts of pyrite. In general, Fe contents 45-65%, SiO₂ contents are 10-15%, and S contents are 1-2%. These ore lenses comprise masses ranging from 20 thousand to 5

million tones and have a reserve of about 11 million tones (Öztürk et al., 1983). Faults detected around the pits are in NW-SE direction and give rise to transportation of ore-bearing fluids.

PETROGRAPHY OF DRILLING SAMPLES

A total of 481 core samples was systematically collected from a number of 10 wells drilled in the Kesikköprü iron deposit by MTA in the years between 1977 and 1982. A total of 150 thin sections was systematically prepared from the Kes-2 well in which ore-country rock relation is well displayed. As a result of macroscopic and microscopic examinations, it was determined that the dominant rock type of the drilling with a depth of 173 m is generally gabbroic type mafic rocks that are partly subjected to hydrothermal alteration. In addition, altered ultramafic rocks were also observed.

Mafic rocks

Examination of drilling samples from surface to depth reveals that in hand specimens to the first 100 m, light and dark colored mineral alternations are repeated in a narrow space and dark gray, gray, and green colored, partly fine grained materials with a tight appearance are dominated.

Microscopic investigations indicate the presence of polysynthetic twinnings in subhedral medium, fine, and very fine grained plagioclases and xenomorphic medium to fine grained plagioclases. In places, intense argillization and lesser amounts of sericitization are also observed.

Diopside-augite type of clinopyroxenes of medium to fine grained, getting coarser in places, are also present. Fine grains are in euhedral and prismatic shapes and as the grain size gets coarse, they appear as subhedral and anhedral forms. They seem to be transformed to amphiboles along fracture and margins.

Medium to fine grained, subhedral, anhedral, platy hastingsite type pleochroic primary amphiboles are observed in light green and brown colors and ac-

company the pyroxenes. Moreover, fibrous, radial, bar-like tremolite type secondary amphiboles formed as a result of amphibolitization of pyroxenes are widely detected.

Medium to fine grained, subhedral, anhedral, disseminated three type opaque occurrences as thin veinlets are observed along the cleavage traces associated with amphibolitization of pyroxenes.

In addition, medium to fine grained, subhedral to anhedral, zoned, locally radial, green colored pleochroic tourmalines and xenomorphic, stockwork type yellowish brown colored, optic, isotropic garnet group minerals, and lesser amounts of fine grained xenomorphic epidot group minerals are also observed.

A granular texture is detected among the plagioclase and pyroxenes that are the main components of the rock. However, these two components display a distinctive banded texture as alternations of plagioclase and pyroxene in both hand specimens and thin sections (Plate I, fig. 1). This appearance may indicate the presence of a complex consisting of ultramafic and mafic lithologies.

Mafic rocks subjected to hydrothermal alteration

In hand specimens from 100 to 130th meters of core samples, a fractured structure in light gray to white colors with intense carbonatization and magnetic susceptibility is distinctive.

The main components of the rock are composed of two different associations unique to the same rock that is subjected to hydrothermal alteration also accompanying the ore.

Opaque minerals are generally medium to coarse grained, subhedral to anhedral, subjected to cataclysm and observed as fractured and fissured and being replaced by hematite along the edges. Lesser amounts of fine grained, anhedral opaque minerals associated with carbonates are also detected.

In some of altered mafic rocks accompanying the ore, carbonate-rich levels are observed derived from carbonatization of light colored minerals (plagioclase). While in some samples, dark colored minerals show amphibolitization, carbonatization, and lesser amount of chloritization signs. These transformations are detected even only one thin section.

Along the fracture and fissures of medium to fine grained, anhedral light brown opaque minerals, two types of carbonates are observed: one is iron-rich ankerite type carbonates and another is coarse, medium, and fine grained, anhedral calcite type carbonates, in those of coarse to medium grained, pressure twinnings are also observed. A little amount chlorite filled space is also detected in the rock.

In other samples showing amphibolitization, carbonatization, and little amount of chloritization, a large amount of pyroxene relicts together with tremolites formed a result of amphibolitization of pyroxenes are observed. Tremolites are fine to medium grained, platy, fibrous, locally radial, chloritized, and intensely carbonaceous.

Ultramafic rocks subjected to hydrothermal alteration

In hand specimens from 130 to 165th meters of core samples, they are observed as light gray to beige colored, schistose carbonaceous levels.

Completely carbonated serpentines with a distinctive sieve texture, which also locally bear relicts of opaque minerals, comprise the main component of the rock. In the places of intense serpentinization, a significant orientation is observed (Plate I, fig. 2).

Two different carbonate types were determined in the rock. First is fine, medium to coarse grained, subhedral to anhedral calcite type carbonates with widespread pressure twinnings, while the second is fine grained, anhedral, light brown colored ankerite type carbonates particularly accumulated where serpentinization is present.

Opaque minerals as fine to medium grained, euhedral, subhedral disseminations are detected together with veins associated with serpentinization (Plate I, fig. 3). In disseminated opaque minerals, silicate minerals are observed along cleavage traces and fractures (Plate I, fig. 4).

Samples from 165 to 173rd meters of well are composed of light green-beige colored, fine grained rocks of tight appearance and mostly resemble hydrothermally altered mafic rocks. These levels in previous studies are evaluated as "skarn occurrences" and/or fels (Öztürk et al., 1983). In these levels, medium to coarse grained, euhedral to subhedral, locally anisotropic lamellae-bearing, optically isotropic garnet type minerals and light green colored, fine to medium grained, subhedral, fibrous, pleochroic epidot group minerals together with lesser amounts of fine grained euhedral to subhedral, prismatic pyroxenes also observed. In addition, within the pores of the rock, green colored, pleochroic possibly iron-rich chlorites together with quartz are also detected.

ORE MINERALOGY

As a result of petrographic examinations of the surficial and drilling samples collected around the Kesikköprü iron deposit, a total of 29 polished sections was prepared, from 9 source rock and 4 country rock samples, 4 samples from the pits, and 12 from ore samples, and described with the ore microscopy. Non-opaque minerals accompanying opaque minerals were also examined with thin sections prepared parallel to polished sections.

Ultramafic and mafic rocks

Ore microscopy examinations of ultramafic rocks were performed under two different rock assemblages as peridotite and serpentinite type rocks and gabbro-diabase type rocks together with pyroxenite resembling the composition of ultramafic rocks. It was also determined that, like in the silicate minerals, ore minerals of ultramafic rocks display similarities. Therefore, textural and compositional relations in the ore minerals of

both groups are presented on the basis of each ore mineral.

Peridotite and serpentinites. - These source rocks are represented with dunite, harzburgite, lherzolite, and serpentinites of peridotite family.

Microscopic examinations reveal that coarse grained, euhedral to subhedral, chromites locally subjected to an intense cataclysm appear to be transformed to chrome spinel and magnetite along fracture, fissure, and edges (Plate I, fig. 5).

Magnetites of the rock can be divided into 4 groups. 1 st group is observed as transformation of chromites to magnetite along fracture, fissure, and edges, 2nd group is detected as fine grained, anhedral, skeleton- and veinlet-shaped, silicate inclusion-bearing magnetites within serpentines, 3rd group appears to be fine grained, subhedral to anhedral, magnetites along the cleavage plains of orthopyroxenes (Plate I, fig. 6), and 4th group is observed as fine grained, anhedral, cloudy magnetite grain accumulations appearing along the cleavage plains of orthopyroxenes as a result of serpentinization. Moreover, transforming of magnetite occurrences to maghemite and mushketovite are also frequently observed.

Magnetites together with lesser amounts of fine grained, anhedral, pyrite occurrences are detected along the cleavage plains of serpentinized orthopyroxenes.

Chalcopyrites surrounded by magnetites are generally observed as fine grained and subhedral to anhedral. They are intensely subjected to limonitization.

Fine grained, anhedral pyrrhotite is also found in the rock.

Lesser amounts of pentlandite-gersdorffite are generally associated with fine grained, subhedral to anhedral and rarely with euhedral magnetite. Mackinawite fibers are detected within pentlandites and along its cleavages (Plate II, fig. 1).

Siderite and ankerites are observed as veinlets locally being transformed to goethite and limonite. Little amount of goethite and limonite occurrences is also found as transformation of chalcopyrites to limonite.

Pyroxenite-gabbro and diabases.- Rocks of this group is characterized by pyroxenite, plagioclase pyroxenite, websterite, gabbro, spinel gabbro, olivine gabbro, and diabase. Although pyroxenites are associated with ultramafic rocks, they also exhibit transition to mafic rocks.

Subhedral, anhedral, skeleton-shaped magnetites are observed along the cleavage plains, fracture, and fissures of orthopyroxenes. They are transformed to hematite as a result of intense magnetization. In some cases, magnetites seem to be associated with garnets (hydrogrossular?: rodingitization?) both formed in diopside and augite.

Chalcopyrites are generally fine grained, mostly subhedral, rarely anhedral, and intensely subjected to limonitization.

Fine grained, subhedral, anhedral spinel minerals (possibly hercynite) are rarely developed along the cleavage plains of orthopyroxenes (Plate II, fig. 2).

In addition, lesser amount of pentlandite, chromite, ilmenite, and sphene together with secondary limonitization are also observed.

Ore properties

Petrography and XRD studies reveal that gangue minerals of the ore samples are generally composed of chlorite, tremolite-actinolite, carbonate minerals, pyroxene, and lesser amounts of garnet, quartz, and clay minerals, and in some cases, talc and little amount of olivine which are vitally important in origin.

In order of abundance, ore minerals can be listed as follows:

Magnetites may be examined under 4 different groups. 1st group is composed of fine grained silicate in-

clusion-bearing magnetites (Plate II, fig. 3) and they gradually change to magnetites with no inclusion to the crystal margins and form zoning matrix. 2nd group is coarse grained, subhedral to anhedral, sutured, and has a cataclastic structure and has been widely changed to martite along fracture, fissure, and cleavage plains (Plate II, fig. 4). 3rd group is composed of fine grained, anhedral, cloudy magnetites in which coarse grained magnetites appear to fill the spaces. They change to martite in places. 4th group is observed as fine to medium grained, euhedral to subhedral, skeleton- and lattice-shaped magnetites that are mostly replaced by siderite and ankerites.

A little amount of fine to medium grained, subhedral, chalcopyrite was determined to be associated with magnetite within siderite and ankerites. Tremolite, actinolite, and chlorite type silicate inclusions are found in magnetite and chalcopyrite and they seem to change to chalcocite, bornite, and covellite along their edges (Plate II, fig. 5).

Fine grained, euhedral to subhedral, anhedral pyrites traversing the magnetites contain silicate inclusions.

Little amount of fine grained, subhedral, chromite in calcite and dolomite is completely changed to chrome spinel and magnetite along the edges (Plate II, fig. 6).

Siderite-ankerite veins are observed in fracture and fissures of ore minerals also as replacing magnetites.

Lesser amounts of limonite formed as a result of surficial alteration is detected in magnetites.

COMPARISON OF ORE MINERALOGY AND PETROGRAPHY STUDIES

Data obtained from ore mineralogy studies were compared with those from source and country rock petrography studies.

Considering rock systematic, there is a large consistency between petrography and ore mineralogy stu-

dies. Findings of ore mineralogy of source rocks and ore samples are also well in accordance with each other.

Primary magnetites in serpentinites are represented with fine grained, silicate inclusion-bearing magnetite occurrences. They are recrystallized as pure magnetites due to indirect effect of granitic rocks, that is by the effect of hydrothermal convection systems providing the fluid circulation within the country rocks heated by the granitic rocks, while fine grained silicates in magnetites give rise to crystal growths of coarse grained non-opaque minerals. During this process, depending on O and S fugacities, magnetites change to hematite also accompanied by pyrites. Thus, hydrothermally altered serpentinites are formed and hydrothermal alteration causes siderite, ankerite, and/or dolomite and calcite minerals to form as a result of reactions between mobile iron element and carbonatization which is another important characteristic of the system, like silicification. It is believed that most of the iron-carbonate minerals are formed by metasomatic effect of iron element leached from former magnetite and iron silicates.

During the hydrothermal alteration process, particularly mafic rocks and rocks with Ca-rich minerals give easily rise to formation of "skarn type" components. At the same time, cements of diabase type rocks may largely develop fels-like textures. However, it should also be considered that small relicts of limestones being observed as blocks within ultramafic and mafic rocks may also form country rock and lay the groundwork for skarn minerals.

As the loss on ignition of the whole rock increases (it is generally -2%, but it may be up to 4-5% or 7-9%, Table 1), impact of hydrothermal alteration is also increased. This, in turn, provides change of magnetites to hematite via martitization and/or bounding of iron element to the carbonates as vein type mineralizations traversing the structure. Late stage magnetite veinlets cut all the components. However, as the impact of hydrothermal alteration is decreased, that is rate of

loss on ignition is lowered, magnetites become stable to be observed in serpentinites.

Tourmaline-bearing veinlets that are believed to be associated directly with granitic fluids traverse the structures mentioned above. However, isolated states of such veinlets (separate from other gangue minerals) indicate that they have no direct effect on the mineralization. Traversing of these veinlets through the hydrothermal alteration matrix, that is fed by hydrothermal convection systems, may indicate that granitic rocks in the region have different ages but are derived from the same thermal conduit with different compositions.

GEOCHEMISTRY

Sampling and analysis method

Geochemical analyses were performed on a number of 25 selected samples collected from ore (12 samples), source and country rocks (13 samples) of the Kesikköprü iron deposit. The sampling localities are given in Doğan (1996).

Chemical analyses were carried out at the laboratories of the General Directorate of Mineral Research and Exploration of Turkey (MTA). Si, Ti, Al, Fe, Ca, K, and P elements were determined by XRF (X-ray Fluorescence method) while Mg, Na, Mn, Cr, Co, B, Sc, and Pb concentrations were found with AAS (Atomic Absorption Spectrophotometry) and OSA (Optical Spectral Analysis), loss on ignition and Cl with gravimetry, S element with Leco method (Iodimetric), N, Cu, Zn, Ba, Sr, Zr, V, La, Ga, Y, Nb, Ce, and Nd elements were determined by ICP (Induced Coupled Plasma) method. Detection limits of the instruments are given in Doğan (1996). As a result, chemical analyses of 11 major and 20 trace elements for 25 samples were obtained.

Presentation of results of chemical Analysis

Results of chemical analysis of the samples collected from Kesikköprü iron deposit are shown in Table 1.

Table 1- Chemical analyses results of source-country rock and ore samples of the Kesikköprü iron deposit (Fe₂O₃ total iron, G: concentration below the detection limit of the instrument).

No	SOURCE ROCKS															COUNTRY ROCKS															ORE														
	1	2	3	4	5	6	7	8	9	10	11	12	13	14	15	16	17	18	19	20	21	22	23	24	25																				
Sample Number	80.S.10	80.S.11	80.S.14	80.S.16	H-1	H-5	H-33	H-34	H-36	C-18	C-19	K-11	BE-9	K-21	K-26	K-35	C-30	C-33	C-40	C-49	SD-42	82.D.19	82.D.14	82.C.7	82.L.1																				
Lithology	Dense Sandstone	Herzschg. Litharenite	Wolfsberg. Litharenite	Hetzschg. Litharenite	Spinn. Gabbro	Spinn. Gabbro	Wolfsberg. Litharenite	Urtuff	Wolfsberg. Litharenite	Wolfsberg. Litharenite	Pyroxenit. Pyroxenit	Pyroxenit. Pyroxenit	Gabbro	Diorite	Magnet. Pyroxenit	Magnet. Pyroxenit	Magnet. Pyroxenit	Magnet. Pyroxenit	Magnet. Pyroxenit	Magnet. Pyroxenit	Magnet. Pyroxenit	Magnet. Pyroxenit	Magnet. Pyroxenit	Magnet. Pyroxenit	Magnet. Pyroxenit																				
Major Element (%)																																													
SiO ₂	87.50	87.50	85.00	85.00	85.00	85.00	85.00	85.00	85.00	85.00	85.00	85.00	85.00	85.00	85.00	85.00	85.00	85.00	85.00	85.00	85.00	85.00	85.00	85.00																					
TiO ₂	<0.10	<0.10	0.10	0.10	0.10	0.10	0.10	0.10	0.10	0.10	0.10	0.28	0.50	<0.10	<0.10	0.10	<0.10	<0.10	<0.10	0.10	<0.10	<0.10	<0.10	0.10																					
Al ₂ O ₃	<0.10	<0.10	3.40	3.40	3.40	3.40	3.40	3.40	3.40	3.40	3.40	7.49	16.00	<0.10	<0.10	1.20	<0.10	<0.10	<0.10	<0.10	<0.10	<0.10	1.30	2.20																					
Fe ₂ O ₃	16.10	16.10	14.00	14.00	14.00	14.00	14.00	14.00	14.00	14.00	14.00	3.88	3.88	78.26	88.26	88.53	94.00	81.69	72.12	81.20	64.66	88.84	88.46	51.28																					
MnO	0.37	0.25	0.28	0.27	0.17	0.17	0.25	0.28	0.22	0.21	0.22	0.21	0.24	0.08	0.08	0.45	0.25	0.25	0.22	0.24	0.27	0.15	0.27	0.15																					
MgO	81.00	84.00	28.00	24.00	26.00	11.30	28.00	28.00	18.00	18.00	11.30	12.00	5.50	3.10	2.80	3.20	1.40	3.30	5.30	2.90	4.80	8.50	1.00	12.50																					
CaO	2.80	1.70	9.40	12.00	7.10	15.80	3.80	6.80	15.50	21.00	21.50	20.59	16.00	5.70	4.50	3.00	1.80	3.28	1.80	3.80	7.90	11.00	10.00	3.60																					
Na ₂ O	0.05	<0.01	0.18	0.16	0.05	0.38	0.01	0.09	0.25	0.60	0.40	0.30	3.00	0.01	<0.01	0.01	<0.01	<0.01	<0.01	0.02	0.02	<0.01	<0.01	<0.01																					
K ₂ O	0.10	<0.10	0.10	0.10	<0.10	0.10	<0.10	<0.10	0.10	0.10	0.10	0.28	0.10	<0.10	<0.10	0.10	<0.10	<0.10	<0.10	0.10	<0.10	<0.10	<0.10	<0.10																					
P ₂ O ₅	<0.10	<0.10	<0.10	<0.10	<0.10	<0.10	<0.10	<0.10	<0.10	<0.10	<0.10	0.10	0.26	0.10	<0.10	<0.10	<0.10	<0.10	<0.10	<0.10	<0.10	<0.10	<0.10	<0.10																					
Loss On Ignition (LOI)	8.04	11.48	4.50	2.84	7.00	1.72	9.52	7.10	1.85	2.25	1.15	1.30	1.40	1.61	1.85	1.55	1.20	4.00	7.00	8.10	4.40	2.00	2.80	6.65																					
Total	97.27	99.20	100.07	100.45	96.37	100.04	98.72	98.90	100.00	99.43	98.67	97.81	99.74	99.89	101.58	101.11	103.34	98.82	100.88	100.10	100.68	100.28	100.05	98.74																					
Trace Element (ppm)																																													
Cr	2200	2000	1000	900	700	400	700	700	1800	1100	1300	1400	800	G	70	70	70	180	70	40	200	70	100	100																					
V	71	50	133	151	100	115	55	86	200	139	54	177	211	G	72	58	G	G	G	116	G	G	57	G																					
Ni	754	1156	445	470	466	359	555	487	288	478	149	418	252	135	130	284	188	457	202	620	513	304	404	262																					
Co	700	100	100	70	70	70	70	70	70	70	G	G	G	G	70	70	70	150	150	40	40	40	G	G																					
Cu	80	14	881	47	38	101	43	44	33	25	44	147	34	114	18	81	18	1062	281	88	46	64	184	26																					
Zn	227	142	209	107	165	120	169	138	180	121	207	187	119	250	288	161	320	310	272	151	334	257	292	132																					
S	1400	200	600	300	200	200	100	200	100	100	9400	200	200	24000	100	100	300	24000	25000	300	100	<10.000	300	160																					
Cl	<500	<500	<500	<500	<500	<500	<500	<500	<500	<500	<500	700	<500	<500	<500	<500	<500	<500	<500	<500	<500	<500	<500	<500																					
Ba	21	12	26	63	84	114	46	53	80	34	18	28	23	20	21	22	46	87	37	26	38	30	34	36																					
Pb	70	G	G	40	G	70	G	G	G	40	40	G	100	G	G	G	G	G	G	40	40	G	G	G																					
Sr	29	15	18	132	21	78	74	22	23	257	46	20	89	80	80	74	144	128	108	190	97	88	127	84																					
Zr	G	G	G	184	G	G	G	G	G	87	G	G	G	G	G	G	G	G	G	G	G	G	G	G																					
Y	70	70	40	G	70	G	200	40	40	150	1500	2000	190	G	G	G	G	G	G	G	G	G	G	G																					
Sc	G	G	150	70	40	70	G	G	100	150	100	100	40	G	G	G	G	G	G	G	G	G	G	G																					
La	G	G	G	G	G	G	G	G	G	90	G	G	G	G	G	G	G	G	G	G	G	G	G	G																					
Ga	G	G	G	G	G	G	G	G	G	G	G	G	G	G	G	G	G	G	G	G	G	G	G	G																					
V	G	G	G	G	G	G	G	G	G	G	G	G	G	G	G	G	G	G	G	G	G	G	G	G																					
Nb	G	G	G	G	G	G	G	G	G	G	G	G	G	G	G	G	G	G	G	G	G	G	G	G																					
Ce	G	G	G	G	G	G	G	G	G	G	G	G	G	G	G	G	G	G	G	G	G	G	G	G																					
Hf	G	G	G	G	G	G	G	G	G	G	G	G	G	G	G	G	G	G	G	G	G	G	G	G																					
N.T.A. Analy. Lab No.	62485	62486	62487	62488	62489	62500	62501	62502	62503	62504	62505	62506	62507	62508	62509	62510	62511	62512	62518	62514	62515	62516	62517	62518																					

sections. However, some points are needed to be explained for understanding of the evaluations.

Geochemical analyses performed on the samples from source and country rocks were compared with the; mean values of similar rock assemblages given in Table 3. Based on this, SiO₂ contents (37.50%) of dunite and serpentinite samples with sample nos. 1 and 2 are lower in comparison to those of normal harzburgite and dunite (Table 3) while their MgO contents are

high while their MgO content is somewhat low. 3000-ppm B content of gabbro with sample no. 12 is also high. It is noticeable that pyroxenite with sample no. 11 and gabbro with sample no. 12 with the highest B contents (1500 and 3000 ppm, respectively) have the lowest total iron oxide contents of all, 4.50 and 3.80%, respectively. Cr, V, Ni, and Co contents of all source and country rock samples (sample nos. 1-13) are within the limit values of ultramafic and mafic rocks presented in Table 3.

Table 3- Some major and trace element contents of ultramafic and mafic rocks (Oman, Burro Mountain, Twin Sisters, and Troodos) (from Boudier and Coleman, 1981).

	Harzburgite	Dunite	Websterite	Gabbro
Major Element (%)				
SiO ₂	43.50-44.00 (23)	40.40-40.60 (18)	48.30-54.30 (6)	45.50-50.00 (8)
MgO	45.30-46.20 (23)	48.60-50.60 (18)	13.00-17.60 (6)	8.80-19.00 (8)
CaO	0.50-0.91 (23)	0.15-0.59 (18)	12.60-20.50 (6)	7.10-16.40 (8)
Fe ₂ O ₃	7.20-8.20 (23)	7.70-8.80 (18)	3.00-4.30 (6)	2.60-5.60 (8)
Al ₂ O ₃	0.47-0.94 (23)	0.14-0.63 (18)	1.70-4.60 (6)	5.70-16.30 (8)
TiO ₂	Not reported	Not reported	0.05-0.14 (6)	0.03-0.17 (8)
Trace Element (ppm)				
Cr	2669-3491 (23)	2806-4107 (18)	1780-8214 (6)	411-4449 (8)
V	20-80 (17)	15-100 (14)	115-194 (6)	46-125 (8)
Ni	2123-2630 (23)	1887-3361 (18)	670-1400 (6)	515-1850 (8)
Co	88-120 (17)	96-140 (14)	38-75 (6)	36-90 (8)

extremely low (31.00-34.00%). However, CaO values are somewhat high. Total iron oxide concentrations with 14.10-16.10% indicate an enrichment. CaO contents of lherzolites (sample nos. 3, 5, 7, and 8) show excess values while Al₂O₃ concentrations display a little increase. SiO₂, MgO, and total iron oxide relations of dunite and serpentinite samples are also valid for these samples. MgO contents of websterite (sample nos. 4 and 9) and pyroxenites (sample nos. 10 and 11) are a little higher while their total iron oxide concentrations are significantly higher when compared to those of websterite in Table 3. In addition, Sr contents of websterite with sample no. 4 (132 ppm) and pyroxenite with sample no. 10 (257 ppm) and B content of pyroxenite with sample no. 11 (1500 ppm) are significant. CaO and total iron oxide contents of spinel gabbro with sample no. 6 and gabbro with sample no. 12 are also

Except total iron content, SiO₂ (37.50-52.50%), MgO (5.50-34.00%), CaO (1.70-21.50%), Al₂O₃ (0.10-18.00), Fe₂O₃ (3.80-17.50%) contents of source and country rocks display a wide element distribution within the limits of ultramafic and mafic rocks. Low contents of K₂O, P₂O₅, TiO₂, MnO, and Na₂O also accompany this association. Cr, V, Ni, Co, Cu, Zn, S, Cl, Ba, Pb, Sr, Zr, B, and Sc contents of source and country rocks are also variable. However, La, Ga, Y, Nb, Ce, and Nd contents of source and country rocks were not detected.

Total iron contents of ore samples in Table 2a are between 51.39 and 94.60% which are significantly higher than those of other elements. Their Al₂O₃ contents range from 0.10 to 2.20% and CaO contents are 1.80 and 11.00%, MgO contents are 1.40-12.50%, and SiO₂

contents are 2.80-20.50%. However, Na₂O, K₂O, and P₂O₅ contents are quite low. Cr, Ni, and Co contents are significant. Cu and Zn concentrations are somewhat high while Pb and Ba contents are significantly low. Another important point is that low B contents detected in ore samples (in whole rock analyses) are not consistent with Sc, La, Ga, Y, Nb, Ce, and Nd element contents.

Interpretation of results of chemical analysis

A total of 13 major element geochemical data obtained from source and country rocks were plotted on the AFM diagram and compared with those on typical localities of ultramafic and mafic rocks. What is shown in this diagram that samples are generally concentrated along the FM axis and display some similarities to the ophiolitic rocks of Hatay region in Turkey (Doğan, 1996).

Careful examination of Table 1 reveals that MgO and SiO₂ contents of source and country rocks (sample nos. 1-13) are lower while their CaO contents are higher than those of ultramafic and mafic rocks at other localities. However, there is a significant increase (!) in their total iron oxide concentrations. Total iron oxide concentration of only a few samples display a decrease. Trace element content of source and country rocks are generally similar to those of ultramafic and mafic rocks at other localities. Table 1 displays the element behavior unique to serpentinite and hydrothermally altered serpentinite lithologies.

Ore samples (sample nos. 14-25) given in Table 1 resemble an iron ore with a wide range of major element concentration accompanied by Ca- and Mg-silicates. On the basis of whole rock analyses, particularly Zr, B, Sc, La, Ga, Y, Nb, Ce, and Nd trace element contents, that were not detected in ore samples, indicate that granitic fluids were not circulated in the ore or granitic rocks have no direct effect on the ore formation. However, high B but low total iron contents determined in only two country rock samples traversed by tourmaline veins may yield that granitic rocks possibly affected the system and they may be activated during at least one stage of frequently renewable iron element

mobilization thus indicating that granitic rocks should not be precluded from the system. Absence of elements characterizing the granitic fluids within the ore rejects an iron expelling from granitic rocks or the model on iron enrichment deriving from granitic rocks.

Cr, V, Ni, and Co element enrichments in the ore samples indicate a possible genetic relation between mineralization and ultramafic-mafic rocks. Cu, Zn, S, and Ba contents may be due to hydrothermal circulation. Among the trace-elements, Cr has the most important role in the ore formation. Cr with a concentration range of 40-200 ppm in the ore samples seem to be a major element rather than a trace element and indicates the necessity of ultramafic-mafic rocks for the ore formation. Therefore, all samples (sample nos. 1-25) were reanalyzed at the laboratories of Ankara Nuclear Research and Training Center (ANRTC) (Sarayköy, Ankara) for their Cr contents. Table 4 shows Cr concentrations analyzed at the laboratories of both MTA and ANRTC. Cr contents of ore samples range from 36 to 113 ppm that absolutely indicate the necessity of ultramafic-mafic rocks for the ore formation.

Table 4- Cr contents of source-country rock and ore samples analyzed with AAS method.

No.	Sample number	MTA (ppm)	ANRTC (ppm)
1	93.S.10	2300	3962 ± 51
2	93.S.11	2600	3636 ± 103
3	93.S.14	1000	527.5 ± 98
4	93.S.18	900	495.5 ± 16
5	H-1	700	376.5 ± 5
6	H-5	400	246.5 ± 0.7
7	H-33	700	327 ± 18.4
8	H-34	700	not analyzed
9	H-36	1800	1148 ± 29.7
10	Ç-18	1100	222.5 ± 7.8
11	Ç-19	1300	306.5 ± 0.7
12	K-1.1	1400	429.5 ± 20.5
13	BE-9	600	381.5 ± 3.5
14	K-21	n.d.	36 ± 1.4
15	K-28	70	39 ± 0
16	K-35	70	59 ± 0
17	Ç-30	70	47 ± 0
18	Ç-33	150	113 ± 1.4
19	Ç-40	70	49 ± 0
20	Ç-49	40	39 ± 0
21	SD-42	200	98 ± 0
22	92. D.13	70	56 ± 0
23	92.D.14	100	92 ± 1.4
24	92. C.7	100	53.5 ± 0.7
25	92.X.1	70	63.5 ± 9.7

All the geochemical data yield that iron occurrences of hydrothermal origin are derived from ultramafic-mafic rocks and that serpentinization process has also contributed to the ore formation. The effect of granitic rocks on the system should not be neglected.

Graphical presentation of results of analysis

Chemical analyses of 19 elements from 13 source and country rocks, 17 elements from 12 ore samples, and 22 elements from 25 whole rock samples were plotted on variation diagrams and distribution and trends between element pairs were determined. Thus, for each element pair consisting totally of 22 elements, a number of 538 variation diagrams were constructed with the use of computer.

Examination of variation diagrams of the element pairs of the Kesikköprü iron deposit reveals that there are similarities in distribution and trends of some element pairs. Since it is impossible to present all these graphics, considering their distribution relations and consistencies, only 7 positively correlated and 6 negatively correlated variation diagrams will be displayed (Figs. 3, 4, and 5). Correlation coefficients on the variation diagrams are separately presented in order to make distribution and trends more understandable.

It is shown in CaO vs. SiO₂ diagram of Fig. 3a that 13 source and country rock samples have similar trends. Graphic yields a positively correlated distribution extending from ultramafic to mafic rocks. V vs. SiO₂ diagram (Fig. 3b) shows that, except pyroxenite with sample no. 11, all the data points exhibit a positive correlation with a wide distribution from beginning. SiO₂ increase of sample nos. 10, 11, 12, and 13 is significant. It is shown in MgO vs. Fe₂O₃ diagram of Fig. 3c that 13 source and country rock samples display similar trends. Low Fe and Mg contents of sample nos. 10, 11, 12, and 13 are significant. MgO vs. Ni diagram (Fig. 3d) shows a positively correlated distribution with a wide distribution from beginning. However, in the diagram, two different trends are observed. Diabase with sample no. 13, gabbro with sample nos. 6 and 12, pyroxenite with sample no. 10, and serpentinite with sample no. 2 display a trend parallel to that of other

samples. Mg and Ni contents of these samples are also low.

It is shown in Fe₂O₃ vs. CaO diagram of Fig. 3e that 13 source and country rock samples have similar trends. There is a negative correlation with a tight distribution from beginning. As CaO contents decrease from mafic to ultramafic rocks, Fe₂O₃ contents are increased. SiO₂ vs. Fe₂O₃ diagram of Fig. 3f indicates the presence of a negatively correlated distribution with a tight distribution from beginning. It is shown in SiO₂ vs. Ni variation diagram (Fig. 3g) that there is a negatively correlated distribution with a wide distribution from beginning. These diagrams also exhibit that Fe₂O₃ and Ni contents are decreased from ultramafic to mafic rocks. Al₂O₃ vs. MgO variation diagram (Fig. 3h) yields that, except gabbro with sample no. 6, all other samples have a negatively correlated distribution.

It is shown in SiO₂ vs. MgO variation diagram of Fig. 4a that 12 ore samples have similar trends. There is a positive correlated distribution with a wide distribution from beginning.

In the Fe₂O₃ vs. SiO₂ variation diagram of Fig. 4b, 12 ore samples show similar trends. In the diagram, there is a negative correlated distribution with a wide distribution from beginning.

There are two different parallel orientations in SiO₂ vs. CaO variation diagram of Fig. 5a constructed for 25 samples from source and country rocks. Ore samples at the left side of diagram yield a positive correlation with a wide distribution from beginning while source and country rock samples at the right side of diagram show a positive correlation with a tight distribution from beginning. In the MgO vs. Cr variation diagram of Fig. 5b, samples of ore, source and country rock samples indicate a positively correlated distribution with a wide distribution from beginning. Data points in these graphics may be evaluated as two separate parallel trends belonging to source and country rock samples.

There are two different trends in the variation diagram of Fe₂O₃ vs. SiO₂ built for ore, source, and country rock samples. However, these different variations se-

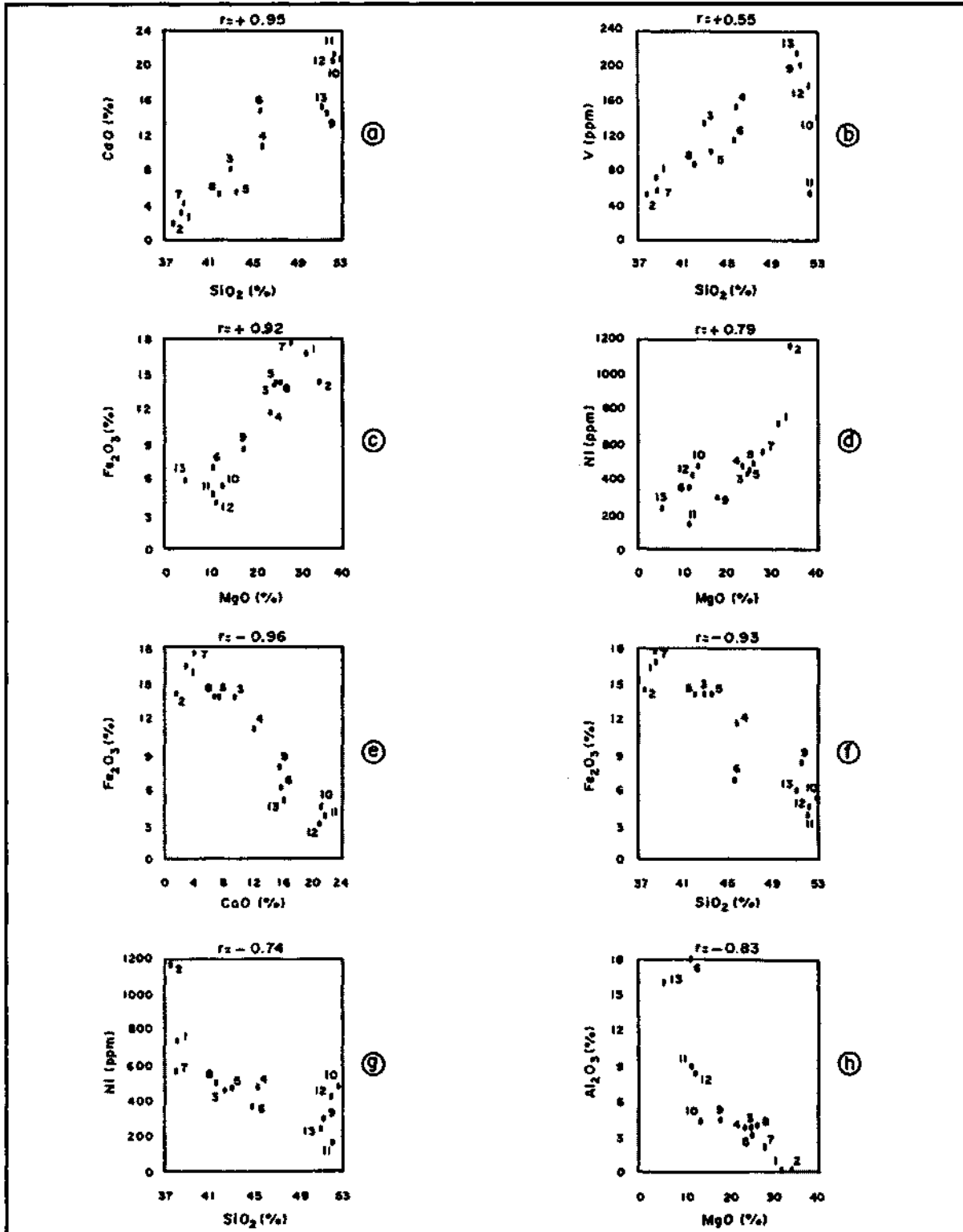


Fig. 3- Variation diagrams for different components of source and country rock samples.

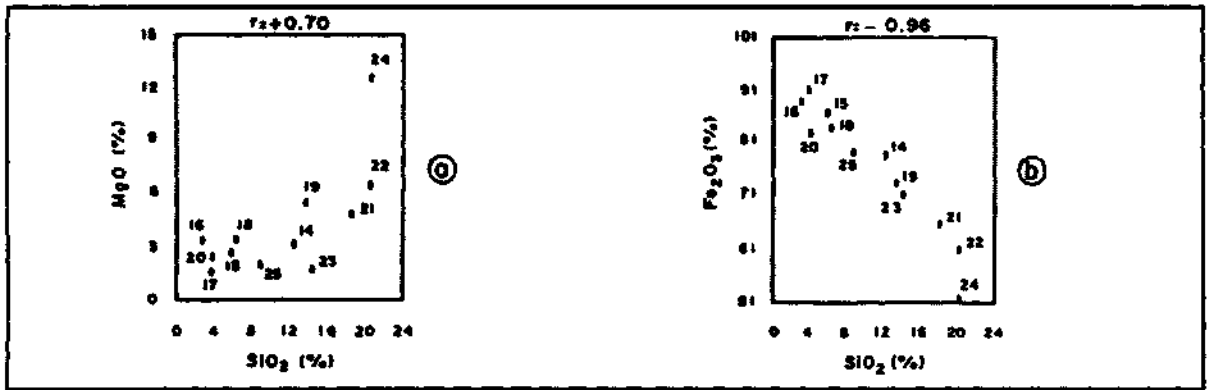


Fig. 4- Variation diagrams for different components of ore samples.

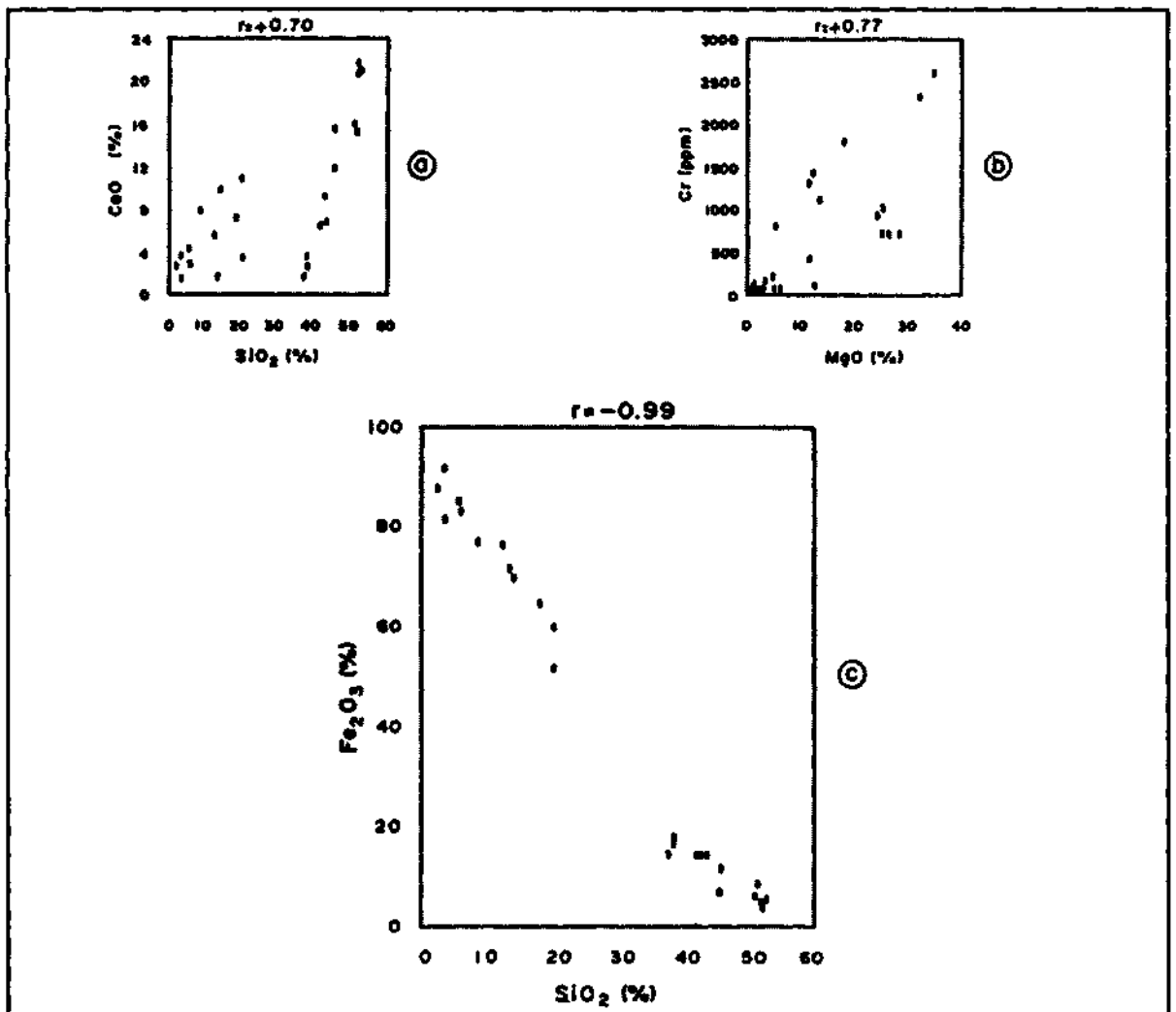


Fig. 5- Variation diagrams for different components of all samples (source-country rock and ore samples).

em to be continuation of each other. Samples yield a negatively correlated distribution (distribution of points observed along the same line) with a tight distribution from beginning.

Interpretation of graphical presentations

In Fig. 6, a number of 10 graphics are presented that are selected out of 538 constructed based on source, country, ore, and whole rock samples.

At the top of Fig. 6, Ca-Si and Mg-Fe element groups are shown on first, second, and third rows of source and country rock graphics. These two groups inversely behave, in other words, they resemble the complex of ultramafic and mafic lithologies. In addition, Mg-Fe association indicates that iron element is dependent on ferromagnesian minerals in the source rocks.

At the center of graphics in Fig.6 constructed for ore samples, Mg-silicate forms a group. Contrary to the graphics of total iron oxide vs. MgO and the features observed in source rocks, there is a negatively correlated distribution. That is, iron element is differentiated from ferromagnesian minerals within the source rocks and becomes a source for iron minerals accompanied by Mg-silicates.

In the last row of Fig. 6, the variation diagram of SiO_2 vs. total iron oxide for all the samples are illustrated. Because, ultramafic and mafic rocks at one side and ore samples at another show almost the same trends with $r = -1.00$, in the diagram, the negative correlation with $r = -0.99$ is noticeable. Under these circumstances, searching of a source (e.g. granitic rocks) for the origin of iron element is unreasonable. The fact that laboratory methods are costly hinders the analyzing of granitic rocks. However, a distribution with $r = -0.99$ does not necessitate the performance of chemical analyses of granitic rocks.

Geostatistics

Although a limited number of samples is available for the geostatistical methods to be applied, Cluster and Factor Analyses on the basis of linear regression

were tested on different element pairs from a total of 25 samples (13 from source and country rocks and 12 from ore samples). Correlation coefficients of element pairs of 171 from source and country rocks, 136 from ore samples, and 231 from total samples were utilized. Considering high and medium and intermediate, positive, and negative correlation coefficients (Doğan, 1996), qualitative results and/or element group and associations are presented in Table 5.

In Table 5 in which Cluster Analyses were tested for source and country rocks, there seems to be two groups with a high positive correlation ($r > +0.65$). First group is represented with Ca, Si, and V elements. In this limited association, each three element behaves in the same way, that is if one of them increases, another also increases or vice versa. Second group of Table 5 with a high positive correlation is characterized by Fe, Mg, Ni elements and loss on ignitions (LOI). Elements of second group behave with a positive correlation. They are also two groups with a positive correlation ($+0.65 > r > +0.40$) in the table. First group is composed of Ca, Si, V, Na, and Al elements. The difference of this association from the former first group that it includes Na and Al elements. Second group consists of Fe, Mg, Ni, Cr, Co elements and LOI. The main difference between the two second groups is that the latter group includes Cr and Co elements.

Two main groups with a high negative correlation ($r < -0.75$) appear in testing of Factor analyses for source and country rocks (Table. 5). First group is characterized by Ca, Si, and Al elements while second group is represented with Fe and Mg elements together with LOI. It seems that elements of first and second groups as a whole behave with a high positive correlation with respect to each other while elements of these groups display an association of a high negative correlation individually. In other words, as the elements of first group increase, elements of second group are decreased or vice versa. In last part of Table 5 belonging to source and country rocks, an association with an intermediate negative correlation ($-0.45 > r > -0.75$) is observed. Differing from the former first group with a high negative correlation, V and Na elements are included to the first group while Ni, Cr, Co, and Mn elements are included to the second group.

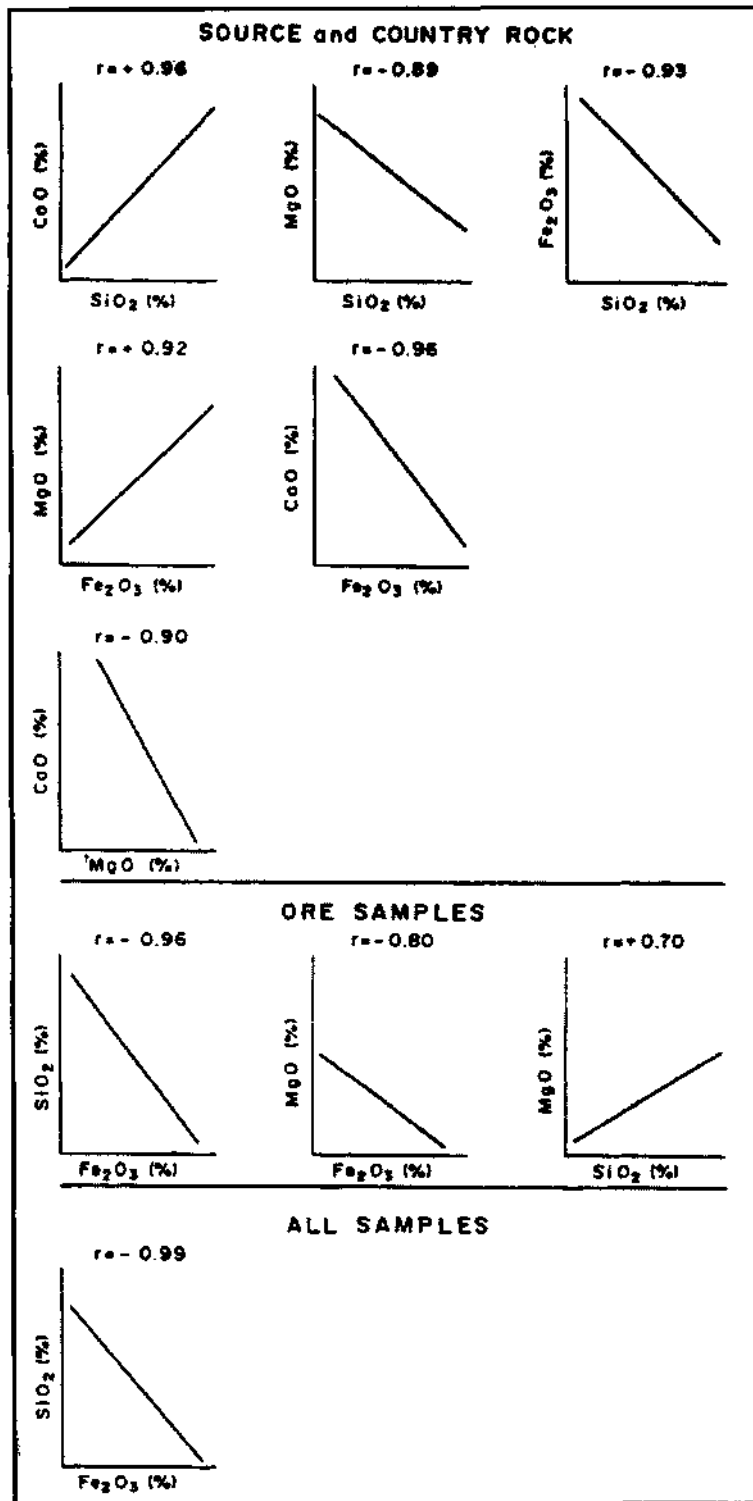


Fig. 6- Variation diagrams of some elements in source-country rock, ore, and whole rock samples. Distribution relations are characterized by regression lines and correlation coefficients.

Table 5- Element group and associations and their possible origins.

SOURCE and COUNTRY ROCKS (for 13 samples)		
1st Group: Ca, Si, V	$r > +0.65$	Mafic rocks
2nd Group: Fe, Mg, Ni, LOI		Ultramafic rocks
	$+0.65 > r > +0.40$	
1st Group: Ca, Si, V, Na, Al		Mafic rocks
2nd Group: Fe, Mg, Ni, LOI, Cr, Co		Ultramafic rocks
	$r < -0.75$	
Ca, Si, Al Fe, Mg, LOI		Complex of mafic and ultramafic lithologies
	$-0.45 > r > -0.75$	
Ca, Si, Al, V, Na Fe, Mg, LOI, Ni, Cr, Co, Mn		
ORE (for 12 samples)		
1st Group: Mg, Si	$r > +0.70$	Silicate occurrences
	$+0.70 > r > +0.30$	
1st Group: Mg, Si, Ca, LOI		Silicate (\pm carbonate) occurrences
2nd Group: Ni, Mn		Late hydrothermal effects
	$r < -0.60$	
Mg, Si Fe		Silicate (\pm carbonate) occurrences and ore
	$-0.30 > r > -0.60$	
Mg, Si, Ca, LOI Fe, Mn, Co, Zn		
ALL SAMPLES (for 25 samples)		
1st Group: Mg, Cr	$r > +0.73$	Ultramafic rocks
	$+0.73 > r > +0.39$	
1st Group: Ca, Si, V, Na, Al		Mafic rocks
2nd Group: Mg, Ni, LOI		Ultramafic rocks
	$r < -0.77$	
Si Fe		Differentiation of iron associated with serpentinization (Serpentinites subjected to Hydrothermal alteration)
	$-0.36 > r > -0.77$	
Mg, Cr, Ca, V Fe, Zn, LOI		

There is only one group with a high positive correlation ($r < +0.70$) appearing in testing of Factor analyses for ore samples (Table 5). This group is represented with Mg and Si elements. There are two groups in

the table with an intermediate positive correlation ($+0.70 > r > +0.30$). First group is characterized by Mg, Si, Ca elements and LOI. The difference of this group from the former first group is the including of Ca ele-

ment and LOI. Second group is composed only of Ni and Mn elements.

Two main groups with a high negative correlation ($r < -0.60$) appear in testing of Factor analyses for ore samples (Table 5). First group consists of Mg and Si elements while second group is represented with only Fe element. In last part of Table 5 belonging to ore samples, an association with an intermediate negative correlation ($-0.30 > r > -0.60$) is observed. Differing from the former first group with a high negative correlation, Ca element and LOI are included to the first group while Mn, Co, and Zn elements are included to the second group.

There is only one group with a high positive correlation ($r < +0.73$) appearing in testing of Factor analyses for all samples (Table 5). This group is represented with Mg and Cr elements. There are two groups in the table with an intermediate positive correlation ($+0.73 > r > +0.39$). First group is characterized by Ca, Si, V, Na, and Al elements while second group is composed only of Mg and Ni elements together with LOI.

Two main groups with a high negative correlation ($r < -0.77$) appear in testing of Factor analyses for ore samples with (Table 5). First group is represented with only Si element while second group is represented with only Fe. In last part of Table 5 belonging to ore samples, an association with an intermediate negative correlation ($-0.36 > r > -0.77$) is observed. First group is represented with Mg, Cr, Ca, and V elements. Second group is composed of Fe and Zn elements together with LOI. Differing from the former second group with a high negative correlation, Zn element and LOI are included to the latter second group.

XRD studies on core samples

Minerals found with XRD studies performed on 74 samples taken from Kes-2 well with a thickness of 173 m and the general petrographic features determined by microscope are described in Doğan (1996). In XRD studies, intensity values of each peak was also individually evaluated by the computer. Using the inten-

sity values of 100 peaks, mineral components of each sample were semi-quantitatively calculated.

Quantitative distribution of main components of 74 samples from Kes-2 well determined with XRD studies is displayed in Fig. 7. Examination of the graphic reveals the presence of an association consisting of plagioclase, pyroxene, and hastingsite (plus tremolite) at the first 100-m part of the well. In the part to the depths from 100 meter, clay, quartz, calcite, dolomite, ankerite, siderite, and magnetite become dominant.

Correlation coefficients calculated on the basis of component pairs of 74 samples generally yield 3 different groups (Doğan, 1996). 1st group consists of magnetite, hematite, ankerite, and pyroxene minerals and comprises the ore-based group, 2nd group consists of tremolite, hastingsite, serpentine, and calcite minerals and comprises serpentinized lithologies and locally hydrothermally altered serpentinites, and finally 3rd group consists of only plagioclase and comprises plagioclase-rich lithologies. Minerals of each group display positive correlations while 2nd group minerals negatively correlate with those of 1st and 3rd group minerals negatively correlate with those of 1st and 2nd group. This generalization indicates the presence of an alternation of plagioclase-rich lithologies at one side and the lithologies composed of altered mafic minerals (plus ore) at another side. In addition, correlation coefficients of some component variations were also computed such as hastingsite + tremolite = amphibole and hastingsite + tremolite + pyroxene = amphibole + pyroxene. This process yields the presence of 3 groups. 1st group consists of hematite, magnetite, ankerite, siderite, and pyrite minerals and comprises the ore-based group, 2nd group consists of calcite, serpentine, and hastingsite + tremolite + pyroxene minerals and comprises serpentinized lithologies and locally hydrothermally altered serpentinites, and finally 3rd group consists of only plagioclase and comprises plagioclase-rich lithologies. Relations among these groups are similar to those of previously described ones. However, some increases in correlation coefficients are noticeable.

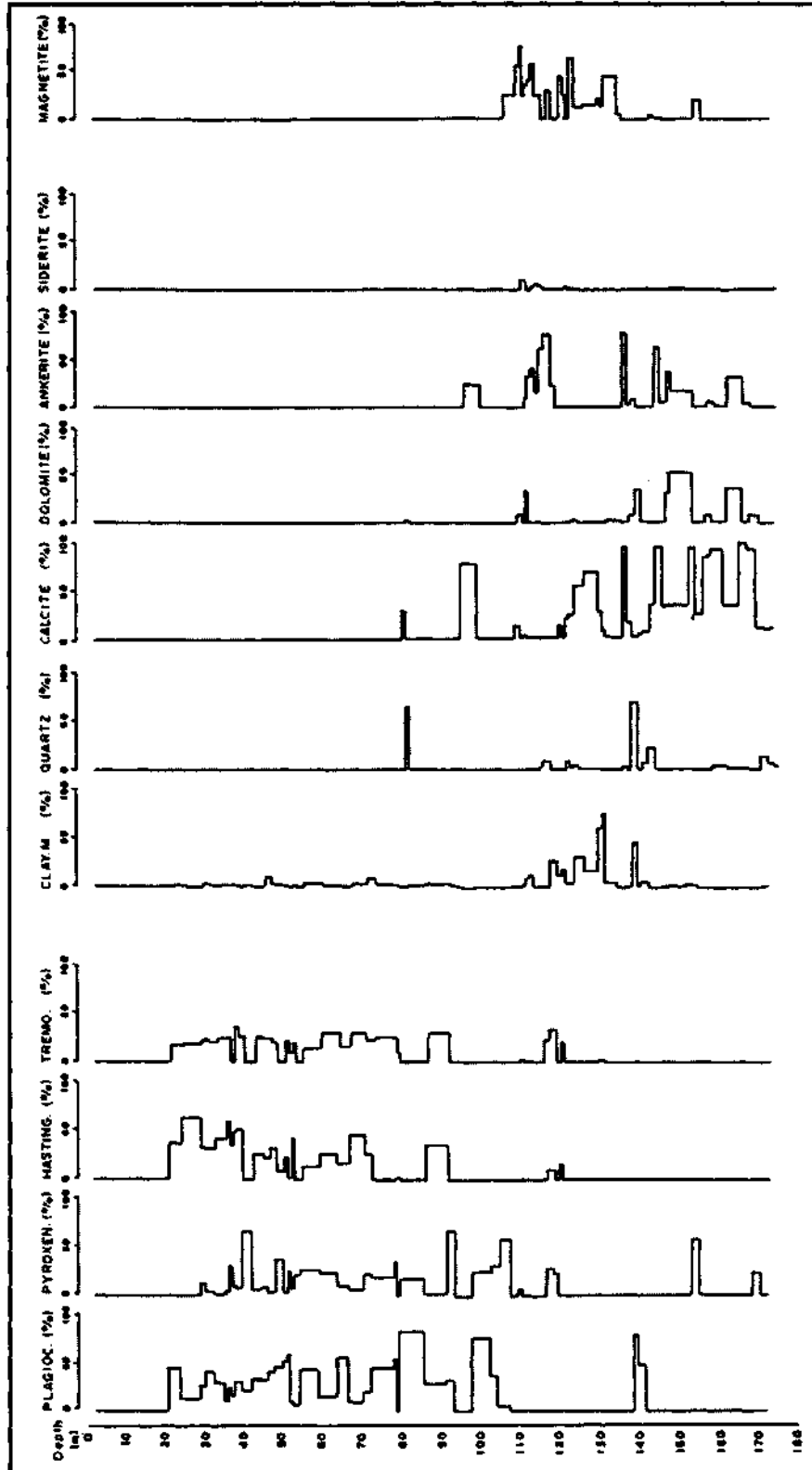


Fig. 7. Quantitative vertical distribution graphic of components from Kes-2 well samples.

Correlation coefficients of some major components and component variations are given in Table 6 that are based on 28 samples selected out of 74 core samples from plagioclase- and pyroxene-rich parts of the well to the depth of 100 m. The purpose is to clarify the relations among silicate components. Table 6 yields that hastingsite and tremolite display a positive correlation with respect to each other while pyroxene shows a negative correlation to both hastingsite and tremolite, and finally plagioclase has a negative correlation to all three minerals. In Table 6b, pyroxene shows a negative correlation with hastingsite + tremolite while plagioclase shows a negative correlation with hastingsite +

tremolite and pyroxene. In Table 6c, there is a negative correlation between plagioclase and hastingsite + tremolite + pyroxene with $r = -0.97$. These circumstances reveal two original results. One is the change of hastingsites to tremolite. The second is sequential association among plagioclase, pyroxene, and hastingsites. Among the component percents in Fig 8, graphical presentation of distribution of plagioclase vs. hastingsite + tremolite + pyroxene is symbolically given.

Correlation coefficients of some major components and component variations are computed that are based on 27 ore samples selected out of 74 core samp-

Table 6- Correlation coefficients of component pairs for plagioclase- and pyroxenerich parts of well samples [a: plagioclase, tremolite, hastingsite, and pyroxene, b: plagioclase, hastingsite + tremolite (Amp) and pyroxene, c: plagioclase and hastingsite + tremolite + pyroxene (Amp-pyx) component variations].

	Plg	Tre	Hst	Pyx
Plg	1.00			
Tre	-0.53	1.00		
Hst	-0.69	0.59	1.00	
Pyx	-0.02	-0.57	-0.56	1.00

a

	Plg	Amp	Pyx
Plg	1.00		
Amp	-0.70	1.00	
Pyx	-0.02	-0.63	1.00

b

	Plg	Amp-Pr
Plg	1.00	
Amp-Pr	-0.97	1.00

c

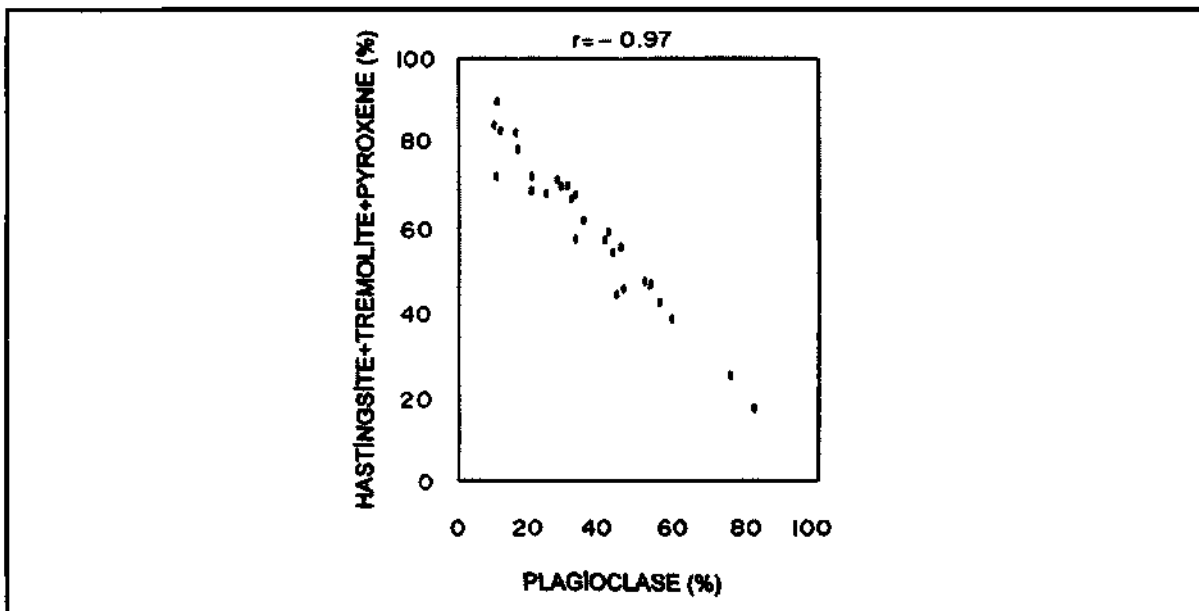


Fig. 8- Graphical presentation of plagioclase vs. hastingsite + tremolite + pyroxene distribution given in Table 60.

les from ore- and carbonate-rich parts of the well to the level deeper than 100 m (104.00-133.00 m). The purpose here is to clarify the relations among oxide-rich and carbonate-rich components which yielded two main groups. 1 st group consists of hematite, siderite, and ankerite minerals and comprises the ore while 2nd group is composed of calcite and serpentine minerals and comprises serpentinized lithologies. Each group displays a positive correlation internally while both groups show a negative correlation with respect to each other. Testing of some other component variations reveals once more the presence of two main groups. 1 st group consists of magnetite + hematite and ankerite + siderite while 2nd group is composed of calcite + dolomite and serpentine mineral variations. Evaluation of these groups yields the results similar to the previous one. The only difference is the accompaniment of dolomite occurrences.

XRD studies on chemically analyzed samples

Minerals found with XRD studies performed on a number of 13 source and country rock and 12 chemically analyzed ore samples and the general petrographic features determined by microscope are described in Doğan(1996).

Component percents of 13 source and country rock samples were determined and correlation coefficients of all component pairs were computed. Moreover, correlation coefficients of some variations of components were also found. Examination of Table 7 reveals the presence of three groups. 1 st group consists of serpentine + olivine and magnetite minerals, 2nd group consists of only plagioclase, and 3rd group is compo-

sed of-hastingsite + tremolite + pyroxene minerals. In the first group, there is a positive correlation with $r = +0.94$ among serpentine + olivine and magnetite minerals yielding an information in origin. 2nd group negatively correlates with 1 st group while 3rd group with 2nd and-1 st groups.

Calculation of correlation coefficients of all component and component variation pairs of 6 peridotite samples out of 13 source and country rock samples yields that serpentine, magnetite, and olivine minerals form one group and hastingsite, tremolite, chlorite, and pyroxene form another group. In general, there is a negative correlation between the two groups. Testing of some component variations indicates the presence of two main groups. 1st group consists of serpentine + olivine and magnetite minerals and yields a high positive correlation with $r = +0.94$. 2nd group is composed of hastingsite + tremolite + pyroxene minerals. This group negatively correlates with the first group with $r = -0.98$.

Calculation of correlation coefficients of all component and component variation pairs of 4 pyroxenite and 2 gabbro samples out of 13 source rock samples yields that hastingsite, tremolite, chlorite, and spinel comprise the first group while pyroxene comprises the second group and plagioclase makes up the third group. Minerals of first group are positively correlated with each other. Correlation coefficient of $r = +0.99$ between hastingsite and tremolite is significant. 2nd group negatively correlates with 1st group while 3rd group with 1st and 2nd groups. Testing of some component variations indicates the presence of two groups. 1 st group consists of hastingsite + tremolite + pyroxene minerals while 2nd group consists of only plagioclase mineral.

Table 7- Correlation coefficients of component pairs for source and country rocks [serpentine + olivine (Se-Ol), hastingsite + tremolite + pyroxene (Amp-pyx), plagioclase and magnetite component variations].

	Se-Ol	Amp-Pyx	Plg	Mgn
Se-Ol	1.00			
Amp-Pr	-0.82	1.00		
Plg	-0.39	-0.18	1.00	
Mgn	0.94	-0.77	-0.43	1.00

There is a significant negative correlation between the two groups with $r = -0.98$.

Furthermore, component percents together with correlation coefficients of component and component variables of chemically analyzed 12 ore samples were calculated that yielded the presence of two main groups. 1st group consists of serpentine, chlorite, talc, siderite, ankerite, and hematite minerals while 2nd group is composed of quartz, calcite, magnetite, and pyroxene minerals. 1st group minerals are positively correlated with each other while minerals of 2nd group are partly positively and negatively correlated. Therefore, there seems to be some difficulties in reevaluation of 2nd group minerals and in their grouping. However, testing of some component variables could be beneficial. Testing of magnetite + hematite, magnetite + hematite, and siderite + ankerite associations yields the 4th group. 1st group has almost the same assemblage with the former first group. Serpentine, chlorite, talc, siderite + ankerite minerals comprise this group. This group is the indicative of vein mineralizations within hydrothermally altered country rocks. 2nd group is composed of quartz and calcite. These minerals indicate gangue minerals associated with vein mineralizations. 1st and 2nd groups are the indicative of ore veins. 3rd group is composed of only magnetite + hematite mineral assemblage and indicates the change of magnetites to hematite. 4th group is made of pyroxene mineral. These 4 groups are negatively correlated with each other. Negative correlation between 1st and 2nd groups reflects the presence of gangue and vein type ore formation while negative correlation between 3rd and 1st groups may probably indicate that ore minerals comprising the 1st group are derived from magnetite.

Results of XRD studies

Vertical distribution of non-mineralized country rock samples from the Kes-2 well indicates the presence* of alternation of plagioclase, pyroxene, and hastingsite (plus tremolite) while the mineralized parts reveal the association of clay, quartz, dolomite, ankerite, siderite, and magnetite (Fig. 7).

High positive correlation observed between hastingsite and tremolite minerals in non-mineralized parts of the same well indicates that most of hastingsites change to tremolite. However, negative correlation and inconsistency detected between pyroxene and tremolites hinder the searching of tremolite source in pyroxenes. In this respect, the relation of pyroxene hastingsite tremolite and changing of primary hastingsites to tremolite may be considered.

High negative correlation ($r = -0.97$) among plagioclase, pyroxene, and hastingsite + tremolite + pyroxene observed in non-mineralized part of the well yields the presence of a sequential association among plagioclase, pyroxene, and hastingsite minerals. In this case, it is believed that geostatistical expressions of cumulate textures of ultramafic cumulates are generally approached in accordance with negative correlation criteria.

In ore- and carbonate-dominated components of Kes-2 well, two different groups with negative correlations are detected. One is composed of magnetite + hematite + and ankerite + siderite while 2nd group consists of calcite + dolomite and serpentine minerals and their varieties which indicating that serpentinization accompanies and/or associated with the ore formation.

In addition to ore samples, Cluster Analyses of chemically analyzed peridotite samples of source and country rocks yield the presence of two groups, one is composed of serpentine + olivine and magnetite while the second consists of hastingsite + tremolite + pyroxene. In pyroxenite and gabbro samples, hastingsite + tremolite + pyroxene minerals comprise the first group while plagioclase comprises the second group. There is a negative correlation among these groups. In this case, it is thought that geostatistical expression of cumulate textures is approached with the correlation relation among mineral associations of each rock group.

Studies conducted on currently exploited massive ore samples indicate that 1st and 2nd groups are made up with serpentine, chlorite, talc, siderite + ankerite, and quartz and calcite minerals. These groups corres-

pond to ore-vein stage accompanied by hydrothermally altered gangue minerals in the country rock. 3rd group consists of hematitized magnetite while 4th group consists of pyroxene. Negative correlation between these 4 groups is distinctive.

Considering all the synthesis mentioned above, negative correlation between pyroxene observed in the ore samples and other 3 groups may indicate that minerals comprising the source of other groups should have been derived from plagioclase in pyroxenite and gabbro and from olivine in peridotite. Since derivation of iron mineral from plagioclase is not possible, the source of this group seems to be olivine.

RESULTS

1- Sediments of syntectonic basin that was developed under the control of ophiolitic rocks lying above the Paleozoic-Mesozoic basement of the Kırşehir Massive is characterized by a volcanosedimentary sequence consisting of sedimentary and volcanic rocks of upper Cretaceous Kasımağa formation that is laterally and vertically transitional with an ophiolite complex composing of ultramafic-mafic rocks together with crystallized limestone blocks. All these lithologies are intruded by Çelebi and Kesikköprü granitoids of Maastrichtian to Paleocene age. Typical skarn occurrences are observed along the contacts between granitic rocks and limestones while "skarn-like" and "fels-like" occurrences are detected far from granitic rocks and particularly within the mafic rocks. All these units are unconformably covered with post-tectonic basin sediments of Eocene Çayraz formation, Miocene-Pliocene (?) İncik formation, volcanic rocks, and Pliocene-Quaternary Kızılırmak formation.

2- As a result of petrographic and XRD studies, rocks associated with mineralization are divided into two parts, one is ultramafic rocks consisting of peridotite, pyroxenite, and serpentinites and the second is mafic rocks consisting of gabbro and diabase. Petrologic examination of core samples taken from the wells drilled in the Kesikköprü iron deposit reveals a stratigraphy, to a depth of 175 m, consisting of, from top to bottom, mafic rocks and hydrothermally altered mafic and ultramafic rocks. Alternated association between

particularly olivine, pyroxene, and plagioclase minerals becomes distinctive in thin sections of hand specimens collected from the field and the area subjected to a detail ore geology study. Moreover, a banded texture is noticeable towards the surface. Petrographic studies on ultramafic and mafic rocks reveal the presence of ultramafic cumulates. However, since cumulate concept is a genetic description and it necessitates some petrologic studies, it should be avoided from using of such a concept. At the same time, cumulate texture should also be described in the field. Because the subject is related to ore geology, it is believed that a further study, on whether it is a typical ophiolitic sequence or it is crystallized as a result of insitu differentiation, is not needed.

3- Data from geochemical analyses on source rocks were plotted on a AFM diagram indicating that most of the samples are concentrated along FM axis. This yields a very close relation to the ophiolitic rocks of the Hatay region and partly to ophiolitic rocks of the Divriği area.

4- Findings on ore mineralogy of ore samples and ultramafic-mafic rocks are consistent. That is, granitic fluids may be directly associated with the ore formation. Ore is mainly composed of magnetite, lesser amounts of pyrite, chalcopyrite, chromite, siderite, ankerite, and trace amounts of pentlandite, gersdorffite, ilmenite, and sphene. Transformation products are frequently observed. Ore is accompanied by some silicate minerals, such as olivine, pyroxene, and tremolite, in addition, calcite and dolomite are also found along fracture and fissures.

Very fine grained, silicate mineral inclusion-bearing magnetites observed in ultramafic rocks have been intensely subjected to cataclysm due to tectonic settlement and early impacts of granitic rocks and they change to pure magnetites and are remobilized and recrystallized due to the circulations formed by hydrothermal convection cells in the country rocks which are heated by granitic rocks. This event may be observed within one same crystal size as changes to pseudo-zoned pure magnetites from crystal included parts towards the edges of crystal as well as zonings of centimeters in thickness. These indirect effects of granitic rocks may

redissolve such iron minerals during syngenetic and/or postgenetic processes and may also give rise to formation of siderite-ankerite veinlets traversing the structure.

Hydrothermal convection cell affecting the country rocks comprise the hydrothermal alteration models accompanied by "skarn-type minerals" and "fels-like textures". Tourmaline-rich isolated veinlets traverse the whole structure that are formed at later stages directly by the granitic fluids of different compositions following the same conduit. The whole structure in a wide region are also cut younger fluorite veins.

5- Absence of Zr, B, Sc, La, Ga, Y, Nb, Ce, and Nd elements in the ore samples indicates that granitic fluids are not effective for the ore formation.

Geochemical studies performed on the ore samples yield that source of iron element may be derived from ultramafic rocks. Ultramafic rocks being enriched in iron due to serpentinization are leached by indirect effects of granitic rocks, and thus country rocks become iron-poor and the iron expelled may form the mineral associations, hence the iron deposits, at suitable Eh and pH conditions (Fig. 9).

Therefore, as a result of serpentinization, expelling of iron element in ferromagnesian minerals of ultramafic rocks, such as olivine and partly pyroxene, is the primary source of iron. Their secondary enrichment by the granitic fluids indicates another important stage in the formation of Kesikköprü iron deposit.

DISCUSSION-COMPARISON AND SUGGESTIONS

In the previous studies (Kraeff, 1962; Boroviczeny, 1964a, b, c, d, Sözen, 1970; Öztürk et al., 1983), Kesikköprü iron deposits was thought to be a skarn type deposit associated directly with granitic rocks. However, recent works on the formation of modeling of iron deposits (Ünlü, 1989; Ünlü and Stendal, 1986 a, b; 1989; Stendal and Ünlü, 1991; Ünlü et al., 1995) state that iron enrichments deriving from ophiolitic rocks due to indirect effects of granitic rocks. It is also suggested

that ophiolitic rocks are the source of iron element in synsedimentary-volcanogene or exhalative-sedimentary deposits within the basins formed on the ophiolitic complex (Ünlü, 1983; Stendal et al., 1995; Çiftçi et al., 1996; Ünlü et al., 1996).

In the frame of this study, it is suggested that Kesikköprü iron deposit is a Divriği type deposit (Gümüş, 1979: pyro-mobile-metasomatic, Ünlü et al., 1995: metamorphic + hydrothermal alteration type), that is, iron is not derived from granitic rocks but formed by the enrichment resulting from dissolution of source rocks. The fact that country rocks are not mostly carbonaceous rocks restricts to use of the term of "skarn-type deposits". Therefore, in general, Kesikköprü iron deposits may be described as a deposit associated with "magmatism-metamorphism" processes (Guilbert and Park, 1986). However, although small limestone relicts observed as blocks within ultramafic and mafic rocks seem to be not directly affected from this process, considering the field observations and theoretic assumptions, it should not be precluded that such a process may facilitate formation of skarn minerals and fels textures.

It seems inevitable that an investigations should be directed to discovering of new magnetite deposits in the lithologies belonging to ophiolitic melange around the Kesikköprü area, and then, studying the altered rocks by air-borne electric and magnetic methods while ore occurrences by means of air-borne magnetic method, and by justifying the data obtained with those from magnetic method performed in the field, target areas have to be selected and finally detailed geological studies should be carried out. It should be always considered that during these studies, new iron and manganese deposits could be discovered in volcanosedimentary sequences.

ACKNOWLEDGEMENTS

This work comprises a part of first author's M. Sc. study conducted in the Department of Geological Engineering of the Ankara University under the guidance of

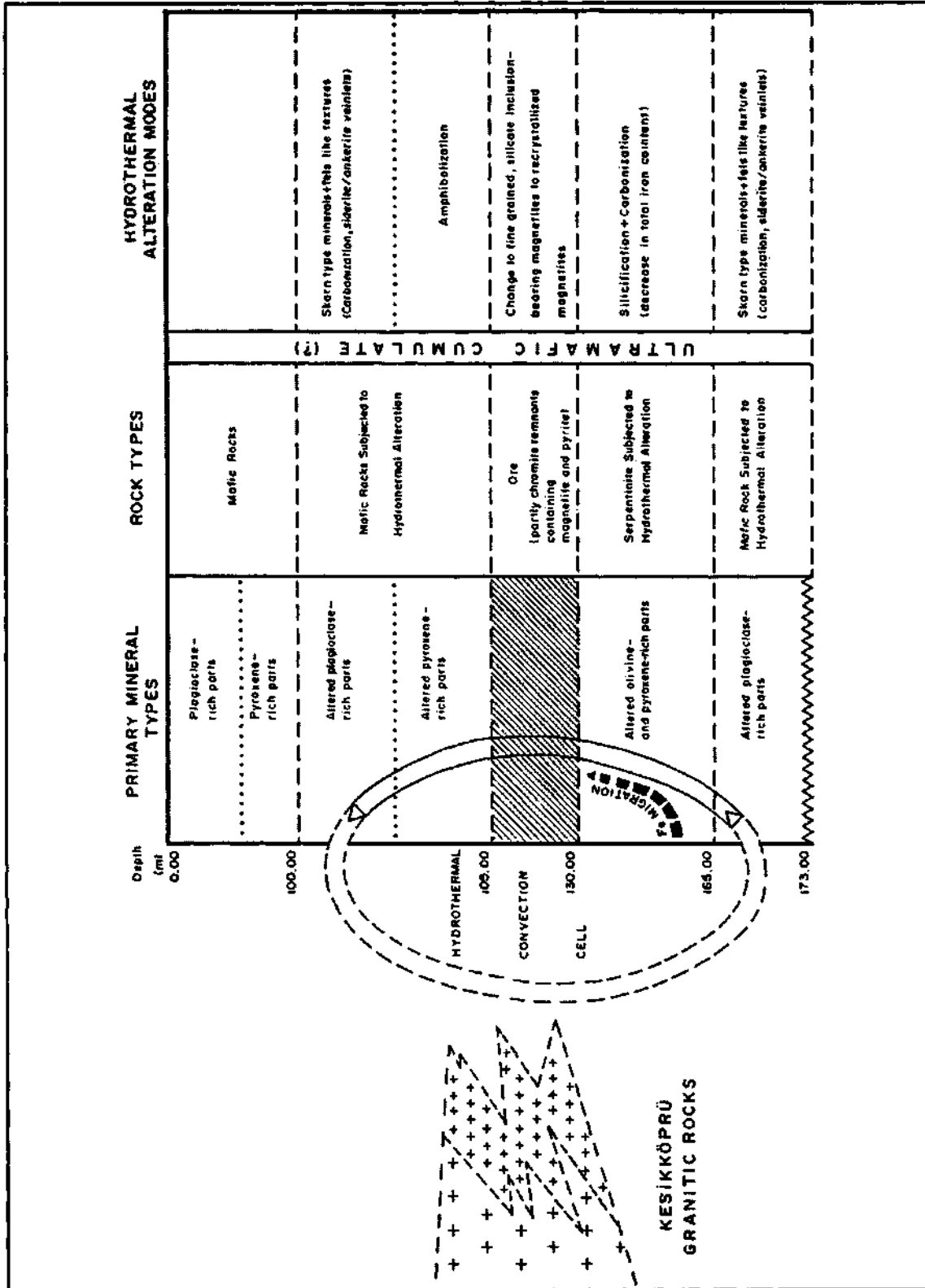


Fig. 9- Probable formation model of Kesikköprü iron deposit (figure is produced from the data of Kes-2 well. No scale).

second and third authors. Authors thank to Prof. Ayhan Ertler, Dr. Ahmet Çağatay, Prof. Baki Varol, and Assoc. Prof. Okan Tekeli for their criticism on the manuscript. Appreciation is extended to General Directorate of MTA for the access of geochemical studies. Thin sections and duplicate samples of rocks are stored at the laboratories of Department of Geological Engineering of the Ankara University.

Manuscript received November 22, 1996

REFERENCES

- Akıman, O.; Ertler, A.; Göncüoğlu, M.C.; Güleç, N.; Geven, A.; Türeli, T.K. and Kadioğlu, Y.K., 1993, Geochemical characteristics of granitoids along the western margin of the Central Anatolian Crystalline Complex and their tectonic implications: *Geological Journal*, 28, 371 - 382.
- Akyürek, B.; Bilginer, E.; Akbaş, B.; Hepşen, N.; Pehlivan, S.; Sunu, O.; Dağ, Z.; Çatal, E.; Sözeri, B.; Yıldırım, H. and Hakyemez, Y., 1984, Ankara - Elmadag - Kalecik dolayının temel jeoloji özellikleri: *Jeol. Müh.*, 20, 5-19, Ankara.
- Atabey, E.; Tarhan, N.; Akarsu, B. and Taşkıran, A., 1987, Şereflikoçhisar, Şanlı (Ankara) - Acıpınar (Niğde) yöresinin jeolojisi: MTA Derleme Rep., 8155, (unpublished), Ankara.
- Ataman, G., 1972, Ankara'nın güneydoğusundaki granit-granodiyoritik kütlelerden Cefalık dağ'ın radyometrik yaşı hakkında ön çalışma: *H. Ü. Yerbilimleri Derg.*, 2/1, 44 - 49, Ankara.
- Ayan, M., 1963, Contribution a l'etude Petrographique et geologique de la region situee au Nord-Est de Kaman (Turquie): *MTA Bull.*, 115, 332 s.
- Bailey, E. B. and Mc Callien, W.J., 1950, Ankara Melanji ve Anadolu Şariyajı: *MTA Bull.*, 40, 17 - 21, Ankara.
- Bayhan, H., 1984, Kesikköprü skarn kuşağının (Bala - Ankara) mineralojisi ve petrojenezi: *H. Ü. Yerbilimleri Derg.*, 11, 45-57, Ankara.
- Bayhan, H., 1986, İç Anadolu granitoid kuşağındaki Çelebi Sokulumu'nun jeokimyası ve kökensel yorumu: *Jeol. Muh.*, 29, 27 - 36, Ankara.
- Bilgin, Z.R.; Akarsu, B.; Erbaş, A.; Elbol, E.; Yaşar, T.; Esentürk, K.; Güner, E. and Kara, H., 1986, Kinkale - Kesikköprü - Çiçekdağı alanının jeolojisi: MTA Gen. Müd., Derleme Rep., 7876, (unpublished), Ankara.
- Boroviczeny, F., 1964a, 200/240 no'lu ruhsat sahasının Kesikköprü yakınındaki demir yatağı hakkındaki rapor: MTA Rep., 3481, (unpublished) Ankara.
- , 1964b, 200/212 no'lu ruhsat sahasında yapılan jeolojik etütler hakkında sunulan rapor. MTA Rep., 3570, (unpublished), Ankara.
- , 1964c, Kesikköprü yakınındaki 200/240 no'lu ruhsat sahasında yapılan jeolojik etütler hakkında rapor: MTA Rep., 3591, (unpublished), Ankara.
- , 1964d, 200/248 no'lu ruhsat sahasında yapılan jeolojik etütler hakkında sunulan rapor: MTA Rep. 3584, (unpublished), Ankara.
- Boudier, F. and Coleman, R.G., 1981, Cross section through the peridotite in the Samail Ophiolite, Southeastern Oman Mountains: *Journal of Geophys. Res.*, 86, B4, 2573 - 2593, Londra.
- Brennich, G., 1960, Çelebi - Kesikköprü - Hirfanlı Bölgesinde manyetit zuhurları hakkında rapor: MTA Rep., 2755, (unpublished) Ankara.
- Çapan, U.Z. and Buket, E., 1975, Aktepe - Gökdere bölgesinin jeolojisi ve ofiyolitli melanji: *TJK Bül.*, 18, 11 -16, Ankara.
- Çiftçi, D., Ünlü, T. and Sayılı, I.S., 1996, Otluklise (Gürün-Sivas) demir yatağının kökenine bir yaklaşım: *MTA Bull.*, 118, 65-92, Ankara.
- Doğan, B., 1996, Kesikköprü Demir Yatağı'nın (Bala - Ankara) maden jeolojisinin incelenmesi: *A.Ü.F.F. Jeol. Müh. Bölümü, Yüksek Lisans Tezi*, 258 p. (unpublished), Ankara.
- Egeran, N. and Lahn, E., 1951, Note on the tectonic position of the northern and central Anatolia: *MTA Bull.*, 41, 23-27, Ankara.

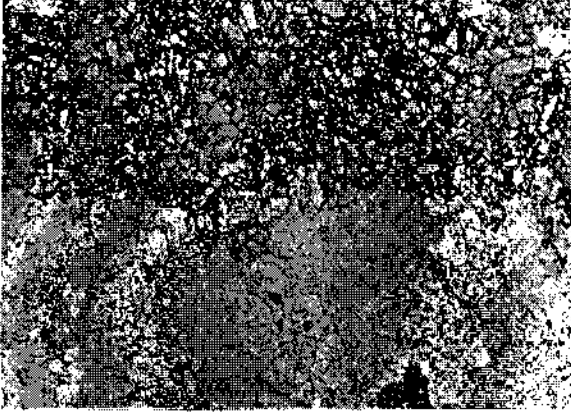
- Erkan, Y., 1981, Orta Anadolu Masifinin metamorfizması üzerinde yapılmış çalışmalarda varılan sonuçlar: İç Anadolu'nun Jeolojisi Simpozyumu TJK Bull., 9-11, Ankara
- and Ataman, G., 1981, Orta Anadolu Masifinin (Kırşehir Yöresi) metamorfizma yaşı üzerinde K/Ar yöntemi ile bir inceleme: TJK 35. Kurultay, Bildiri Özetleri, 33, Ankara.
- Erler, A; Akıman, O.; Unan, C.; Dalkılıç, F.; Dalkılıç, B.; Geven, A. and Önen, A.P., 1989, Kaman (Kırşehir) ve Yozgat yörelerinde Kırşehir Masifi magmatik kayaların petrolojisi ve jeokimyası: TÜBİTAK Proje No: TBAG 677,119 p., Ankara.
- ; ———; ———; ———; ——— and ———, 1991, Kaman (Kırşehir) ve Yozgat yörelerinde Kırşehir Masifi magmatik kayaların petrolojisi ve jeokimyası: TÜBİTAK, Doğa, 15, 76-100, Ankara.
- and Bayhan, H., 1995, Orta Anadolu granitoidlerinin genel değerlendirilmesi ve sorunları: Yerbilimleri, 17, 49-67, Ankara.
- Göncüoğlu, M.C., 1977, Geologie des westlichen Niğde Massivs: Bonn Üniv. Doktora Tezi, 181 p. (unpublished), Bonn.
- Guilbert, J. M. and Park, C.F., 1986, Skarn Deposits: The Geology of Ore Deposits. 436 - 451, A.B.D.
- Güleç, N., 1994, Rb - Sr Isotope data from the Ağaören Granitoid (east of Tuz Gölü). Geochronological and genetical implications: J. of Earth Sciences, 3, 39 - 43, TÜBİTAK, Ankara.
- Gümüş, A., 1979, Nouvelles observations sur la genese du gisement de Fer de Divriği (Sivas, Turguie): Verh. Geol. B-A, 3, 347-355.
- Kara, H. and Dönmez, M., 1990, 1/100.000 ölçekli açınasma nitelikli Türkiye jeoloji haritaları serisi: Kırşehir - G17 paftası No: 34, MTA Bull., Ankara.
- Ketin, İ., 1955, Yozgat Bölgesi'nin jeolojisi ve Orta Anadolu Masifi'nin tektonik konumu: TJK Bull., 6, 1 - 40, Ankara.
- Ketin, İ., 1963, 1/500.000 ölçekli Türkiye Jeoloji Haritası Kayseri Paftası izahnamesi: MTA Bull., Ankara.
- Kraeff, A., 1962, Kesikköprü konsesyonu: MTA Gen. Müd., Derleme Rep., 3349, (unpublished) Ankara.
- Norman, T., 1972, Ankara-Yahşihan bölgesinde Üst Kre-tase-Alt Tersiyer istifinin stratigrafisi: TJK Bull., 15/2, 180-276, Ankara.
- Önen, P. and Unan, C., 1988, Kaman (Kırşehir) kuzey doğusunda bulunan gabroların mineralojisi, petrografisi ve jeokimyası: TJK Bull., 31, 23 - 28, Ankara.
- Öztürk, M., 1981, Ankara-Keskin-Çelebi; Kırşehir-Kaman; Nevşehir-Hacibektaş yörelerindeki demir zuhurlarının jeoloji raporu: MTA Gen. Müd., Rep., 7158, (unpublished), Ankara.
- Öztürk, K. and Öztürk, M., 1983, Ankara-Bala-Yukar-tepe-köy-Kartalkaya demir cevherleşmesi Jeoloji Etüt ve Arama Raporu, MTA Gen. Müd., Rep. 7357, (unpublished), Ankara.
- , Kurt. M.; Öztürk, M. and Sarı, İ., 1983, Ankara-Bala-Kesikköprü, Madentepe, Büyükocak, Çataldere, Camiisagır demir yatakları jeoloji ve rezerv raporu: Cilt 1, 2, 3, MTA Gen. Müd. Rep. 7355, (unpublished), Ankara.
- Schmidt, C.G., 1960, Mem. 365-367 no'lu ruhsat sahalarının nihai terk raporu: Petrol İşleri Gen. Müd., (unpublished), Ankara.
- Seymen, İ., 1982, Kaman dolayında Kırşehir Masifinin Jeolojisi: ITU Maden Fakültesi Doçentlik Tezi, 164 p., İstanbul.
- Sözen, A., 1970, Kesikköprü, Madentepe manyetit zuhur hakkında rapor: MTA Gen. Müd. Rep. 4212, (unpublished), Ankara.
- Stendal, H. and Ünlü, T., 1991, Rock geochemistry of an iron ore field in the Divriği region, Central Anatolia, Turkey. A new exploration model for iron ores in Turkey: Journal of Geochemical Exploration, 40, 281 - 289, Amsterdam.
- , ——— and Konnerup-Madsen, J., 1995, Geological setting of iron deposits of Hekimhan Province, Malatya, Central Anatolia, Turkey: Trans. Instn Min. Metall. (Sect. B: Appl. earth sci.), 104, 46 - 54, London.

- Sungurlu, B., 1970, Kesikköprü-Çelebi-Hirfanlı Bölgesinin manyetit zuhurları hakkında (Yaz and Sözen) isimli rapordan Kesikköprü Ltd. Şirketine ait Ar: 200/248 ruhsat no'lu demir sahası için derlenen rapordur: MTA Gen. Mud. Rep. 4231, (unpublished) Ankara.
- Tülümen, E., 1980, Akdağmadeni (Yozgat) yöresinde petrografik ve metalojenik incelemeler: KTÜ Doktora Tezi, 157 p., Trabzon.
- Ünlü, T., 1983, Die Genese der Siderit-Lagerstätte Deveci in der Hekimhan-Provinz Malatya/Turkei und ihre wirtschaftliche Bewertung: Doktora çalışması, Berlin Teknik Üniversitesi, 84 p., Almanya.
- , 1989, Türkiye demir yatakları arama çalışmalarında 1. derecede ağırlıklı hedef saha seçimi ve madden jeolojisi araştırmaları ile ilgili proje teklifi: MTA Gen. Mud. Rep., 8593, 48p., (unpublished), Ankara.
- , Sayılı, I.S. and Çiftçi, D., 1996, An approach on genesis of Otlukilise iron deposit Gürün - Sivas, Middle Anatolia - Turkey: UNESCO, IGCP, Project No 356, Alpine metallogeny and plate tectonics in the Carpatho - Balkanides, v. 2,15-22, Sofya, Bulgaristan.
- and Stendal, H., 1986a, Divriği Bölgesi demir yataklarının element korelasyonu ve jeokimyası (Orta Anadolu - Türkiye): Jeo. Müh., 28, 5-19, Ankara.
- Ünlü, T. and Stendal, H., 1986b, Jeokimya verilerinin çok değişkenli jeostatistik analizlerle değerlendirilmesine bir örnek. Divriği bölgesi demir yatakları, Orta Anadolu: MTA Bull., 109, 127-140, Ankara.
- and ———, 1989, Divriği Bölgesi demir cevheri yataklarının nadir toprak element (REE) jeokimyası. Orta Anadolu, Türkiye: TJK Bull., 32 (1- 2), 21-38 Ankara.
- , ———, Makovisky, E. and Sayılı, I. S., 1995, Divriği (Sivas) demir yatağının kökeni, Orta Anadolu, Türkiye - Bir cevher mikroskobisi çalışması: MTA Bull., 117,17 - 28, Ankara.
- Yaz, N. and Sözen, A., 1965, Kesikköprü Madencilik Ltd. Şirketi Kesikköprü Demir Ruhsat sahaları hakkında rapor: MTA Rep., 3810, (unpublished), Ankara.
- and ———, 1967, Kesikköprü - Çelebi - Hirfanlı bölgesinin manyetit + hematit zuhurları hakkında rapor: MTA Rep., 4440, (unpublished), Ankara.
- Wondemagegnehu, T. W., 1990, Mineralogy, chemistry and physical properties of the magnetite ore deposits around Kesikköprü village and the surrounding areas: ODTÜ Yüksek Lisans Tezi, 128 s., Ankara.

PLATES

PLATE-I

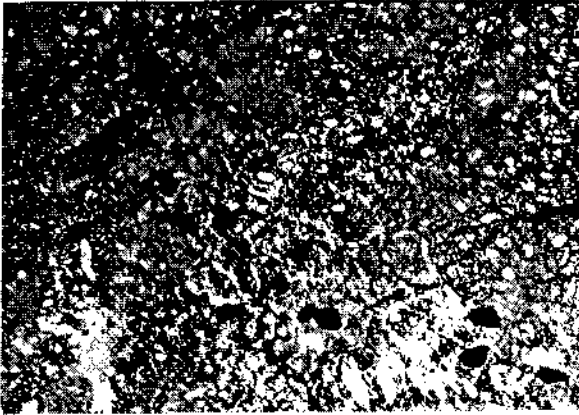
- Fig. 1 - Pyroxenes (grained parts at the top) of banded texture and plagioclases (light colored part at the bottom) within the gabbro. XPL. Magnification x16 .
- Fig. 2- Carbonated (subjected to hydrothermal alteration) magnetite crystals (small black grains on the left center) oriented in the serpentinite. XPL. Magnification x16 .
- Fig. 3- Magnetite veinlets (black) and chromite grains (four black grains on the right bottom) within serpentinitized ultramafic rock (dunite). XPL. Magnification x16 .
- Fig. 4- Magnetite (black) and silicate occurrences (light gray) within magnetite in carbonated serpentinite (subjected to hydrothermal alteration). XPL Magnification x16 .
- Fig. 5- Chromite (black margin at the right bottom) in serpentinite (dark gray at left) - cataclastic textured chromite-magnetite assemblage associated with spinel (light gray spots) and magnetite (white) transitions. In oil. Magnification x200.
- Fig. 6- Deformed orthopyroxene (gray) and magnetite occurrences (white) along the cleavages. In oil. Magnification x200.



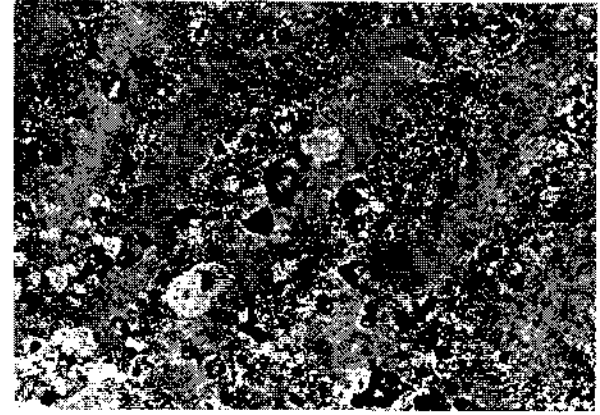
1



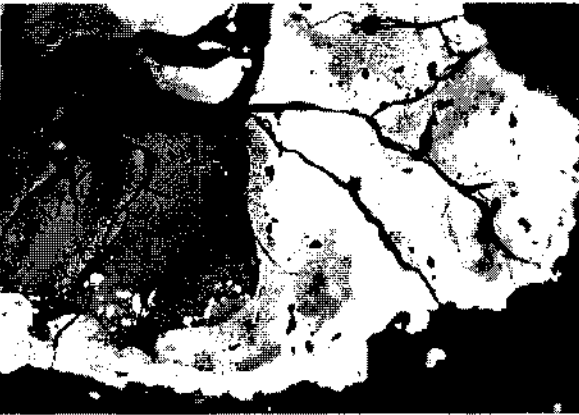
2



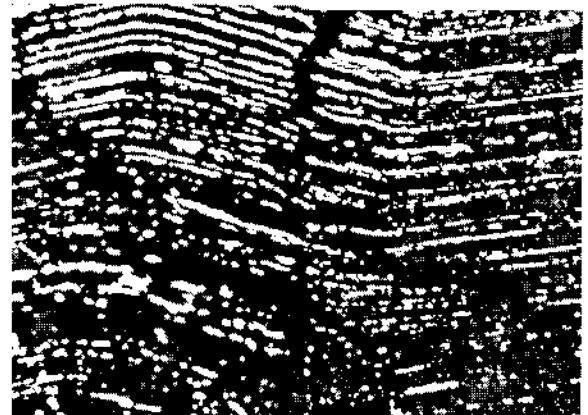
3



4



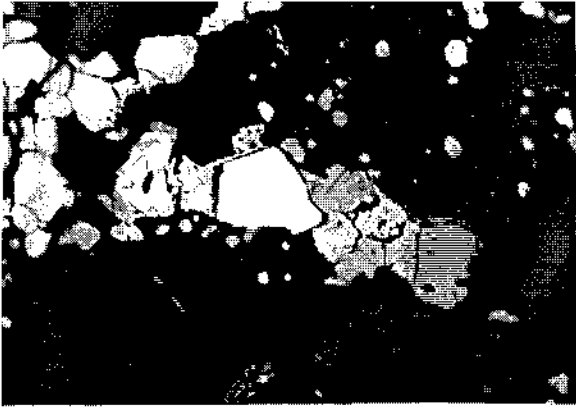
5



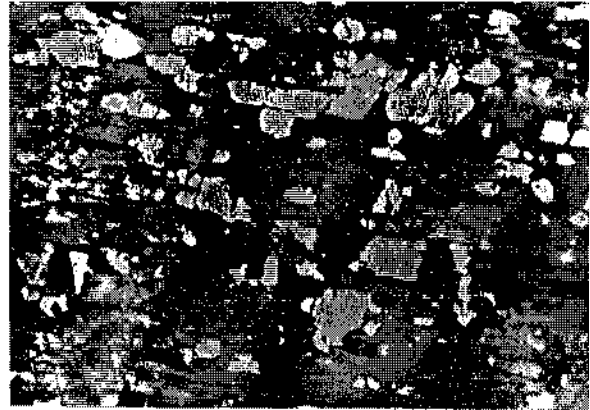
6

PLATE-II

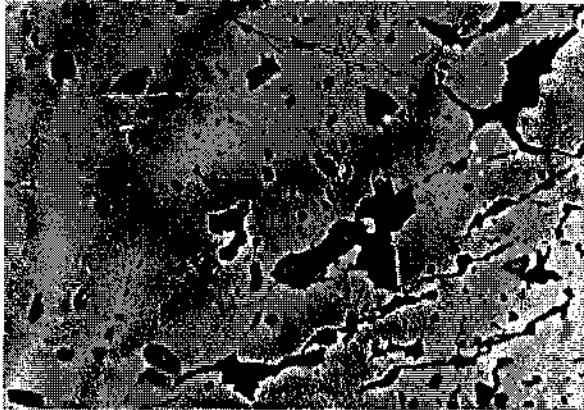
- Fig. 1- Magnetite (gray) and pentlandite (dirty white, anhedral at the left center) growths and a gersdorffite grain (white, subhedral at the center) in serpentinites (black). In oil. Magnification x200.
- Fig. 2- Hercynite occurrences (gray) along cleavage plains of orthopyroxene (dark gray). In oil. Magnification x200.
- Fig. 3- Silicate inclusion-bearing (small black spots) magnetite occurrences (gray) associated with siderite-ankerite type carbonates (black coarse grains) along fracture and spaces. In oil. Magnification x200.
- Fig. 4- Cataclastic magnetite occurrences (gray) transforming to martite along the edges. In oil. Magnification x200.
- Fig. 5- Tremolite, actinolite, and chlorite (horn-shaped dark gray part at the center) inclusions-bearing chalcopyrite occurrences (gray) locally transformed to bornite (dark gray cloudy appearance at the left center) in siderite-ankerite (black). In oil. Magnification x200.
- Fig. 6- Chromite and chrome spinel (gray central parts of the same crystal) occurrences in calcite-dolomite (cloudy gray background) transformed to magnetite (the most outer light gray zone of drop-shaped crystals) along the margins. In oil. Magnification x200.



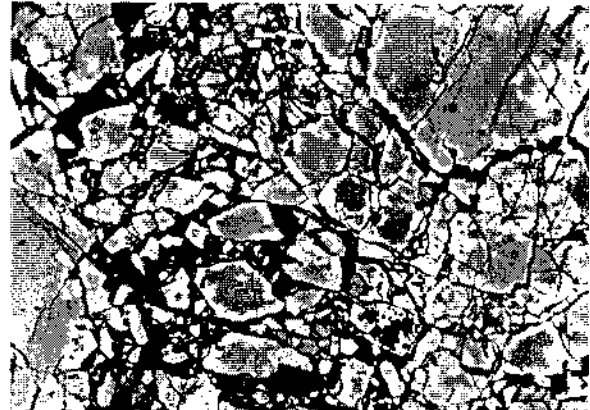
1



2



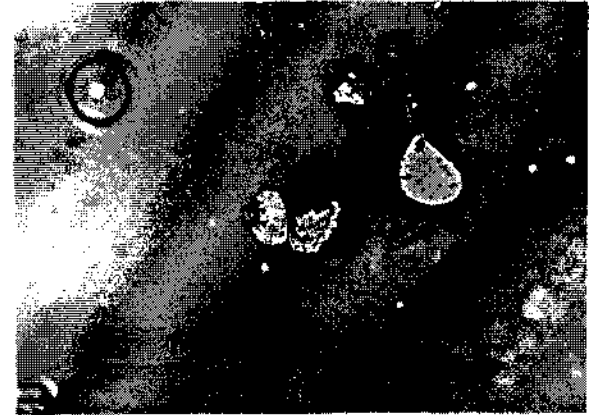
3



4



5



6

QUATERNARY FRESHWATER FAUNA OF THE KILBASAN AREA, NORTHERN KARAMAN

Ümit ŞAFAK* and Güler TANER**

ABSTRACT.- Clastic units exposing around the Kilbasan village at north of the city of Karaman contain the relicts of a dry lake basin. In this basin, the presence of an extensive fauna even detectable with necked eye is noticeable. Seven of wash samples collected as point sampling from the basin were subjected to detail works. As a result of examinations on the fauna, a number of 3 ostracods, 4 gastropods and 1 pelecypod species characteristic for typical freshwater environment were determined.

STRATIGRAPHIC AND TECTONIC FEATURES OF MIOCENE BASIN SOUTH OF İMRANLI AND HAFİK (SİVAS)

Yavuz ÇUBUK*** and Selim İNAN****

ABSTRACT.- Basement of the autochthonous units cropping out in the south- southeast of İmranlı (Sivas) and south-southwest of Hafik (Sivas), comprises the Refahiye ophiolitic complex, whose time of emplacement is Late Cretaceous-Early Eocene. This basement is overlain unconformably by the Middle Eocene Bozbel formation, composed of marine sediments with occasional volcanic components. The Bozbel formation is overlain again unconformably by the Oligocene Selimiye formation, comprising shallow marine (possibly lagoonal) sediments. Chattian-Burdigalian aged Ağılkaya formation, which is composed of red colored aluvial fan-sabkha-limited cycle sediments, overlies transgressively the Selimiye formation. The Ağılkaya formation crosses gradually into the Lower Miocene Karayün formation of red colored fluvialite-playa sediments. The Karayün formation and Ağılkaya formation are overlain unconformably by the Lower-Middle Miocene age Sarıhacı formation, which comprise green colored mudstone, with shallow marine sandstone-limestone interlayers. All these units are overlain by the Upper Miocene-Pliocene Eğerci formation, comprising fluvialite sediments. Sivas Tertiary basin, whose evolution started in Early Eocene, has been subject to the influence of N-S trending compressive regime in Late Eocene. Chattian-Aquitaniaian gypsum deposits have caused the first period of salt uprisal which shaped the recent structural units of the basin in Early Miocene. This salt tectonics has been effective in the basin up to Late Pliocene. In this epoch, abundantly salt uprisals and related folds and overthrust have been developed in the basin.

AN EXAMPLE FOR A PRE-EARLY ORDOVICIAN ARC MAGMATISM FROM NORTH TURKEY: GEOCHEMICAL STUDY OF THE ÇAŞURTEPE FORMATION (BOLU, W PONTIDES)

P. Ayda USTAÖMER* and Erdinç KİPMAN*

ABSTRACT.- Three different units are exposed underneath the Palaeozoic sequence of W Pontides in the Bolu-Yedigöller area. These are, from the structural base to the top: i) high grade metamorphic rocks (the Sunnice group), ii) granitoids and, iii) a volcanic sequence (the Çaşurtepe formation) into which the granitoids intruded. The granitoidic intrusions are a part of an extensive group of intrusions, called the "Bolu Granitoid Complex" (BGC) and, together with the Çaşurtepe formation, they crop out structurally on top of the Sunnice group along a NE-SW trending, NW-dipping tectonic contact. The granitoids are cut by a number of lamprophyre dykes. The Çaşurtepe formation, the main subject of this paper, comprises of andesitic lavas at the base, overlain by an ignimbrite serie in which rhyolitic volcanoclastics are dominant. Both the volcanic sequence and the granitoids were metamorphosed to greenschist facies and as a result, an albite+epidote+chlorite+actinolite mineral assemblage was developed, together with relict igneous minerals. An extensive pyrite mineralization is developed along sinuous shear zones in locally developed intense hydrothermal alteration areas. Massive lavas of the volcanic sequence are calc-alkaline andesitic and locally rhyo-dasitic in composition with high SiO₂ content (> % 54). These have LIL-element enrichment relative to N-type MORB and show Nb depletion relative to LREE (La, Ce, Nd). The dykes within the granites have similar chemical characteristics. One sample analysed from the Çaşurtepe formation gave ⁸⁷Sr/⁸⁶Sr 550 Ma model age value of 0.706482, ¹⁴³Nd/¹⁴⁴Nd model value of 0.512450 and ^εNd value of 10.2. Both major and trace elements of volcanic rocks indicate that the lavas are products of calc-alkaline active margin arc volcanism, developed above a subduction zone. ¹⁴³Nd/¹⁴⁴Nd - ⁸⁷Sr/⁸⁶Sr isotope ratios depart from typical MORB values and are compatible with those of intra-oceanic arcs. The Sunnice group, the Çaşurtepe formation and the BGC are unconformably overlain by Lower Ordovician continental elastics of the Palaeozoic of Istanbul. Therefore, the data presented here points out to the existence of subduction-related magmatism during the pre- Early Ordovician period in W Pontides.

INTRODUCTION

The Pontides are a mosaic of amalgamated Palaeozoic-Early Mesozoic continental and oceanic assemblages that differ in their metamorphism, magmatism and tectonic settings (Şengör et al., 1984; Robertson and Dixon, 1984). The study area is in the western part of the Pontide tectonic belt, within what is termed the Istanbul nappe (Şengör et al., 1984), the Istanbul zone (Okay, 1989) or the Istanbul fragment (Ustaömer and Robertson, 1993); geographically it is located in the north and northeast of the Bolu city, between Bolu and Yedigöller (Fig. 1). Although the post-Ordovician geological evolution of the West Pontides is well understood (Şengör and Yılmaz, 1981), there is limited data for the pre-Ordovician period. The Palaeozoic of Istanbul (Abdüsselamoğlu, 1977) and its basement units, composed of high-grade metamorphics (the Sunnice group), low-grade metamorphic plutonic (the Bolu Granitoid Complex-BGC) and volcano-sedimentary rocks (the Çaşurtepe formation), are exposed un-

derneath an Upper Mesozoic-Tertiary volcano-sedimentary cover (Fig. 2). The Palaeozoic of Istanbul and the Upper Mesozoic-Tertiary cover units are outside the scope of this paper. We here describe the basement units but emphasis is given to the Çaşurtepe formation. Stratigraphy, petrography, major- trace- elements and isotope geochemistry of the Çaşurtepe formation will be described in detail and its implication for regional geology will be evaluated. This work brings a different approach to the age and source problem of magmatic rocks, based on field work as well as geochemical studies on massive lavas of the Çaşurtepe formation, and petrographically and mineralogically similar dykes that intrude the granitoids. In this paper, an active margin magmatism of pre- Early Ordovician period is described.

HISTORY OF RESEARCH

The Çaşurtepe formation was considered part of metamorphic basement rocks (the Sunnice group of

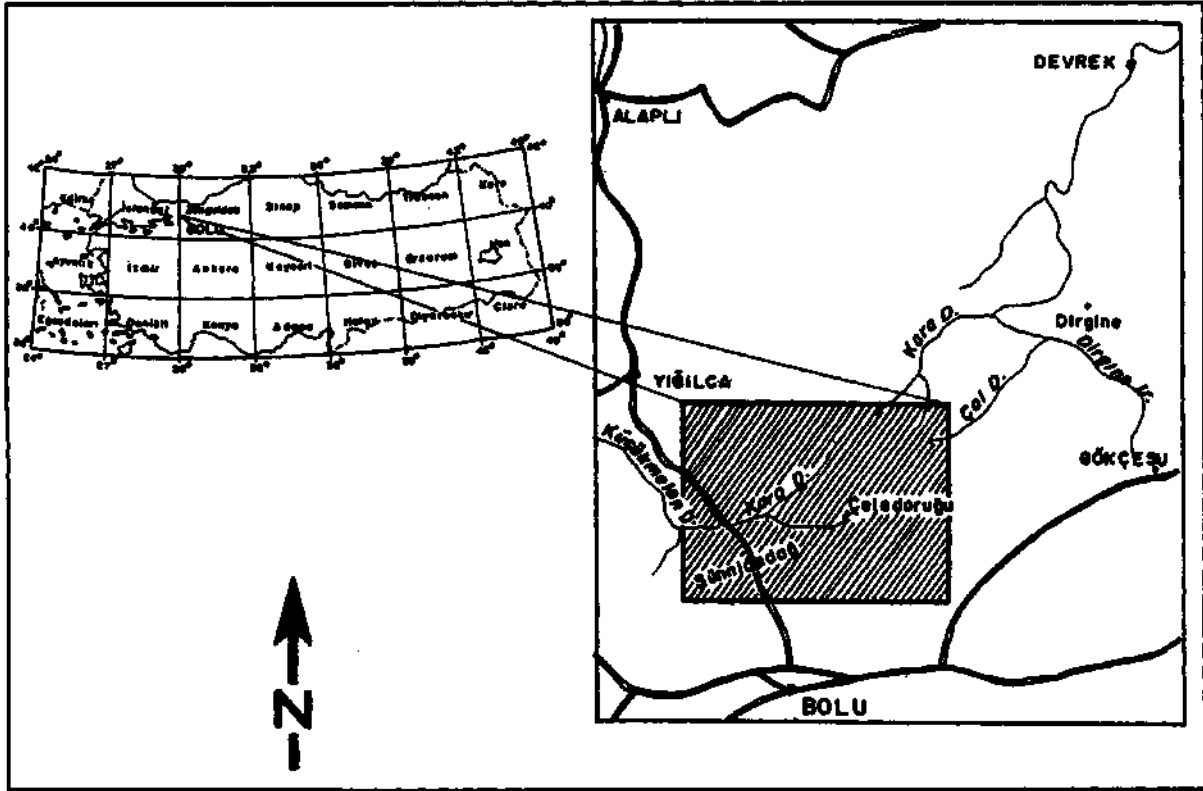


Fig. 1- Location map of the study area.

this study) and its metamorphosed basic volcanic and volcanoclastic member (Kaya, 1978; Canik, 1980; Serdar and Demir, 1983). Aydın et al., (1987) termed the unit the "Orhandağ metabasics", and Erendil et al., (1991) named it the "Yellice member" of the "Bolu massif". The volcanic rocks, however, during this study and a previous work (Cerit, 1990) are considered as a separate formation (Fig. 3).

Cerit (1990) called the unit the "Yellice formation or Yellice metavolcanics" and assumed it to be the oldest unit of the Palaeozoic sequence. He separated five different rock group within the formation; metavolcanics, metasandstones, contact metamorphic felsic rocks, quartzites and cataclastics. According to Cerit (1990) and Cerit and Batman (1992), the Dirgine granitoids (The BGC of this study) of Early Palaeozoic (Ordovician?) age and the Cambro-Ordovician aged metavolcanic rocks (the Yellice formation) are products of the same magmatic event and this magmatism took place during the early stages of the Caledonian orogeny.

Thus the yanitoids (based on 23 major element analysis) and the metavolcanics emplaced onto southern margin of Eurasia as products of arc magmatism. Later Cerit changed his view and thought that the "Dirgine granitoids" are of S-type, products of partial melting of the Karadere metamorphics (the Sünnice group of this study) of sedimentary origin (Cerit, 1995).

Erendil et al., (1991) considered the granitoids and the volcanic rocks as "Magmatic core rocks" of the "Bolu massif" (Blumenthal 1949). They gave a post-Devonian-Valangian emplacement age to the granitoids. They observed that the granitoids and the "Yellice member" cut each other, thus, they are the products of the same magmatic event.

Interpretation of the volcanic rocks by the previous workers is wholly based on field observation, contact relations and petrographic work. No geochemical data was provided.

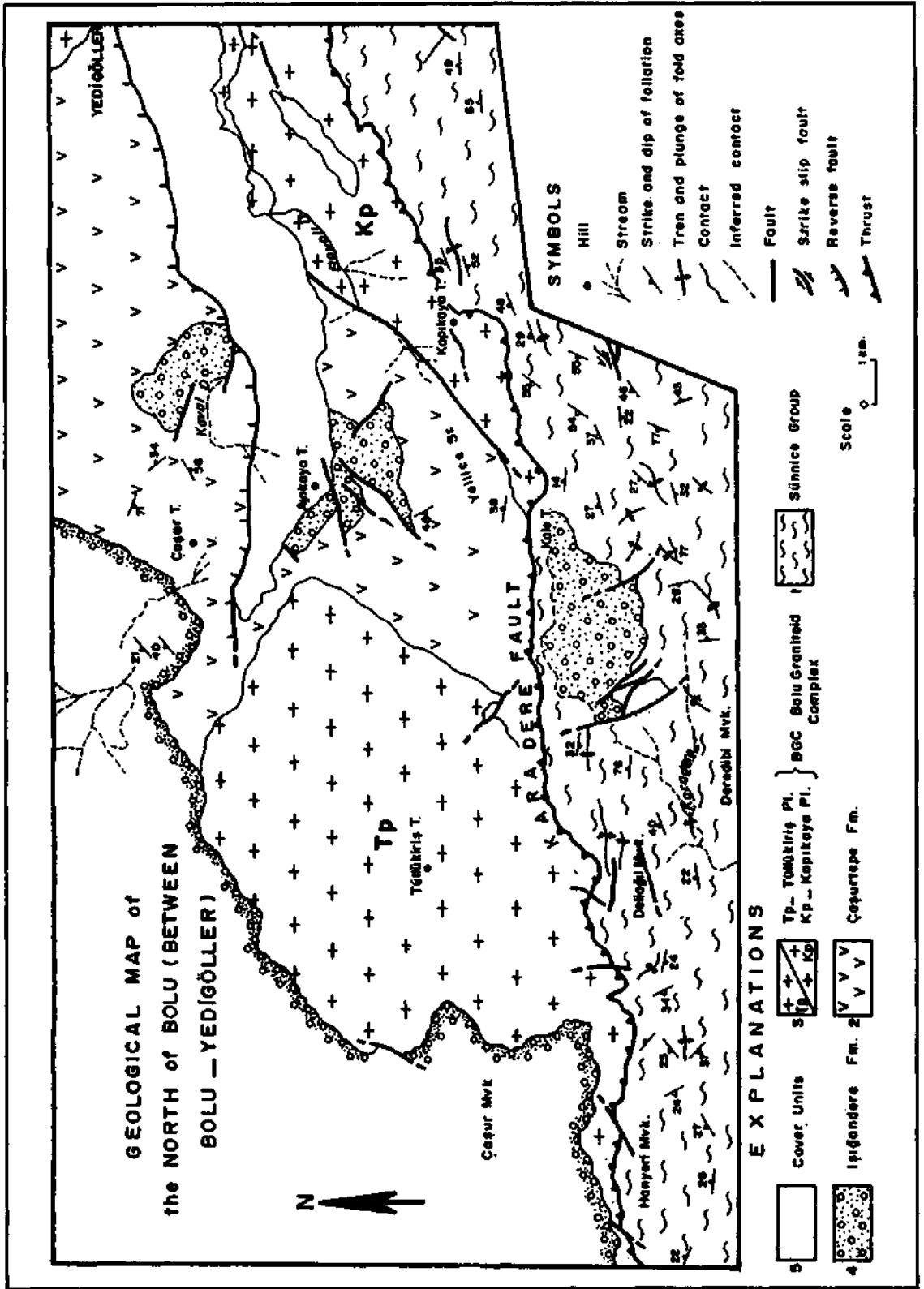


Fig. 2- Geological map of the study area. Simplified after Ustaömer (1996).

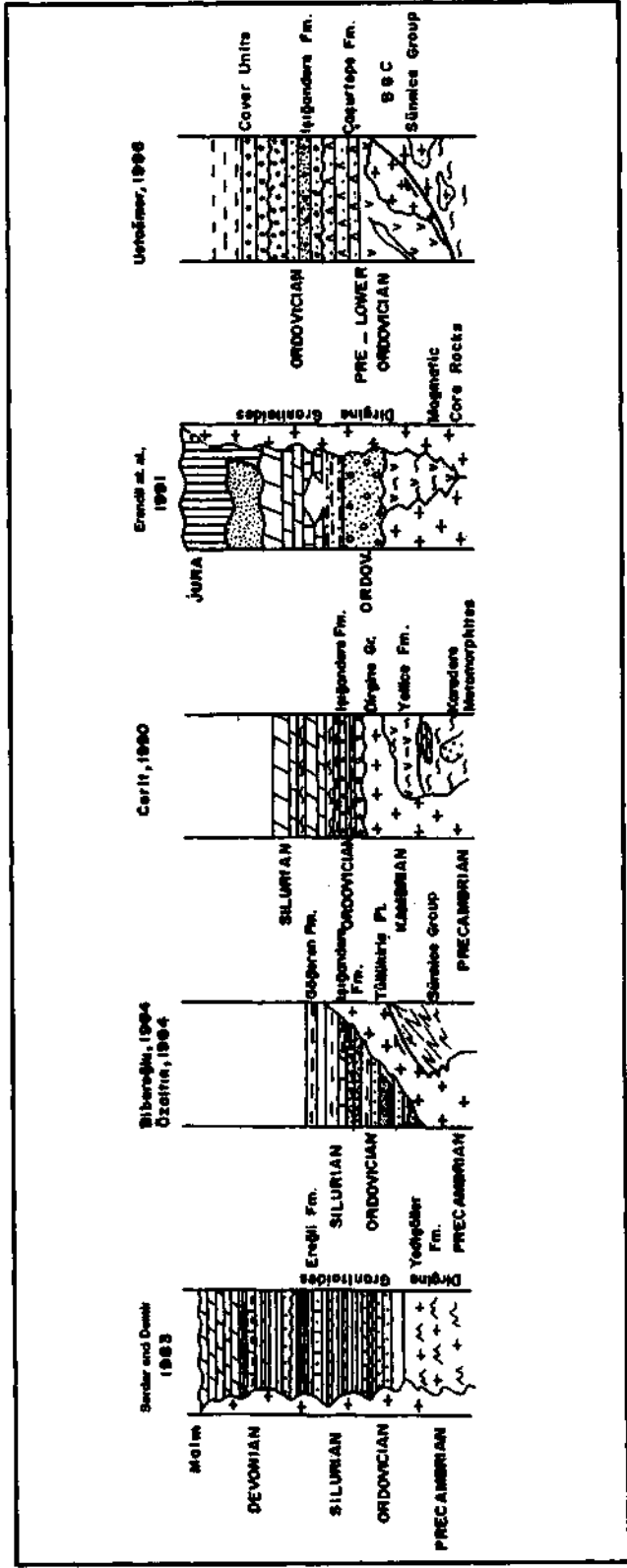


Fig. 3- Stratigraphic column sections of the study area proposed by previous workers and this study (not to scale).

TECTONO-STRATIGRAPHY

In the study area (Fig. 1), three different units are exposed underneath the Palaeozoic of Istanbul sequence. Structurally lowest unit is the Sünnice group (Biberoğlu, 1984; Özaltın, 1984; Seyitoğlu, 1984), comprises of gneisses and amphibolites cut by metagranitic intrusions. Structurally above is the Çaşurtepe formation (P.A. Ustaömer, 1996). This unit is made up of andesitic lavas at the base, overlain by dacite-rhyodacites and meta-ignimbrites, consisting of rhyolitic volcanoclastic sediments. The third rock group is the intrusions of the "Bolu Granitoid Complex" (BGC) (Mugan-Ustaömer, 1992) that cut the volcanic rocks of the Çaşurtepe formation and are in tectonic contact with the Sünnice group along a NE-SW trending fault zone. All these three units are unconformably overlain by continental elastics (the Işığandere formation) that are lateral equivalent of the Kurtköy formation (Haas, 1968; Kaya, 1978) of the Istanbul and adjacent areas. The Işığandere formation is conformably overlain by quartzites and shales in the NW of the study area. These are equivalents of the Aydos and Gözdağ formations (Önalın, 1981) of the İstanbul area. Following Middle Ordovician fossils were found within the study area from the shales (Özaltın, 1984; Biberoğlu, 1984): *Orthambonites* sp., *Mcewanella* sp., *Mcewanella* sp. cf. *berwynansis* (Mac Gregor), *Glyptorthis* sp., *Dalmanella* aff. *parva* Williams, *Parastrophinella* sp., *Christiania* sp., *Oligorhynchia* aff. *subplana* Cooper, *Protozygasp.*, *Bryozoer*, and *Crinoid*. By its stratigraphic position underneath the Middle Ordovician shales, the age of the Işığandere formation can be given as Lower Ordovician.

The Sünnice group

The Sünnice group, the highest grade metamorphics of the study area comprises of gneisses and amphibolites, retrograded into greenschist facies (P.A. Ustaömer, 1996). The Sünnice group is exposed as a north dipping tectonic slice, sandwiched between the Mesozoic sediments in the south (outside the study area) and the Bolu Granitoid Complex and the Çaşurtepe formation in the north, and unconformably overlain by the Lower Ordovician continental (fluvial) elastics

The Sünnice group is a migmatitic assemblage and consists, at the base (in the south), of pale and dark green, cm to m thick amphibolites, alternated with white, cream coloured quartz- feldspatic bands. The contact between the two is sharp and irregular in places. Further up, the unit is composed of thick gneisses, alternating with thin bands of amphibolites: At the uppermost levels the unit is cut by tonalitic, granodioritic and granitic (sensu stricto) rocks that are a few meters to tens of metres thick and metamorphosed in greenschist facies conditions. The most interesting structural feature of the Sünnice group is existence of extensive extensional structures in the form of normal faults. These structures are observed in the structurally upper levels (close to the northern contact of the unit) and do not exist in the younger (Lower Ordovician and Upper Mesozoic) units (P.A. Ustaömer, 1996).

The age of the unit can be given pre-early Ordovician as it is unconformably overlain by the Lower Ordovician continental elastics (the Işığandere formation). Aydın et al., (1987) described a clastic sequence (Soğuksu formation; Kaya, 1982) of Cambrian age stratigraphically underneath the Işığandere formation (Gormus, 1980). There is no metamorphism within this unit. This unit is not exposed in the study area due to either erosion or non-deposition. Therefore, the age of the Sünnice group can be given as Precambrian. There is a general consensus on the age of the similar units of the area among the previous workers (P.A. Ustaömer, 1996). High grade metamorphosed gneisses and amphibolites crop out in the Central and West Pontide tectonic belt in the Devrekani massif, in the Araç-Karadere area and in Kaplandededağ. These metamorphics are thought to be Precambrian in age by all the researchers (Arpat et al., 1978; Yılmaz, 1980; Ustaömer and Robertson, 1993). Kaya (1982) gave a Precambrian age to the unit as the Ordovician aged elastics unconformably overlies the metamorphic rocks.

The Bolu Granitoid Complex

Structurally above the Sünnice group, two members of the "Bolu Granitoid Complex", the Tüllükiriş pluton (Biberoğlu, 1984) in the west and the Kapıkaya plu-

ton (P.A. Ustaömer, 1996) in the east are exposed along a NE-SW trending thrust zone. Petrographically, the plutons are tonalite, granodiorite and in restricted areas (northern areas for the Tüllükiriş pluton, central and northern areas for the Kapıkaya pluton) granite (*sensu stricto*) in composition, and exhibit a typically granophyric texture, implying that the granitoids were emplaced in shallow crustal levels and are high-level intrusives (emplacement depth is between <5 km and >2 km). Major- trace- elements and isotope geochemistry of the granitoids indicate that they are products of melts of supra-subduction zone arc magmas, contaminated by a crust at a certain degree (P.A. Ustaömer, 1996).

The plutons are cut by a number of lamprophyre and aplite dykes. The dykes are a few cm to a few m thick with a general NE-SW strike, compatible with general trends of the intrusions and their margins. Field and petrographic characteristics of the lamprophyre dykes are similar to those of the lavas of the Çaşurtepe formation. Therefore, chemical characteristics of the dykes are studied along with the volcanic rocks of the Çaşurtepe formation.

There is a general debate on the emplacement age of the granitoids. Suggested ages range from Early Ordovician (Aktimur et al., 1983; Cerit, 1990), post-Devonian (Erendil et al., 1991), post-Silurian (Biberoğlu, 1984; Özaltın, 1984; Seyitoğlu, 1984), End-Carboniferous- Upper Jurassic (Aydın et al., 1987) to pre-Middle Jurassic (Yazman et al., 1984) (Fig. 3).

The age of the intrusions can be given as pre-Early Ordovician as they are unconformably overlain by the continental Işığandere formation. They are, however, younger than the Çaşurtepe formation as they intrude it.

The Çaşurtepe formation

The Çaşurtepe formation is a volcano-sedimentary rock assemblage metamorphosed into greenschist facies. The unit is made up of massive, locally foliated, neutral to acidic lavas and volcanoclastic sediments.

Clastic and carbonate sediments join the assemblage in the east, outside the study area (Fig. 2). The unit is named the Çaşurtepe formation as its best exposures and stratigraphy could be seen in the Çaşurtepe and in the Kaval dere valley adjacent to Çaşurtepe (P.A. Ustaömer, 1996).

The Çaşurtepe formation crops out between the tectonic line that separates the Sünnice group to the south and the Işığandere formation to the north (Fig. 2).

As the area is heavily vegetated, the best exposures can be seen in the road cuts along valleys. White rhyolitic lavas could be seen along the Yedigöller National Park-Homrus village road section. Hydrothermal alteration zones and mineralizations are best exposed on Kapıkaya Tepe-Boyalı Dere road sections. The Bolu river valley that flows in NW-SE direction between Gökçesu and Dirgine (outside the study area in the east) is the section where phyllites and metacarbonates dominate at the expense of volcanics.

At the observable base, there are massive lavas, dark green at altered surface, pale green to gray at fresh surfaces. At these levels, the lavas are represented by aphyric, locally quartz and plagioclase-phyric lavas. Chlorites are seen widely along foliation planes. Upward, the unit is cut by white, acidic lavas. These acidic lavas are 40-50 cm thick, fine grained and altered. These are best exposed to the south of Hümrüs village.

At upper part of the unit, pale green volcanoclastic sediments are seen. These are medium (15-20 cm thick) bedded, silicified and contains sedimentary structures such as grading and lamination. Base of individual beds are tabular, sharp and not erosional. At individual beds where grading is seen, base of the beds are represented by coarse sands, followed by fine sands and then silts. Dark green muds are found at the uppermost part of the beds. In such sandstone dominated sections, the sandstones alternate with 10-20 cm thick, dark green, finely laminated mudstones. The unit appears as a volcanic turbidite sequence in such

areas. Volcanic conglomerates, on the other hand, were not encountered in the unit.

The volcanic rocks exhibit intense hydrothermal alteration at lower levels where massive lavas dominate and in places in the north where volcanoclastic sediments are exposed. Such alteration zones can easily be recognised with their reddish brown and local sulphuric yellow colours. Another characteristics of such areas is existence of associated intense deformation (shear zones). Thus, there is a strong control on genesis of the mineralization. When closely examined, the shear zones separate lensoidal massive lava blocks. Along the shear planes of 2- 3 cm thick, there are pyrite-rich veins in which pyrite crystals are 5-6 mm long. Lava blocks contain disseminated pyrites and are silicified.

It is impossible to give a stratigraphic thickness to the unit as it is faulted at the base and erosional at the top and also as it is composed dominantly of massive lavas with only rare stratigraphic horizons (bedding, lava flows). A 5 km structural thickness is estimated for the exposures within the study area (Fig. 2).

The Çaşurtepe formation is in tectonic contact with the Sünnice group and the Kapıkaya pluton. Along the contact with the Sünnice group, the Çaşurtepe formation is thrust over it. The volcanic rocks are cleaved in the contact zone. The Çaşurtepe formation is thrust over the Palaeocene-Eocene aged volcanic rocks along the northern slopes of the Ayıkaya tepe (Fig. 2).

The Çaşurtepe formation is unconformably overlain by red continental conglomerates of the Işığandere formation in the Kapıkaya tepe, north of the Çaşurtepe and in the southeast of Hümrüs village, outside the study area in the north. The Işığandere formation here contains clasts of volcanics of the Çaşurtepe formation. Another important observation is that the Işığandere formation do not show any trace of hydrothermal alteration where it unconformably overlies zones of intense hydrothermal alteration and mineralization. The Çaşurtepe formation is unconformably overlain by the Upper Cretaceous limestones (Ayıkayası formation; P.A. Ustaömer, 1996) near south of Ayıkaya tepe peak (Fig. 2),

Along the intrusive contact with the Tüllükiş pluton, apophysis (2-3 m thick) of the pluton intrudes the volcanic rocks and large volcanic blocks are seen within the plutonic rocks. A few tens of metres thick contact aureole is developed along this contact.

There is no radiometric age data on the Çaşurtepe formation. Therefore, the age of the unit can be constrained by taking into account of its contact relation with other units. As stated above, the Çaşurtepe formation is unconformably overlain by the Lower Ordovician Işığandere formation. This indicates that the Çaşurtepe formation was uplifted and become a source area for the Işığandere formation elastics before Early Ordovician. The hydrothermal mineralization and deformation that control it must be pre-Early Ordovician in age as such zones are also unconformably overlain by the Işığandere formation. It is obvious that metamorphic grade of the Çaşurtepe formation is lower than that of the Sünnice group. This implies that metamorphism of the Çaşurtepe formation took place at shallower crustal levels in comparison to the Sünnice group. The unit can be said to be older than the granites as it is cut by them.

PETROGRAPHY

When examined under the microscope, the neutral-acidic volcanics and volcanoclastics comprises of plagioclase, quartz, chlorite, actinolite and epidote minerals set in a dark green chloritized. Calcite and pyrite join the assemblage where the rock is heavily deformed, evidenced by development of secondary shear zones.

Plagioclases are found as both large crystals and as microlites within the matrix. They show mainly carlsbad and albite-carlsbad twinning, and appear brownish in colour due to carbonate alterations. Among the plagioclase crystals, there are quartz (5-10 %), chlorite with bluish extinction colour in places, and tabular actinolites. Epidote minerals of various sizes are widely seen in sections rich in plagioclase. Thus, mainly andesitic neutral rocks typically show porphyric textures. In some sections with cryptocrystalline matrix, fine grained quartz minerals are seen to be dispersed through

hout. But, matrix / quartz ratio changes place to place at the expense of each other. In such sections, there are also dispersed fine grained plagioclase, chlorite and actinolite in trace amounts.

Extinction angles of the plagioclase minerals were measured by using universal table and change between 12 to 26°. Thus, anorthite content of the plagioclases varies in a wide interval between An_{28-46} .

The rhyolitic volcanoclastic sediments of the Çaşurtepe formation are made up of large quartz grains as well as plagioclases.

In summary, petrographic examination of the lavas of the Çaşurtepe formation showed that an albite + epidote + actinolite + chlorite ± quartz greenschist facies mineral assemblage was developed on a primary igneous mineral assemblage of neutral plagioclase, quartz and glassy matrix.

GEOCHEMISTRY

6 samples of lavas of the Çaşurtepe formation and 8 samples of dykes that cut the granitoids were collected to analyse for major- and trace- elements. The result is given in Table 1. Major- and trace- elements analysis were carried out by using XRF (X-Ray Fluorescence) technique at Edinburgh University. Sample preparation method is given in Fitton and Dunlop (1985).

Major- and trace- elements geochemistry

LOI (Loss on ignition) values of the lavas and the dykes are up to 5 %. This indicates that these rocks are variably altered. Most of the major oxides, except Ti and P, and Large Ion Lithophile (LIL) elements (Rb, Sr, Ba) are known to be mobile under greenschist facies metamorphism conditions (Pearce and Cann, 1973). It is possible to determine mobility of an element by plotting it against an immobile element. Here, all the elements are plotted against Zr and it is found out that concentrations of K_2O , Na_2O , CaO , MgO , MnO , Sr, Rb, Ba were affected by hydrothermal alterations. When the dykes are taken into consideration, in addition to

above oxides and elements, the SiO_2 concentrations were also affected (P.A. Ustaömer, 1996). Therefore, the discussion below is based on immobile elements.

SiO_2 values of the volcanics is less than 54 %. MgO values are generally < 6 %, varying between 2-3%. Thus, the volcanic rocks appears to be products of fractionated and evolved melts (P.A. Ustaömer, 1996). In Zr-Ti diagram (Pearce 1980; 1982), the lavas plot in evolved IAT (Island Arc Tholeiites) field (Fig. 4a). Therefore, it is not correct to plot these lavas in basalt discrimination diagrams. In the same diagram, two dykes that cut the Tüllükiriş pluton plot in the basic field, five dykes of the Kapıkaya pluton plot in the evolved IAT field and one sample plot in the basic WPB (Within Plate Basalt) field.

In Nb/Y-Zr/Ti nomenclature diagram (Winchester and Floyd, 1977), the lavas of the Çaşurtepe formation plot in the andesite field, of which two samples plot close to the rhyodacite field (Fig. 4b). Four dyke samples of the Kapıkaya pluton plot in the rhyodacite and the two plot in the andesite fields. But one of these two samples plot in the andesite-rhyodacite boundary and the other is on the basaltic andesite-andesite boundary. The two dykes of the Tüllükiriş pluton plot in the basaltic andesite field on the same diagram (Fig. 4b).

When plotted on an AFM diagram (Fig. 5), the Çaşurtepe volcanics show calc-alkaline trends, while the dyke samples plot in the tholeiitic field (care should be taken, however, when using this diagram as the oxides used in constructing this diagram are known to be mobile).

The samples are plotted on spidergrams by using Sun and McDonough (1980) normalizing values (Fig. 6). In MORB-normalized spidergrams, the dykes (Fig. 6 a,b) show light rare earth element (La, Ce, Nd) enrichment relative to Nb. The Kapıkaya pluton dykes show LIL element (Sr, K, Rb, Ba) enrichment and Ti depletion relative to Zr. These are characteristics of the calc-alkaline volcanics. The Tüllükiriş dykes, on the other hand, show relative flat patterns that are similar to those of island arc tholeiites. The Çaşurtepe volcanics

Table 1- Major- and trace-element analysis of the Çaşurtepe formation and the dykes.

Örnek*	93-54	93-11	93-48	93-3	91-42	91-45	93-41	93-64	91-13	91-15	91-17	91-24	91-25	91-26
SiO ₂	63.09	66.08	70.76	62.64	54.92	70.23	50.29	57.06	58.21	62.39	60.07	47.1	53.61	53.8
Al ₂ O ₃	13.32	14.53	13.22	13.21	16.94	13.41	14.66	13.39	17.06	15.88	16.74	15.3	19.48	19.6
Fe ₂ O ₃	9.51	5.94	4.32	8.92	9.11	4.74	17.77	11.59	7.28	6.02	7.46	14.26	7.27	6.65
MgO	4.91	1.95	0.86	6.5	3.59	1.89	3.88	6.28	1.3	1.24	1.75	5.92	4.53	3.31
CaO	0.24	5.08	4.44	0.21	6.14	2.88	3.28	2.54	5.3	2.82	2.29	7.48	7.85	6.57
Na ₂ O	3.93	3.18	3.54	0.07	3.6	3.8	4.38	3.12	4	7.16	5.53	3.79	3.03	4.48
K ₂ O	0.047	0.416	0.497	1.174	0.898	0.719	0.232	0.014	1.727	0.539	2.167	0.949	0.721	1.005
TiO ₂	0.832	0.464	0.465	0.721	0.996	0.496	1.639	0.999	0.798	0.594	0.935	2.825	0.875	0.848
MnO	0.297	0.11	0.104	0.522	0.127	0.121	0.209	0.295	0.131	0.087	0.126	0.237	0.123	0.125
P ₂ O ₅	0.103	0.15	0.082	0.114	0.192	0.098	0.233	0.112	0.328	0.224	0.242	0.387	0.154	0.169
LOI	3.3	2.01	1	4.76	3.59	1.6	3.09	4	3.59	3.36	2.44	1.98	2.65	3.7
Toplam	99.57	99.89	99.28	98.7	100.1	100.09	99.96	99.39	99.74	100.33	99.75	99.83	100.1	100.05
Sc	32.9	16.8	21.7	32.3	45.8	17.1	59.5	34.2	9.4	14.1	19.8	33.1	18.4	13.4
Ba	40.6	202.2	111.4	2355.3	4.3	461.5	78.9	5	388.9	182.2	508.3	223.9	119.2	174.7
V	240.1	84.9	48.6	72.4	486.9	71.9	430.2	331.6	56.7	20.4	59.9	351.5	143.7	118.6
La	4.6	21.1	9.3	6.7	6.6	6.6	2.8	2.6	20.2	21.9	16	8.9	9	15.5
Ce	24.8	41.4	19.3	23.3	6.5	8.6	20.1	13	36.3	38.9	28.7	29.4	19.7	19.9
Nd	15.5	17.5	9.9	16.6	4.6	5.2	13	7.4	17.8	18.3	11.7	16.7	3.3	10.5
Cr					84.2	6.2			4	0.5	0.9	80.3	36.3	9.5
Ni					20.3	7			4.2	4.1	3.1	38.9	20.7	8.9
Cu	139.5	40.8	38.8	24.5	20.4	8.1	86.7	10	11.8	13.2	15.3	36	29.1	23.5
Zn	322.1	76	50.2	634.5	295.2	82.7	114.2	163.8	74.7	64.1	63.2	120.4	52.2	65.5
Pb	3.7	3.2	8.5	3.2	57.2	17.6	6.5	1.9	3.2	7.9	3.5	5.8	3.7	5.5
Th	0.8	0.6	3.4	0.9	0.2	1.6	5.2	1	3.7	3.3	4.2	0.3	1	2.7
Rb	0.9	14.8	14.5	21	0.2	11.2	7.4	1.2	35.2	9.9	49.4	23.4	18.8	23.1
Sr	22.9	309	160.5	10.1	480.5	131.6	288.4	44.3	208.1	210.9	306.4	445.1	247.6	245.6
Y	32.7	20.8	25.3	38.7	38.7	23.9	29.7	26.9	36.3	43.6	39.5	38.1	17.4	19.4
Nb	2.7	5.3	2.4	2.8	2.7	6.5	1.8	1.1	13.8	10.7	9.6	16.3	6.4	7.8
Zr	87.9	75.1	60.2	81.8	103.8	71.6	50.1	67.5	209.4	204	171.7	214.2	94.1	103.6
Zr/Y	2.688	3.611	2.379	2.114	2.682	2.998	1.687	2.509	5.789	4.679	4.347	5.622	5.408	5.34
Nb/Y	0.083	0.255	0.095	0.072	0.07	0.272	0.061	0.041	0.38	0.245	0.243	0.428	0.368	0.402
Fe/Mg	1.937	3.046	5.023	1.372	2.538	2.382	4.58	1.848	4.855	4.263	4.263	2.409	1.605	2.009
Ce/Y	0.798	1.99	0.763	0.602	0.188	0.38	0.677	0.483	1	0.882	0.727	0.772	1.132	1.026
Y/Nb	12.111	3.925	10.542	13.821	14.333	3.677	16.5	24.455	2.83	4.075	4.115	2.337	2.719	2.487
Ce/Nb	9.185	7.811	8.042	8.321	2.407	1.323	11.167	11.818	2.63	3.636	2.99	1.804	3.078	2.551
Zr/Nb	32.556	14.17	25.083	29.214	38.444	11.015	27.633	61.364	15.174	19.065	17.865	13.141	14.703	13.282

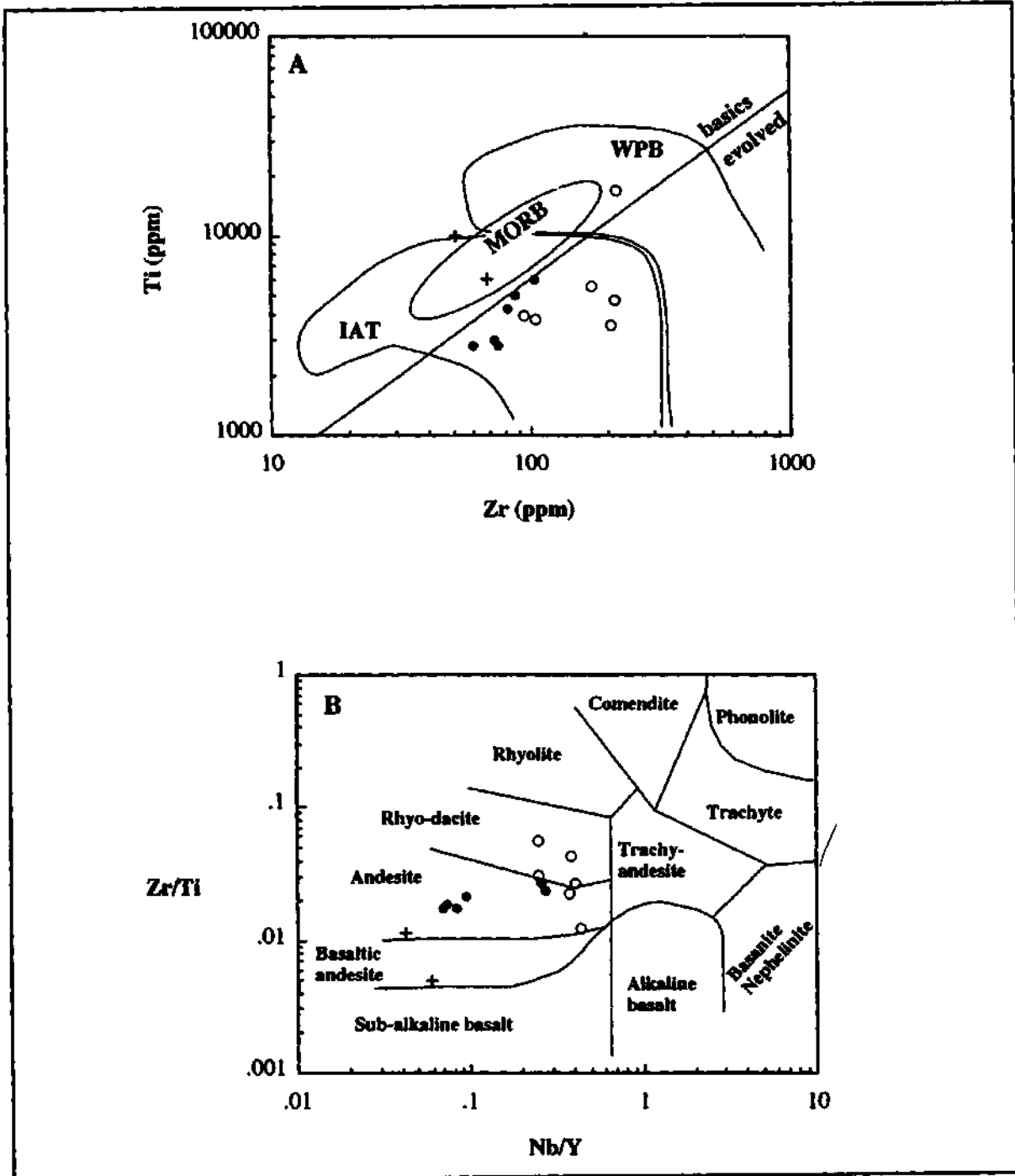


Fig. 4- A. Zr versus Ti diagram (Pearce, 1982) of the Çaşurtepe formation and the dykes (IAT-Island Arc tholeiites; MORB-Mid Ocean Ridge Basalt; WPB-Within Plate Basalt).

B. Nb/Y versus Zr/Ti nomenclature diagram (Winchester and Floyd, 1977) of the Çaşurtepe formation lavas and the dykes. See text for explanation (filled circles: the Çaşurtepe formation; empty circles: Kapıkaya dykes; +: Tüllükiş dykes).

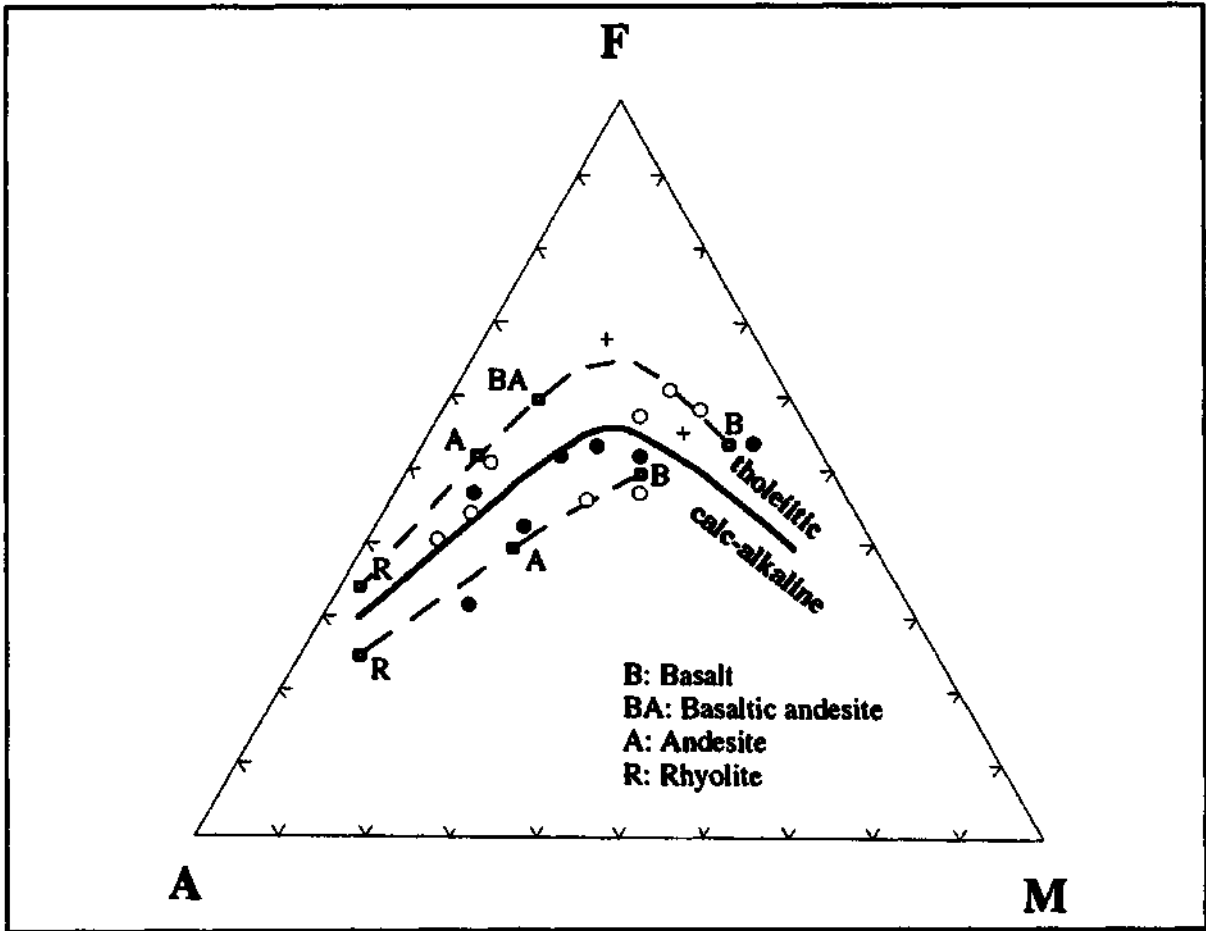


Fig. 5- AFM ternary diagram of the volcanic rocks and the dykes (Boundary line is taken from Irvine and Baragar, 1971). Filled circles: the Çaşurtepe formation; empty circles: the Kapıkaya dykes; + : the Tüllükiriş dykes.

are enriched in LIL elements, there is a marked Nb depletion relative to LREE and Ti depletion relative to Zr (Fig. 6c). The two dykes samples from the Kapıkaya pluton near Dorukhan (outside the study area) show LIL element enrichment, Nb depletion relative to La (Fig. 6d). But the elements between Nb and Y are distinct than the other dykes with these characteristics.

Sr-Nd isotope chemistry

During this study, one sample of the Sünnice group metagranite, one sample of lava from the Çaşurtepe formation and four samples of the granitoids were analysed for Rb, Sr, Sm, Nd isotopes at SURRC (Scot-

tish Universities Research and Reactor Centre). Here Sr, Nd isotope data of one lava sample of the Çaşurtepe formation will be discussed.

$^{87}\text{Sr}/^{86}\text{Sr}$ 550 Ma model values of the sample is 0.706482, $^{143}\text{Nd}/^{144}\text{Nd}$ model value is 0.512450, 550 Ma ϵ_{Nd} value is 10.2.

When plotted on $^{143}\text{Nd}/^{144}\text{Nd}$ versus $^{87}\text{Sr}/^{86}\text{Sr}$ diagram (Wilson, 1989), the sample departs from typical MORB field and plot in the intra-oceanic arc field (Fig. 7). Nd isotope values are not affected by crustal processes such as alteration, sedimentation and metamorphism (Wilkinson, 1982). Therefore, Nd isotopes give reliable results for petrogenetic processes.

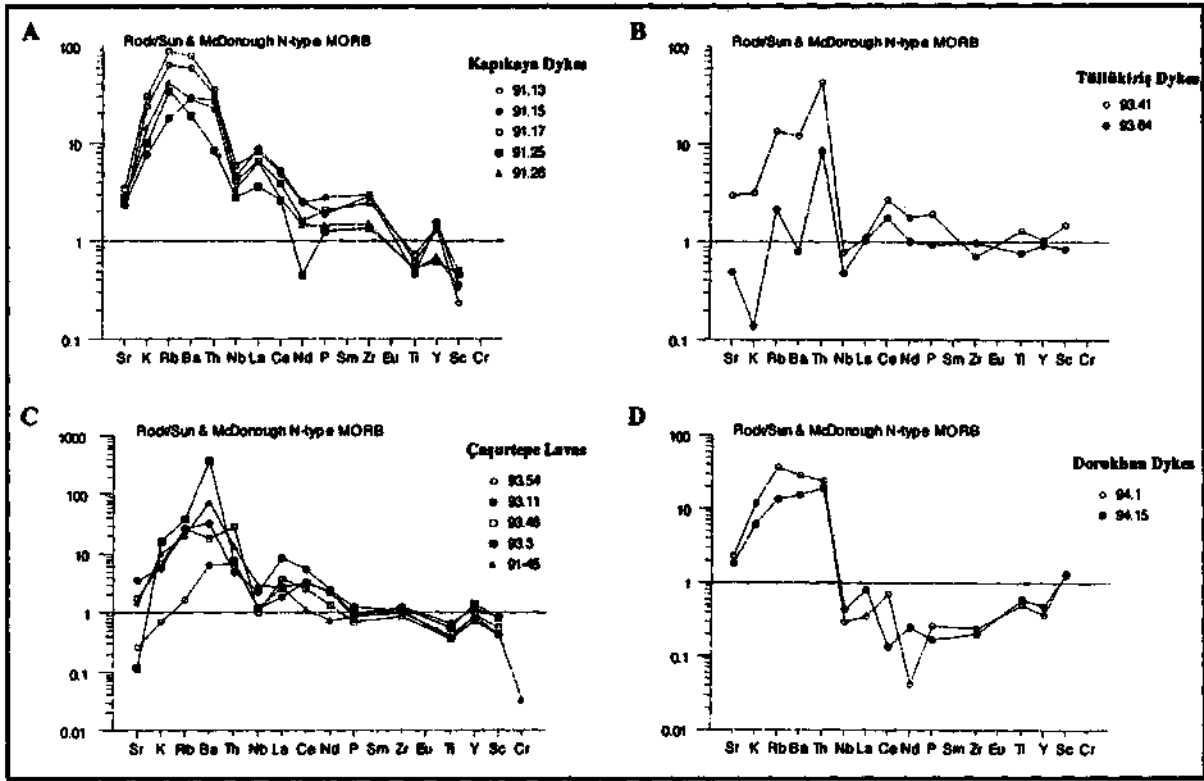


Fig. 6- MORB-normalised spidergrams of the Çarşurtepe formation and the dykes in granites. Normalising values are from Sun and McDonough (1989). See text for explanation.

- A. Dykes of the Kapıkaya pluton
 B. Dykes of the Tüllükiriş pluton
 C. The Çarşurtepe formation lavas
 D. The Dorukhan dykes (from the Kapıkaya pluton outside the study area in the east)

Interpretation of the geochemical data

The geochemical data show that the lavas of the Çarşurtepe formation are calc-alkaline, fractionated andesitic lavas. The patterns observed on the spidergrams are compatible with those of above subduction zone calc-alkaline volcanic rocks. LIL-elements enrichment and Nb depletion relative to LREE (Ce) are the characteristics of supra-subduction zone lavas. Similarly, the dykes of the plutons appear to be above subduction zone melts. The Kapıkaya dykes show typical calc-alkaline trends, while the Tüllükiriş dykes give patterns similar to island arc-tholeiites.

When the plutonic and the volcanic rocks are evaluated together the pre-Early Ordovician magmatic

rocks of the Bolu-Yedigöller area represent half mature arc setting where subduction related tholeiitic and calc-alkaline intrusives and extrusives were accumulated (P.A. Ustaömer, 1996).

DISCUSSION

The Lower Ordovician continental clastic sediments (the Işığandere formation) unconformably overlies the older units. Pebbles of the Sunnice group, the granitoids and the Çarşurtepe formation are widely present within these clastic sediments. This implies that the basement rocks were uplifted a minimum of 5 km before deposition of the Işığandere formation and become a source area for them.

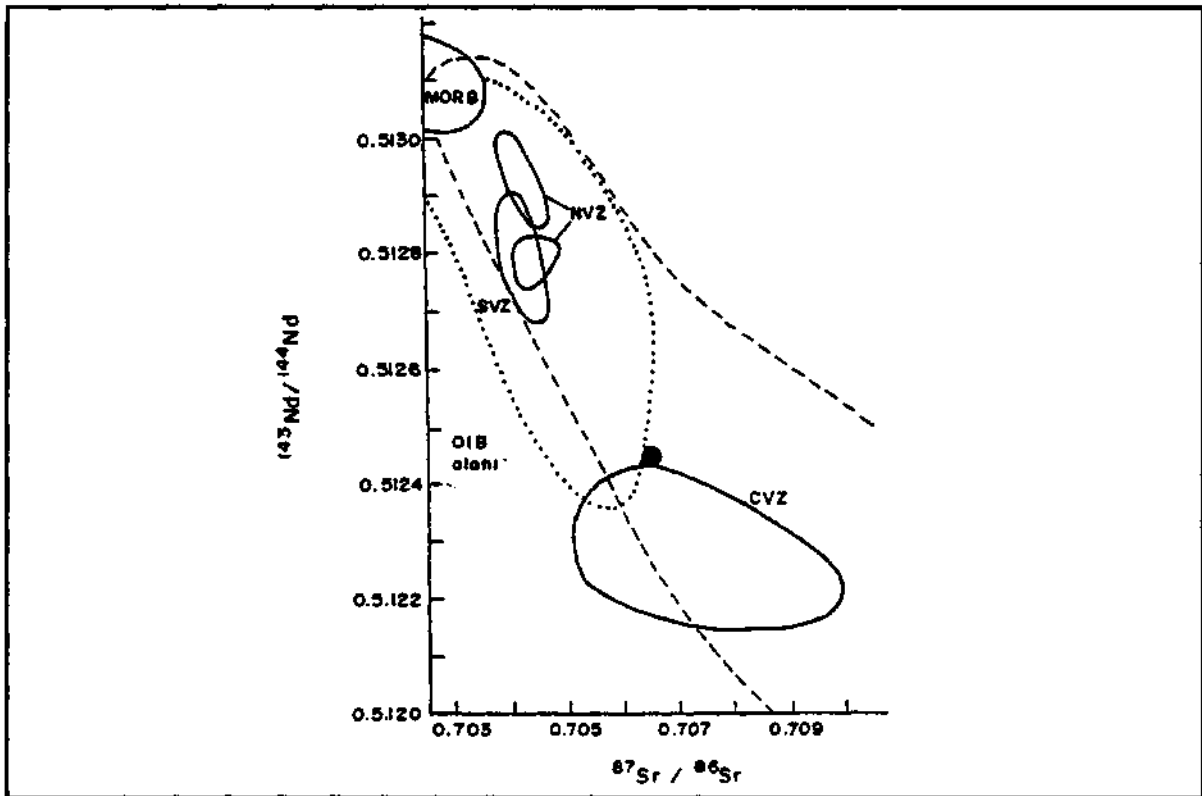


Fig. 7- $^{87}\text{Sr}/^{86}\text{Sr}$ versus $^{143}\text{Nd}/^{144}\text{Nd}$ diagram of one sample of the Çaşurtepe formation. The fields are taken from Wilson (1989). NVZ: North Volcanic Zone; CVZ: Central Volcanic Zone; SVZ: South Volcanic Zone (all from Andean active volcanos); MORB: Mid-Ocean Ridge Basalt; OIB: Oceanic Island Basalt.

The Sunnice group is a migmatitic assemblage metamorphosed in amphibolite facies and its formation corresponds to deeper crustal levels (P.A. Ustaömer, 1996). The granitoids are typical calc-alkaline and show I-type, and locally S-type characteristics due to crustal contamination. They are interpreted as products of mantle derived, crustal contaminated arc magmas that emplaced into shallow crustal levels. Compatibility of both strikes and composition of the dykes and the granitoids suggest that the dykes were the products of relict melts of the granitoids. Major- and trace-element composition of the dykes support this conclusion. In summary, the dykes observed in the granitoids represent a supra-subduction magmatism compatible with the geochemistry of the granitoids.

The Çaşurtepe formation is a 5 km thick (structural-

thickness), subduction related, calc-alkaline volcanic assemblage in which andesitic lavas are dominant with lesser amount of dacite-rhyodacite and rhyolites. At the upper levels, volcanoclastic sediments join the sequence.

In the light of the data given here, it can be said that the granitoids and the volcanic sequence were formed in the same tectonic setting. While volcanic sequence was constructed as surface product of arc magmatism, the granitoids were emplaced into this volcanic pile in later stages of the arc evolution (Fig. 8). Similar evolution can be found in many modern and ancient magmatic arcs (Andean active margin and Cretaceous E Ron-tide arc; Pitcher, 1982; Tokel, 1995).

The data points out the existence of arc magmatism in pre-Early Ordovician time.

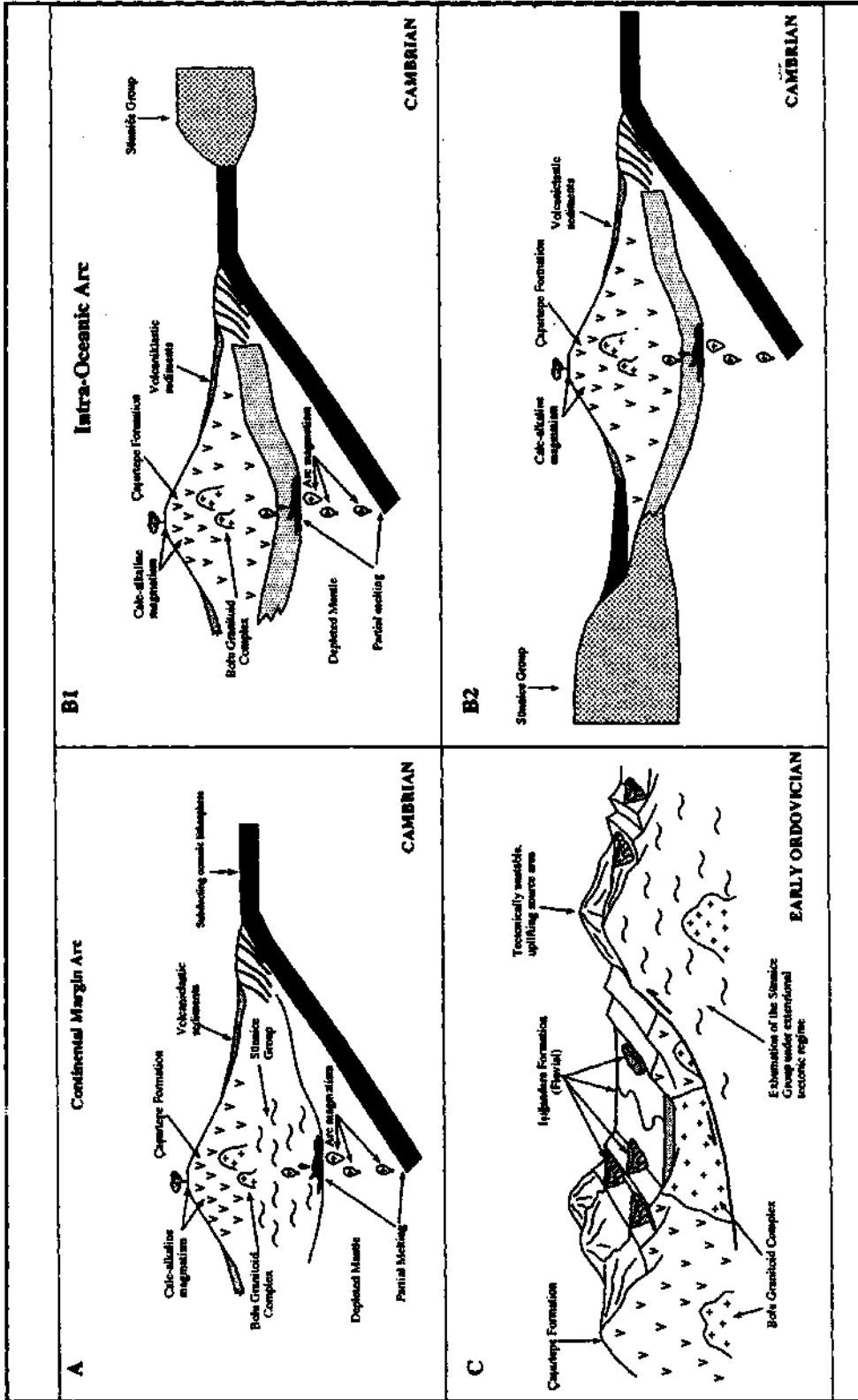


Fig. 8- Proposed alternative tectonic models of the study area. See text for explanation of the models.

Infra-Oceanic versus continental margin arc magmatism

As the stratigraphic basement of the Çaşurtepe formation is not exposed, it is not clear whether it was developed on top of continental or oceanic crust.

Two different models can be proposed for development of the plutonic and volcanic assemblage. In the first model (Fig. 8a), the Çaşurtepe formation represents surface products of active continental margin arc magmatism into which the intrusions of the BGC were emplaced during later stages of arc evolution. In this model, the Sünnice group forms the continental basement of the active margin. This basement was detached and uplifted in pre- Early Ordovician time (Fig. 8c). In the second model, the calc-alkaline magmatism was developed in an intra-oceanic arc (Fig. 8b). In this model, the Sünnice group represents a separate continental siver. This continental block a) collided with the intra-oceanic arc, deeply buried, then detached and uplifted (Fig. 8b1) or b) the intra-oceanic arc was a near continental margin arc and it was thrust onto the continental margin (i.e. the Sünnice group) during pre-Early Ordovician period (Fig. 8b2). The second model requires that the present day outcrop pattern of the region is a result of post-Ordovician tectonism.

The Çaşurtepe formation, together with the granitoids, tectonically overlies the Sünnice group. There is no accretionary complex or an ophiolitic melange along the contact. Therefore, the contact with the Sünnice group is not a suture. The Sünnice group itself is not an accretionary complex either as the unit comprises of gneiss-amphibolite alternation into which granitic melts were emplaced. The unit does not contain ophiolite slices or blueschist blocks. Therefore, the first model is preferred here.

This paper presents first analytical data on existence of arc magmatism during pre-Early Palaeozoic period within West Pontide tectonic belt (P.A. Ustaömer, 1996; Ustaömer and Kipman, 1997). Similar tectonic events took place in Europe along Cadomian margins (Haydudov, 1995; Göncüoğlu, 1997).

ACKNOWLEDGEMENTS

This study was supported by the University of Istanbul Research Fund (Project No:593/171193). Thanks are due to Prof. A.H.F. Robertson for providing laboratory facilities at Edinburgh University. Dr. G. Rogers of SURRC is thanked for carrying out isotope analysis. Prof. Dr. Yücel Yılmaz read an earlier draft of this paper and made useful comments. Drs. T. Ustaömer and M. Keskin are thanked for their help and suggestions to improve the paper. We also thank an anonymous referee for critical appraisal of the paper.

Manuscript received January 20, 1997.

REFERENCES

- Abdüsselamoğlu, M.S., 1977, The Palaeozoic and Mesozoic in the Gebze region-Explanatory text and excursion guidebook. 4th Colloquium on the Aegean Region, Excursion 4. ITU Maden Fak., İstanbul.
- Aktimur, T.; Algan, Ü.; Ateş, Ş.; Oral, A.; Ünsal, Y.; Karatosun, H.; Öztürk, V. and Sönmez, M., 1983, Bolu ve yakın çevresinin yerbilim sorunları ve muhtemel çözümleri. MTA Rep. 1385, (unpublished), Ankara.
- Arpat, E.; Tütüncü, K.; Uysal, S. and Göğer, E., 1978, Safranbolu yöresinde Kambriyen-Devoniyen istifi: TJK 32. Bilimsel ve Teknik Kurultayı, Bildiri Özetleri Kitabı, 67-68.
- Aydın, M.; Serdar, H.S.; Şahintürk, Ö.; Yazman, M.; Çokuğraş, R.; Demir, O. and Özçelik, Y., 1987, Camdag (Sakarya)-Sünnicedağ (Bolu) yöresinin jeolojisi. TJK Bül.,30, 1-14.
- Biberoğlu S., 1984, Yiğilca (Bolu) güneydoğusunun jeolojisi. Yüksek Lisans tezi İTÜ Fen Bilimleri Enstitüsü, 104s. (unpublished).
- Blumenthal, M., 1948, Bolu civarı ile aşağı Kızılırmak mecrası arasındaki Kuzey Anadolu Silsilesinin jeolojisi. MTA Bull., 13, seri: B.

- Canik, B., 1980, Bolu sıcak su kaynaklarının hidrojeoloji incelemesi. Selçuk Üniversitesi Fen Fakültesi Yayl. No. 1, 74 s.
- Cerit, O., 1990, Bolu Masifinin jeolojik ve tektonik incelenmesi. Doktora tezi Hacettepe Üniversitesi Fen Bilimleri Enstitüsü, 217 s, (unpublished).
- , 1995, Bolu Masifinde Alt Paleozoyik yaşlı magmatizma (Bolu kuzeyi). KTÜ Jeoloji Mühendisliği Bölümü 30. Yıl Sempozyumu Bildiri Özleri, 16-20 Ekim, Trabzon, s. 21.
- and Batman, B., 1992, Pre-Mesozoic Stratigraphy and evolution of Bolu Massive (Turkey NW). ISGB-92, Abstract. 20, Ankara.
- Erendil, M.; Aksay, A.; Kuşçu I.; Oral, A.; Tunay, G. and Temren, A., 1991, Bolu Masifi ve çevresinin jeolojisi. MTA Rep. 9425, (unpublished), Ankara.
- Fitton, J.G. and Dunlop, H.M., 1985, The Camerron line, West Africa and its bearing on the origin of oceanic and continental alkali basalts. Earth and Planetary Science Letters, 72, 23- 38.
- , James, D ; Kempton, P.D.; Ormerod, D.S. and Leeman, W.P., 1988, The role of Lithospheric Mantle in the generation of Late Cenozoic basic magmas in the Western United states. J. Petrol. Spec. Lithospheric issue, 331-349.
- Göncüoğlu, C., 1997, Distribution of Lower Palaeozoic rocks in the Alpine terranes of Turkey; Palaeogeographic Constraints. TPJD Sepcial Publication, 3, 13-23.
- Gömüş., S., 1980, Yiğilca (Bolu NW) yöresinin jeolojik incelenmesi. Doktora tezi. Hacettepe Üniversitesi Fen Bilimleri Enstitüsü, 210 s.
- Haas, W., 1968, Das Alt-Palaeozoikum von Bithynien : N., Jb., Gel., Palaont., Abh., 131, 178- 242.
- Haydutov, I., 1995, Pan-African structures along the South European suture zon. A. Erler, T. Ercan, E. Bingöl, S. Orcen (eds): Proceedings of the International Symposium on the Geology of the Black Sea Region, 3-10.
- Irvine, T.N. and Baragar, W.R., 1971, A guide to the chemical classification of the common volcanic rocks. Canadian journal of Earth Sciences, 8, 523-548.
- Kaya, O., 1978, Marmara Denizi doğu çevresinin yaşlı tektoniği: TPAO Arama Grubu Rep. 1020, Ankara.
- , 1982, Ereğli, Yiğilca, Bolu Kuzey, Mengen alanlarının stratigrafi ve yapı özellikleri: TPAO Arama Gurubu Rep. 1639, Ankara.
- Ketin, İ. and Gümüş., Ö., 1962, Sinop, Ayancık ve güneyinde III. Bölgeye dahil sahalarn jeolojisi hakkında rapor: Ml. TPAO Grubu Rep. 213-288.
- Mugan-Ustaömer, P.A., 1992, Tectonic setting and emplacement of the Bolu Granitoid Complex, W Pontides, N Turkey. Abstract, Keele.
- Okay, A.I., 1989, Alpine-Himalayan Blueschists. Ann. Ren. Earth Planet Sci., 17, 55-87.
- Önalın, M., 1981 İstanbul Ordovisiyen ve Siluriyen istifinin Çökeltme Ortamları. İÜ Yerbilimleri Bull., 2, 161-177.
- Özaltın, M., 1984, Yiğilca (Bolu) güneydoğusunun jeolojisi. Yüksek Lisans Tezi İTÜ Fen Bilimleri Enstiusü, 75 s, (unpublished).
- Pearce, J.A., 1980, Geochemical evidence for the genesis and eruptive setting of lavas from Tethyan ophiolites. A. Panayiotou (ed): Proceedings of the International Ophiolite Symposium, Cyprus, 1979, 261-272.
- , 1982, Trace element characteristics of lavas from destructive plate boundaries. Thorpe, R.S. (eds): Orogenic Andesites and Related Rocks, Wiley, London, 525-48.
- and Cann, J.R., 1973, Tectonic setting of basic volcanic rocks determined using trace element analysis. Earth and Platemary Science Letters, 19, 290-300.
- Pitcher, W.S., 1982, Granite type and tectonic environment. In K.J. Hsu (ed) Mountain Building Processes, 19-40.

- Robertson, A.H.F. ve Dixon, J.E., 1984, Introduction: aspects of the geological evolution of the Eastern Mediterranean. J.E. Dixon ve A.H.F. Robertson (eds): The Geological Evolution of the Eastern Mediterranean. Geological Society of London Special Publication 17, 1-74.
- Serdar, H.S. and Demir, O., 1983, Bolu-Mengen-Devrek dolayının jeolojisi ve petrol olanakları. TPAO Arama Grubu Rep. 1781.
- Seyitoğlu, G.G., 1984, Sünnice tepe (Bolu) güneyinin jeolojisi. ITU Fen Bilimleri Enstitüsü, Yüksek Lisans tezi, 30 s, (unpublished).
- Sun, S.S. and McDonough, W.F., 1980, Chemical and isotopic systematics of oceanic basalts: implications for mantle composition and processes. A.D. Saunders ve M.J. Norry (eds): Magmatism in the Ocean Basins. Geological Society of London Special Publication, 42, 313-347.
- Şengör, A.M.C. and Yılmaz, Y., 1981, Tethyan evolution of Turkey: a plate tectonic approach. *Tectonophysics*, 75, 181-241.
- , ——— and Sungurlu, p., 1984, Tectonics of the Mediterranean Cimmerides: nature and evolution of the western termination of Palaeo-Tethys. J.E. Dixon ve A.H.F. Robertson (eds): The Geological Evolution of the Eastern Mediterranean. Geological Society of London Special Publication, 17, 77-111.
- Tokel, S., 1995, Magmatic and geochemical evolution of the Pontide segment of the northern Tethys subduction system. A. Ertler, T. Ercan, E. Bingöl, S. Örcen (eds): Proceedings of the International Symposium on the Geology of the Black Sea Region, 163-170.
- Ustaömer, P.A.M., 1996, Bolu-Yedigöller Granitik Kayaçlarının Petrojenezi ve Metalojenezi. İÜ. Fen Bilimleri Enstitüsü, Doktora tezi Maden Yatakları-Jeokimya programı, 196 s., (unpublished).
- Ustaömer, P.A. and Kipman, E., 1997, Remnant of a pre-Early Ordovician Cadomian active margin in W Pontides, N Turkey. EUG 9 Meeting, Abstract France, p. 382.
- Ustaömer, T. and Robertson, A.H.F. 1993, Late Palaeozoic-Early Mesozoic marginal basins along the active southern continental margin of Eurasia: evidence from the Central Pontides (Turkey) and adjacent regions. *Geological journal*, 28, 3-4, 219-238.
- Wilkinson, J.F.G., 1982, The genesis of Mid-Ocean Ridge Basalts. *Earth Science Reviews*, 18, 1-57.
- Wilson, M., 1989, *Igneous Petrogenesis*. Unwin Hyman. 466s.
- Winchester, J.A. and Floyd, P.A., 1977, Geochemical discrimination of different magma series and their differentiation products using immobile elements. *Chemical Geology*, 20, 325- 343.
- Yazman, K.M.; Aydın, M.; Serdar, H.S.; Şahintürk, Ö; Demir, O. and Çokuğraş, R., 1984, Sakarya-Çamdağ, Akçakoca-Kaplandededağ, Ereğli Orhandağ, Bolu-Sünnicedağ ve Mengen yörelerinin jeolojisi. TJK 38. Bilimsel Teknik Kurultayı Bildiri özetleri.
- Yılmaz, O., 1980, Daday-Devrekani Masifinin kuzeydoğu kesiminin litostratigrafik birimleri ve tektoniği (Batı Pontidler, Türkiye). *Yerbilimleri*, 5-6, 101-135.

FACIES CHARACTERISTICS AND GEOGRAPHIC DISTRIBUTION OF RHODOLITHS AND MAERLS (RED ALGAE) IN SOUTHERN SHELF OF THE SEA OF MARMARA

Nevbahar ATABEY*

ABSTRACT.- Irregular crusts, rhodolith and maerl facies of crustose coralline red algae were determined in the recent sediments of southern shelf of Marmara sea. Rhodoliths are found in western off shore of the Kapıdağ peninsula at a depth of 27-52.5 m. They have a diameter of 1-8 cm and are composed of *Lithothamnion corallioides* Crouan and Crouan (1867). They exhibit different growth shapes depending on the environmental conditions and may be found as laminated, nodular, and ball shapes in high-energy, shallow (0-30 m) aerated waters. Maerls are also composed of *Lithothamnion corallioides*. In between Kapıdağ and Bozburun peninsulas and a depth of 27-52.5 m, they are observed as free, open branch, spheroidal, ellipsoidal, and discoidal shapes. *Phymatolithon calcareum* Adey and McKibbin (1970) is another species of red algae. It forms irregular crusts coiling around the rock fragments, pebbles, and corals. Rhodolith-bearing sandy and large pebbled, maerl-bearing sandy and coarse pebbled, and skeletal sandy facies were described in these rhodolith and maerl-bearing deposits. In addition to these facies, two other facies of bryozoa and serpulites were also determined. Crustose coralline red algae and their depositional environments in the southern shelf of Marmara sea indicate that Mediterranean conditions have prevailed in the sea of Marmara during the interglacial periods along Quaternary and even in the recent time.

Key words: Rhodolith, Maerl, Quaternary, southern Marmara sea.

INTRODUCTION

Rhodoliths are described as clay-originated nodules, nodular clay accumulations, clay associations, and clayey nodules. Bossellini and Ginsburg (1971) and Bates and Jackson (1983) used the term of "rhodolithes" as the accumulation formed by talus of encrusting red algae together with other preserved fauna assemblage. Adey and Macintyre (1973) evaluated the rhodoliths to be a grain enclosure type that shows a bedded internal structure depending on the growth of red algae and as the synonymous of oncoids. Their structure is shaped by intense layering around the nucleus, repetition of enclosing and algae growth (Prager and Ginsburg, 1989). It is also known that this term is used as "rhodoliths" in some studies (Barnes et al., 1970; Ginsburg and Bosellini, 1973). In addition, branches of dead or actual encrusting red algae may develop growth forms so called maerl on algal banks (Alexander, 1977; Bosence, 1977; Ginsburg and Bosellini, 1973). In this study, both terms are used as "rhodolith" and "maerl". Facies characteristics and geographic distribution of rhodoliths and maerls in the southern shelf of the sea of Marmara were investigated.

MATERIAL AND METHOD

This study was carried out in the frame of TÜBİTAK (Turkish Scientific and Technical Research Council) National Program on Sea Geology and Geophysics using the bottom samples collected by the MTA Sisnik-1 research vessel from the sea of Marmara. A total of 182 stations was sampled at depths between 20-134 m. Of these, 77 were examined and encrusting red algae was determined at 22 stations. Rhodoliths were at station no 160 and a depth of 35 m (Table 1 and Fig. 1). Spheroidal maerls were found station nos. 38, 53, 100, 102, 103, 106, 119, 120, and 144 at a depth of 29-50 m, discoidal maerls were at station nos. 52, 66, 67, 69, 82, 85, 144, 166, and 177 at a depth of 27-36.5 m, and ellipsoidal maerls were at station nos. 35, 99, and 144 at a depth of 29-51.5 m (Table 1 and Fig. 1). Those developed as irregular encrustings were determined at station nos. 35, 38, 39, 52, 53, and 55 (Table 1 and Fig. 1). Bryozoas were found at station no. 139 while serpulites at station no. 40 (Table 1 and Fig. 1). Description of encrusting red algae that display some growth forms, such as rhodolith, maerl, and irregular crusts were carried out with macro and micropa-

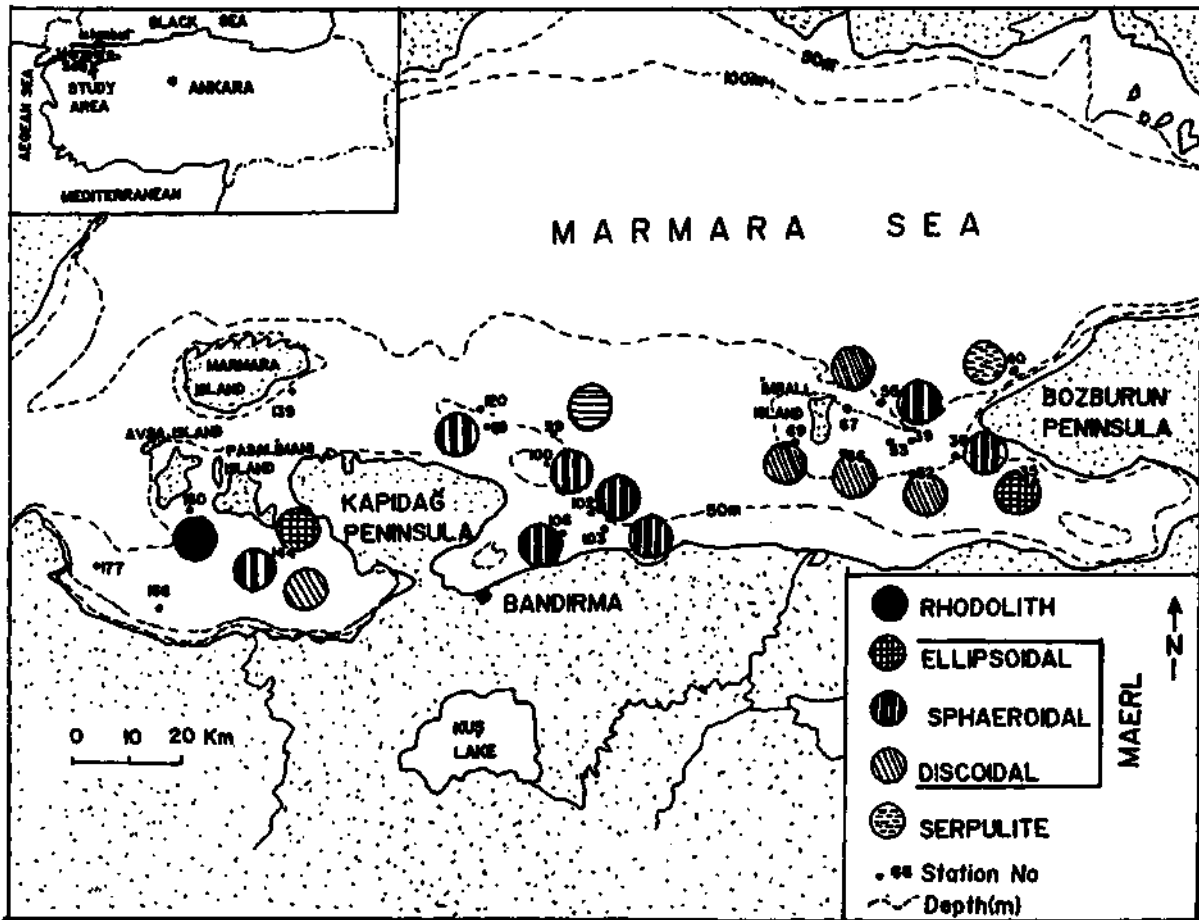


Fig. 1- Distribution of rhodoliths and maerls in southern sea of Marmara.

leontologic studies. For micropaleontologic studies, a number of 30 thin sections was prepared from two rhodolith (with a radius of 8 cm) and four maerl (with a radius of 3-5 cm) samples. Thin sections of rhodoliths and maerls were examined by an ocular microscope and photographed. In order to obtain thin sections, thallus of red algae comprising rhodoliths and maerls were frozen within the Canada balsam. Microtextural features of the samples were determined by scanning electron microscope (SEM). As a result of all these examinations, *Lithothamnion corallioides* and *Phymatolithon calcareum* species were determined. Shape (spheroidal, ellipsoidal, discoidal), size (1-8 cm in radius), and growth forms (rhodolith, maerl, crusts) of rhodolith, maerl, and irregular crusting were determined by macropaleontologic studies.

FORMATION OF RHODOLITHS AND MAERLS AND THEIR BIOLOGIC CHARACTERISTICS

Rhodoliths are characteristic in the sediments in southern shelf of southern part of the sea of Marmara at a depth of 27-52.7 m. *Lithothamnion corallioides* of encrusting red algae forms a laminated structure coiling around a nucleus consisting of small pebble, rock fragment, mollusk, and serpulite type grains under the effect of strong currents and waves (Prager and Ginsburg, 1989). This type of rhodoliths were met at south of the Avsa island at a depth of 35 m (Fig. 1 and Table 1). Internal parts of rhodoliths are generally destroyed by activities of several organisms, such as serpulite worms, some echinoid species, and endolithic blue-green algae (*Ostreobuim queckettii* Bomet and Flaha-

Table 1- Percent distribution of rhodolith, maerl, irregular encrustings, bryozoa, and serpulites.

Station No:	Depth (m)	Sphaeroidal	Discoidal	Ellipsoidal	Irregular Crusts	Rhodolith	Serpulit	Bryozoa
35	45.3			3	0.51			
38	52.7	7			0.8			
39	71.5				2			
40	50						75	
52	36.5	-	7		0.51			
53	50.4	0.62			4			
55	134				1.8			
66	30.5		8.24					
67	30.2		2.66					
69	27.2		18.24					
82	94.5		1					
85	90.5		1					
99	51.2			10.5				
100	45.5	5.6						
102	40	3.5						
103	43.7	9						
106	34.8	22.5						
119	41.9	9.52						
120	60.4	15						
139	50							75
144	29	16	10	8				
160	35					80		
166	28.1		1					
177	28.5		1					

ult, 1889; *Gomontia polyrhiza* (Lagerh) Bornet and Flahault, 1889; *Hyella caespitosa* Bornet and Flahault, 1889) and emptied. Using the epithallus providing its growth, rhodolith-forming algae hinders the destruction of these organisms (Plate I, figs. 1, 2, 3, 4). Epithallus contains the meristem which facilitates the growth of plant. This part of plant that is in contact with oxygen and light provides the organism to be alive. As a result of development of algae, laminated and ball-shaped forms are existed. In southern coasts of the sea of Marmara governed by warm climate conditions, rhodoliths with radius of 1-8 cm are commonly found (Plate-II, fig. 1). Strong currents and waves are the most important factors in formation of such structures. Open and freely branching rhodoliths so called maerl formed by branching species of *Lithothamnion corallioides* are found in southern sea of Marmara at a depth, of 27-52.5 m. Maerls display different shapes depending on water depth, light, temperature, and energy of the

water (Bosence, 1977). As a result of examinations, spheroidal, ellipsoidal, and discoidal maerls were described. Spheroidal maerls were found west of Erdek gulf at a depth of 29 m, east of Bandırma gulf at a depth of 34-52.5 m and around the Bozburun peninsula at a depth of 50 m (Table 1 and Fig. 1 and Plate II, fig 2A). In general, they are formed in shallow (0-30 m) and high-energy environments. Abundant light and heat cause the branches be thick and intense. In this way, they become resistant to strong current and waves. Ellipsoidal forms were determined at west of Erdek gulf at a depth of 29 m, west of Gemlik gulf at a depth of 45.5 m, and northeast of Kapıdağ peninsula at a depth of 51.5 m. Due to decreasing of light, temperature, and the energy of the environment, they are less intense and have thinner branches (Table 1 and Fig. 1 and Plate II, fig. 2B). Discoidal maerls are found at west of Erdek gulf at a depth of 29 m, north of Imralı island at a depth of 30.2 m and southwest and east of

Imrali island at a depth of 30 m (Table 1 and Fig. 1 and Plate II, fig. 2C). Open and thin-branched, discoidal maerls are developed in low-temperature, scarce of light, durable, and low-energy environments. In order to utilize from the light, branches are opened. Insufficiency of light and oxygen cause branches to open. However, since the environment is durable, there is no breaking and disintegration in the branches. They are more stable in comparison to intensely branching forms. Transportation is insignificant (Bosence, 1977). In addition, since spheroidal forms form more strong structures with thicker and intense branches to adapt to high-energy environments, they seem to be more durable in comparison to spheroidal forms. This type of structure gives rise to them transported in less amounts in the water. Broken branches of maerls are shown in (Plate II fig. 3). Transportation by deep currents causes branches of maerls to be broken.

FACIES CHARACTERISTICS

Three different facies types were differentiated in the sediments of encrusting red algae in southern sea of Marmara. These are rhodolith-bearing sandy and coarse-pebbled facies, maerl-bearing sandy and coarse-pebbled facies, and coarse-pebbled together with crust-bearing sandy facies.

Rhodolith-bearing sandy and coarse-pebbled facies

This facies generally covering rhodoliths of 1-8 cm is observed at south of Avşa island at a depth of 35 m (Plate II, fig 1). It is found together with the fauna assemblage containing mollusk-, bryozoa-, echinoid-, and serpulite-forming worm tubes, benthic foraminifera, and lesser amounts of planktonic foraminifera. The environment has abundant amount of light, free water circulation, and high-energy.

Maerl-bearing sandy and coarse-pebbled facies

Maerls cover a wide area on the sea bottom at a depth of 27-52.5 m. (Plate II, figs. 2A, B, C). Very coarse sand and pebble size material is dominant. Maerls

are distributed over the sand as groups or individually. Considering the shape of the maerl reflecting the energy of environment, 3 different zones distinguished. Those in spheroidal shapes (Plate II, figs. 2A-3a) are the products of high-energy, abundant-light, and shallow environments, those in ellipsoidal shapes are characteristic of intermediate-light (Plate II, figs. 2B, 3b) and low-energy environments, and finally the ones with discoidal shapes (Plate II, figs. 2C, 3c) reflect durable, low-energy environments with lesser amounts of light. Fauna assemblage consisting of mollusk- coral- and serpulite-forming worm tubes is rarely observed.

Crusts-bearing sandy facies

This facies comprising intense crust forms at a depth of 36.5-134 m (Fig. 2) is commonly found covering *Phymatolithon calcareum* of encrusting red algae, rock fragments, pebble; mollusk, and coral pieces as thin layers (>1 cm). It is accompanied by also other encrusting organisms, bryozoa, mollusk, and serpulite.

In addition to encrusting red algae facies, serpulite bioherms formed by vermes tubes are observed at west of Bozburun peninsula at a depth of 50 m. They are associated with broken, disintegrated mollusk shells (Plate III, fig. 1). Due to carving and hollowing activities of vermes, they are composed of sediments with micro structures and very fine-grained material (Fig. 2). Moreover, a facies with vast amount of bryozoa was detected at south of the Marmara island. In general, algae form oncolite or rhodolith surrounding the bryozoas (Plate III, figs. 2, 3).

GEOGRAPHIC DISTRIBUTION

Lithothamnion corallioides forming rhodoliths and maerls in southern shelf of the sea of Marmara and *Phymatolithon calcareum* developing as irregular crusts are the indicator of a cold, warm, subtropical climate belt. This type of occurrences are observed in Atlantic Ocean, along the northern coasts of Norway, and northeast Pacific (Leclaire, 1971 ; Bosellini and Ginsburg, 1971; Adey and Macintyre, 1973; Alexanderson, 1977; Basso, 1995).

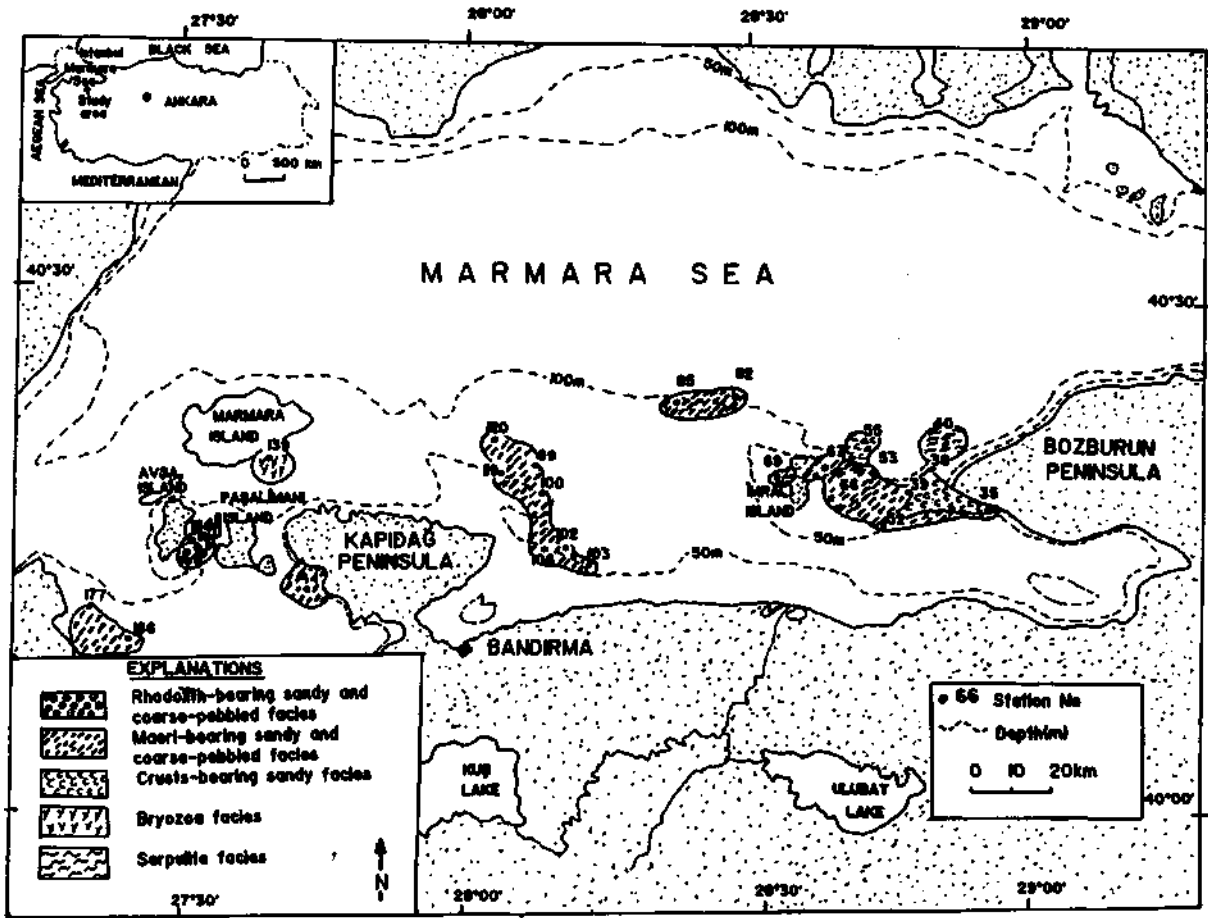


Fig. 2- Distribution of rhodolith, maerl, irregular encrustings, bryozoa, and serpulite facies.

DISCUSSION AND RESULTS

Marine transgressions originated from the Atlantic Ocean were effective in the sea of Marmara along the interglacial periods in Quaternary time. Following the late Walday (Wurm) glacial period at the beginning of Holocene (9-7 thousands years ago), waters of the Mediterranean sea reached to the sea of Marmara via Dardanelles and Bosphorus and then to the Black sea (Ross, 1978; Muratov et al., 1978; Tchepaliga, 1995). Thus, since Holocene the sea of Marmara has resembled the Mediterranean sea with respect to its salinity and fauna and flora content. This was confirmed by paleontologic studies conducted in southern shelf of the sea of Marmara. For example, *Emiliana huxleyi* of calcareous type of nanofossils (V. Toker pers. commu-

nication), *Turboella parva*, *Bittium spira*, *Ringicula conformis*, and *Ostrea edulis* of the mollusk species in Mediterranean origin (Islamoğlu and Tchepaliga, 1997), *Aurila onvexa*, *Bosquetina* sp., and *Loxoconca* sp. of theostracod species (Duru, 1996), *Globigerina bulloides*, *Globigerina quinqueloba*, *Globigerina bermudezi*, and *Orboulina universa* of the planktonic foraminiferas (V. Toker and A. Hakyemez: pers. communication) together with *Lithothamnion corallioides* and *Phymatolithon calcareum* species of encrusting red algae were determined in Pleistocene to Recent sediments. Encrusting red algae forming rhodoliths and maerls can stand for a temperature of 5-24°C and a salinity of 25-35‰. In general, rhodoliths and maerls developing at a depth of 50-150 m are observed at depths 40 to 50 m in the Atlantic Ocean which has a cold climate regime

(Vanney, 1965; Adey and McKibbin, 1970). Lithothamnion genus that is found at a depth of 50-150 m in the Mediterranean sea is generally observed in more deeper parts in the Atlantic Ocean (Milliman and Emery, 1971; Ladd, 1961; Bosellini and Ginsburg, 1971). This is due to the fact that as the depth increases temperature also is decreased, hence in turn providing development of Lithothamnion that favors cold waters. Although development of rhodoliths is controlled by biological, physical, and chemical factors, the primary factor is actions of water that are currents and waves (Adey and Macintyre, 1973). Their morphology depends on the energy regime of the environment in which they are formed. For example, laminated, ball-like coiled rhodoliths characterizing a high-energy environment and spheroidal, ellipsoidal, and discoidal maerls forming at different depths (Bosellini and Ginsburg, 1971; Bosence, 1977). Very strong waves inhibit the light and cause fragile rhodoliths to be broken and disintegrated. Similarly, weak waves and currents inhibits rhodolith development. Fine-grained sediments give rise to welding and burying of shells (Adey and Macintyre, 1973). As a result, it is thought that above mentioned physical, chemical, and biologic conditions necessary for the formation of rhodoliths have been prevailed since interglacial periods of the Quaternary time.

ACKNOWLEDGEMENTS

Author thanks to Dr. Eşref Atabey for his criticism on the manuscript.

Manuscript received January 27, 1997.

REFERENCES

- Adey, W. H. and McKibbin, D.; 1970, Studies on the maerl species *Phymatolithon calcareum* (Pallas) nov. comb. and *Lithothamnion corallioides* Crouan in the Ria de Jigo.: *Botanica Marina*, 13,100-106.
- Adey, W. H. and Macintyre, I. G.; 1973, Crustose Coralline Algae; A-Re evolution in the Geol. Soc. Amer. Bull.: 84, 883-904.
- Alexhderson, T., 1977, Carbonate cementation in recent corallin algal constructions fossil algae, *Recent Results and Developments*: Ed. by Erik Flügel, 262-269.
- Barnes, J.; Bellamy, D.J.; Jones, D.J.; Whitton, B.A.; Drew, E. and Lythogoe, J.; 1970, Sublittoral reef phenomena of Aldabra: *Nature*, 225, 268-269.
- Basso, D., 1995, Living calcareous algae by a Paleontological approach: The genus *Lithothamnion* Heydrich nom. cons. From the soft bottoms of the Tyrrhenian sea (Mediterranean): *Riv. ita. di Paleontologia e stratigrafia* 101, 349-366.
- Bates, R.L. and Jackson, J.A.; 1983, *Glossary of Geology*: Amer. Geol. Inst. Falls Church, Va, 749pp.
- Bornet, E. and Flauhalt, C.; 1889, Sur quelques plantes vivants dans le test calcaire de mollusques.: *Bull. Soc. Bot. France*, 36 CXIII et seq.
- Bosence, D., 1977, Ecological studies on two carbonate sediment-producing algae.: *Fossil algae recent results and developments*, 270-278.
- Bosellini, A. and Ginsburg, N.R.; 1971, Form and internal structure of recent algal nodules (Rhodolites) from Bermuda: *J. of Geology*, 79, 669-682.
- Crouan, P.L and Crouan, H.M.; 1867, *Florolide Finistere*, Brest.
- Duru, M., 1996, Ostracoda assemblage on the southern shelf of Marmara Sea, TÜBİTAK Ulusal Deniz Jeolojisi ve Jeofiziği programı: *Marmara Denizi Workshopu*.
- Ginsburg, R.N. and Bosellini, A.; 1973, Form and internal structure of recent algal nodules (Rhodolites) from Bermuda: a reply: *J. of Geology*, 81, 239-241 .
- İslamoğlu.Y. and Tchepaliga, LA.; 1997, Marmara Denizi Güney şelfinin Neoeuxinian- Holosen Mollusk topluluğu ve Paleoekolojik özelliği *Marmara Denizi Araştırmaları: Workshop III*, 88-92.

- Ladd, H. S., 1961, Reef building: Science, 134, 703-715.
- Leclaire, L, 1971, Aspects of Late Quaternary sedimentation on the Algerian precontinent and in the adjacent. Algiers-Balearic Basin. The Mediterranean Sea: 561-582.
- Milliman, J. D. and Emery, K.O.; 1971, Sea levels during the past 35, 000 years: Science, 162, 1121-1123.
- Muratov, M.V.; Neprochnov, Y.P.; Ross, D.A. and Trimonis, E.S.; 1978, Basic Features of the Black Sea Late Cenozoic history based on the results of deep sea drilling, Leg 42 B. Initial Rep. of the deep sea drilling Project: XLII, 2,1141-1148.
- Prager, E.J. and Ginsburg, R.N.,1989, Carbonate nodule growth on Florida's outer shelf and its implications for fossil interpretations: Palaios, 4:310-317.
- Ross, D.A., 1978, Initial Rep. Deep Sea Drill. Proj. E.T. Degens and D.A.Ross. (Ed.): 1149-1178.
- Tchepaliga, A.L., 1995, Pliyo-Pleyistosen Karadeniz havzaları ve bunların Akdeniz ile ilişkileri, İzmit Körfezi'nin Kuvaterner istifi, Ed.: Engin Meriç.
- Vanney, R., 1965, Etude sedimentologique du mor Bras Bretagne: Marine Geology, 3,195-222.

PLATES

PLATE-I

- Fig. 1- Vertical section of *Lithothamnion corallioides*. (C) Conceptacle (Pe), perithallus. x 63 Ocular microscope.
- Fig. 2- Oblique section of *Lithothamnion corallioides*. (C) multi pores, sexual conceptacles. x 63 Ocular microscope.
- Fig. 3 Perithallus and epithallus in a longitudinal section, x 63 Ocular microscope.
- Fig 1 Scanning electron microscope (SEM) image of opithallus cells Spaces among the cells are filled with early diagenetic high magnesian calcite (ç) Black parts (b) non-tilled areas.

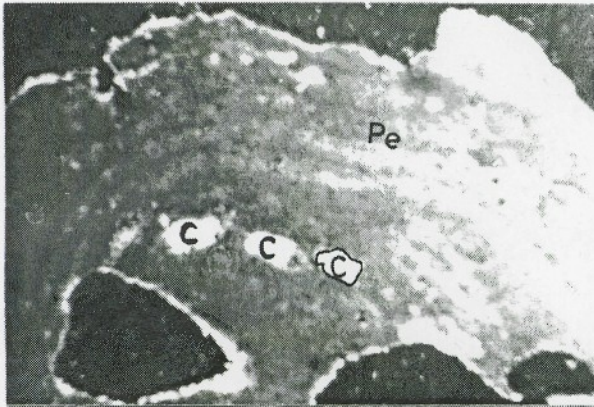


Fig. 1

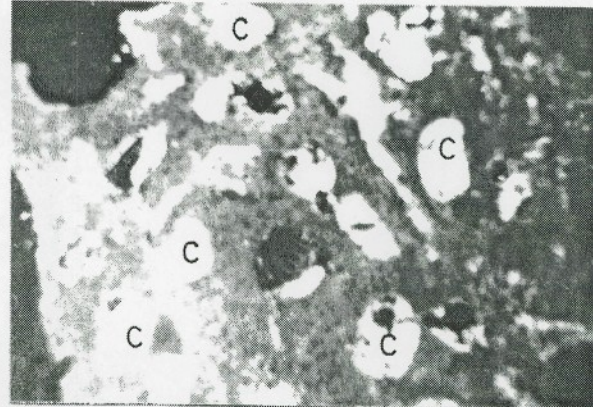


Fig. 2



Fig.3

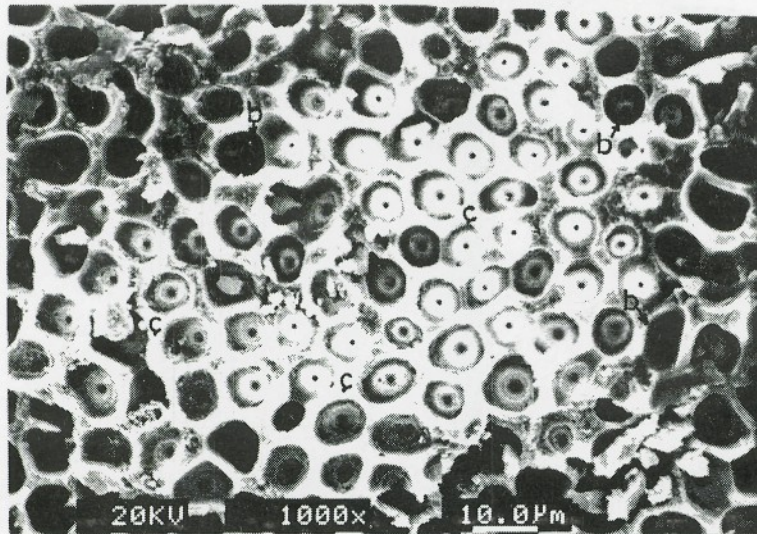


Fig. 4

PLATE-II

- Fig. 1- Rhodoliths. Nodules with a radius of 1-8 cm at south of Avşa island. Station no. Southern Marmara 95/07-160.
- Fig. 2- Maerls. A-Spheroidal, B- Ellipsoidal, C- Discoidal forms. Station no. Southern Marmara 95/07-144.
- Fig. 3- Broken tallus of *Lithothamnion corallioides*. a- Spheroidal, b- Ellipsoidal, c- Discoidal maerls.

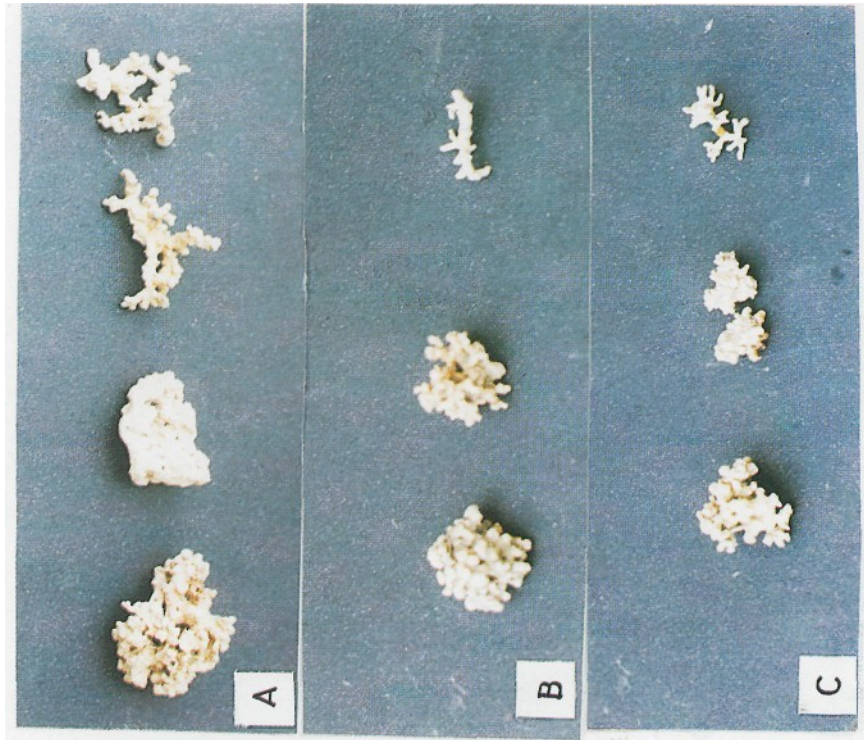


Fig. 2



Fig. 1



Fig. 3

PLATE-III

Fig. 1 - Serpulites formed by vermes tubes.

Fig. 2- Bryozoa.

Fig. 3- Lithothamnion (L.c.) and Bryozoa (B).



Fig. 1

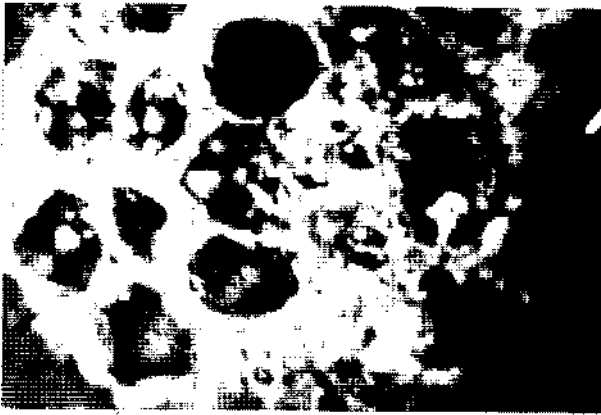


Fig. 2

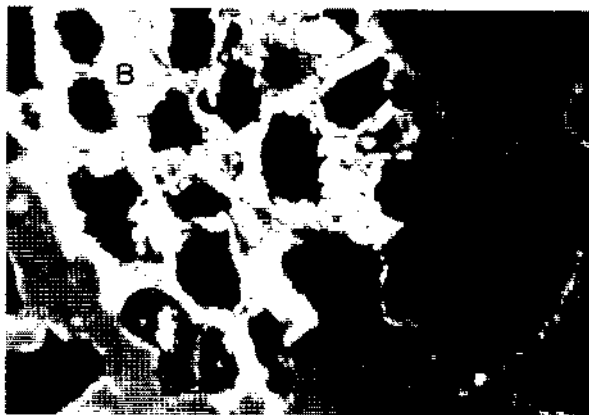


Fig. 3

REVISION ON THE SPECIES OF PSEUDOLACAZINA CAUS 1979 (FORAMINIFERIDA) FROM THE DIFFERENT LOCALITIES OF TURKEY

Ercüment SİREL*

ABSTRACT.- The megalospheric and microspheric specimens of the one fabularid species were first described and figured as *Fabularia alpani* Sirel and *Lacazina blumenthali* Reichel and Sigal respectively by Sirel from the Ilerdian exotic limestone blocks within the ophiolitic melange near the village of Pemavut, S of Kars, Eastern Turkey. This large fabularid species is reexamined on the new material from the foregoing locality. In the result of this study, megalospheric specimens *F.alpani* and microspheric specimens *L. blumenthali* were renamed as a species of *Pseudolacazina Caus* "*Pseudolacazina alpani* (Sirel)" by the following generic features: all the chambers of the megalospheric specimens are arranged in biloculine mode; microspheric specimens start growth with quinqueloculine chambers cycles reduced biloculine and monoloculine; chambers subdivided by continuous, longitudinal partitions (as septula) in both generations. On the other hand, the Anatolian Thanetian species *Pseudolacazina oeztemueri* (Sirel) and the Yugoslavian species *Pseudolacazina donatae* (Drobne) are described and figured. The specific differences of *P. alpani*, *P. oeztemueri* and *P. donatae* are discussed with the other species of *Pseudolacazina*.

INTRODUCTION

Three species *P.alpani*, *P. oeztemueri* and *P. donatae* which have been occurred at the different localities of Turkey (Fig.1) are described with the new illustrations and their specific features are discussed with the other species of *Pseudolacazina*. In 1972, the megalospheric and microspheric forms of large, ovoid trematophorid foraminifera were described and figured as *F.alpani* and *L.blumenthali* respectively by (Sirel, 1972, p. 280-283, Plate II, fig. 1-6; Plate VI, fig. 1-4;- Plate I, fig. 1-3) from the Upper Paleocene (Ilerdian) limestone blocks within the ophiolitic melange near the village of Pernavut, S of Kars (Fig.1). This dimorphic fabularid species is reexamined on the new limestone samples from this locality; as a result of this investigation, the megalospheric *F.alpani* and microspheric *L.blumenthali* were renamed as the one species of *Pseudolacazina* as *P.alpani* (Sirel) by the following generic features: the megalospheric specimens have biloculine chambers throughout ontogeny; microspheric forms start growth with pleuroloculine (probably quinqueloculine) chambers cycles reduce biloculine and morroloculine cycles in the adult; chambers subdivided by continuous longitudinal partitions (as septula) in the both generations. *P.alpani* is associated in the Ilerdian limestone blocks of the Kars region with *Miscellanea*

miscella, (D'Archiac and Haime), *Alveolina minervensis* Hottinger, *Alveolina avellana* Hottinger, *Alveolina (Glomalveolina) lepidula* Schwager, *Alveolina (Glomalveolina) minutula* Reichel and Renz, *Alveolina (Glomalveolina) karsica* Sirel, *Alveolina (Glomalveolina) sp. 1, 2*, (newspecies), *Dictyoconus (Dictyoconus) cf. indicus* Davies, *Sakesaria cf. dukhani* Smout, *Kathina (Smoutina ?) subsphaehca* Sirel, *Ranikothaliasp.*, *Kathina sp.* and *Thomasella labyrinthica* (Grimsdale). The trematophorid species and its subspecies from the Thanetian of Yugoslavia were described and figured as *Fabularia donatae* and *Fabularia donatae libumica* by Drobne (1974). As reported by Caus (1979) *F.donatae* is a species of *Pseudolacazina*. This smallest species of *Pseudolacazina* is found together with *P. oeztemueri* at the various localities, particularly at the Central Turkey (Fig. 1). These two species were found below the algal limestone bed with *Alveolina (Glomalveolina) primaeva* (Reichel) only at the Haymana area, Central Turkey. Unfortunately, so far, we did not find *P. oeztemueri* and *P. donatae* together with *A. (Glomalv.) primaeva* in Turkey, although *P. donatae* had been occurred with *A. (Glomalv.) primaeva* in Yugoslavia (Drobne, 1974, p. 45, Plate XIV, fig. 2).

All the thin sections of the *Pseudolacazina*'s species described and figured in this paper are deposited in

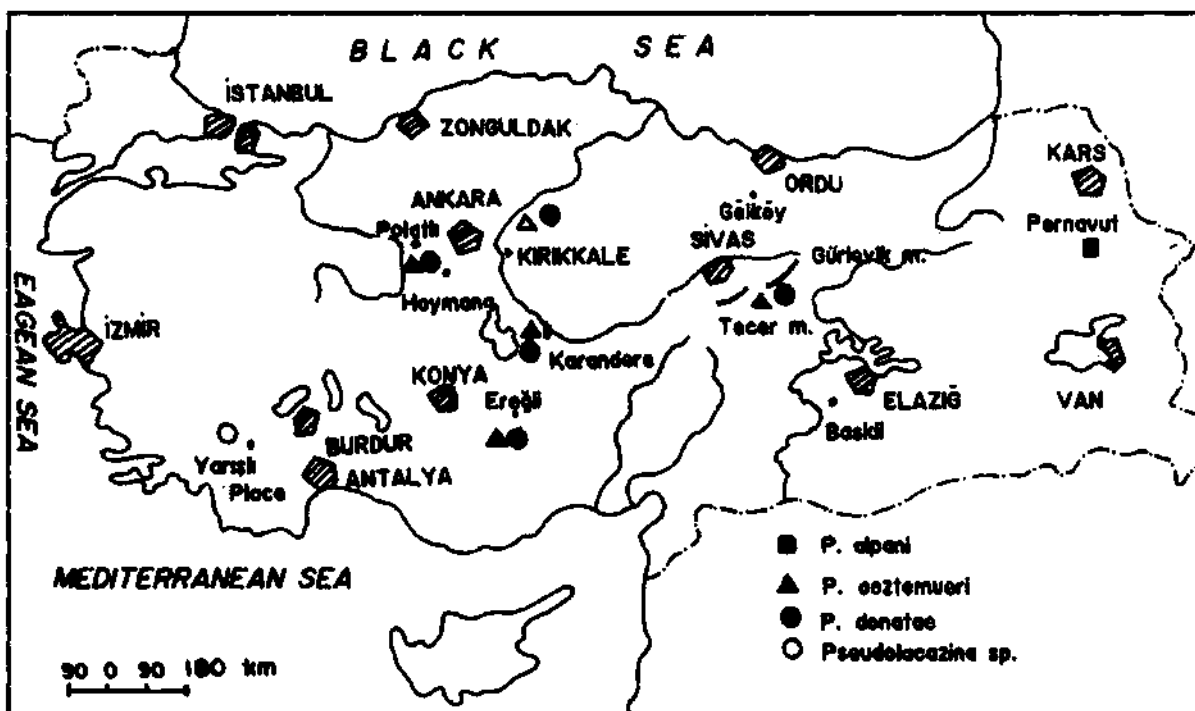


Fig. 1- Geographic distribution of the species of *Pseudolacazina* Caus in Turkey.

the collection of Ankara University, faculty of Science, Geological Engineering, Ankara, Turkey, under the numbers shown in plates 1-5.

SYSTEMATIC DESCRIPTION

Family : Fabulariidae Ehrenberg , 1839
 Genus : *Pseudolacazina* Caus, 1979
 Type species : *Pseudolacazina hottingeri* Caus, 1979

Diagnosis of the genus

Subspheric to ovate, dimorphic, trematophorid fabulariids of large size; megalospheric specimens biloculine throughout ontogeny (Plate I, fig. 4-8; Plate II, fig. 3, 5, 6, 9,10; Plate III, fig. 3, 8,10,11; Plate IV, fig. 3, 4, 6-8; Plate V, fig. 4, 8, 13, 14), in microspheric specimens with numerous whorls: early chambers in quinqueloculine arrangement (Plate IV, fig. 9; Plate V, fig. 1, 3, 7, 9, 11,15) later biloculine (Plate III, fig. 1, 4,

7; Plate V, fig. 1, 3, 9,10,12,16) and finally with wholly embracing chambers monoloculine (Plate I, fig. 1; Plate III, fig. 1, 4, 6, 7; Plate IV, fig. 5, 9; Plate V, fig. 1, 3, 7, 9-12,15,16), adult chambers (biloculine and monoloculine) subdivided by numerous, continuous longitudinal partitions (as septula) that form continuous chamberlets spiralling around the shell, wall calcareous, porcellaneous, basal layer well developed; annular trematophoric aperture with pillars (Plate I, fig. 2, 8; Plate II, fig. 2, 8, 10; Plate IV, fig. 1,2; Plate V, fig. 2, 17) alternating crowning the upper or lower flattened surface of the shell; Paleocene- Eocene.

Pseudolacazina ooztemueri (Sirel) 1981
 (Plate III, fig. 1-7; Plate IV, fig. 1-9; Plate V, fig. 16,17)

1981 *Lacazina dztemuri* Sirel, p. 82, Plate IV, fig.1-6; Plate V, fig. 1-6.

1986 *Pseudolacazina ooztemueri* (Sirel), Sirel, p. 125, Plate I, fig. 1-6; Plate II, fig.1-6, Plate III, fig. PA, PB.

1988 *Pseudolacazina oeztemueri* (Sirel), Drobne, fig. 9/10,17.

DESCRIPTION

Microspheric specimens ovoid, large *Pseudolacazina* with a striking dimorphism, equatorial diameter varies between 2.7 mm and 4.9 mm, axial diameter reaches 3.4 mm, elongation (in the direction of the apertural axis) reaching an index 1.4 but the main value is around 1.3; the microsphere is small, spherical (0.022-0.025 mm in diameter). The first three undivided cycles which follow the microsphere are arranged in quinqueloculine (Sirel, 1986, Plate I, fig. 2, 6). Their diameter vary 0.248 mm to 0.266; they are followed by 4-5 divided bilocular cycles with a diameter 0.719-0.892 mm, all the later chambers are monoloculine.

Megalospheric specimens ovoid to subspheric, the equatorial diameter 1.2-1.8 mm, axial diameter 1.29-1.35 mm, megalosphere ovate to subspheric with bottle-neck (goulot) and large when compare to the size of the shell, its diameter varies between 0.235 mm and 0.310 mm; chambers arrangement biloculine throughout ontogeny.

Differential diagnosis

P. donatae is distinguished from *P. oeztemueri* by small size by much lower chambers producing very narrow chamber lumina, therefore *P. donatae* has 11 divided biloculine and monoloculine chambers in an axial diameter of the shell of 2 mm (Drobne, 1974, Plate IV, fig. 21; Plate IX, fig. 1) and in this paper (Plate V, fig. 1, 9, 12), whereas, *P. oeztemueri* has 11 divided chambers in an axial diameter of the shell of 3.6 mm (Plate III, fig. 4). Furthermore, the megalospheric specimens of *P. donatae* has much lower chambers when compare to the megalospheric specimens of *P. oeztemueri*. Type species *P. hottingeri* differs from *P. oeztemueri* by smaller size, by much lower chambers and by under developed quinqueloculine and biloculine stages, llerdian species *P. alpani* is easily distinguished from *P. oeztemueri* by its larger size and megalosphere, by higher chambers with bigger chamberlets, particularly in the megalospheric specimens.

Stratigraphic and geographic distribution

P. oeztemueri is associated at the type locality, Til-kitepe and Kocaağildere, approximately 2 km southwest of Karandere village, NW of Aksaray, Central Turkey, Sirel (1981) with *Bolkarina aksarayi* Sirel, *P. donatae*, *Idalina sinjarica* Grimsdale, keramospherid specimens, Miliolidae and Algae of Thanetian age.

It occurs in Thanetian limestone of Mahmutlar village, NW of Kırkkale, Central Turkey. It is associated at this locality with *B. aksarayi*, *Miscellanea ? primitiva*, Rahaghi, *Miscellanea ? globularis* Rahaghi, keramospherid specimens, Miliolidae and Algae.

It has been found in the Çaldağ section (Sirel, 1995, fig. 2 and Sirel, 1999, fig. 2); W of Haymana, Central Turkey (Fig. 1). It is accompanied by *B. aksarayi*, *Laffitteina mengaudi* (Astre), *P. donatae*, *M. ? primitiva*, *M. ? globularis*, *I. sinjarica*, keramospherid specimens, Miliolidae and Algae.

It is found in the Thanetian limestone of Sirakayalar gediği, approximately, 25 km SE of Eregli, SE of Konya, Central Turkey, with *B. aksarayi*, *P. donatae*, *M. ? primitiva*, *Idalina* sp., Miliolidae and Algae.

It occurs in the Thanetian limestone with *B. aksarayi*, *P. donatae*, *Miscellanea* sp., Miliolidae and Algae at the Tecer and Gürlevik mountains, S of Sivas, Central Turkey.

Pseudolacazina donatae (Drobne), 1974 (Plate V, fig. 1-15)

- 1974 *Fabularia donatae* Drobne, p. 167, Plate II, fig. 1-6; Plate II, fig. 1-3; Plate IV, fig. 1-9, 17-21; Plate IX, fig. 1.
- 1979 *Pseudolacazina donatae* (Drobne), Caus, p. 36.
- 1981 *Fabularia donatae* Drobne, Sirel, p. 84, Plate V, fig. 8-10.
- 1986 *Pseudolacazina donatae* (Drobne), Sirel, p. 125.
- 1988 *Pseudolacazina donatae* (Drobne), Drobne, p. 658, fig 9/7-9.

DESCRIPTION

Ovoid, small *Pseudolacazina* with distinct dimorphism, elongation reaching an index of 1.29 in microspheric, 1.09 in megalospheric specimens; maximum length 2.2 mm and 1.5 mm, maximum breadth 1.9 mm and 1.1 mm in the microspheric and megalospheric specimens respectively.

Megalospheric specimens have large megalosphere (0.200-0.250 mm in diameter) followed by bottle-neck with thin wall; chambers arrangement bilocular throughout ontogeny, it has 6 biloculine chambers in an axial diameter of the shell of 1.15 mm; low biloculine chambers subdivided by longitudinal partitions that form continuous very small chamberlets; trematophore simple, supported by a single central pillar (Plate V, fig. 4).

Microspheric specimens are more than twice the size of the megalospheric specimens, all the chambers are strikingly low when compare to the microspheric specimens of *P. oeztemueri*, quinqueloculine stage reaches 0.200 mm in diameter, biloculine stage consists usually of four cycles, the following monoloculine stage composed of about nine concentric chambers of low height; trematophore simple, supported by a single, central pillars (Plate V, fig. 2, 5, 6).

Its stratigraphic level and the geographic distribution are given in the chapter of the distribution of *P. oeztemueri*.

Pseudolacazina alpani (Sirel), 1972

(Plate I, fig. 1-8; Plate II, fig. 1-10; Plate III, fig. 8-11)

1972 *Fabularia alpani* Sirel, p. 280, Plate II, fig. 1-6.

1974 *Fabularia alpani* Sirel, Drobne, p. 45.

1988 *Fabularia alpani* Sirel, Drobne, p. 656, fig. 8/3.

Emended diagnosis

Ovoid, large *Pseudolacazina* with a striking dimorphism, elongation reaching an index of 1.3 in megalospheric, 1.5 in microspheric specimens; maximum length 3.7 mm and 5.3 mm; maximum breadth 3 mm and 4.2

mm in the megalospheric and microspheric specimens respectively.

Megalospheric specimens with a large, spherical megalosphere of 0.5 mm in average diameter, followed by distinct bottle-neck with thin wall; chamber arrangement bilocular throughout ontogeny (Plate I, fig. 4-6; Plate II, fig. 3, 5, 6, 9); all the chambers are strikingly higher when compare to the megalospheric specimens of *P. oeztemueri* and *P. donatae*; it has 5 bilocular chambers in an axial diameter of the holotype of this species of 2.6 mm, biloculine chambers subdivided by longitudinal partitions that form continuous chamberlets; Chamberlets generally low elliptical in shape and their height is more smaller than their width; ovoid elongated forms with trematophore, supported by at least one, central pillars (Plate I, fig. 5, 8; Plate II, fig. 6, 10).

Microspheric specimens are very rare, microspherere can not be observed, early chambers pleuroloculine (quinqueloculine ?), later biloculine and finally monoloculine; chambers are strikingly higher when compare to the microspheric specimens of *P. oeztemueri* and *P. donatae*.

REMARKS

The megalospheric and the microspheric specimens of the one fabularid species were described and figured as *Fabularia alpani* (Sirel, 1972, p. 280, Plate II, fig. 1-6) and *Lacazina blumenthali* respectively (Sirel, 1972, p. 282, Plate VI, fig. 1-4; Plate VII, fig. 1-3) from the Upper Paleocene (Ilerdian) of the Pernavut village, S of Kars (Fig. 1). This ovoid, large, dimorphic fabularid species is reexamined on the new material collected from the type locality. As a result of this study, megalospheric *F. alpani* and microspheric *L. blumenthaliv/ere* renamed as a species of *Pseudolacazina* (*P. alpani*) by the presence of the following generic features: all the chambers of the megalospheric *P. alpani* are arranged in biloculine mode (Plate I, fig. 4-6, 8; Plate II, fig. 3, 5, 6, 9-10); microspheric *P. alpani* start growth with pleuroloculine (quinqueloculine ?) chamber cycles (Sirel, 1972, Plate VII, fig. 1-2) reduced biloculine (Plate I, fig. 1; Plate II, fig. 2), (Sirel, 1972, Plate VII, fig. 1, 2) and monoloculine cycles in the adult (Plate I, fig. 1,2); adult chambers (biloculine

and monoloculine) subdivided by continuous, longitudinal partitions (as septula) in both generations (Plate I, fig. 2; Plate II, fig. 1, 2, 7, 8). Ilerdian species *P.alpani* differs from the Eocene species *P.hottingeri*, and the Thanetian species *P.oeztemueri*, *P. donatae* in possessing large size and large meglosphere.

DISTRIBUTION

Strigraphic, geographic distribution and foraminiferal assemblage of *P. alpani* are given in the introduction chapter.

DISCUSSION AND CONCLUSION

As mentioned by Hottinger et al., (1989, p. 103) there is a general consensus to define the genera of Mesozoic to Recent larger complex foraminifera by the presence or absence of structural elements such as septula, pillars, pre- and post-canals etc. While the species are characterized by proportions and/or absolute sizes of the shell and its components. Chamber arrangement is neither a structural element nor a size character of the shell. However, many authors have to apply the chamber arrangement in the definition of the larger complex foraminifera, particularly larger trematophorid genera (Caus, 1979; Drobne, 1984; Loeblich and Tappan, 1964, 1987 and Hottinger et al., 1989), in spite of the fact that the chamber arrangement is unsuitable to this general consensus. The Tertiary genus *Pseudolacazina* has its chambers with chamberlets and the numerous opening on a trematophore in common with the calcareous, porcellaneous foraminiferal genera *Fabularia* Defrance, *Lacazina* Munier-Chalmas and *Periloculina* Munier-Chalmas and Schlumberger. In that case whether the presence or absence of the chamber arrangement is being important in the definition of the trematophoric, complex foraminiferal genera, on condition that we use the chamber arrangement combined with the particular characteristic of the chamber subdivision (partitions and/or septula, pillars and their position from one chamber to the next) of the both generations together. The Thanetian species, *P.oeztemueri*, *P. donatae*, and Ilerdian species *P.alpani* which have been found at the different localities of Turkey (Fig.1) showing the following same diagnostic generic features with the Eocene species *P. hottingeri*

(type species): the chambers arrangement (biloculine in megalospheric forms, quinqueloculine, later biloculine and finally monoloculine chambers cycles in microspheric forms) and by continuous, longitudinal partitions in both generations.

Pillared species *Pseudolacazina loeblichii* Hottinger and Drobne and Caus and *Pseudolacazina contabrica* Hottinger and Drobne and Caus were described and figured from the Santonian of Spain by Hottinger et al., (1989). *P.loeblichii* and *P.contabrica* have their chamber arrangement (biloculine throughout ontogeny in megalospheric forms, pleuroloculine, biloculine and monoloculine in microspheric forms) in both generations in common with all Tertiary representatives of *Pseudolacazina*, but the former two Upper Cretaceous species differ from the Tertiary species by having longitudinal, discontinuous pillars (Hottinger et al., 1989, Plate 24, fig. 2, 3; Plate 26, fig. 3) instead of the continuous longitudinal partitions. These two species have a tendency to the new genus of Fabulariidae by possessing chambers arrangement combined with the diagnostic structure discontinuous, longitudinal pillars.

Manuscript received January 28, 1997.

REFERENCES

- Caus, E., 1979, *Fabularia roselli* n.sp., et *Pseudolacazina* n.gen., foraminifères de l'Eocene moyen du Nord-Est de l'Espagne: *Geobios*, 12/1, 29-45.
- Drobne, K., 1974, Les grandes miliolides des couches paléogènes de la Yougoslavie du nord-ouest: *Razprave 4.razr. SAZU* 17, 125-184.
- , 1984, *Periloculina slovenica*, B form, from the Paleogene of Majeвица MT. (Yugoslavia) and the new family Fabulariidae. *Razprave 4.razr. SAZU*, 26, 159-176.
- , 1988, Elements structuraux et répartition stratigraphique des grands miliolides de la famille Fabulariidae. *Rev. Paleobiologie*, vol spec. 2, Benthos, 86, 643-661.

- Hottinger, L.; Drobne, K. and Caus, E., 1989, Late Cretaceous, larger, complex miliolides (Foraminifera) endemic in the Pyrenean faunal province. *Facies*, 21,99-134.
- Loeblich, A. and Tappan, H., 1964, Sarkodina, chiefly Thecamoebians" and Foraminiferida. In Moore, R.C. (ed.). *Treatise on invertebrate paleontology*, part C, Protista 2, 1-653, Lawrence Kansas (Kansas Univ. Press).
- and ———, 1987, Foraminiferal genera and their classification. Vol. I, 1-970; vol. II, 212 p, 847 Pl. New York (Van nostrand Reinhold).
- Sirel, E., 1972, Systematic study of new species of the genera *Fabularia* and *Kathina* from Paleocene: *Bull. Geol. Soc. Turkey*, XV, 2, 277- 294.
- Sirel, E., -1981, *Bolkarina*, new genus (Foraminiferida) and some associated species from the Thanetian limestone (Central Turkey): *Eclogae geol. Helv.*, 74/1,75-95.
- , 1986, *Lacazina öztemuri* Sirel 1981 renamed as *Pseudolacazina öztemuri* (Sirel) from the Thanetian limestone (Central Turkey): *Bull. Min. Research Expl.*, vol 105/106, 123-126.
- , 1995, Description and geographic, stratigraphic distribution of the species of *Laffitteina* Marie from the Maastrichtian and Paleocene of Turkey. *Rev. Paleobiologie*, 15, (1), 9-35.
- , 1999, On four new genera (*Haymanella*, *Kayseriella*, *Elaziğrella*, and *Orduella*) and a new species of *Hottingerina* from the Paleocene of Turkey. *Micropaleontology*, 45, 2, 113-137.

PLATES

PLATE-I

Pseudolacazina alpani (Sirel)
(Early Ilerdian, Pernavut village, S of Kars, Eastern Turkey)
All figs, x 20

Figs. 1-2 Microspheric forms.

Figs. 3-8 Megalospheric forms.

Fig. 1- Almost centered section perpendicular to apertural axis, 5/30.

Fig. 2- Oblique longitudinal section, 5/30.

Fig. 3- Oblique longitudinal section, 5/41/3.

Fig. 4- Centered section perpendicular to apertural axis, note large megalosphere and biloculine chambers throughout ontogeny, 5/26/4.

Fig. 5- Slightly oblique longitudinal section in apertural axis, note weakly developed central trematophorean pillars in the apertural foramina, 5/24/1.

Fig. 6- Centered section perpendicular to apertural axis, holotype of *Fabularia alpani* (Sirel, 1972, Plate-2, fig. 1), 5/31/1.

Fig. 7- Almost longitudinal section in apertural axis, 5/30.

Fig. 8- Almost longitudinal section in apertural axis showing trematophorean pillars in the apertural foramina, 5/30.

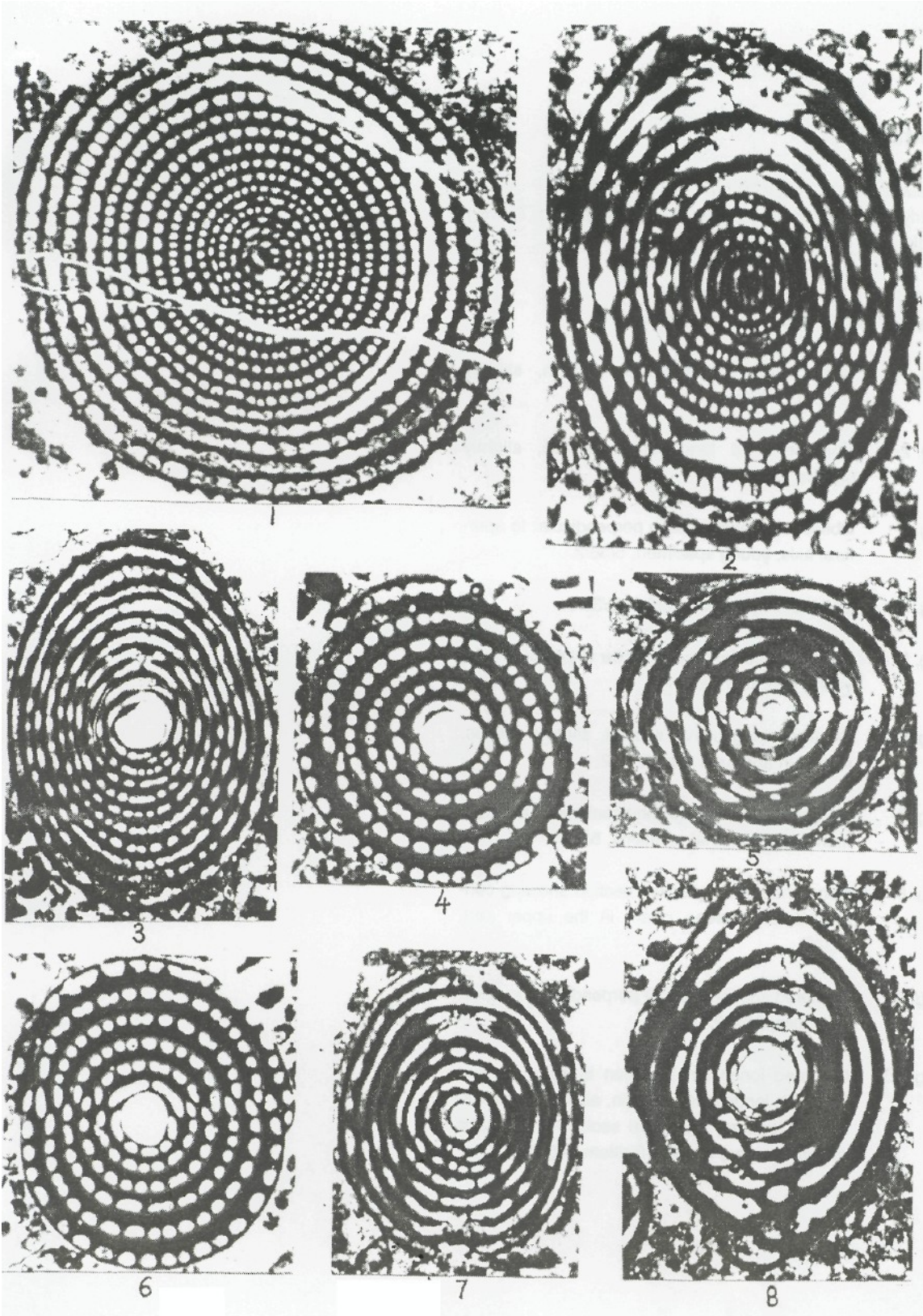


PLATE-II

Pseudolacazina alpani (Sirel)
(Early Ilerdian, Pernavut village, S of Kars, Eastern Turkey)
All fig. x 20 except fig. 2x10.

Figs. 1, 2, 8 Microspheric forms.

Figs. 3-7, 9, 10 Megalospheric forms.

Fig. 1- Non centered longitudinal section, slightly oblique, 5/36/5.

Fig. 2- Non centered longitudinal section, slightly oblique, 5/30.

Fig. 3- Oblique centered section perpendicular to apertural axis, young specimen, 5/36/2.

Fig. 4- Oblique longitudinal section, 5/38/3.

Fig. 5- Centered section perpendicular to apertural axis, young specimen, 5/41/4.

Fig. 6- Centered longitudinal section, slightly oblique, almost in apertural axis, 5/37/2.

Fig. 7- Tangential section, showing continuous arrangement of longitudinal partitions, 5/30.

Fig. 8- Non centered longitudinal section showing central trematophorean pillars in the upper part, 5/37/2.

Fig. 9- Centered section, almost perpendicular to apertural axis, 5/38/2.

Fig. 10- Centered longitudinal section in apertural axis (top left), longitudinal section, almost in apertural axis (bottom) and axial section of *Alveolina* (*Glomalveolina*) *lepidula* (bottom left), 5/41/1.

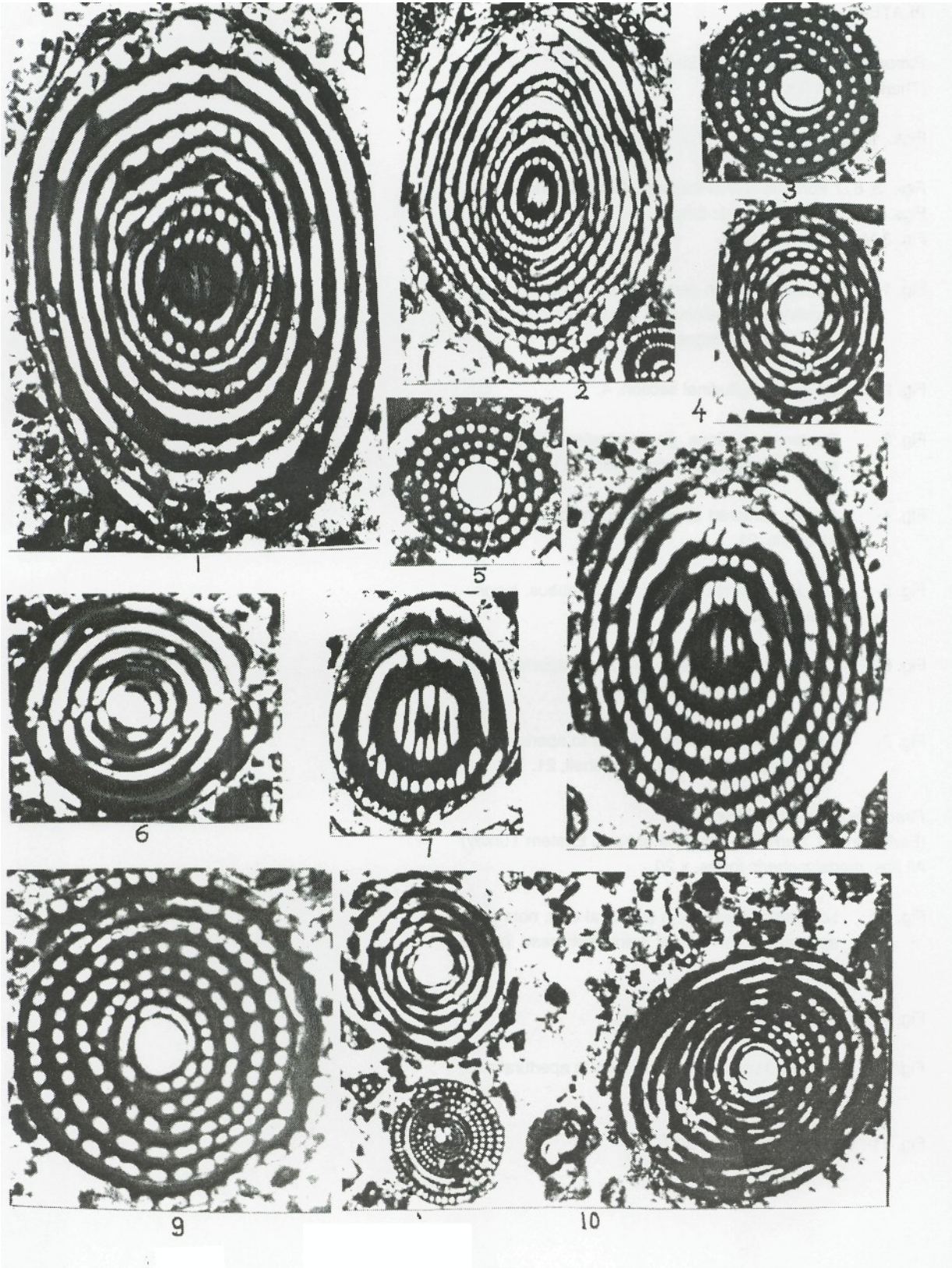


PLATE-III

Pseudolacazina oeztemueri (Sirel)

(Thanetian, all figs, x 20)

Figs. 1, 2, 4, 5 from the NW of Kırkkale, E of Ankara,
Central Turkey

Figs. 3, 6, 7 from the NW of Aksaray, Central Turkey.

Figs. 1, 2, 4-7 Microspheric forms.

Fig. 3 Megalospheric form.

Fig. 1 - Centered section perpendicular to apertural axis showing quinqueloculine, biloculine and monoloculine growth stages, 21.

Fig. 2- Oblique longitudinal section, 4.

Fig. 3- Centered sections perpendicular to apertural axis and tangential section (top). (Y).

Fig. 4- Almost centered section perpendicular to apertural axis, 21.

Fig. 5- Tangential section showing continuous, longitudinal partitions, 46.

Fig. 6- Centered section perpendicular to apertural axis showing growth stages, Ak-18.

Fig. 7- Centered section perpendicular to apertural axis showing growth stages of the shell, 21.

Pseudolacazina alpani (Sirel)

(Early Ilerdian, Pernavut village, S of Kars, Eastern Turkey)

All figs, megalospheric forms, x 20.

Fig. 8- Longitudinal section in apertural axis, note early appearance of central trematophorean pillars, 5/58/1.

Fig. 9- Oblique section, 5/41/2.

Fig. 10- Centered section perpendicular to apertural axis, 5/38/8.

Fig. 11- Oblique sections, 5/37/1.

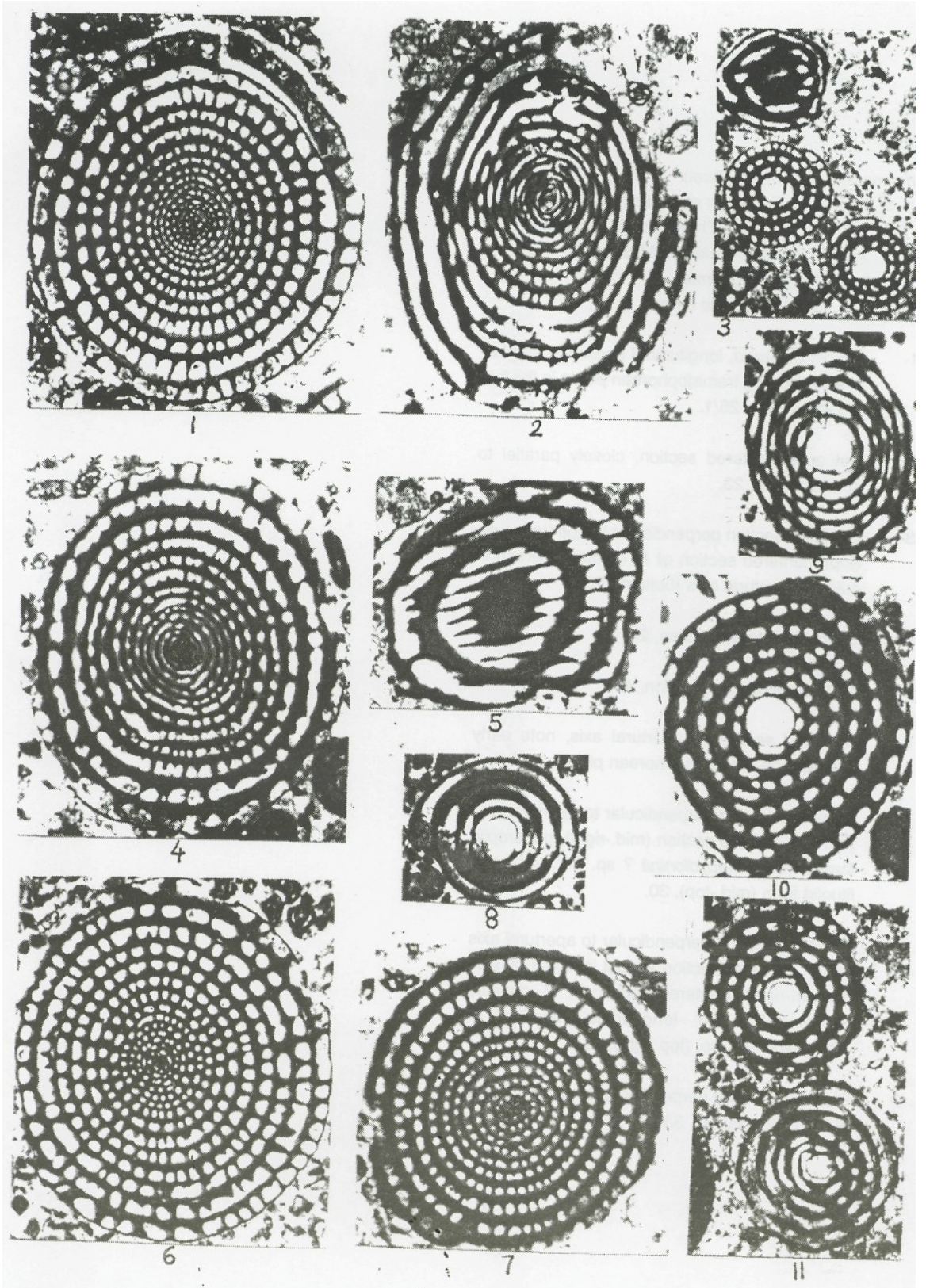


PLATE-IV

Pseudolacazina oeztemueri (Sirel)

Figs. 1, 5, 8 from the Thanetian of Aksaray, Central Turkey.

Figs. 2-4, 6, 7, 9 from the Thanetian of Kırkkale, E of Ankara, Central Turkey. All figs, x 20.

Figs. 1, 2, 5, 9 Microspheric forms.

Figs. 3, 4, 6-8, 9 Megalospheric forms.

Fig. 1- Almost centered, longitudinal section in apertural axis showing trematophorean pillars in the late ontogeny, Aks. 25/1.

Fig. 2- Not quite centered section, closely parallel to apertural axis, 23.

Fig. 3- Centered section perpendicular to apertural axis, (top), centered section of *P. donatae*, perpendicular to apertural axis (bottom), 28.

Fig. 4- Oblique centered section, 24.

Fig. 5- Non centered axial section, 40.

Fig. 6- Centered section in apertural axis, note early appearance of trematophorean pillars, 34.

Fig. 7- Centered section perpendicular to apertural axis (top left), oblique section (mid.-right), peneroplid form (mid.), *Rhapydionina* ? sp. (mid.-left) and lituolid form (mid.-top), 30.

Fig. 8- Centered section perpendicular to apertural axis (mid.), centered section almost in apertural axis (bottom-right), centered section of *P. donatae* (bottom-left) and. longitudinal section of *Rhapydionina* ? sp. (top right), 23/3.

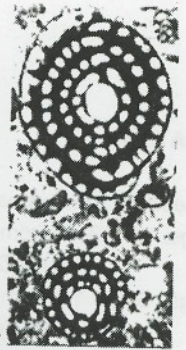
Fig. 9- Centered section perpendicular to apertural axis of both generations, 33.



1



2



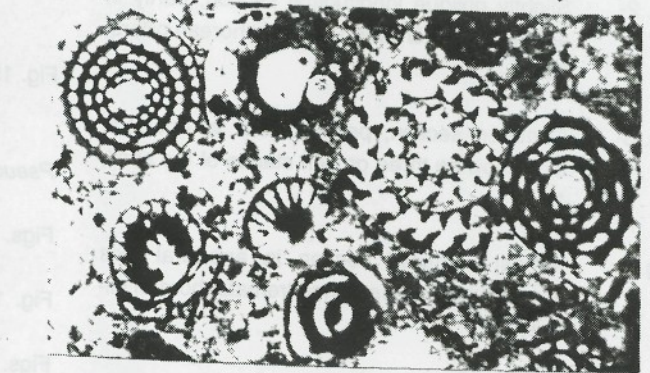
3



4



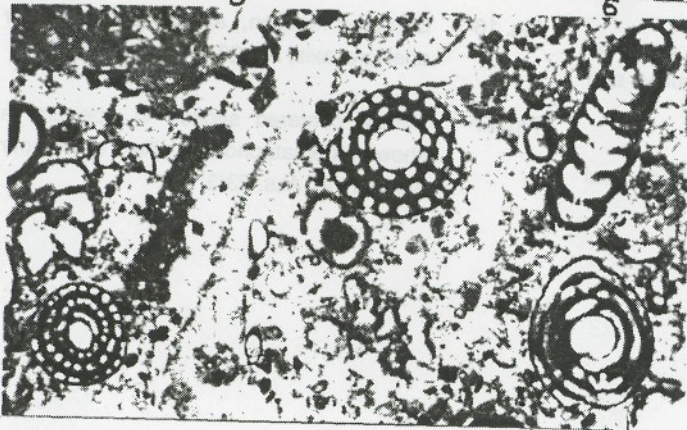
5



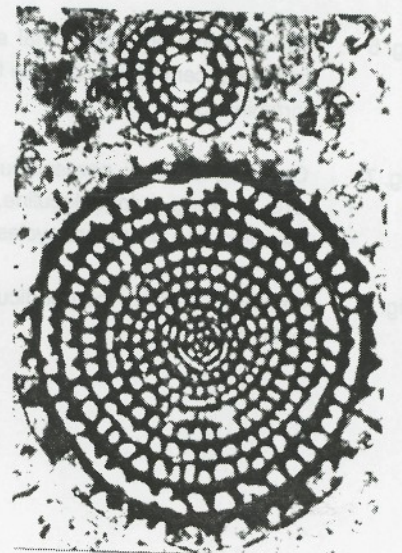
6



7



8



9

PLATE-V

Pseudolacazina donatae (Drobne)

Figs. 1-7,13,15 from the Thanetian of Kirikkale area, E of Ankara, Central Turkey.

Figs. 8-12, 14 from the Thanetian of Aksaray region, Central Turkey. All figs, x 20.

Figs. 1, 2, 3, 5-7, 9-12, 15 Microspheric forms.

Figs. 4, 8, 14 Megalospheric forms.

Fig. 1- Centered section perpendicular to apertural axis (top), tangential section (bottom right) and oblique section (bottom left), 6.

Fig. 2- Slightly oblique longitudinal section, partly in apertural axis, showing trematophorean pillars, 36.

Fig. 3- Centered section, perpendicular to apertural axis showing three growth stages of the shell, 17.

Fig. 4- Almost centered section in apertural axis showing early appearance trematophorean pillars, x.

Fig. 5- Oblique longitudinal section, 21.

Fig. 6- Almost centered longitudinal section in apertural axis, central pillars in the trematophorean foramina, 36.

Fig. 7- Centered section, perpendicular to apertural axis showing quinqueloculine, biloculine and monoloculine chambers Cycles, 38.

Fig. 8- Centered section, perpendicular to apertural axis, 24.

Fig. 9- Centered section, perpendicular to apertural axis showing growth stages of the shell, 14.

Fig. 10- Centered section, perpendicular to apertural axis, 15.

Fig. 11- Centered section perpendicular to apertural axis, 24.

Fig. 12- Almost centered, section perpendicular to apertural axis, 36.

Fig. 14- Centered section perpendicular to apertural axis, Ak. 27/1.

Fig. 15- Centered section perpendicular to apertural axis, 36.

Pseudolacazina oeztemueri (Sirel)

Figs. 16,17- From the Thanetian of Aksaray region, Central Turkey.

Fig. 13- From the Thanetian of Kirikkale area, East of Ankara, Central Turkey. All figs, x 20.

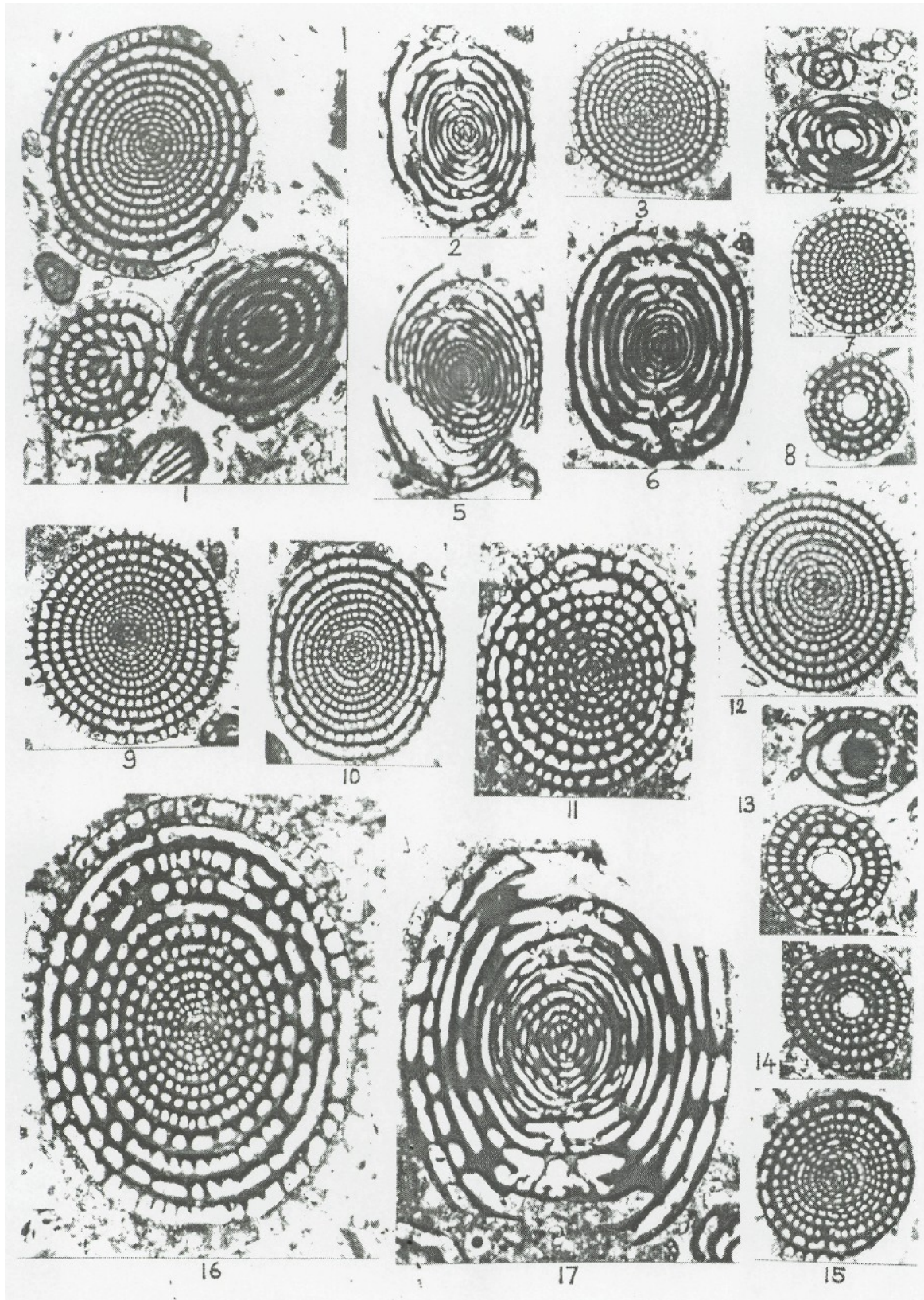
Figs. 16, 17- Microspheric forms.

Fig. 13- Megalospheric form.

Fig. 13- Centered section, perpendicular to apertural axis (bottom), tangential section (top), Kir. 3.

Fig. 16- Centered section, almost perpendicular to apertural axis, Ak. 23.

Fig. 17- Almost centered section in apertural axis, showing trematophorean pillars in the apertural foramina, Aks. 23/3.



SEDIMENTOLOGY OF CALICHE (CALCRETE) OCCURRENCES OF THE KIRŞEHİR REGION

Eşref ATABEY*; Nevbahar ATABEY* and Haydar KARA*

ABSTRACT.- Study was conducted in the Kirşehir region. Carbonate occurrences within the upper Miocene-Pliocene deposits forming the subsidence basins surrounded by the Kirşehir massive, are described as caliche. These caliche deposits in the alluvial fan-meandering river and lacustrine environments are found in three different zones. In the measured sections, conglomerate comprises the basement and is overlain by a transition zone made of sandy mudstone (Zone I). Above them is the rarely nodular carbonaceous zone with horizontal and vertical positions in the reddish mudstone-siltstone (Zone II). Finally, laminated caliche (calcrete) comprises the upper most part (Zone III). Carbonates in the basement, country rocks, and in the soil are dissolved in the acidic environment and become a solution saturated with calcium bicarbonate. This solution is transported to the sediments and capillary rises through the sediments during arid-semi arid seasons. Carbondioxide in the Ca and HCO_3^- bearing solution is removed from the system and as a result, calcium carbonate nodules and laminated caliche are formed. These stromatolite-like laminated caliche occurrences show a cryptoalgal structure under polarized microscope and scanning electron microscope (SEM), and they contain microerosional surfaces and caliche pisolites that are formed by dissolution. Caliche occurrences are believed to be source of carnotite, thorium, vanadium, sepiolite, huntite, dolomite, and magnesite.

INTRODUCTION

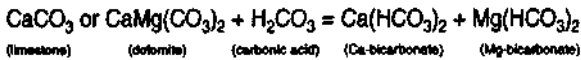
Study area comprises around of the city of Kirşehir in the Central Anatolia (Fig. 1A and 1B). In this region, nodular and laminated carbonate occurrences are observed particularly in upper Miocene-Pliocene rock units that are bordered by the Kirşehir metamorphic basement at north of Kızılırmak river. In the previous studies, these occurrences are stated to be the products of shallow lake-playa (caliche) environment (Atabey et al., 19875; Atabey, 19895; Kara and Dönmez, 1990). This study revealed that this type of laminated carbonate occurrences are in fact caliche (calcrete) deposits that are found as nodules in a vertical position in soil zones of upper Miocene-Pliocene rock units, mudstone-siltstone, and partly in conglomerates at the upper most section of the sequence. The purpose of the present study is also to investigate sequence characteristics, position, geometry, lithology features, microtextural properties, and formation mechanism of such occurrences.

In a general sense, caliche is described as secondary carbonate formation and calcareous, semi-consolidated aragonite or early diagenetic calcite forming in loose materials (Walls et al., 1975), such as pebble,

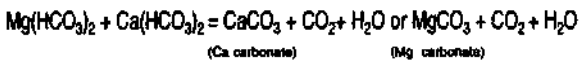
sand, silt, and soil under semi-arid and arid climate regimes. The term of caliche is used as a synonymous of calcrete and also known as calcrete crust and limestone crust (Bretz and Horberg, 1949; Brown, 1956; Mutter and Hoffmeister, 1968; Aristarain, 1970; Reeves, 1970; Goudie, 1972; Esteban, 1976; Hay and Reeder, 1978; Read, 1976; Hubert, 1978; Esteban and Klappa, 1983). Wright et al., (1988) used the term of laminated calcrete for limestone and calcrete-bearing deposits. Klappa 1980b, Seminiuk and Meagher (1981), Arakel and McConchie (1982), and Carlisle (1983) point out that these occurrences are formed in capillary zones of wide soil areas. Textural classification of calcretes is made by Knox (1977) and Reeves (1970). Calcretes were mineralogically and petrologically described by Hay and Reeder (1978). Kahle (1977) and Aristarain (1970) studied calcretes biologically and chemically. Hubert (1978) and Arakel (1979) worked on climatic and geographic features of calcretes.

It is given in the literature that caliche occurrences are associated with some element and minerals, such as carnotite, thorium, vanadium, sepiolite, magnesite, huntite, and dolomite (Szalay, 1964; Goudia, 1972; Arakel and McConchie, 1982; Esteban and Klappa, 1983; Carlisle, 1983).

Some conditions required for the formation of caliche are country or basement rocks be a carbonate type, presence of carbonate in the soil zone of the area, climate regime of semi-arid to arid, widespread capillary activity, and the presence of CO_2 in the environment. As a result, caliche occurs to be a product of carbonization process. Carbonization is defined as reacting of carbonate (CO_3) and bicarbonate (HCO_3) ions with bases to form carbonates (Ketin, 1982). Carbonic acid facilitates disintegration of rocks. CO_2 content of air and rain water is 0.03% and 0.45%, respectively. Carbonic acid is existed with the reaction between water (H_2O) and carbondioxide (CO_2). $\text{CO}_2 + \text{H}_2\text{O} = \text{H}_2\text{CO}_3$. This acid dissolves Ca- and Mg-bearing rocks and forms solutions saturated with calcium and magnesium carbonates.



These Ca- and Mg-bicarbonate saturated waters move downward percolating generally through loose soil and mudstones. Then, they rise to the surface by capillary effect and evaporation during arid and semi-arid seasons. Carbondioxide (CO_2) in the solution on the surface is evaporated while water becomes stagnant. Thus, carbondioxide (CO_2) and water (H_2O) are removed from bicarbonate-saturated solution. Following this separation, as shown in the reaction given below, nodules consisting of calcium carbonate (CaCO_3) and magnesium carbonate (MgCO_3) form vertical and lateral carbonate occurrences. Carbonate rock of this type is described as caliche in a geological sense.



Caliche is mostly observed in lacustrine, river, and alluvial fan deposits (Reeves, 1970; Platt, 1989; Esteban and Klappa, 1983; Hubert, 1978) and fresh water and vadose diagenetic environments (Steinen and Mathews, 1973; James, 1972; Land, 1970). Many studies were carried out on definition, facies features, diagenesis, chemistry, mineral content, occurrence, and deposition environment of caliche in Lebanon, Syria, Spain, Australia, Unites States of America, South Africa, and several other countries in North Africa. In Tur-

key, caliche occurrences are commonly observed in young rock units in Aegean, Mediterranean, and Central Anatolia. Studies on such deposits in Turkey are recently initiated. The city of Kırşehir was selected for a new investigation area and measured sections on caliche exposures in Seyrek village, Malhüyük hill at south of Çoğun village, city center of Kırşehir, Tilkideresi at south of Tepesidelik village, Kepez village, and Yenifakılı town were studied (Fig. 1B and 2). Samples collected were examined with polarizing microscope and scanning electron microscope (SEM). Samples were also analyzed with XRD and their microtextural features were determined by a paint technique. In addition, considering lithologic data, sedimentologic features and depositional environments of caliche occurrences in the area were examined.

STRATIGRAPHIC SETTING

The basement in the area is represented with a Paleozoic-Mesozoic unit composing of metamorphic and magmatic rock assemblages (Fig. 1B and 2a). Above this metamorphic-magmatic basement, is the sedimentary upper Miocene-Pliocene rock units with an angular unconformity. This unit is described as the Kızılırmak formation by Birgili et al., (1975), Oktay (1981), and Kara and Dönmez (1990) and later as the Pecenek formation by Uygun (1982), Atabey et al., (1987a), Atabey (1989a), and Atabey (1989b). The same unit at north and east of Çiçekdağı was defined to be Kızılırmak and Bozkır formations by Erdoğan et al., (1996) and based on the palinologic data, its age was assigned as middle-upper Miocene. This unit is widely observed around the Kızılırmak valley and subsidence basins in the vicinity of the city of Kırşehir. Unit is composed of loosely cemented conglomerate, red mudstone-siltstone, and thin bedded carbonate cover in the upper parts of the sequence, all deposited in alluvial fan, meandering river, and lacustrine environments (Fig. 1B and 2a). Based on some vertebrate fossils, such as *Cyprideiscf. ventroundulata* Kırstic, *Cyprideis torosa* Jones, and *Hypparion gracile* Kaup, and molar tooth of *Choerolophodan pentelici*, bone and tooth pieces of *Proboscidea family* (elephants), the unit is aged to be upper Miocene-Pliocene (Kara and Dönmez, 1990). Its thickness is about 15-300 m. White-gray, yellowish colored, clastic, porous, banded, lenti-

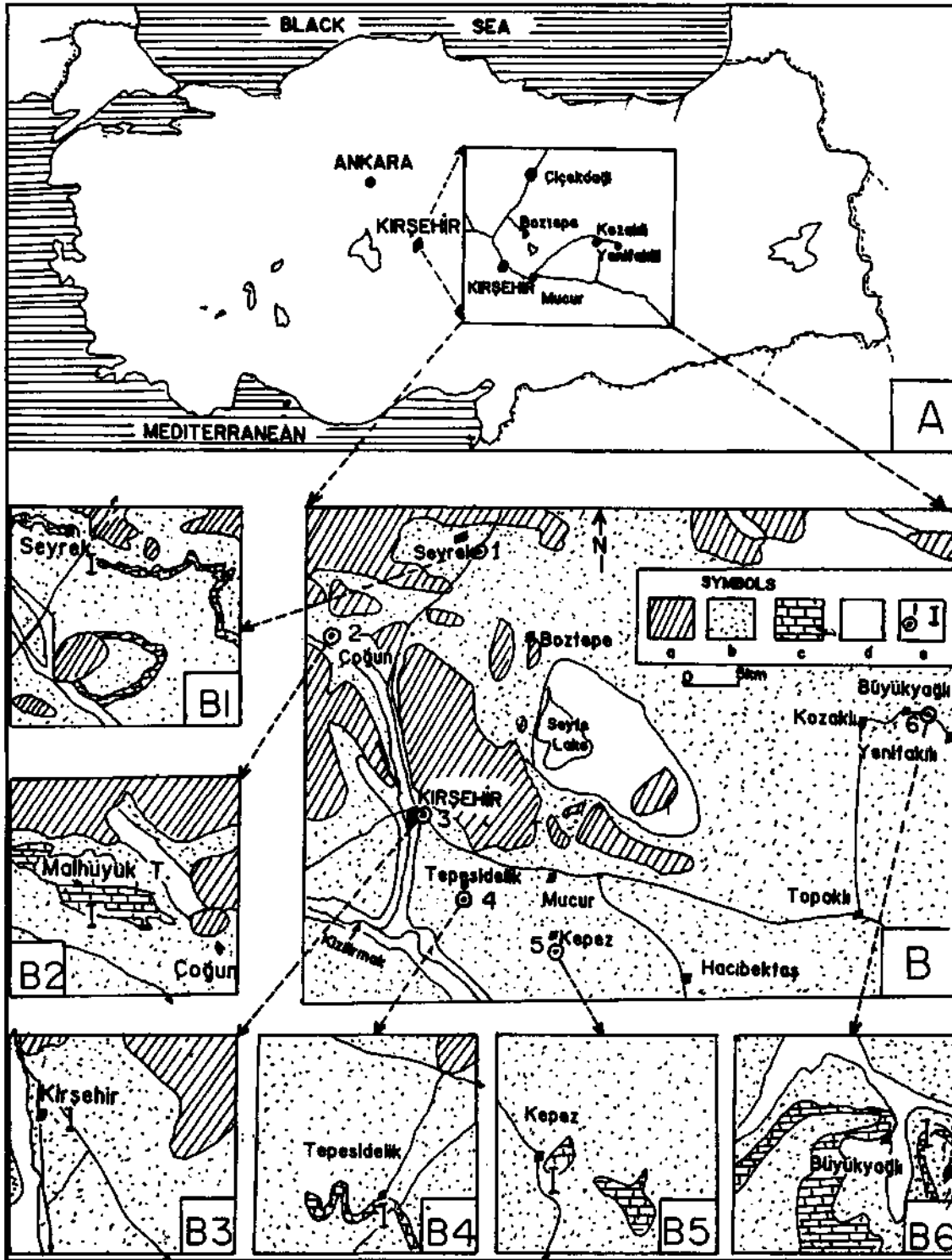


Fig. 1- A- Location map, B- Geology map (a- Metamorphic-magmatic rock units, b- Upper Miocene-Pliocene clastics, c- Upper Miocene-Pliocene carbonates, d- Alluvium), B1, B2, B3, B4, B5, and B6- Location of measured sections and their detailed geology maps.

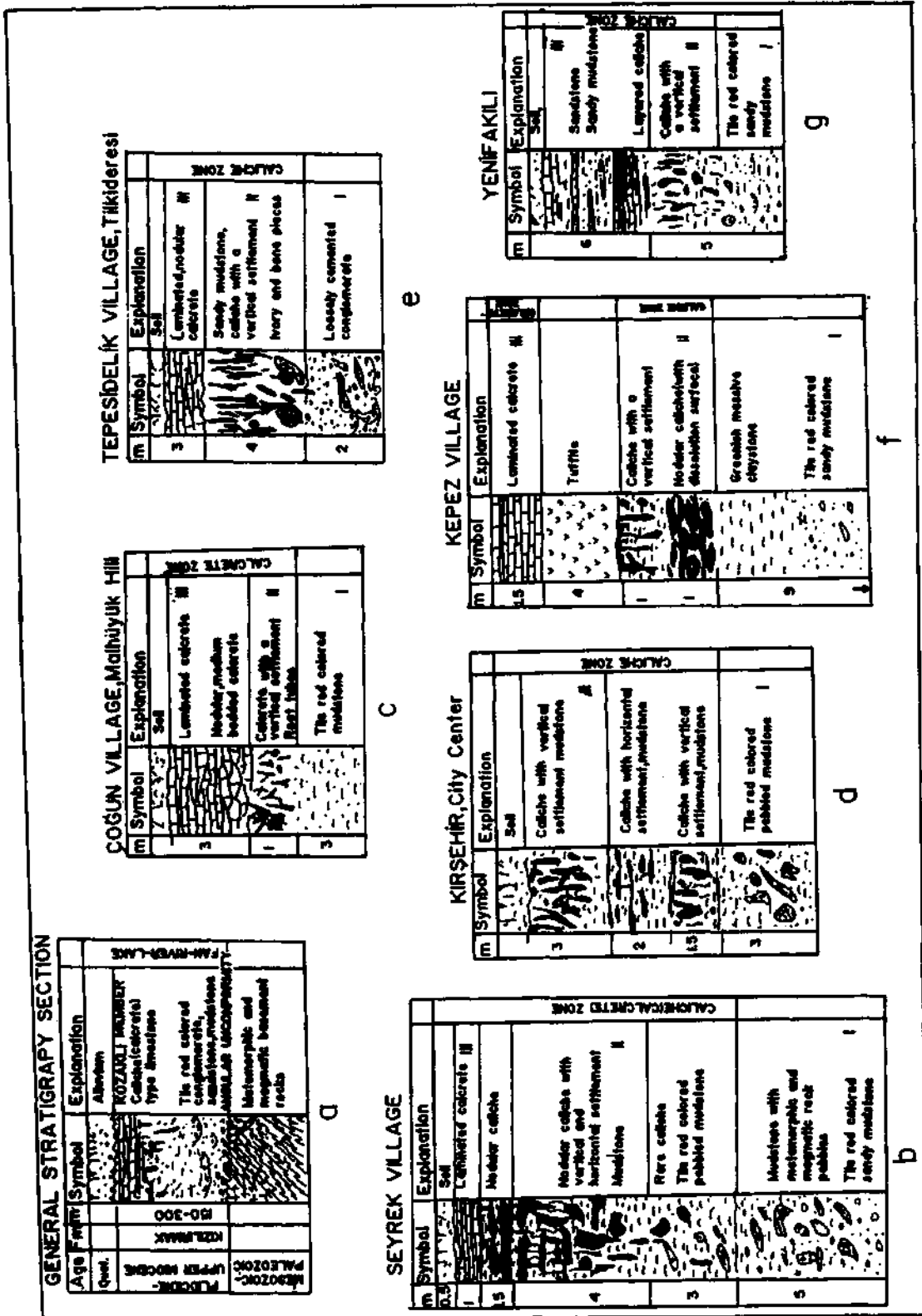


Fig. 2- a- General stratigraphic section, b, c, d, e, f, and g- Measured sections.

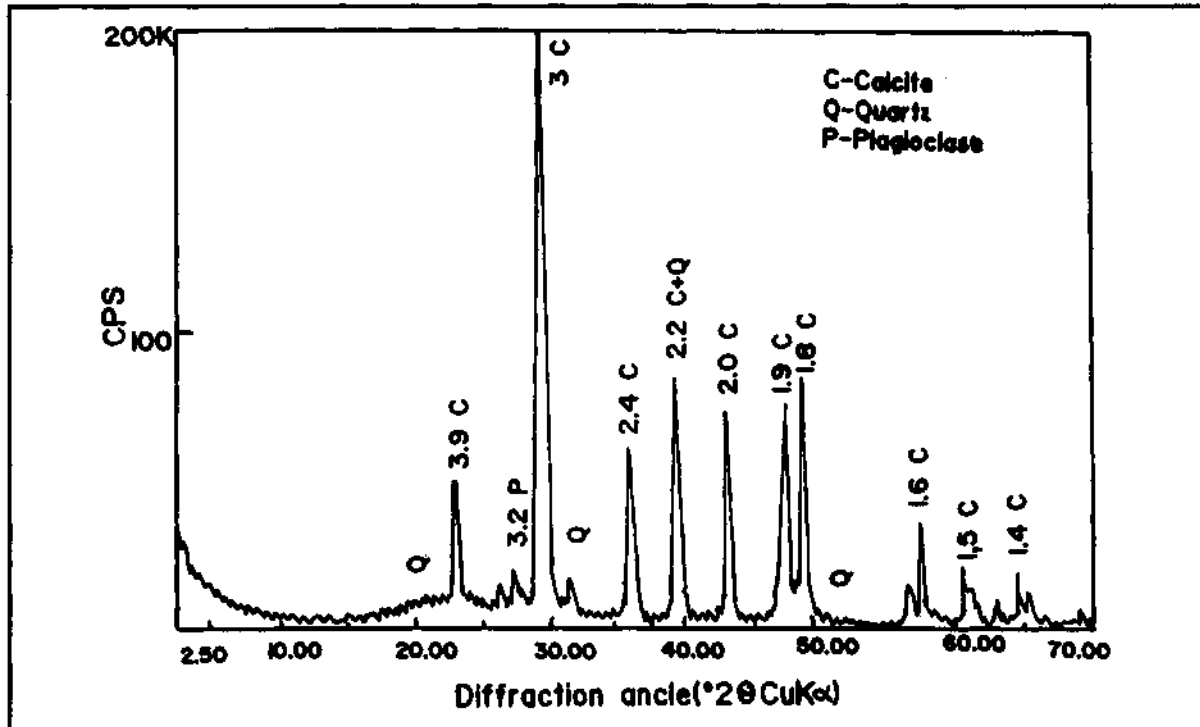


Fig. 3- X-Ray diffractometry chart of caliche (calcite) (Seyrek village). Calcite is the dominant mineral phase.

cular lacustrine limestones covering upper parts of the Kızılırmak formation are named as Kozaklı limestone member (Kara and Dönmez, 1990), while laminated, thin bedded lacustrine limestones are called as Aksaklı limestone member (Atabey et al., 1987b; Atabey, 1989b) (Figs. 1 B1, 1 B2, 1 B4, 1 B5, 1 B6, and 2a). Caliche occurrences under investigation are observed as white colored, nodular calcite occurrences with horizontal and vertical settlements in sandstone and mudstone- siltstone levels of the unit mentioned above. Laminated lacustrine limestones at the top of the sequence are also defined as caliche (calcrete).

Descriptions of measured sections

Sections measured from caliche exposures in the Kırşehir region are described as below (Figs. 1 and 2).

Measured section from the Seyrek village.- It is at 40th km of the Kırşehir-Çiçekdağı road and located in J32-b1 quadrangle (Section marked with 1 in Fig. 1.B and with b in Fig. 2). Its coordinates are x: 66600 and

y: 10250 and has a thickness of 15 m. Sequence at the bottom is composed of mudstone 5 m in thickness containing metamorphic and magmatic pebbles, tile red colored sandy mudstone, and nodular calcite of 2-15 cm in size (Fig. 2b and Plate I). It changes to tile red colored pebbled mudstone with a thickness of 3 m containing rare caliche nodules and to mudstones of 4 m consisting of calcite nodules with horizontal and vertical long axes. Above that is partly nodular carbonaceous mudstone with a horizontal long axis of 1.5 m (Plate I, fig. 2, 4). The top of sequence is made up with laminated and thin bedded carbonates (caliche) (Plate I, fig.2).

Measured section of Malhüyük hill at south of Çoğun village.- It was measured in the Malhüyük hill southwest of Çoğun village at north of Kırşehir and is located in J32-a4 quadrangle (Section marked with 2 in Fig. 1 B and with c in Fig. 2). Its coordinates are x: 53800 and y: 92800 and has a thickness of 7 m. The basement is composed of tile red colored sandy mudstone level with a thickness of 3 m. Above that is a level

consisting of root tubes and pipes with a vertical long axis of 1 m (Fig. 2c and Plate II, fig. 1). To the top, nodular, massive and layered limestone (calcrete) of 3 m is observed.

Measured section from the city center of Kırşehir- It was measured on the Kayseri road in the city center of Kırşehir and is located J32- d2 quadrangle (Section marked with 3 in Fig. 1 B and with d in Fig. 2). Its coordinates are x: 33800 and y: 01700 and has a stratigraphic thickness of 9.5 m. Section is composed of mudstones consisting of rare carbonate nodules overlain by carbonaceous mudstone- siltstone level with vertical horizontal long axes of 3.5 m. The upper most part consist carbonaceous mudstone with a vertical settlement of 3 m (Fig. 2d and Plate II,fig.3).

Measured section from the Tilkideresi at south of Tepesidelik village. - It was measured from the Tilkideresi at south of Tepesidelik village in Kırşehir city and is located in J32-d3 quadrangle (Section marked with 4 in Fig. 1 B and with e in Fig. 2). Its coordinates are x: 22000 and y: 07500. Its thickness is 9 m. At the basement of the section it is composed of loosely cemented conglomerate of 2 m in thickness that is overlain by tile red colored sandy mudstone of 4 m. In the mudstone, nodular carbonates with vertical long axes, ivory, and bone pieces are detected. The top of section consists of laminated calcrite (Fig. 2e and Plate II, figs. 2, 4).

Measured section from the Kepez village. - It was measured in the Kepez village of the city of Nevşehir and is located in K32-b1 quadrangle (Section marked with 5 in Fig. 1 B and with f in Fig. 2). Its coordinates are x: 16700 and y: 18750. It has a stratigraphic thickness of 16.5 m. The basement of section is composed of tile red colored mudstone and greenish blue colored massive limestone of a total of 9 m in thickness. They change to nodular carbonate (caliche) zone of 1 m with a surface of dissolution signs. Above that is volcanic tuffite of 1 m. The most upper part is made up with layered-laminated partly massive carbonate (caliche) of 4 m in thickness (Fig. 2f and Plate III, figs. 1, 3).

Measured section from the west of Yenifakılı town. - It was measured on the road excavation between Büyükyaylı village and Yenifakılı town of the city of Yoz-

gafarid is located in J33-b1 quadrangle (Section marked with 6 in Fig. 1 B and with g in Fig. 2). Its coordinates are x: 44250 and y: 69800. It has a thickness of 11 m. Section is represented at the basement by sandy mudstone of 5 m in thickness and calcite (caliche) zone with a vertical settlement overlain by a thin bedded (6 m) calcite zone (Fig. 2g and Plate III, fig. 4).

CALICHE FACIES

Considering the lithologic descriptions of measured sections; three main caliche zones were differentiated. They are transition zone nodular calcareous zone, and laminated caliche (calcrete) zone described by Esteban (1976) and Esteban and Klappa (1983) (fig. 2).

Transition zone (1st zone): It is the transition zone found at the bottom of sections. It is composed of pebbled-sandy mudstone, sandstone, and partly loosely cemented lenticular conglomerates. Pebble components are derived from metamorphic-magmatic basement. Grains are 2-15 cm in size, angular, sub-angular, sub-rounded, and poorly sorted (Plate I, fig.1). In addition, grains display some signs of orientation and brick-like packing. Tile red color is dominant. They rarely contain nodular, white colored chalk-like carbonate occurrences of 5-10 cm in size (Plate I, Plate II; figs. 1, 2, 3, 4 and Plate III, figs. 1, 4). This zone is repeated in the section measured from the city center of Kırşehir (fig. 2d).

Nodular zone (2nd zone): This zone is composed of red tile colored mudstone-siltstone and nodular, chalky carbonate (caliche) occurrences with vertical and horizontal settlement. It is observed in all the sections. It is partly erosional and transitional with rarely nodular, mudstone at the basement (1st zone). 1st and 2nd zones cannot be exactly distinguished from each other (Plate I, figs. 1, 2; Plate II, figs. 1, 4 and Plate III, figs. 1, 4). Calcite nodules are 5-10 cm in size and spherical or oval in shape. In some cases, nodules are laterally adjacent (Plate I, fig. 4). Root remnant and molds, root tubes, and vertical pipe structures are also observed (Plate II, fig. 1).

Laminated zone (3rd zone): It is the zone in which layered and laminated calcite (caliche) is vastly detected.

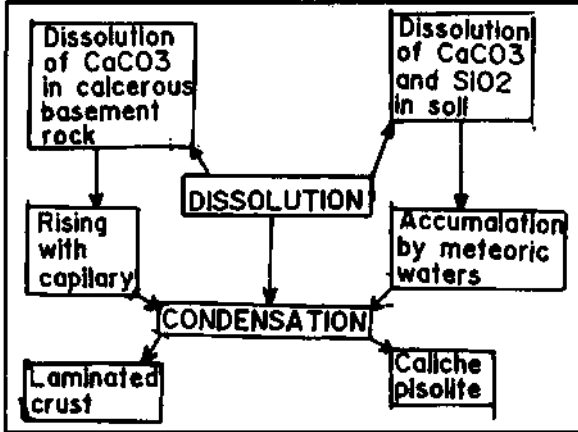


Fig. 4- Evolution of caliche pisolite in the study area.

ted. It is observed in the sections from the city center of Kirşehir and Yenifakılı town. (Plate II, fig. 3 and Plate III, fig. 4). It is widely exposed in the sections of Seyrek and Kepez villages. Zone consists of thin bedded, laminated locally massive, horizontal carbonate occurrences. It is gray, white, dirty yellow colored. Surface of carbonate layer shows dissolution signs and stromatolite-like algal structure. Their view from the top reveals that calcareous crust covers alluvial-lacustrine sediments (1st and 2nd zones) (Walls et al., 1975) (Fig. 2; Plate I, fig. 2; Plate II, figs.1, 2, 4 and Plate III, fig.1). Freydet and Plaziat (1982) used the term of exposing calcareous crust zoning for laminated calcrites.

MICROTEXTURAL FEATURES

In order to determine microtextural features of samples collected from caliche exposures, thin sections were examined by means of polarizing microscope while rock samples were examined with scanning electron microscope (SEM), X-Ray diffractometry (XRD), and paint technique.

Samples from transition zone of caliche facies (1 st zone) have a completely porous texture (Plate IV, fig. 1). Detritic quartz and volcanic and magmatic rock fragments are the dominant grain component. Overlying rarely nodular chalky caliche (2nd zone), however, display a carbonaceous mud texture (Plate IV, fig. 2). Nodules in this zone are accompanied by detritic grains (Plate IV, figs. 3, 4). Root molds, root tubes and pi-

eces are also observed. These root tube and molds are circular- and ellipsoidal-shaped and are generally filled by a low-magnesium calcite cement (Klappa, 1980b). In thin section, dissolution voids (Plate IV, fig. 2), vadose silt structure (Plate IV, fig. 3), and micro fissures (Plate IV, fig. 4) around the grains and within the carbonaceous mud are widely detected. According to Esteban and Klappa (1983), this type of micro fissures within or around the grains are formed by washing and drying. These micro fissures and voids forming by dissolution are filled with sparry calcite (Plate IV, figs. 2, 3, 4). Stylolite cement is developed in massive calcrites (Plate V, fig. 1). Samples collected from laminated calcrites at the top (3rd zone) exhibit cryptoalgal structures (Plate V, figs. 2, 4). They are undulated like stromatolites but differ from stromatolites with their texture consisting of very fine calcite crystals (Read, 1976) and forming of blue-green algae. In thin section, in addition to laminated structure, micro erosion surfaces (Hay and Reeder, 1978) and caliche pisolites with micritic membrane are also observed (Plate V, figs. 2, 3, 4). These caliche pisolites have irregular membrane and their nucleus is asymmetrical and larger than membrane (Plate V, fig. 3). Due to dissolution and reworking, micro erosion surfaces and lamina may be repeated. Following the dissolution process, this laminated structure is formed by recementing of calcium bicarbonate (CaHCO₃) of micritic size (Harrison and Steinen, 1978).

SEM studies of cryptoalgal laminated caliches reveal that dissolution process is effective (Plate VI, fig. 3). Dissolution process is indicative of an acidic environment and fresh water effect. Voids formed are filled by late diagenetic calcite (Plate VI, fig. 1) and autogenic quartz crystals (Plate VI, fig. 2). Root tubes are partly observed in the rock (Plate VI, fig. 4).

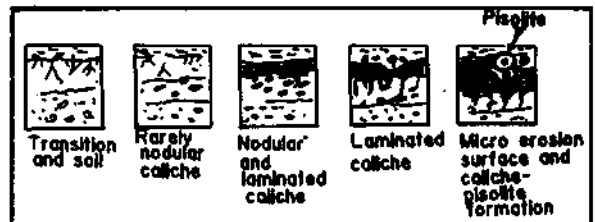


Fig. 5- Development model for laminated caliche and caliche pisolite in the area.

When thin sections are painted with a mixture obtained from alizarin-Red S and potassium ferrocyanide, all samples show a pink color. This indicates that caliche nodules and laminated carbonates are completely composed of calcite and that they do not yield any color indicative of iron or manganese enrichment.

X-Ray diffractometry results of six examined samples also indicate that calcite is the dominant mineral phase (Fig. 3 and Table 1). In addition to calcite, smectite, illite, chlorite, plagioclase, and kaolinite are the other minerals observed (Table 1). Smectite and illite most probably originated from alteration of plagioclase- and K-feldspar-bearing micaceous rocks while chlorite is formed due to shallow diagenesis in acidic soils as a result of washing and oxidation (Tucker, 1981).

1-Carbonates in basement rocks are dissolved by carbonic acid. As stated previously, carbonic acid is formed by the reaction between rain water and carbon-dioxide (CO_2) in the air and expelling from fracture and fissures around $\text{CO}_2 + \text{H}_2\text{O} = \text{H}_2\text{OCO}_3$ (Fig. 4). Carbonate dissolved by carbonic acid then changes to a calcium bicarbonate-rich solution. It is carried as calcium bicarbonate in alluvial fan, river, and lake sediments. This solution that can also be percolated to the ground water level rises to the surface by capillary during arid and semi-arid seasons. Rising solution loses carbon-dioxide (CO_2) being in contact with air and precipitates as calcium bicarbonate (CaCO_3) (calcite). This calcium carbonate (CaCO_3) forms caliche type nodules (Fig. 6 and 1 st and 2nd zones shown in figure and sections).

Table 1- X-Ray diffractometry results of some caliches and laminated calcrites collected from measured sections in the area.

SAMPLE LOCATION	SAMPLE NO	MINERALS
Seyrek village	9	Calcite, quartz
	10	Calcite, smectite, illite, quartz, plagioclase
	19	Calcite, plagioclase, quartz
Çoğun village-Malhüyük hill	21	Calcite, plagioclase, mica, quartz
Kepez village	67	Calcite, plagioclase, mica, quartz
Yenifakılı	128	Calcite, plagioclase, quartz, mica
	105	Calcite, plagioclase, mica, quartz, chlorite
Tepesidelik village	122	Calcite, plagioclase, smectite, chlorite, illite, quartz, kaolinite

CALICHE FORMATION

The area where caliche deposits are exposed is a subsidence basin comprising upper Miocene-Pliocene sediments on the Paleozoic-Mesozoic basement (Fig. 1 B and 6). Nodular and laminated carbonates (caliche) with vertical and horizontal settlements within mudstone and siltstone are derived from two different sources.

2- Percolating of calcium-bicarbonate solution, forming by redissolution of caliche or carbonate available within carbonate caps (lacustrine carbonates) and soil, through the mudstone-siltstone and conglomerate (Fig. 6). Solution concentrated along the ground water level rises by capillary effect during arid and semi-arid seasons (Fig. 4). Carbon-dioxide (CO_2) in rising solution is removed and, like in first case, it is precipitated as CaCO_3 and forms caliche type carbonates. At the top

of the sequence, depending on the position of ground water level, a laminated carbonate crust or massive type caliche with a horizontal settlement is developed (3rd zone) (Plate I, fig. 2; Plate II, fig. 1; Plate III, fig. 1 and fig. 5, 6). This accumulation may be also associated with meteoric waters (Walls et al., 1988). Laminated crust developing due to condensation is dissolved in acidic conditions (high pH) in time and as a result, microerosional surfaces are formed (Plate V, figs. 2, 4). In places where alluvial fan-meandering river intersect with the lake water (Fig. 6), due to fluctuation of ground water level, irregular-shaped caliche pisolites are formed (Hubert, 1978) (Plate V, figs. 2, 3, 4 and fig. 5). Intense accumulation of these pisolites is appeared to be brecciated (Dunham, 1969b). As dissolution and reaccumulation processes are repeated (Fig. 4), laminated

carbonate crust is also alternated and thus, stromatolite-like structures with no stromatolite origin (Read, 1976) are developed (Plate V, fig. 2).

Tectonism plays an important role in the caliche formation. Carbon dioxide expelling along the fracture and fault systems combines with rain water to form carbonic acid. Carbon dioxide-rich an acidic environment is created due to heavy industrialization as widely observed in various European countries. Carbonaceous rocks or carbonaceous soils in the acidic environment are dissolved and transformed to calcium-bicarbonate saturated solutions. This solution generally facilitates the formation of caliche type carbonate nodules or laminated caliche in soils.

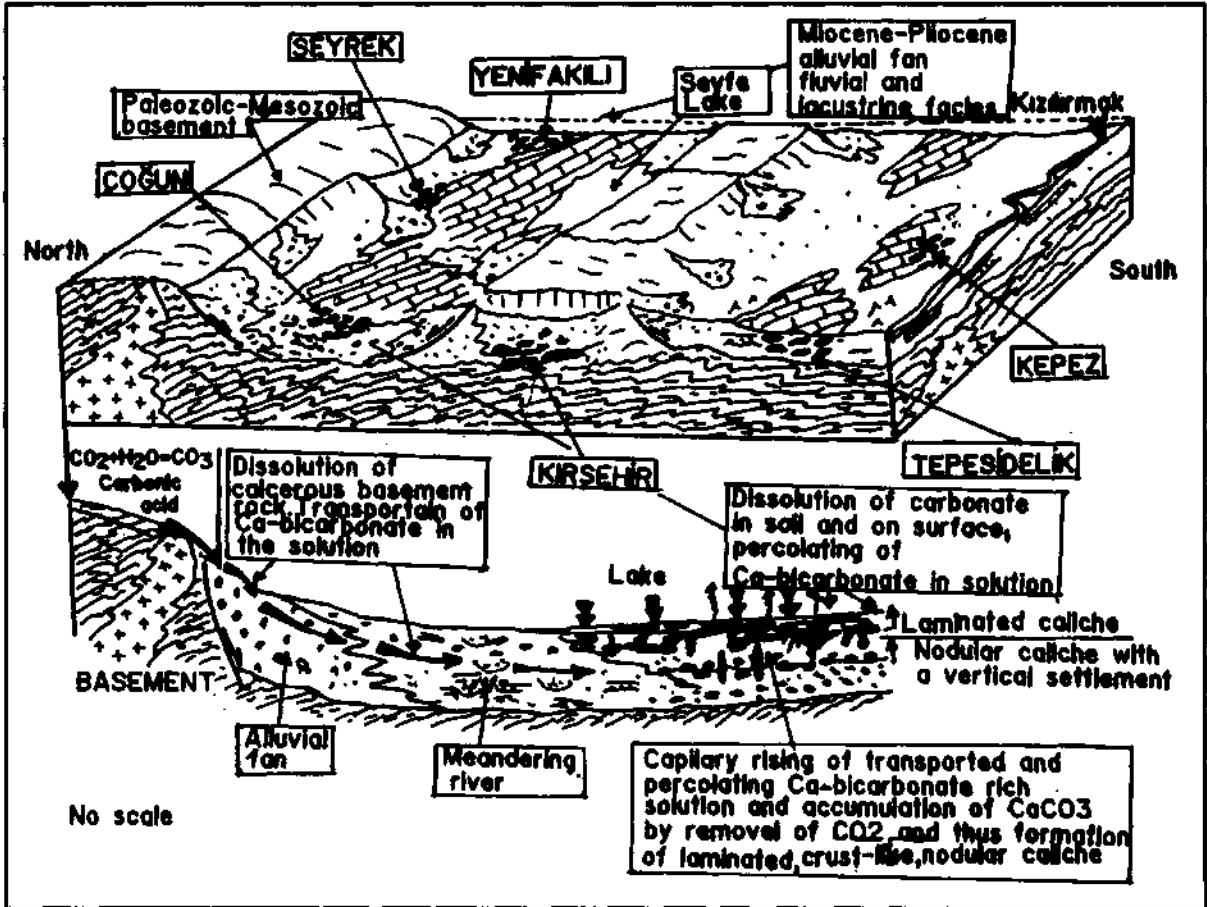


Fig. 6- Formation model for caliches in the area.

RESULTS

Caliche occurrences in the study area are found in conglomerate, sandstone, mudstone, and siltstone belonging to alluvial fan, meandering river, and lacustrine environments. Based on deposit character, water chemistry, and water movement, these caliche deposits are observed in three different zones. Basement rock and carbonates in the soil are the main sources of the occurrences. These carbonates are dissolved and form bicarbonate-rich solutions, which are transported through the sediments and rise by capillary effect, and finally form calcium carbonate nodules and caliche crusts observed in the area. In the present study, carbonates previously described as lacustrine carbonates were determined to be the laminated caliche (calcrete) occurrences and are composed completely of cryptoalgal structures.

ACKNOWLEDGEMENTS

Author thanks to Serap İçöz for conducting X-ray diffractometry analyses and to Dr. Mustafa Albayrak for taking SEM images.

Manuscript received January 30, 1997

REFERENCES

- Arakel, A.V., 1979, Genesis of calcrete in Quaternary soil profiles, Hutt and Leman Lagoons, Western Australia: *J. Sed. Petrol.*, 52, 109-125.
- and McConchie, D., 1982, Classification and genesis of calcrete and gypsite lithofacies in paleodrainage systems of Inland Australia and their relationship to carnotite mineralization: *J. Sed. Petrol.*, 52, 1149-1170.
- Aristarain, L.F., 1970, Chemical analysis of caliche profiles from the high plains, New Mexico: *J. Geol.*, 78, 201-212.
- Atabey, E.; Tarhan, N.; Akarsu, B. and Taşkıran, A., 1987a Şerefilikoçhisar, Panlı (Ankara) - Acıpınar (Niğde) yöresinin jeolojisi MTA Rep.: 8155, (unpublished), Ankara.
- Atabey, E.; Tarhan, N.; Papak, I.; Akarsu, B. and Taşkıran, A., 1987b, Ortaköy-Tuzköy (Nevşehir) - Kesikköprü (Kırşehir) yöresinin jeolojisi, MTA Rep.: 8156, (unpublished), Ankara.
- , 1989a, 1:100000 ölçekli açın-sama nitelikli Türkiye Jeoloji Haritaları Serisi, Aksaray-H18 paftası: MTA Bull.
- , 1989b, 1:100000 ölçekli açın-sama nitelikli Türkiye Jeoloji Haritaları Serisi, Aksaray-H17 paftası: MTA Bull.
- Birgili, Ş.; Yoldaş, R. and Ünal, G., 1975, Çankırı-Çorum havzasının jeolojisi ve petrol olanakları, MTA Rep.: 5621 (unpublished), Ankara.
- Bretz, J.H. and Horberg, L, 1949, Caliche in southeastern New Mexico: *J. Geol.*, 57, 492-511.
- Brown, C.N., 1956, The origin of caliche on the northeastern Llano Estacado Texas, *J. Geol.*, 64, 433-457.
- Carlisle, D., 1983, Concentration of uranium and vanadium in calcretes and gypsites, In: *Residual Deposits: Surface Related weathering processes and materials* (Ed. by R.C.L. Wilson). Spec. Publ. Geol. Soc. Lond. 11, 185-195.
- Dunham, R.J., 1969b, Vadose pisolite in the Capitan reef (Permian), New Mexico and Texas, In: *Depositional Environments in Carbonate Rocks* (Ed. by G.M. Friedman): Spec. Publ. Soc. Econ. Paleont. Miner., 14, 182-190.
- Erdoğan, B.; Akay, E. and Uğur, M.Ş., 1996, Geology of the Yozgat Region and Evolution of the Collisional Çankırı Basin: *International Geology Review*, 38, 788-806.

- Esteban, M.C., 1976, Vadose pisolite and caliche: Amer. Assoc. Petrol. Geol. Bull., 60, 2048-2057.
- and Klappa, C.F., 1983, Subaerial exposure environments: Carbonate Depositional Environments (Eds. by P.A. Scholle, D. G. Bebout ve C. H. Moore): AAPG. Mem.,33, 2-54.
- Freytet, P. and Plaziat, I.C., 1982, Continental carbonate sedimentation and pedogenesis - Late Cretaceous and Early Tertiary of southern France.: Contrib. Sediment., 12,213.
- Goudie, A., 1972, The chemistry of world calcrete deposits: J. Geol., 80, 449-463.
- Harrison, R.S. and Steinen, R.P., 1978, Subaerial crusts, caliche profiles, and breccia horizons: Comparison of some Holocene and Mississippian exposure surfaces, Barbados and Kentucky: Geol. Soc. Amer. Bull., 89, 385-396.
- Hay, R.L. and Reeder, R.J., 1978, Calcretes of Olduvai Gorge and the Ndolanya Beds of northern Tanzania: Sedimentology, 25, 649-673.
- Hubert, J.F., 1978, Paleosol caliche in the New Haven Arköse, Newark Group, Connecticut: Palaeogeography, Palaeoclimatology, Palaeoecology, 24, 151-168.
- James, N.P., 1972, Holocene and Pleistocene calcareous crust (caliche) profiles: Criteria for subaerial exposure: J. Sed. Petrol., 42, 817-836."
- Kahle, C.F., 1977, Origin of subaerial Holocene calcareous crusts: Role of algae, fungi, and sparmicritization: Sedimentology, 24, 413-435.
- Kara, H. and Dönmez, M., 1990, 1:100000 ölçekli açınasma nitelikli Türkiye Jeoloji Haritaları Serisi, Kırşehir-G17paftası:MTABull.
- Ketin, I., 1982, Genel jeoloji: Yerbilimlerine giriş: Cilt 1,-İTÜ Maden Fak. yayını, 597s.
- Klappa, C.F., 1980b, Rhizoliths in terrestrial carbonates; classification, recognition, genesis and significance: Sedimentology, 27, 613-629.
- Knox, G.J., 1977, Caliche profile formation, Saldanha Bay (South Africa): Sedimentology, 24, 657-674.
- Land, L.S., 1970, Phreatic versus vadose diagenesis in limestone; evidence from a fossil water table: Sedimentology, 14, 175-185.
- Leeder, M.R., 1975, Pedogenic carbonates and field sediment rates: a quantitative model I for alluvial arid-zone lithofacies: Geol. Mag., 112, 257-270.
- Mutter, H.G. and Hoffmeister, J.E., 1968, Subaerial laminated crusts of the Florida Keys: Geol. Soc. Amer. Bull., 79, 183-192.
- Oktay, F.Y., 1981, Savcılı Büyükoba (Kaman) çevresinde Orta Anadolu masifi tortul örtüsünün jeolojisi ve sedimentolojisi: İTÜ Maden Fak. Doç. Tezi (unpublished).
- Platt, N.H., 1989, Climatic and tectonic controls on sedimentation of a Mesozoic lacustrine sequence: The Purbeck of the Western Cameros Basin, Northern Spain: Paleogeography, Paleoclimatology, Paleogeology, 70,187-197.
- Read, J.F., 1976, Calcretes and distinction from stromatolites (ed. by M.R. Walter): Developments in Sedimentology, 20. Amsterdam, Elsevier Sci. Pub., 55-71.
- Reeves Jr.C.C., 1970, Origin, classification and geologic history of caliche on the southern high plains, Texas and Eastern New Mexico: J. of Geol., 78, 352-362.
- Seminiuk, V. and Meagher, T.D., 1981, Calcrete in Quaternary coastal dunes in southwestern Australia: A capillary rise phenomenon associated with plants: J. Sed. Petrol., 51,47-68.

- Steinen, R. P. and Matthews., 1973, Pheratic vs. vadose diagenesis, stratigraphy and mineralogy of a cored borehole on Barbados, W.I.: J. Sed. Petrol., 43, 1012-1021.
- Szalay, A., 1964, Cation exchange properties of humic aside and their importance in the geochemical enrichment of VO₂ and other cations: Geoc. et Cosm. Acta., 28, 1605-1614.
- Tucker, M.E., 1981, Sedimentary Petrology: an introduction, Blackwell Sci. 251p.
- Uygun, A., 1982, Tuzgözü havzasının jeolojisi: MTA Rep.: 7188 (unpublished), Ankara.
- Walls, R.A.; Harris, W.B. and Nunan, W.E., 1975, Calcareous crust (caliche) profiles and early subaerial exposure of Carboniferous carbonates, northeastern Kentucky: Sedimentology, 22, 417-440.
- Wright, V.P.; Platt, N.H. and Wimbleton, W.A., 1988, Biogenic laminar calcretes evidence of calcified root-mat horizons in paleosoils: Sedimentology, 35, 603-620.

PLATES

PLATE-I

Caliche exposure in the Seyrek village:

Figs. 1, 2- Metamorphic-magmatic pebbled-sandy mudstone zone (1st zone), zone of calcite nodules with vertical and horizontal long axes (kn) (2nd zone) and layered-laminated caliche (calcrete) (Lk) zone (3rd zone).

Fig. 3- Calcite nodules of lateral continuity within red mudstone-siltstone (kn).

Fig. 4- Close view of metamorphic pebbles (mç) and calcite nodules (kn).

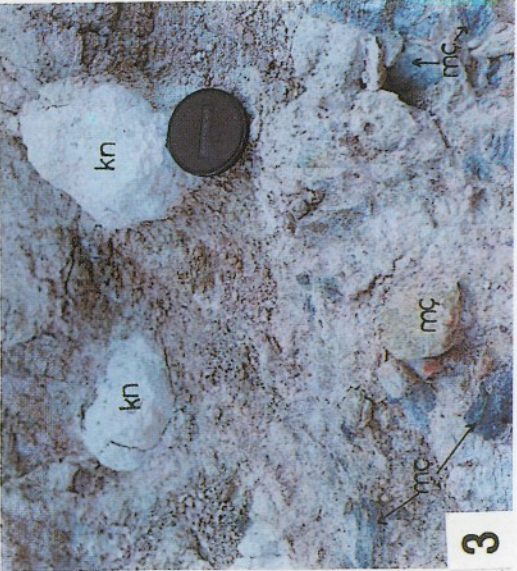
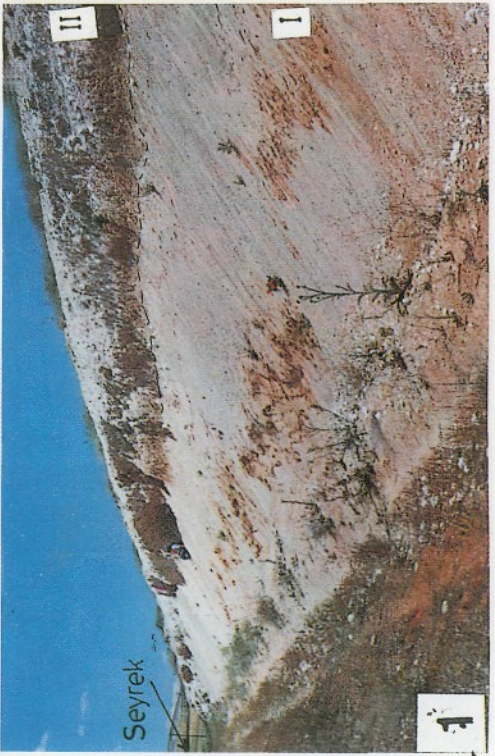


PLATE-II

Fig. 1- Caliche exposure in Çoğun village-Malhüyük hill: I- Transition zone, II- Root tubes (kt) and calcite occurrences with vertical settlement in red mudstones, III- Massive caliche (calcite) zone.

Figs. 2, 4- Tepesidelik caliche exposure:I-Conglomerate-sandstone zone. II- Caliche zone of nodular calcite with vertical long axes in red mudstone-siltstone, ivory (fd) and bone pieces are also observed in mudstone. III- laminated caliche zone.

Fig. 3- Central Kırşehir section: I- Calcite nodules (kn) in red mudstone-siltstone and calcareous caliche zone with vertical longaxes. II- Caliche zone with horizontal long axes. Repetition: I- Caliche zone with vertical long axes, e- Erosion surface.

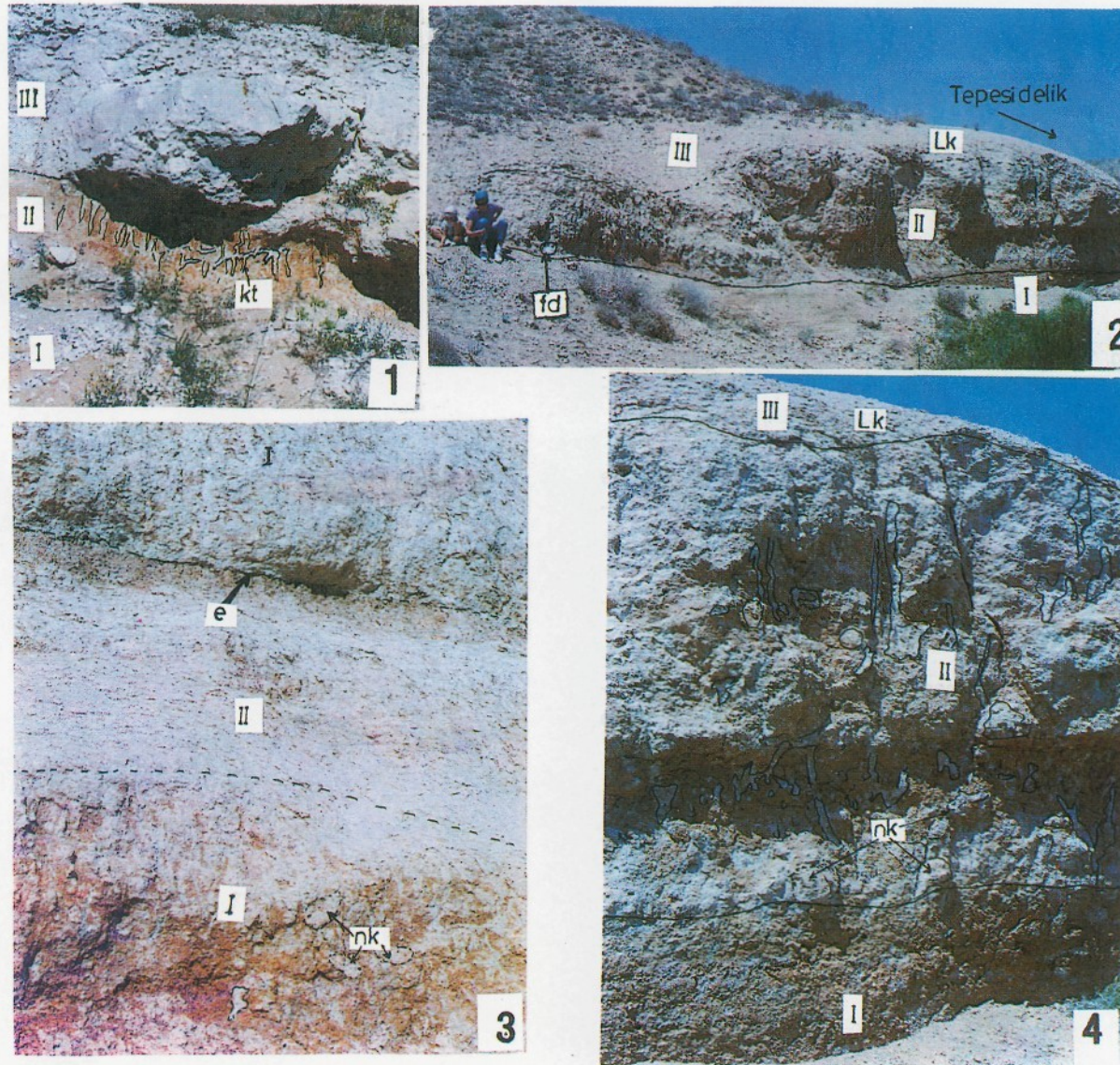


PLATE-III

Figs. 1, 2,3- Caliche occurrence in lacustrine sequence of Kepez village:

Fig. 1- I- Claystone-mudstone zone, II- Platy and nodular calcite (nk) zone. T-Tuffite. III- layered-laminated caliche (calcite) (Lk) zone.

Fig. 2- Calcite nodules (their upper surfaces are bowl-shaped and rough due to dissolution process).

Fig. 3- Calcite nodule and caliche pisolites (kp). T-Tuffite level, e- Erosion surface.

Fig. 4- Caliche exposure in Yenifakılı town: I- Mudstone-siltstone zone. II- Nodular carbonaceous caliche zone with vertical settlement.

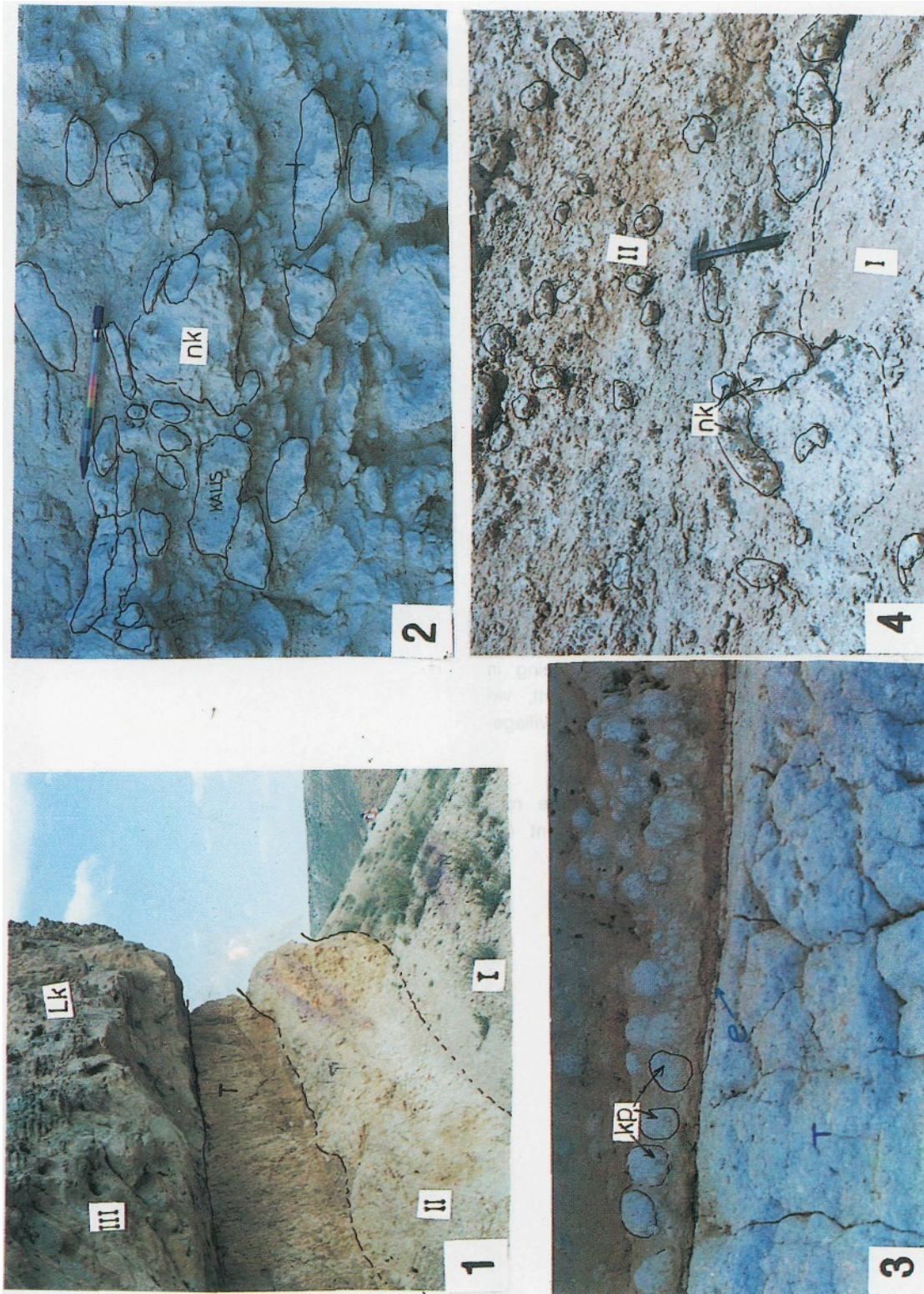


PLATE-IV

Polarizing microscope view of caliches (calcite):

- Fig. 1- Calcrite. Micritic textured and detritic quartz-grained. Tepesidelik village - Tilkideresi.
- Fig. 2- Dissolution voids and sparry calcite (sk) filling these voids, root mold (kk) and pieces (kp). Seyrek village.
- Fig. 3- Vadose silt structure (vs) developing in dissolution void. Ç- Calcite cement, vk- Volcanic rock fragment. Çoğun village- Malhüyük hill.
- Fig. 4- Circular micro fissures around the rock fragment filled with caliche cement (ç). Tepesidelik village - Tilkideresi.

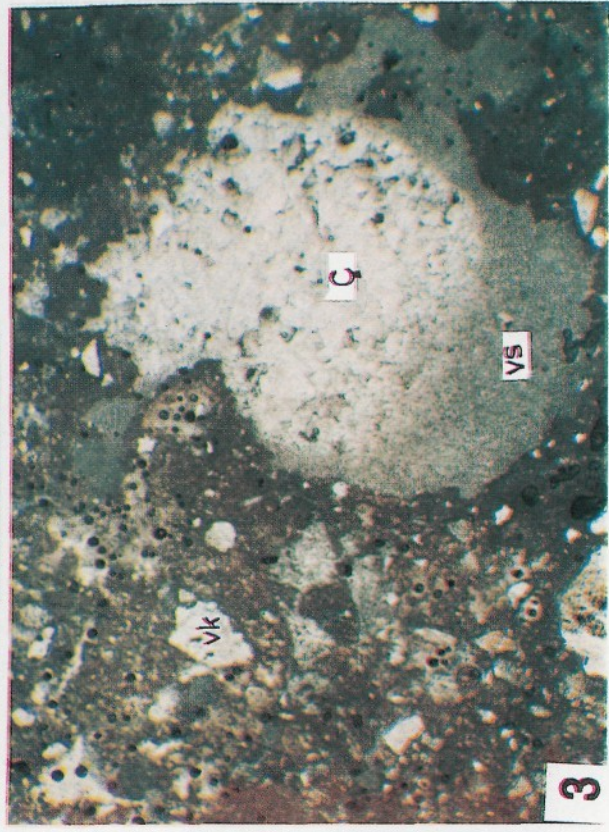
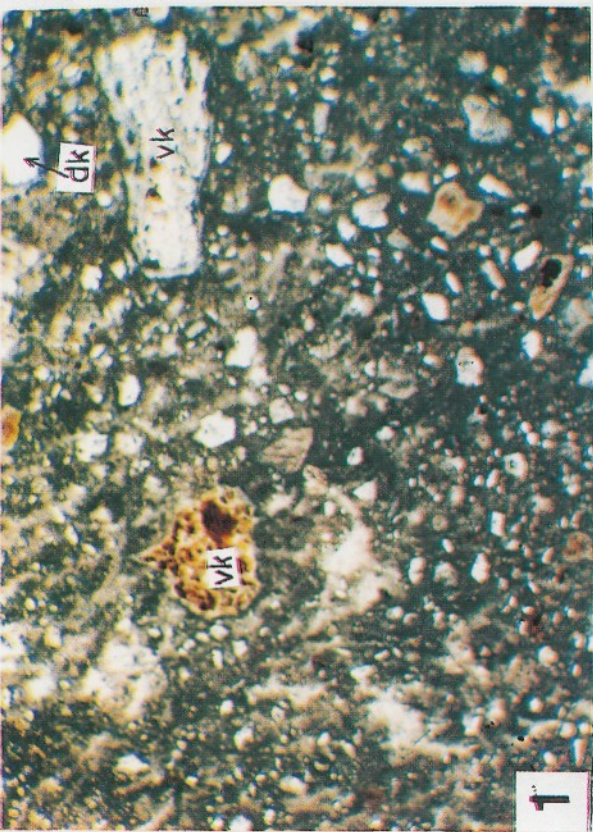
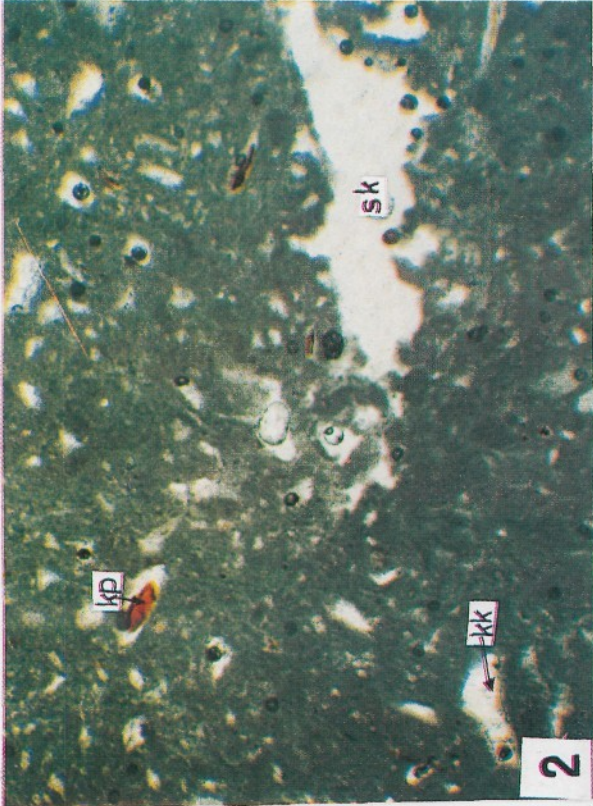


PLATE-V

Fig. 1- Caliche cement. Çoğun village - Malhüyük hill and Figs. 2, 3, 4- Caliche pisolites (Seyrek village): Caliche cement: ç- Stylolite cement, b- Void not filled with calcite.

Figs. 2, 3, 4- Cryptoalgal structures and caliche pisolites (p). me-Microerosion surface, micritic laminated caliche pisolite (p), ml-micritic lamina (membrane), 5- calcite cement (white parts) cryptoalgal laminae (kal).

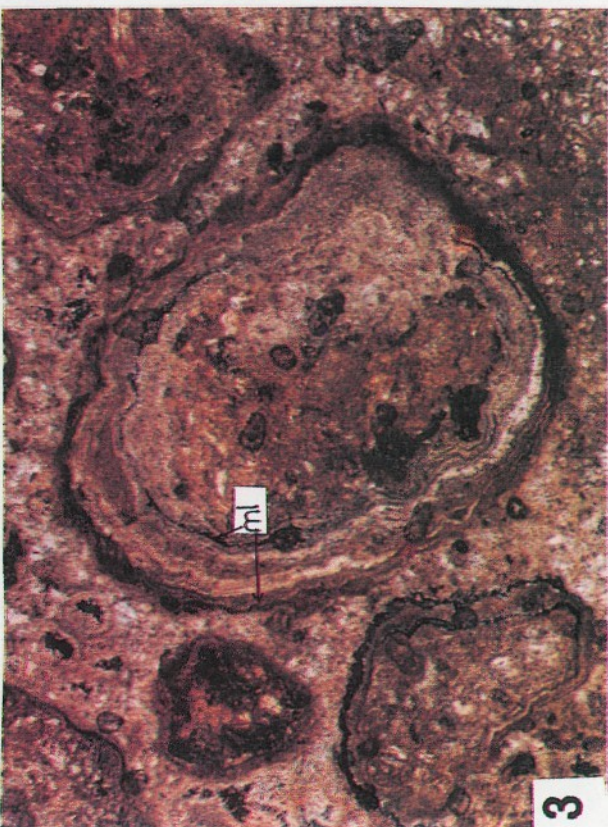
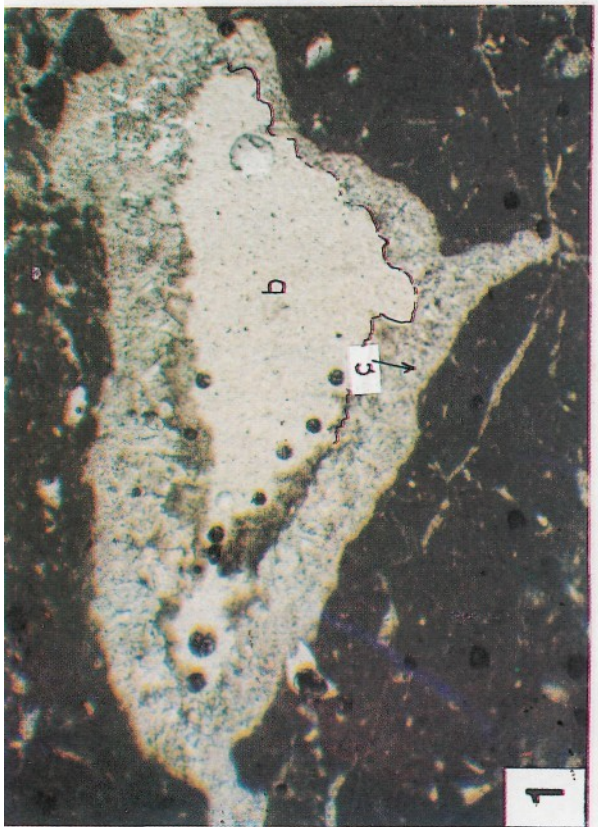
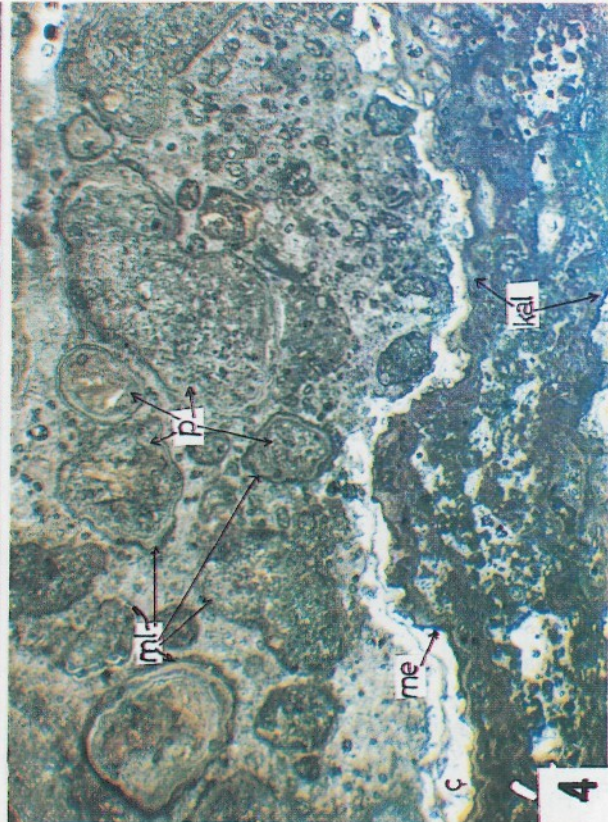
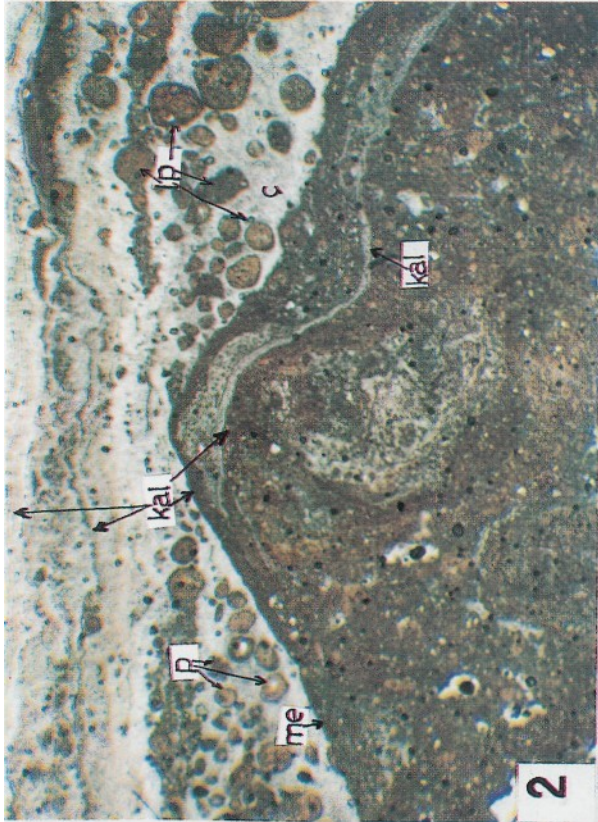


PLATE-VI

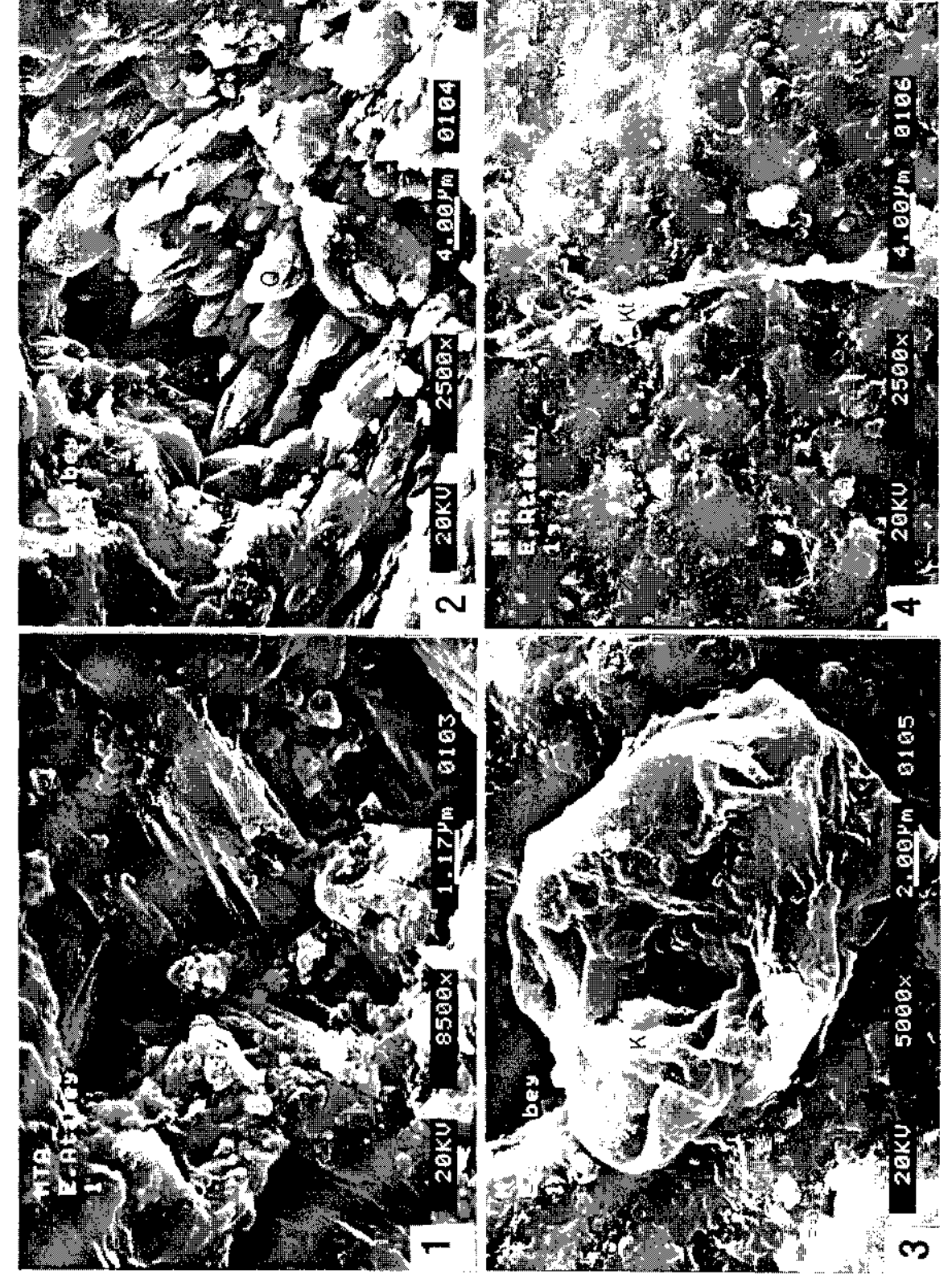
SEM image of laminated caliche (Seyrek village):

Fig. 1- Space-filling secondary calcite crystals (K).

Fig. 2- Autogenic quartz crystals (Q) growing towards the center of space.

Fig. 3- Calcite crystals (K) with dissolution surface.

Fig. 4- Root tube (Kt) within the carbonaceous mud.



THE GEOLOGY OF THE SOUTH OF MANYAS (BALIKESİR) AND TECTONIC SIGNIFICANCE OF BLUESCHISTS

H. Serdar AKYÜZ* and Aral I. OKAY*

ABSTRACT.- The study area comprises mainly Karakaya complex units of Sakarya zone, a granodioritic pluton which cuts the Karakaya complex and unconformably overlying Neogene sedimentary and volcanic rocks. Apart from these, a small blueschist klippe rests on the Karakaya complex. The Karakaya complex in the area studied is made up of Nilüfer unit and tectonically overlying Triassic detritics (Hodul unit and Orhanlar greywacke). Nilüfer unit consists of metabasite-metapelite-marble intercalation at the base and monotonous marbles at the top. Nilüfer unit has undergone greenschist facies metamorphism probably during Late Triassic. Nilüfer unit is in tectonic contact with detritic rocks bearing neritic limestone blocks of Carboniferous-Permian age and rare spilite blocks. A blueschist klippe, which consists of metabasites, is observed on the Nilüfer unit and on the Triassic detritics to the south of Manyas. The metamorphic age of the blueschist is Late Cretaceous as reported from south of Mustafakemalpaşa. The exhumation of blueschists mainly occurred during the latest Cretaceous. Thus, the thrusting of blueschist onto Karakaya complex units took place probably during the Paleocene continent-continent collision. Main blueschist belt is located to the south of klippe which indicates a northward vergence. This shows that back-thrusting occurred during continent-continent collision in the western Anatolia.

INTRODUCTION

Western Anatolia comprises different tectonic units which came together as a result of continent-continent collisions during the Tertiary (Fig.1, Şengör and Yılmaz, 1981; Okay et al., 1996). These continental fragments are separated by suture zones. Izmir-Ankara suture is one of the most important suture, which separates Pontides to the north from the Anatolidae Tauride units in the south. Tavşanlı zone, which consists of ophiolite, ophiolitic melange and blueschist, formed during the northward subduction of Neo-Tethys ocean, is observed to the south of the Izmir-Ankara suture between Bursa and Ankara (Okay, 1984), while Sakarya zone is located to the north of the suture (Fig. 1). The Sakarya zone is made up of Permo-Triassic arc-trench rocks named as Karakaya complex (Tekeli, 1981; Okay et al., 1990, 1996; Akyüz and Okay, 1996) that formed during the closing of Paleo-Tethys and unconformably overlying Jifrassic-Cretaceous sediments (Fig. 2). Izmir-Ankara suture, which constitutes the boundary between Sakarya and Tavşanlı zones, is represented by a strike-slip fault between Bursa and Eskişehir, which was active even after the Miocene (Harris et al., 1994). The area to the south of Manyas is important as shows the pre-Miocene relation between the Tavşanlı zone and Sakarya zone. In this area, blueschists lie on the Karakaya complex as a horizontal klippe.

For these reasons, the region south of Manyas was studied and mapped in detail (Akyüz, 1995). This paper comprises the main results of this study.

In the study area there are only very few previous studies. The most important is a published geological map in the scale of 1:100.000 and its explanations, which comprises the eastern part of the study area (Ergül et al., 1986); another study is related to general geology and Tertiary volcanism of the area (Ercan et al., 1990). Moreover, there are some MTA reports which constitute the base to these publications.

There are three main units in the study area. These are Permo-Triassic Karakaya complex units, which cover nearly half of the study area, a small blueschist klippe and Neogene magmatic and sedimentary rocks, which unconformably cover or cut the older units (Fig. 3).

KARAKAYA COMPLEX

The major part of the study area is made up of Karakaya complex units (Fig. 3). The previous studies in the Biga peninsula have indicated that Karakaya complex is composed of four tectono-stratigraphic units. Permo-Triassic Nilüfer unit is made up of metabasite, marble and phyllite which is undergone

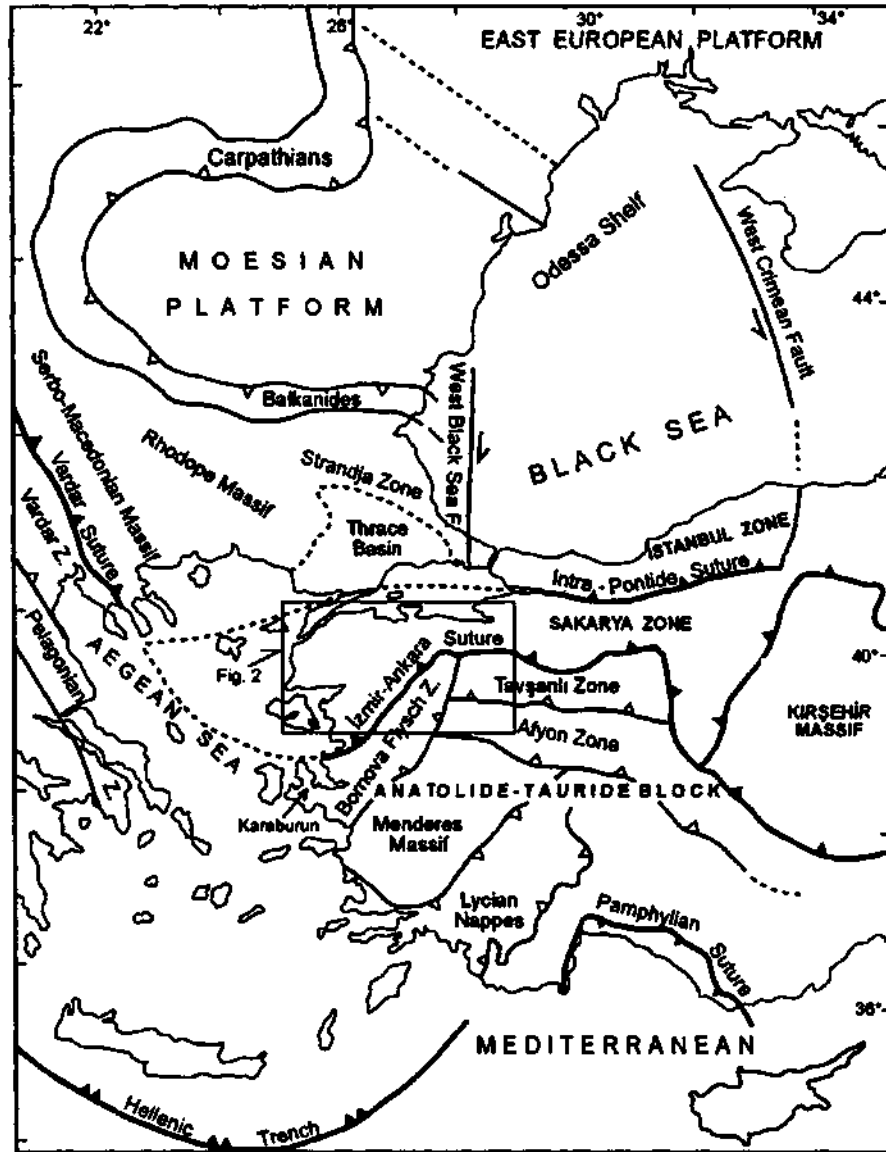


Fig. 1- Tectonic map of western Turkey and the surrounding area. The thick barbed lines show the Mesozoic sutures with their primary subduction polarities. The thinner lines with open triangle indicate major intra-continental thrusts (after Okay et al., 1996).

greenschist facies metamorphism, tectonically overlying clastic rocks with Permian limestone blocks (Hodul unit and Orhanlar greywacke) and Permo-Triassic Çal unit, which is composed of basic volcanic rock, greywacke and pyroclastic rock (Okay et al., 1990). All Karakaya complex units except Çal unit exist in the study area.

Nilüfer unit

This unit was named as Fazlıkonağı formation by Ergül et al., (1986) and Ercan et al., (1990) and in the absence of paleontological data was considered as Upper Paleozoic. This unit is similar to Nilüfer unit

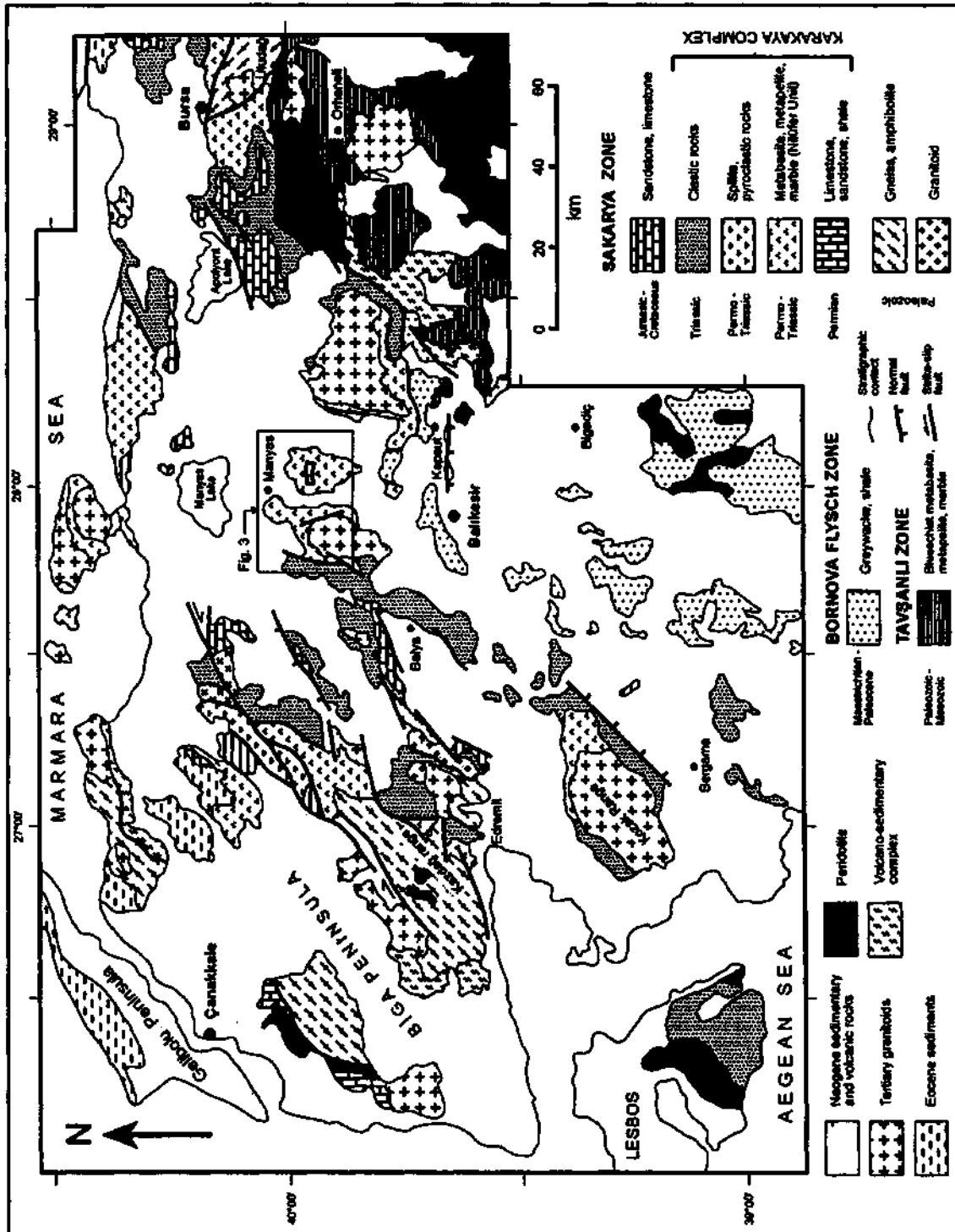


Fig. 2- Simplified geological map of northwestern Turkey (modified after Okay et al., 1996).

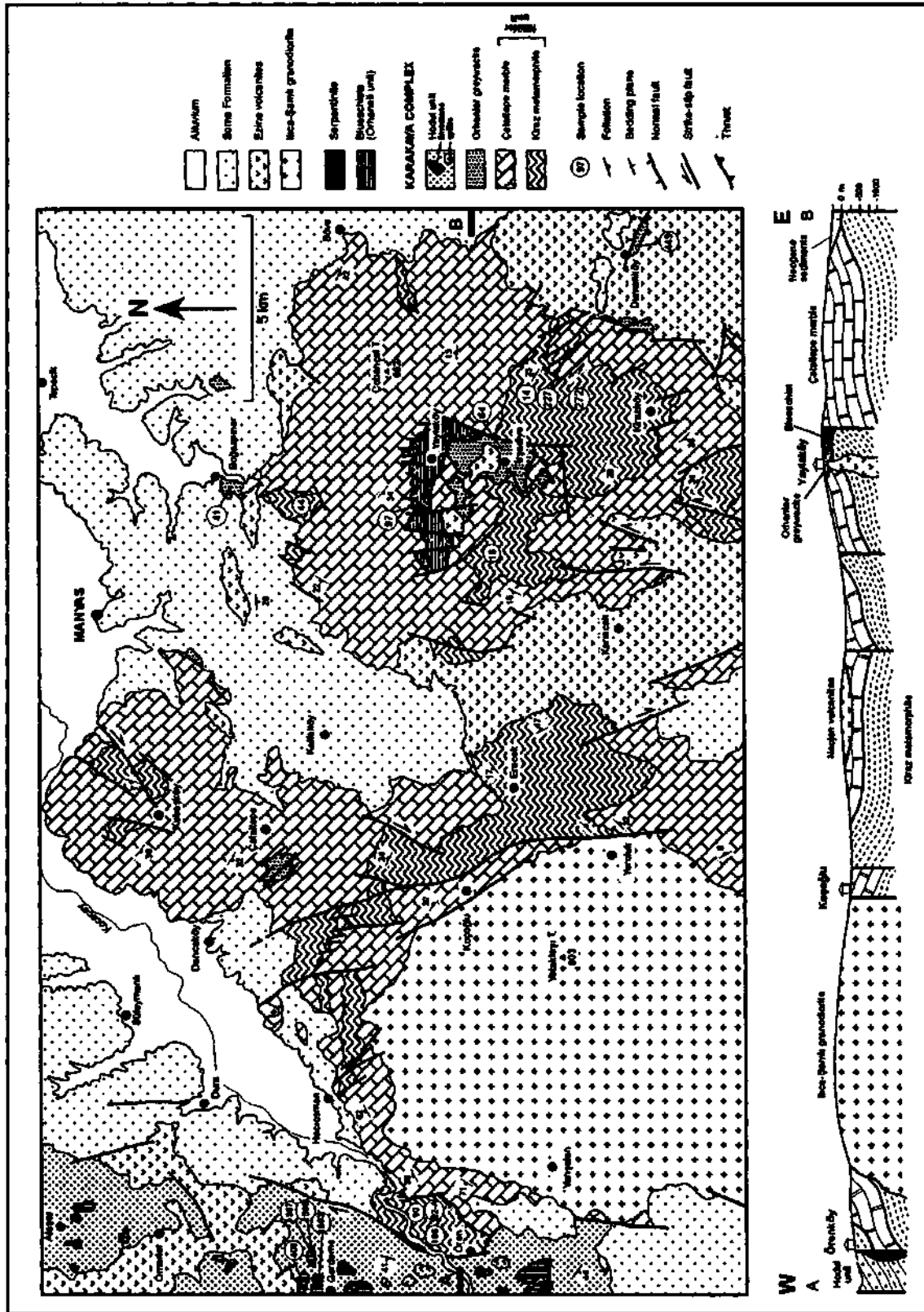


Fig. 3- Geological map and section of the Manyas region. For location see Fig. 2.

lithologically and stratigraphically that crops out extensively in NW Anatolia. Moreover, the name of Fazlıko-nağı formation is also used for Upper Cretaceous blueschists (Ergül et al., 1986). Thus, the Nilüfer unit was used in this study.

Nilüfer unit was divided into two formations. These are Kiraz metamorphite at the base, composed of volcano-sedimentary rocks, and Çataltepe marble at the top (Fig. 3 and 4).

Kiraz metamorphite. - It consists of mainly metabasite and metapelite and rarely quartzschist and calcschist. The best outcrops are around Erecek and north of Kirazköy (Fig. 3). All outcrops have a foliation and locally formed preferred mineral orientation. Kiraz metamorphite is in tectonic contact with Hodul unit to the

samples (samples 18, 44, 90, 92-A and 106) are analysed geochemically (Table 2) to understand the origin and tectonic setting of metabasites of Kiraz metamorphite. Si ratios range between %48-56 and Al %13-16. The results are concentrated on basalt area on Le Maitre (1989) diagram. These samples represent island arc tholeiite in Mullen (1983) diagram.

Micaschists constitute %25-30 of Kiraz metamorphite. Their common mineral assemblage is muscovite + biotite + quartz + chlorite + plagioclase ± epidote ± calcite ± opaque. One sample (sample 14), which is composed of muscovite, biotite, quartz and plagioclase, was analysed under the electron microprobe (Table 1). Quartzschist and calcschist are seen as interbeds of 5-30 m in thickness or as lenses and comprise %5-10 of Kiraz metamorphite. These lithologies are intercala-

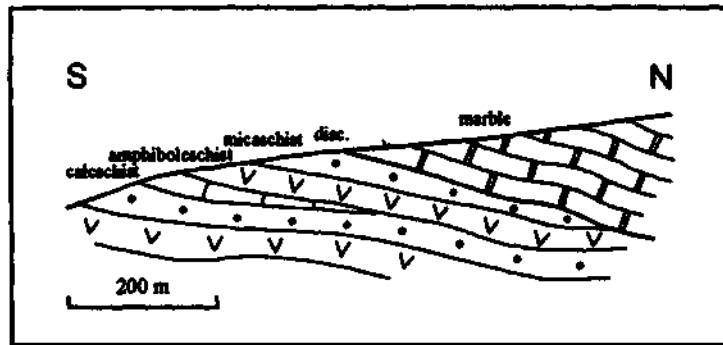


Fig. 4- Sketch section showing the relation between Kiraz metamorphite and Çataltepe marble to the north of Kirazköy.

west of the study area. The thickness of the Kiraz metamorphite in the study area is about 1500 m.

Metabasite constitutes %50-60 of Kiraz metamorphite. The common mineral assemblage of metabasite is calcic amphibole + albite/oligoclase + epidote + chlorite + sphene ± calcite ± quartz ± opaque. Calcic amphibole locally shows strong zoning. Two samples from metabasite were analysed with electron microprobe and mineral analyses were given in Table 1. In zoned amphibole, actinolitic composition is found in the core while tschermakitic composition occurs in rim (Table 1; Fig. 5). Plagioclase is either oligoclase or albite in composition. In some samples they occur together. Five

metabasites are analysed with electron microprobe and mineral analyses were given in Table 1. Mineral paragenesis of metabasite and metapelite indicate that Kiraz metamorphite has undergone upper greenschist facies metamorphism.

Çataltepe marble. - Kiraz metamorphite is overlain by marble around Kirazköy and Erecek. In these areas, marbles are underlain by metabasite, micaschist and quartzschist in short distances. This probably indicates that there was an unconformity between them before regional metamorphism. Kiraz metamorphite was thrust on Çataltepe marble around Örenköy to the west of the study area. Çataltepe marble is tectonically overlain by blueschist and Omanlar greywacke around Yaylaköy (Fig. 3 and 4).

Table 1- Chemical compositions of some index minerals from metabasite of Kiraz metamorphite.

	amphibole				epidote			chlorite			plagioclase	
	227	272	core	rim	227	272	272	227	272	272	272	14
SiO ₂	53.34	45.00	54.09	44.05	37.36	37.73	27.98	27.47	65.07	62.43		
TiO ₂	0.07	0.45	0.09	0.41	0.08	0.12	0.08	0.07	0.01	0.11		
Al ₂ O ₃	3.58	11.87	3.47	13.19	22.62	22.96	21.85	21.89	23.02	24.71		
Cr ₂ O ₃	0.25	0.04	0.06	0.07	0.02	0.02	0.12	0.08	0.01	---		
Fe ₂ O ₃	8.78	12.86	8.58	13.72	12.15	11.92	13.62	14.26	0.11	0.16		
MgO	16.93	12.21	17.95	11.60	0.01	0.02	21.99	22.29	0.01	0.00		
MnO	0.23	0.23	0.18	0.22	0.11	0.08	0.15	0.16	0.00	---		
CaO	12.43	11.53	12.30	11.42	23.61	23.54	0.16	0.26	4.23	3.88		
Na ₂ O	0.56	1.70	0.43	1.81	0.05	0.02	0.00	0.02	6.75	8.42		
K ₂ O	0.12	0.09	0.09	0.29	0.01	0.01	0.02	0.06	0.06	0.28		
Total	96.29	95.98	97.24	96.78	96.02	96.42	85.97	86.56	99.27	100.00		
Structural formula based on:												
	23 O	23 O	23 O	23 O	25 O	25 O	28 O	28 O	28 O	8 O	8 O	8 O
Si	7.61	6.47	7.62	6.29	3.23	3.24	5.62	5.51	2.86	2.76		
Ti	0.01	0.05	0.01	0.05	0.01	0.01	0.01	0.01	0.00	0.00		
Al ^{IV}	0.39	1.53	0.36	1.71								
Al ^{VI}	0.21	0.49	0.20	0.52	Al 2.30	2.32	5.18	5.18	1.19	1.28		
Cr	0.03	0.01	0.01	0.01	0.00	0.00	0.02	0.01	0.00	---		
Fe ³⁺	0.04	0.49	0.33	0.60								
Fe ²⁺	1.01	1.06	0.68	1.04	Fe 0.88	0.86	2.29	2.39	0.00	0.01		
Mg	3.60	2.62	3.77	2.47	0.00	0.00	6.59	6.67	0.00	0.00		
Mn	0.03	0.03	0.02	0.03	0.01	0.01	0.03	0.03	0.00	---		
Ca	1.90	1.78	1.86	1.75	2.19	2.17	0.03	0.06	0.20	0.18		
Na	0.16	0.47	0.12	0.50	0.01	0.00	0.00	0.01	0.58	0.72		
K	0.02	0.02	0.02	0.05	0.00	0.00	0.01	0.02	0.00	0.02		
Total	15.01	15.02	15.02	15.02	8.63	8.61	19.80	19.89	4.63	4.97		
									alb 74.0	78.4		
									or 0.4	1.7		
									an 25.6	19.9		

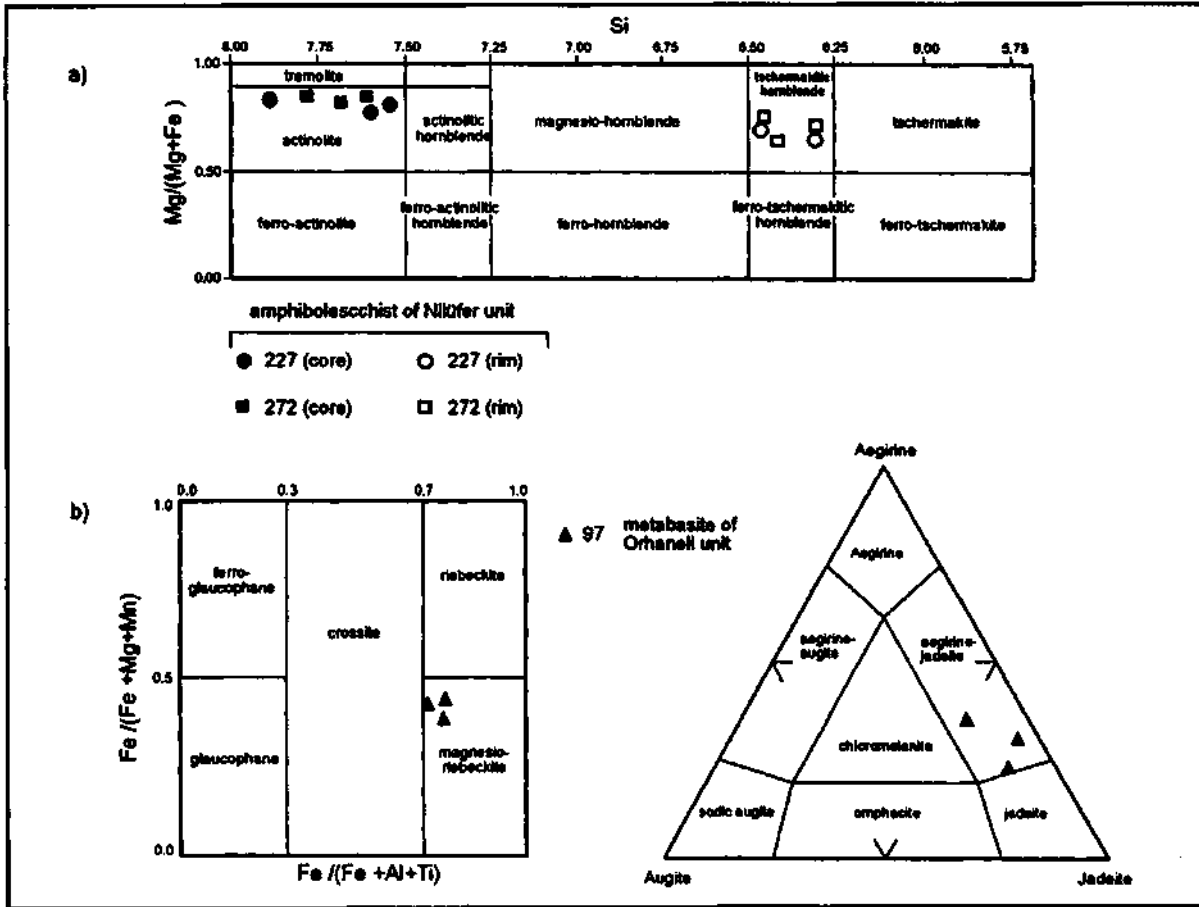


Fig. 5- Amphibole and pyroxene compositions from metabasites of Nilüfer (a) and Orhanlı (b) units.

Çataltepe marble is white-grey, holocrystalline and forms a homogenous sequence. Rare siliceous bands, whose thickness ranges from several cm to 4 cm, are seen within the marble. It is observed that marbles locally preserved primary bedding on the roadway between Manyas-Darıcaköy and that they have middle to thick bedding. This data indicates that marbles are deposited in shallow marine environment. The thickness of the marble is more than 700 m.

The age and tectonic environment of the Nilüfer unit. - No fossils have been found in the Nilüfer unit within the study area. However, Kaya and Mostler (1992) reported Middle Triassic conodonts in carbonate interbeds intercalated with metabasites from the Kozak

range in northwest Anatolia. Moreover, it is known from different parts of NW Anatolia that Nilüfer unit is unconformably overlain by Liassic sediments (Okay et al., 1990), thus, the depositional age of the Nilüfer unit is Triassic and metamorphic age is Late Triassic.

Nilüfer unit covers large areas throughout the Sakarya zone extending from Biga peninsula to eastern Black Sea area (Okay et al., 1990, 1996). Such thick and extensive volcano-sedimentary successions represent basins which is adjacent to active island-arc (Dickinson and Seely, 1979). Similar volcano-sedimentary successions were reported from New Zealand (Houghton and Landis, 1989) and from present-day Fiji volcanic arc (Hathway, 1994).

Table 2- Geochemical analyses of metabasites in Kiraz metamorphite.

Sample	18	44	90	92-A	106
SiO ₂	56.40	54.03	48.68	50.06	48.97
TiO ₂	1.65	1.30	1.13	0.87	1.07
Al ₂ O ₃	15.25	13.05	16.10	12.93	15.88
Fe ₂ O ₃ *	10.27	12.28	11.18	13.33	11.63
MgO	3.61	6.37	6.72	7.64	6.46
MnO	0.19	0.20	0.17	0.22	0.17
CaO	7.13	8.24	11.89	10.54	11.69
Na ₂ O	3.97	3.38	3.03	3.11	3.14
K ₂ O	0.11	0.22	0.10	0.22	0.22
P ₂ O ₅	0.45	0.14	0.07	0.10	0.11
LOI**	0.46	0.62	1.48	0.68	0.16
Total	99.49	99.82	100.65	99.70	99.51
Cr	26.8	33.8	---	370.3	487.4
Ni	11.4	32.5	---	115.8	100.6
Co	27.6	42.0	---	47.6	33.3
V	289.0	477.7	---	353.4	257.3
K	913.0	1826.0	---	1826.0	1826.0
Rb	2.4	6.6	---	2.6	4.4
Ba	9.0	6.6	---	22.8	12.1
Sr	282.4	114.0	---	176.6	172.0
Ga	20.7	13.7	---	10.7	13.4
Nb	2.7	1.9	---	4.2	2.2
Zr	54.3	68.4	---	48.5	62.3
Ti	9892.0	7793.0	---	5261.0	6415.0
Y	20.9	20.7	---	18.1	21.6
* Fe ₂ O ₃ represents total Fe (FeO+Fe ₂ O ₃)					
** LOI: Lost of ignition					

Orhanlar greywacke

This unit is composed of greywacke and shale with limestone and rare spilite blocks. Ercan et al., (1990) defined this unit together with Late Cretaceous units and called them Yayla Melange. However, the lithological characteristics of this unit and the fact that it contains Permian limestone blocks indicate that it belongs to the Orhanlar greywacke which was described in the Biga peninsula. The Orhanlar greywacke technically overlies Nilüfer unit in area to the west of Çataltepe village and around İrşadiye, while it is covered by Neogene sedimentary rocks (Fig. 3 and 6).

The sandstone of Orhanlar greywacke is made up of semi-angular, medium to poorly sorted quartz, feldspar, lithic fragments, mica, chert and opaque grains within, a clay matrix of % 16-20. Quartz is mostly polycrystalline and rarely monocrystalline. K- feldspar-plagioclase ratio is nearly equal. Lithic fragments were derived mostly volcanic and rarely metamorphic and sedimentary rocks. Rare, grey-brownish shale interlayers changing from several cm to 3 m were observed within greywackes. The matrix of Orhanlar greywacke is intensely sheared and its primary structures have been destroyed. It is hard to understand the stratigraphic features and thickness of the Orhanlar greywacke due to intense shearing, its homogenous features and absence of a stratigraphic basement.

Grey-bluish, middle bedded limestone and rare spilite blocks are important components of the Orhanlar greywacke. Limestone blocks are seen around Dumanköy and Boğazpınar and between İrşadiye-yayla. Their size range from 0.5 to 150 m. Spilite blocks are rare and their sizes are less than 20 m.

While, there is no paleontological data from the matrix of Orhanlar greywacke, the limestone blocks in the Orhanlar greywacke are highly fossiliferous. Samples collected from Boğazpınar, İrşadiye and Dumanköy have the following fossils: Schwagerinidae, *Schubertella* sp., *Deckerella* sp., *Paleotextularia* sp. (Permian, sample no: 41); *Globivalvulinasp.*, *Tetrataxissp.*, (Carboniferous-Permian, sample no: 64); *Climacammina* sp., *Cribrogenerina* sp., *Eotuberitina* sp., *Glomospira* sp. (Upper Permian, sample no: 449). Orhanlar greywacke is unconformably overlain by Liassic sediments as well as other Karakaya complex units (e.g. Aygen, 1956; Okay et al., 1990), thus, its age is constrained as Permian-Triassic.

The blocky and intensely sheared structure of Orhanlar greywacke points out that it was formed in a tectonically active environment. Similar sequences were reported from present-day trench zones (e.g. Peru-Chile: Thornburgh and Kulm, 1987; Middle America: McMillen et al., 1982; Aleutian: Underwood, 1986; Cascadia: Schweller and Kulm, 1978; Japan: Boggs, 1984; Hellenic trench: Stanley and Maldonado, 1981), thus, Orhanlar greywacke is accepted as trench deposit.

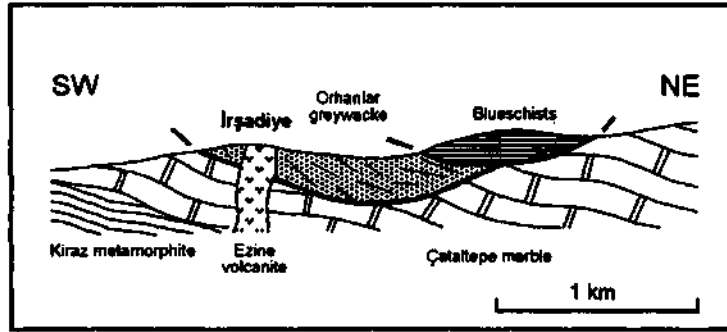


Fig. 6- Sketch section showing the relations among Nilüfer unit, Orhanlar greywacke and blueschist around Yaylaköy.

Hodul unit

Hodul unit is composed of grey-yellowish white arkosic sandstone and dark shale with Permian limestone and spilite blocks. It crops out to the west of Örenköy and around Ömerler to the NW of the study area (Fig. 3). These outcrops form the northern end of a belt trending NNE-SSW, 8-10 km in width and 80 km in length extending from İvrindi to Manyas (Fig. 2, Okay et. al., 1990, 1996). This unit is also defined as Karakaya complex by Ercan et. al., (1990).

Hodul unit is in subvertical tectonic contact with the Nilüfer unit in the east and is covered by Neogene volcanic and sedimentary rocks in the north and south (Fig. 3). Hodul unit has a monoclinical structure younging westward in the study area. The bottom part of the sequence in the study area starts with middle bedded sandstone intercalated with rare shale and micritic limestone (Fig. 7). Small and rare limestone and spilite blocks are seen upward. Sandstone gets dirty in this part due to increasing amount of the matrix and lithic fragments while shale interbeds thicken. The upper part of the sequence has a olistostromal character with limestone blocks (Fig. 7 and 8). The presence of a sheared zone and plastic deformation of several cm around limestone blocks indicates that the limestone blocks have slid into the detritics during the sedimentation. The thickness of Hodul unit in the study area is 1200 m. The Hodul unit shows no regional metamorphism in the study area.

Arkosic sandstone of Hodul unit is made up of semi-angular, well-sorted quartz, feldspar, mica, chert and lithic fragments in clay matrix of %6-10. Quartz are both mono- and polycrystalline. K-feldspar is represented by microcline and its amount is relatively more than plagioclase. The presence of microcline shows that sandstone took the material from a granitic source. Lithic fragments increase towards the top of the sequence which have mostly volcanic and rarely sedimentary rock origin.

The amount and size of limestone blocks increases towards the top of the unit. These grey-bluish blocks are sparitic and mostly middle to thick bedded and rarely massive. The size of blocks range from several cm to 600 m. The samples taken from the blocks gave Upper Carboniferous to Upper Permian ages. Two samples (no: 1503 and 1568) from just east of Gerdeme village contain fusulinid and small forams giving a Moscovian age: *Eostaffella* sp., *Pseudoendothyra* sp., *Verella* sp., *Profusulinella latispinalis* Safonova, *Profusulinella* aff. *parva* (Lee and Chen), *Eotuberitina* sp., *Tuberitina* sp., *Diplosphaerina* sp., *Endothyra* sp., *Globivalvulina* sp., *Monotaxinoides* sp., *Glomospira* sp. (Leven and Okay, 1996). Another sample (no:1499) from west of Gerdeme village has a rich fusulinid and small foram fauna giving Upper Permian age: *Nankinella* sp., *Schubertella* sp.; *Verbeekina* sp., *Eotuberitina* sp., *Tuberitina* sp., *Diplosphaerina* sp., *Globivalvulina* sp., *Glomospira* sp., *Nodosaria* sp., *Pachyphloia* sp., *Climacammina* sp., *Lasioliscus* sp. In a limestone block to the north of Gerdeme (no:409), *Glomospira*

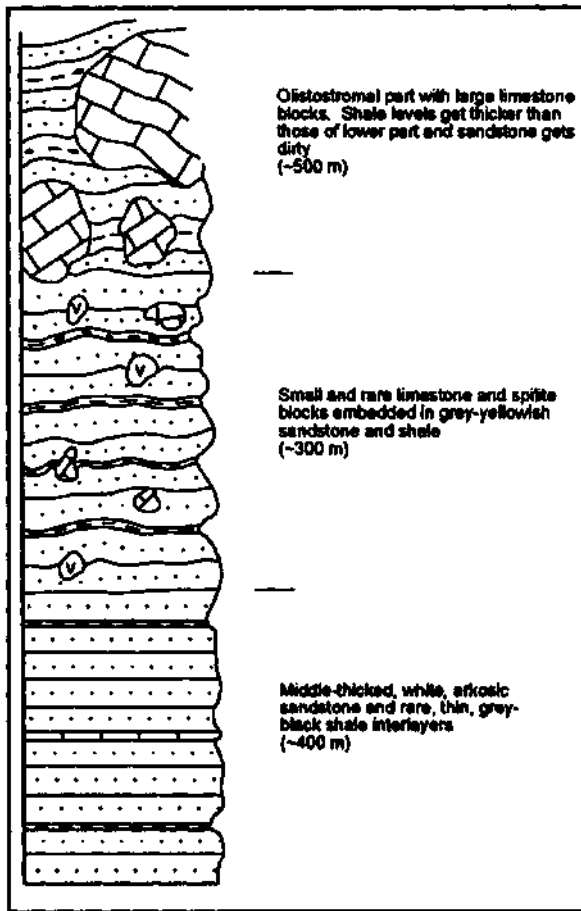


Fig. 7- Generalized columnar section of Hodul unit to the north of Ören.

sp., *Dunbarula* sp., *Paleotextularia* sp. giving Upper Permian age has been determined. Moreover, limestone pebbles in a debris flow which lies under limestone block have Upper Permian fossils: *Eopolydiexodina* sp., *Tuberitina* sp.

A few spilitic blocks are present within the Hodul unit. They have amygdaloidal texture and are composed of feldspar microliths and phenocrysts, monoclinic pyroxene and chlorite in vitrophyric groundmass. Amygdaloids were filled by mostly chlorite and rarely quartz.

There are no paleontological data within the detritic matrix of Hodul unit in the study area. The youngest age determined from limestone blocks is Upper Permian

(Murgabian-Midian). However, Norian macrofossils were reported in shale and siltstones which are equivalent to the upper part of Hodul unit in the Balya and İvrindi areas in the southern continuation of this olistostromal belt (Aygen, 1956; Leven and Okay, 1996). Hodul unit is covered by Liassic sediments outside the study area (e.g. Aygen, 1956; Genç, 1986; Okay et al., 1990). These data show that the age of the Hodul unit is Late Triassic. The presence of abundant feldspar indicates that Hodul unit was rapidly deposited in a fault-controlled basin. Okay et al., (1990, 1996) proposed that Hodul unit represents a fore-land environment.

BLUESCHISTS

Blueschists cover a large area between Orhaneli, Tavşanlı, Eskişehir and Sivrihisar in NW Anatolia (Okay, 1984, 1986). This belt, which was named as Tavşanlı zone by Okay (1984), consists of regionally metamorphosed, thick and regular sequence of blueschists (Orhaneli unit) at the base, and tectonically overlying ophiolitic melange and peridotite. Orhaneli unit is composed of metapelitic rocks bearing jadeite, glaucophane, chloritoid and lawsonite (Okay and Kelley, 1994) at the base with more than 1 km in thickness. They are conformably overlain by a thick homogeneous marble sequence. At the top of the Orhaneli unit, there are metabasites, metacherts and metashales (Okay, 1981). The basement of the blueschist sequence is not observed in the Tavşanlı zone. According to Ar/Ar dating on phengite and sodic amphibole in blueschist, the age of HP/LT metamorphism is late Cretaceous (Okay and Kelley, 1994; Harris et al., 1994). Orhaneli unit represents the passive northern margin of Anatolide-Tauride platform. This passive margin was subducted in an intra-oceanic subduction zone following the consumption of Neo-Tethyan oceanic lithosphere and underwent blueschist facies metamorphism (Okay et al., 1984, 1986) similar to the case in Oman (e.g. Goffe et al., 1988; Searle et al., 1994; Michard et al., 1994).

The most significant feature of the area studied is the exposure of the basal tectonic contact of the blueschist. A small blueschist klippe rests on marbles of Nilüfer unit around Yaylaköy, 10 km south of Manyas (Fig. 6). Thrust plane is marked by serpentinite

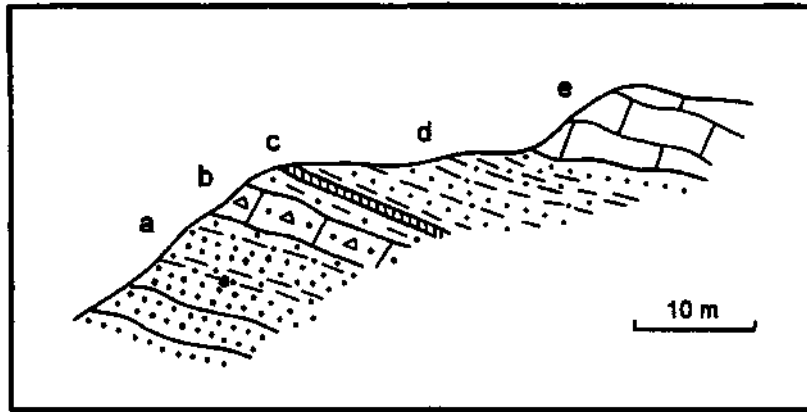


Fig. 8- The transition from arkosic sandstones to limestone olistoliths in the Hodul unit (northeast of Gerdeme village, locality 1568). a- arkosic, white sandstone, b- debris flow with limestone pebbles of 10-15 cm of size, c- black chert, d- brown-greenish brown micaceous sandstone, siltstone, shale, e- Middle Carboniferous (Moskovian) limestone olistolith; the determined fusulinid and small forams: *Eostaffella* sp., *Pseudoendothyra* sp., *Verella* sp., *Profusulinella* aff. parva (Lee and Chen), *Profusulinella latispiralis* Safonova, *Tuberitina* sp., *Diplosphaerina* sp., *Endothyra* sp., *Eotuberitina* sp., *Globivalvulina* sp., *Monotaxinoides* sp.

slices. Serpentinites become dominant westward. Metabasites have a bluish color due to common presence of sodic amphibole. Metamorphic mineral paragenesis in the metabasite is sodic amphibole + lawsonite + sodic pyroxene + chlorite + sphene \pm quartz. Sodic amphibole and lawsonite comprise %70-80 of rock. Sodic pyroxene has formed during the first stage of metamorphism and substitutes igneous augite. Relic igneous augite is preserved in some massive metabasites. The mineral paragenesis and petrographic characteristics of these blueschists are similar to blueschists reported from Tavşanlı zone (Okay, 1980, 1981). One metabasite sample (no: 97) was analysed under the electron microprobe. In this sample, sodic amphibole is magnesio-riebeckite and sodic pyroxene is aegirine-jadeite and contain %65 of jadeite (Table 3; Fig. 5). P-T conditions of metamorphism based on 65 % jadeite, content of sodic pyroxene, and the presence of lawsonite are temperatures less than 450 °C and pressures more than 9 kbar. Okay and Kelley (1994), who analysed blueschist metapelite to the south of Mustafakemalpaşa, reported that the condition of blueschist metamorphism was 430 ± 30 °C and 20 ± 2

kbar based on chlorite-glaucophane jadeite paragenesis in metapelites.

NEOGENE MAGMATIC AND SEDIMENTARY ROCKS

İlica-Şamlı granodiorite

İlica-Şamlı granodiorite is a large leucocratic pluton located to the SW of the study area. The petrology and petrography of the pluton was studied by Bürküt (1966). The age of the pluton was determined as 23-25 Ma based on K/Ar method on orthoclase and hornblende (Ataman, 1973) and 20-23 Ma based on Rb/Sr method on biotite (Bingöl et al., 1982). Thus, the age of the pluton is Late Oligocene-Early Miocene.

İlica-Şamlı granodiorite cuts the Nilüfer and resulted in contact metamorphism. Aplite, quartz and rare pegmatite dykes and veins cut both granodiorite and country rocks. İlica-Şamlı granodiorite is made up of quartz, plagioclase, K-feldspar, rare biotite, hornblende,

and accessory epidote, sphene, tourmaline, zircon, ilmenite and apatite. This pluton is granodiorite in the Le Bas and Streckeisen (1991) classification.

Ilica-Şamlı granodiorite is surrounded by marble. Especially to the northern contact of pluton, a contact metamorphic zone is seen represented by idocrase-garnet bearing skarn zone with 0.5-2 km in width. The porphyritic texture of the Ilica-Şamlı granodiorite and its sharp contact with country rocks point out to shallow level emplacement of the pluton.

Table 3- Representative mineral analyses from metabasites of Orhaneli unit (no: 97).

	sodic amphibole	sodic pyroxene	lawsonite	chlorite
SiO ₂	55.33	57.28	40.83	27.57
TiO ₂	0.09	0.06	0.34	0.04
Al ₂ O ₃	3.03	15.94	31.57	15.85
Cr ₂ O ₃	0.01	0.01	0.04	0.02
Fe ₂ O ₃	21.92	7.56	1.80	23.64
MgO	8.46	1.98	0.09	18.73
MnO	0.30	0.09	0.03	0.69
CaO	0.64	3.73	16.98	0.27
Na ₂ O	7.02	13.00	0.03	0.04
K ₂ O	0.04	0.01	0.01	0.02
Total	96.84	99.66	91.72	86.87
Structural formula based on:				
	23 O	6 O	8 O	28 O
Si	7.94	2.00	2.07	5.80
Ti	0.01	0.00	0.01	0.01
Al ^{IV}	0.06	0.00	0.00	2.20
Al ^{VI}	0.46	0.65	1.89	1.74
Cr	0.00	0.00	0.00	0.00
Fe ³⁺	1.54	0.22	0.08	0.44
Fe ²⁺	1.09	0.00	---	3.72
Mg	1.77	0.10	0.01	5.88
Mn	0.04	0.00	0.00	0.13
Ca	0.10	0.14	0.92	0.06
Na	1.95	0.88	0.00	0.02
K	0.01	0.00	0.00	0.01
Total	14.97	3.99	4.98	20.01
	jad. 065			
	aeg. 0.23			
	aug. 0.12			

Volcanic and sedimentary rocks

Volcanic succession of Lower to Middle Miocene composed of volcanic breccia, massive lava and rare tuff and volcanogenic clay was named as Ezine volcanites. These rocks were studied by Ercan et al., (1990) in detail. Dacitic-andesitic lavas of Ezine volcanite are common around Boğazpınar while volcanic breccias are seen around Ömerler, Karıncalı and Dumanköy (Fig. 3). There is no radiometric data within the study area but the age of volcanic rocks from neighbouring areas were reported as 17-21 Ma (e.g. Borsi et al., 1972; Benda et al., 1974; Gündoğdu, 1984; Ercan et al., 1990, 1995).

Volcanic activity was interrupted in the Middle Miocene and terrigenous sediments were deposited in river and lacustrine environment. The age of this formation is accepted as Middle Miocene-Pliocene from mammal fossils around Sünnük village to the east of the study area (Fig. 2) determined by Bernor and Tobien (1990) and pollen analysis and lacustral gastropods reported by Ercan et al., (1990).

DISCUSSION

The most important feature of the study area is that blueschists lie technically on the Permo-Triassic Karakaya complex units as a klippe. The main blueschist belt occurs to the south of this klippe (Fig. 2), then it means the vergence of the blueschist was north-northwestward. This vergence is contrary to the general southward vergence of Alpid orogen in western Anatolia and points out that northward back-thrusting developed along the suture as the case in the western Alps.

There is no direct data on the time of northward thrusting of blueschist within the study area, however, there is no doubt that this event occurred after blueschist facies metamorphism. The age of blueschist metamorphism is isotopically determined by Okay and Kelley (1994) as 80-90 Ma (Turonian-Santonian) in the region south of Mustafakemalpaşa (Fig. 2). The fact, that blueschist grains and pebbles were found in Upper Senonian-Paleocene clastic rocks of Sakarya zone (Norman and Rad, 1971; Batman, 1978) indicates that blueschists which metamorphosed in 50-60 km depth

during Turonian-Santonian were partly exhumed during Maastrichtian to Paleocene. Moreover, blueschist blocks were reported within Upper Maastrichtian-Lower Paleocene wild-flysch deposited to the south of Tavşanlı zone (Göncüoğlu et al., 1992).

The continent-continent collision between Sakarya zone and Anatolid-Tauride platform occurred probably during the Paleocene. The evidence of this opinion is the passing from flysch deposition to molasse deposition in Sakarya, zone during Paleocene followed by thrusting in the Sakarya zone (Saner, 1980). Thus, the exhumation of blueschists occurred during the Latest Cretaceous before continent-continent collision. Blueschists, which were partly exhumed, were thrust northward over the Sakarya zone during continental collision.

CONCLUSION

A small blueschist klippe lies on Permo-Triassic Karakaya complex units with a low angle tectonic contact. The age of thrusting is post-Late Cretaceous (probably Paleocene) and has occurred during the continent-continent collision. Blueschists were thrust northward onto Sakarya zone during this collision. This indicates that back-thrusting occurred along the Izmir-Ankara suture such as the case in western Alps.

ACKNOWLEDGEMENTS

We thank to E. Yiğitbaş and C. Genç for constructive criticism, B. Arman for helping with the microprobe analysis, E. Leven for paleontological determinations and N. Gündoğdu and B. Kürkçüoğlu for the geochemical analysis. This study is partly supported by TÜBİTAK-Glotek Unit.

Manuscript received January 21, 1997

REFERENCES

- Akat, U.; Çağlayan, A. and İvak, M., 1978, Dursunbey-Orhaneli-Susurluk-Kepsut arasındaki bölgenin jeolojisi: MTA Rep., 6618 (unpublished), Ankara.
- Akyüz, H.S., 1995, Manyas-Susurluk-Kepsut (Balıkesir) civarının jeolojisi: PhD Thesis, İTÜ Fen Bilimleri Enstitüsü, 239 p., (unpublished).
- and Okay, A.I., 1996, A section across a Tethyan suture in northwest Turkey: *Int. Geol. Rev.* V. 38, 405-418.
- Ataman, G., 1973, Ilıca-Şamlı (Balıkesir) granodiyoritinin radyometrik yaşı ve Kuzeybatı Anadolu granitik magması hakkında düşünceler: Cumhuriyetin 50. Yılı Yerbilimleri Kongresi Tebliğleri, MTA Publ., 518-523.
- Aygen, T., 1956, Balya bölgesi jeolojisinin incelenmesi: MTA Publ., D11,95 p.
- Batman, B., 1978, Haymana kuzeyinin jeolojik evrimi ve yöredeki melanjın incelenmesi, I: Stratigrafi birimleri: *Yerbilimleri*, 4, 95-124.
- Benda, L.; Innocenti, F.; Mazzuoli, R.; Radicati, F. and Steffens, P., 1974, Stratigraphic and radiometric data of the Neogene in northwest Turkey: *Zeitschrift der deutschen geologischen Gesellschaft*, 125, 183-193.
- Bemor, R. and Tobien, H., 1990, The Mammalian Geochronology and Biogeography of Paşalar (Middle Miocene, Turkey): *J. Human Evol.*, V. 19, no: 4/5, 551-568.
- Bingöl, E.; Delaloye, M. and Ataman, G., 1982, Granitic Intrusions in western Anatolia: a contribution to the geodynamic study of this area: *Eclogae Geol. Helv.*, 75, 437- 446.
- Boggs, S., 1984, Quaternary sedimentation in the Japan arc-trench system: *Geol. Soc. Amer. Bull.*, 95, 669-685.
- Borsi, S.; Ferrara, G.; Innocenti, F. and Mazzuoli, R., 1972, Geochronology and petrology of recent volcanics in the eastern Aegean Sea (West Anatolia and Lesbos Island): *Bull. Volcan.*, 36, 473-496.
- Bürküt, Y., 1966, Kuzeybatı Anadolu'da yer alan plutonların mukayeseli jenetik etüdü: PhD Thesis, İTÜ, Maden Fak., 272 p.

- Dickinson, W.R. and Seely, D.R., 1979, Structure and stratigraphy of the fore-arc regions: AAPG Bull., 63, 2-31.
- Ercan, T.; Satır, M.; Kreuzer, H.; Türkecan, A.; Günay, E.; Çevikbaş, A.; Ateş, M. and Can, B., 1985, Batı Anadolu Senozoyik volkanitlerine ait yeni kimyasal, izotopik ve radyometrik verilerin yorumu: Türkiye Jeol. Kur. Bull., 28,121-136.
- ; Ergül, E.; Akçören, F.; Çetin, A.; Granit, S. and Asutay, J., 1990, Balıkesir- Bandırma arasının jeolojisi, Tersiyer volkanizmasının petrolojisi ve bölgesel yayılımı: MTA Bull., 110, 113-130.
- ; Satır, M.; Steinitz, G.; Dora, A.; Sarfakioğlu, E.; Adis, C., Walter, H.J. and Yıldırım, T., 1995, Biga yarımadası ile Gökçeada, Bozcaada ve Tavşan adalarındaki (KB Anadolu) Tersiyer volkanizmasının özellikleri: MTA Bull., 117, 55-86.
- Ergül, E.; Öztürk, Z.; Akçören, F. and Gözler, Z., 1980, Balıkesir ili-Marmara denizi arasının jeolojisi: MTA Rep. 6760 (unpublished), Ankara.
- ; Gözler, Z., Akçören, F. and Öztürk Z., 1986, Türkiye Jeoloji Haritaları Serisi, Balıkesir F6 Paftası: MTA Publ., Ankara.
- Genç, Ş., 1986, Geology of the region between Uludağ and the İznik Lake: Guide Book for the field excursion along western Anatolia, Turkey: MTA Publ., 19-25.
- Goffe, B.; Michard, A.; Kienast, J.R. and Le Mer, O., 1988, A case of obduction-related high pressure-low temperature metamorphism in upper crustal nappes, Arabian continental margin, Oman: P-T paths and kinematic interpretation: Tectonophysics, 151, 363-386.
- Göncüoğlu, C.M.; Özcan, A.; Turhan, N. and Işık, A., 1992, Stratigraphy of the Kütahya region: in a Geotraverse across Tethyan suture zones in NW Anatolia: Field Guide Book for the Symposium on the Geology of the Black Sea Region, Ankara, 3-11.
- Gündoğdu, N., 1984, Bigadiç gölsel Neojen baseninin jeolojisi: Yerbilimleri, 11, 91-104.
- Harris, N.B.W., Kelley, S.P. and Okay, A.I., 1994, Post-collision magmatism and tectonics in northwest Turkey: Contrib. Mineral. Petrol., 117, 241-252.
- Hathway, B., 1994, Sedimentation and volcanism in an Oligocene-Miocene intra-oceanic arc and fore-arc, southwestern Viti Levu, Fiji: J. Geol. Soc. London, 151,499-514.
- Houghton, B. F. and Landis, C.,A., 1989, Sedimentation and volcanism in a Permian arc-related basin, southern New Zealand. Bull. Volcan. 51, 433-450.
- Kaya, O. and Möstler, H., 1992, A Middle Triassic age for low grade greenschist facies metamorphic sequence in Bergama (İzmir), western Turkey: the first paleontological age assignment and structural-stratigraphic implications: Newsletter for Stratigraphy, 26, 1-17.
- Le Bas, M.J. and Streckeisen, A.L., 1991, The IUGS systematics of igneous rocks: J. Geol. Soc. London, 148, 825-833.
- Le Maitre, R.W., 1989, A Classification of Igneous Rocks and Glossary of Terms: Blackwell, Oxford, 193 p.
- Leven, E. and Okay, A.I., 1996, Foraminifera from the exotic Permo-Carboniferous limestone blocks in the Karakaya Complex, Northwest Turkey: Rivista Italiana di Paleontologia e Stratigrafia, 102, 2, 1-10, 139-171.
- McMillen, K.J.; Enkeboll, R.H.; Moore, J.C.; Shipley, T.H. and Ladd, J.W., 1982, Sedimentation in different tectonic environments of the Middle America Trench, southern Mexico and Guatemala: Leggett, J.K., ed., Trench-forearc geology: Sedimentation and tectonics of modern and ancient active plate margins: Geol. Soc. London, Spec. Publ., 10,107-120.
- Michard, A.; Goffe, B.; Saddıçı, O.; Oberhansli, R. and Wendt, A.S., 1994, Late Cretaceous exhumation of the Oman blueschist and eclogites: a two-stage extensional mechanism: Terra Nova, 6, 404-413.
- Mullen, E.D., 1983, MnO/TiO₂/P₂O₅: a minor element discriminant for basaltic rocks of oceanic environments and its implications for petrogenesis: Earth Planet. Sci. Letters, 62, 53-62.

- Norman, T. and Rad, M.R., 1971, Çayraz (Haymana) civarındaki Harhor (Eosen) Formasyonunda alttan üste doğru doku parametrelerinde ve ağır mineral bolluk derecelerinde değişmeler: Türkiye Jeol. Kur. Bull., 14, 205-225.
- Okay, A.İ., 1980, Mineralogy, Petrology and Phase Relations of Glaucophane-Lawsonite Zone Blueschists from the Tavşanlı Region, Northwest Turkey: Contrib. Mineral. Petrol., 72, 243-255.
- , 1981, Kuzeybatı Anadoludaki Ofiyolitlerin Jeolojisi ve Mavişist Metamorfizması: Türkiye Jeol. Kur. Bull., 24, 85-95.
- , 1984, Kuzeybatı Anadolu'da yer alan metamorfik kuşaklar: Ketin Simpozyumu, Türkiye Jeol. Kur. Publ., 83-93.
- , 1986, High pressure/low temperature metamorphic rocks of Turkey: Ewans, B.W. and Brown, E.H., eds., Blueschists and Eclogites: Geol. Soc. Amer. Memoir, 164, 333-347.
- ; Siyako, M. and Bürkan, K.A., 1990, Biga Yarımadası'nın Jeolojisi ve Tektonik Evrimi: TPJD Bull. 2/1, 83-121.
- and Kelley, S.P., 1994, Tectonic setting, petrology and geochronology of jadeite+glaucophane and chloritoid+glaucophane schists from north-west Turkey: J. Metamorphic Geol., 12, 455-466.
- ; Satır, M.; Maluski, H.; Siyako, M.; Metzger, R., and Akyüz, H.S., 1996, Paleo- and Neo-Tethyan events in northwest Turkey: Geological and geochronological constraints: Yin, A. and Harrison, T.M., eds. Tectonic Evolution of Asia: 420-441.
- Saner, S., 1980, Mudurnu-Göynük havzasının Jura ve sonrası çökelim nitelikleriyle paleocoğrafya yorumlaması: Türkiye Jeol. Kur. Bull. 23, 39-52.
- Schweller, W.J. and Kulm, L.D., 1978, Depositional patterns and channelised, sedimentation in active eastern Pacific trenches: Stanley, D.J. and Kelling, G., eds., Sedimentation in submarine canyons, fans and trenches: 311-324.
- Searle, M.; Waters, D.J.; Martin, H.N. and Rex, D.C., 1994, Structure and metamorphism of blueschist-eclogite facies rocks from the northeastern Oman Mountains: J. Geol. Soc. London, 151, 555-576.
- Stanley, D.J. and Maldonado, A., 1981, Depositional models for fine-grained sediment in the western Hellenic Trench, eastern Mediterranean: Sedimentology, 28, 273-290.
- Şengör, A.M.C. and Yılmaz, Y., 1981, Tethyan evolution of Turkey: a plate tectonic approach: Tectonophysics, 75, 181-241.
- Tekeli, O., 1981, Subduction complex of pre-Jurassic age, Northern Anatolia, Turkey: Geology, 9, 68-72.
- Thronburgh, T.M. and Kulm, L.M., 1987, Sedimentation in the Chile Trench: Depositional morphologies, lithofacies and stratigraphy: Geol. Soc. Am. Bull., 98, 33-52.
- Underwood, M.B., 1986, Transverse infilling of the central Aleutian Trench by unconfined turbidity currents: Geo-Marine Letters, 6, 7-13.

GEOLOGIC AND MINERALOGIC INVESTION OF THE NORTHERN KONYA LACUSTRINE UNITS

Zehra KARAKAŞ** and Selahattin KADİR*****

ABSTRACT.- Neogene lacustrine sediments of Northern Konya consist of limestone, clayey limestone, claystone, mudstone, marl, sandstone and conglomerate. Widely observed limestones are fine grained, white-beige-cream coloured and contain remnants of the plant root. Brecciation, calcretion, drying cracks and dissolution voids are also common. Laminates are widely seen in claystone and sandstone. Ooid, pellet, intraclast and ostracod are the main components of limestones. Ooids and intraclasts are surrounded by meniscus type cement which represents a vadoze environment. SEM studies indicate that hexagonal and rhombic type calcite and dolomite minerals of meniscus cement are covered by sepiolite and palygorskite clay fibre. XRD analyses show that sepiolite and palygorskite minerals are associated with smectite, chlorite, feldspar, illite and quartz minerals. Carbonate units of Neogene lacustrine of Konya area are alternated and intercalated with conglomerate, sandstone and mudstone lenses. These indicates that, from time to time, the lacustrine area is fed by flowing water. Considering the mineral paragenesis and their textural features of the study area, precipitation was occurred due to continuous changes in climate conditions. Climate conditions changes the lacustrine water chemistry and thus facilitating precipitation of carbonate and detrital units. Because of continuous climate changes, sepiolite and palygorskite were formed as a result of calchification of carbanate units.

ERZURUM - KARS PLATOSUNUN ÇARPIŞMA KÖKENLİ VOLKANİZMASININ VOLKANO-STRATİGRAFİSİ VE YENİ K/Ar YAŞ BULGULARI IŞIĞINDA EVRİMİ, KUZEYDOĞU ANADOLU

Mehmet KESKİN*

ÖZ. - Kuzeydoğu Anadolu'da Erzurum ile Kars arasında kalan bölge, denizden ortalama 2.5 km. yüksekte yer alan bir plato morfolojisi sunar. Erzurum-Kars Platosu olarak isimlendirilen bu yüksek alan, Anadolu ve Arap kıtaları arasında Neotetis Okyanusunun güney kolunun kapanmasını izleyen evrede kıtasal çarpışma ve kabuksal kalınlaşma sonucu bugünkü özgün morfolojisini kazanmıştır. Söz konusu platonun büyük kısmı, çarpışma ile kökensel ilişkili (collision-related) bir volkanizmanın ürünü olan lavlar ve piroklastik birimlerle örtülmüştür. Volkanizma 11 my önce, bölgesel yükselmeden hemen sonra bazik lavlarla başlamış, yaklaşık 5-7 my önce doruğa ulaşmış ve 2.5 my önceye dek sürerek plato üzerinde kimi yerde 1 km.yi aşan kalınlıkta istifler oluşturmuştur. Magma yüzeye genel olarak, bölge neotektoniğinin ana hatlarını oluşturan doğrultu atımlı fay sistemlerine bağlı yerel gerilme alanlarını izleyerek çoğunlukla çatlak erüpsiyonlar şeklinde ulaşmıştır. Çıkan malzemenin önemli bir kısmı, yakındaki fay sistemlerine bağlı pull-apart havzalarında depolanmıştır. Volkanik etkinliğin 6-11 my arasındaki dönemi, yaygın felsik piroklastikler/domlar ile bazik lavların oluşturduğu bimodal bir volkanizma ile temsil edilmiştir. Yaklaşık 5-6 my önce, derinde mafik fazda amfibol fraksiyonel kristalizasyonu geçirmiş olan ortaç porfiritik lavlar yüzeye ulaşarak domlar oluşturmuşlardır. Volkanizmanın 2.7-5 my döneminde ise olivinli bazik lavlar özellikle doğu alanlarda egemen olmuşlar, plato oluşturan lav yaygıları oluşturarak geniş alanlar kaplamışlardır. Yeni K/Ar yaş bulgularına göre, plato üzerindeki volkanik etkinlik zaman içinde batıdan doğuya göç etmiş ve bu sırada genel olarak bazikleşmiştir. Bu, doğrultu-atımlı fay sistemleri içindeki yerel gerilmelerin zamanla batı yönünde artması nedeniyle ortaya çıkmış olmalıdır.

GİRİŞ

Doğu Anadolu Bölgesi, kıtasal bir çarpışma zonu içinde çarpışmayla kökensel ilişkili gelişmiş volkanizmanın dünyada en iyi görüldüğü alandır. Bölgenin kuzeydoğusunda yer alan Erzurum-Kars Platosu ise, çarpışma-kökenli (collision-related) volkanik aktivitenin 11 ile 2.5 milyon yıl arasındaki tüm kaydını son derece iyi mostralara şeklinde içermesi nedeniyle özel bir öneme sahiptir.

Bu makale, Erzurum-Kars Platosunun Erzurum'un kuzeybatısında bulunan Dumlu dağı ile Kağızman'ın kuzeyi arasında kalan yaklaşık 3000 km²lik bir kesiminin volkano-stratigrafisini ele almaktadır (Şek. 1). Platonun batıda Dumlu dağı ile doğuda Pasinler kuzeydoğusunda kalan Harabedere vadisi arasındaki yaklaşık 800 km²lik bir kesimi haritalanmıştır (Şek. 2), diğer kesimleri ise belirli jeo-traversler boyunca keşif (reconnaissance) türünde çalışılmıştır. Makalenin temel amacı, platoyu oluşturan farklı volkanik fasiyeslerdeki birimleri erüptif, petrografik, mineralojik ve ortamsal karakterlerindeki farklılıklarına göre ayırtlayıp, plato üzerinde mekân içinde ve yeni K/Ar yaş verileri ışığında zaman içinde dağılımlarını belirlemektir. Böylece volkanitlerin bölge çapında bir korelasyonu yapılacak ve ardından

volkanizmanın plato üzerindeki evrimi ortaya konulacaktır. Erzurum-Kars Platosu ve civarında, çarpışma kökenli volkanitler üzerinde daha önce bu çalışmada sunulan ayrıntıda haritalama ve birim ayırımı yapılmış olduğundan, makalede kullanılan formasyon isimlerinin çoğu, bu çalışmada verilen isimlerdir. Bu isimler, çoğunlukla birimlerin en karakteristik monstralarının görüldüğü yer isimlerine göre belirlenmişlerdir (Keskın, 1994).

Makalede, istifleri oluşturan birimlerin petrografisi ve mineral bileşiminin tanımlanmasında, polarizan mikroskobu ile yapılan petrografi çalışmaları ve volkanik kaya örneklerinin parlatma kesitleri üzerinde yapılmış elektron mikro-prob analizleri (70 numune üzerinden 890 nokta analizi) kullanılmıştır. Volkanik birimleri oluşturan minerallerin tanımlanması sırasında parantez içinde "(An₅₁₋₅₆)" şeklinde yapılan açıklamalar, prob analizlerine dayandırılanlardır. Plato volkanitlerinin isimlendirilmesinde ve sınıflanmasında ise, petrografik çalışmalara ek olarak platodan derlenen 350 temsilci numunenin yüksek hassasiyete sahip majör ve iz element analizlerinin oluşturduğu geniş bir veri tabanından da yararlanılmıştır. Söz konusu analitik veriler, makalenin amaçları dışına taşmaması açısından burada sunulmamışlardır.

ÖNCEKİ ÇALIŞMALAR

Bölge tektoniğinin genel özellikleri ve bölgede meydana gelen tektonik, morfolojik olaylar ve volkanizma, daha önce pek çok makaleye konu olmuştur (Şaroğlu ve diğerleri, 1980; Şengör, 1980; Şaroğlu ve Güner, 1981; Yılmaz, 1984; Tokel, 1984; Şaroğlu ve Yılmaz, 1986). Önceki çalışmalar, Arap ve Anadolu levhaları arasında gerçekleşmiş olan çarpışmanın bölgedeki yaygın volkanizmanın gelişmesinden sorumlu olduğunu göstermiştir (Lambert ve diğerleri, 1974; Innocenti ve diğerleri, 1976, 1982 a, b; Gülen, 1980 a, b; Yılmaz ve diğerleri, 1987; Ercan ve diğerleri, 1990; Pearce ve diğerleri, 1990; Keskin, 1994; Notsu ve diğerleri, 1995).

Çalışma alanını kapsayan ve Neoteknotik dönemi ilgilendiren çalışmalar ise, alanın tektoniği ve volkanizması olmak üzere başlıca iki konuda yoğunlaşmışlardır. Bu makalede ele alınan sahanın tektoniği konusundaki çalışmalarda, izleyen paragraflarda Erzurum-Tiflis fay hattı olarak isimlendirilmiş olan (R. Westaway, kişisel görüşme) fay zonu, Koçyiğit ve diğerleri (1985), inan (1987) tarafından da çalışılmış ve haritalanmıştır. Tekman ile Çıldır arasında uzanan ve Horasan dolayında volkanik istif keserek geçen doğrudan atımlı sol yönlü fay hattı ise, Koçyiğit (1985) tarafından çalışılmıştır ve Çobandede fay kuşağı olarak isimlendirilmiştir. Çalışma alanı ve civarındaki volkanizma konusunda Innocenti ve diğerleri (1982 b), Yılmaz ve diğerleri (1987), Pearce ve diğerleri (1990) tarafından çalışmalar yapılmışsa da, bunlar (Yılmaz ve diğerleri, 1987 dışında) volkanik istifin volkano-stratigrafisinden çok neo-volkanizmadaki bölgesel jeokimyasal değişimler üzerinde yoğunlaşmışlardır.

VOLKANİK STRATİGRAFI

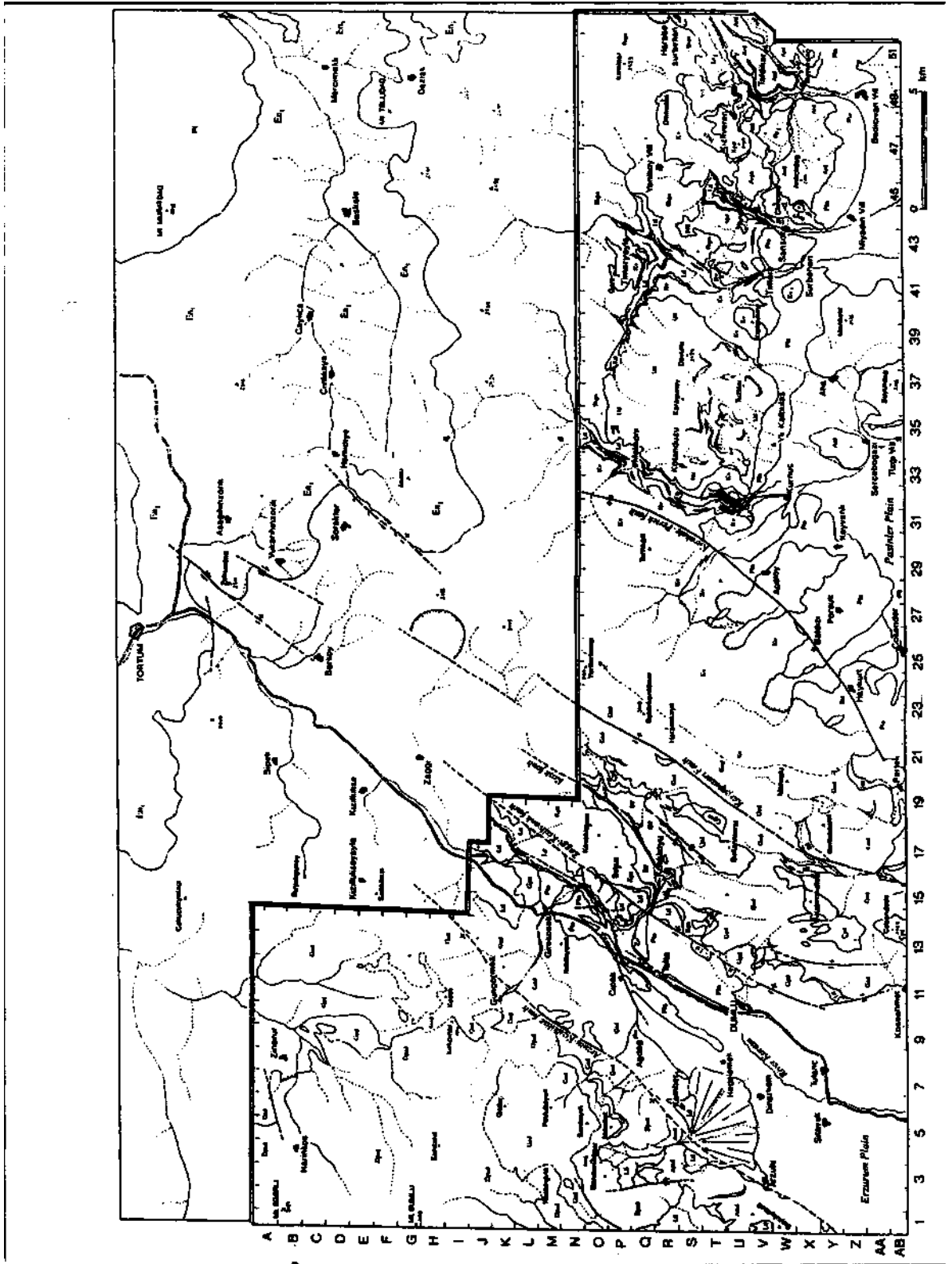
Bilindiği gibi volkanik arazilerde birimlerin dağılımı, son derece karmaşık paternler izleyebilir. Volkanik sahalarda birimlerin ilişkilerinin yorumlanması ve volkano-stratigrafisinin kurulması, diğer kayaçlar üzerinde yapılan çalışmalardan farklıdır ve volkanik fasiyeler konusunda bilgi birikimi ile özel bir çalışma stili gerektirmektedir. Farklı ortamlarda gelişen volkanik istiflerin özelliklen, içlerinde barındırdıkları çok sayıda volkanik fasiyelerin nitelikleri ve ayırtman özellikleri ile bu tür arazilerde yapılması gereken saha çalışması yönteminin güzel bir tanımlaması Cas ve Wright'ta (1998) verilmektedir.

Erzurum-Kars platosu volkanizmasının genel erüptif karakteri






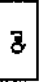

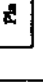
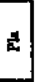


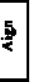



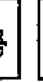



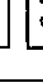

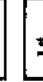





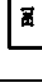
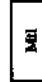

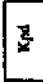


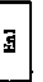
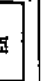

Erzurum-Kars platosu (EKP) volkanizmasına ait lav ve piroklastik ürünlerin büyük çoğunluğu, çatlak püskürmelerine (fisure eruptions) bağlı olarak oluşmuşlardır. Ayrıca volkanik istif içinde Aladağ, Büyük ve Küçük Yağlıca dağları gibi merkezî püskürmeleri belgeleyen bazı volkanik koniler ve çok sayıda felsik dom da vardır.

EKP volkanizmasının volkano-stratigrafik kesitlerinin oluşturulmasında ve ardından platonun volkano-stratigrafisinin belirlenmesinde birim ve fasiyeler ayırıcı için Cas ve Wright'ın (1988) önerdiği kriterler dikkate alınmıştır. Aşağıda sunulan kesitlerde farklı formasyon isimleri altında tanımlanan volkanik birimler, platodaki volkanizmanın belirli zaman aralıklarında yüzeye ulaşmış olan, belirli erüptif, petrografik ve jeokimyasal karaktere sahip olan düzeylerine karşılık gelmektedirler. Bunlardan bir kısmı aynı litoloji, doku ve kimyasal-mineralojik bileşimdeki volkanik ürünlerden oluşan monoton istiflerdir, diğer bir kısmı ise kökensel olarak birbirleriyle ilişkili olarak aynı erüptif periyot içinde yüzeye çıkan ancak dokusal ve bileşimsel olarak birbirinden çok büyük farklılıklar sunabilen kaya türlerinin ardalandıkları istif veya birimlerdir. Bu ikincisine iyi bir örnek, platonun tabanında bulunan ve Taban Tüf düzeyi olarak adlandırılan, gri ve beyaz ignimbritler ile piroklastik döküntü katmanları ile bazik lav merceklerinin ardalanmasından oluşan birimdir (Şek. 2). Bu tür birimlerin oluşmasında, magma odalarındaki fraksiyonel kristalizasyon ile diferansiyasyon, ısıl ve bileşimsel zonlanmalar gibi prosesler (magma Chamber processes) esas denetleyici rolü taşımaktadır (Keskin, 1994). Sunulan birimler bazen tek bir lav veya piroklastik akıntı/döküntü düzeyinden oluştukları gibi bazen de çok sayıda lav akıntıları veya piroklastikleri üstüste istiflenmesinden de meydana gelmişlerdir. Bazen istif içindeki bir lav veya piroklastik birim, anahtar düzey oluşturacak biçimde uzun mesafeler izlenebilmekte, yüzlerce km.² alan kaplayabilmektedir (ör. Kargapazarı volkanitleri, Pasinler kuzeyinde Siyah ignimbrit ve Horasan kuzeyinde Horasan Plato düzeyi olarak adlandırılan birimler). Bu tür düzeyler, istifte korelasyonların yapılmasını kolaylaştırmışlardır.

izleyen paragraflarda, çarpışma-kökenli volkanik istifin anatomisi, plato üzerinde en iyi mostra verdiği sa-



AÇIKLAMALAR

DUMLU DAĞI ALANI		KARGAPAZARI DAĞI ALANI		PASINLER ALANI	
	Alıvyan yelpazeleri		Höveler		Höveler
	Kuvaterner Alıvyan		Kuvaterner Alıvyan		Kuvaterner Alıvyan
	Eski Alıvyan		Pliosen Aras Formasyonu		Pliosen Aras Formasyonu
	Pliosen Aras formasyonu		Kargapazarı volkaniti		Ardıcıladağ ignimbriti öyesi
	Dumlu volkaniti		Göllerizal dazit		Ardıcıladağ rhyolit öyesi
	Güreliök volkaniti		Kargapazarı bezahı		Orta Tuf düzeyi
	Güngörmez volkaniti		Güreliök volkanik öyesi		Kargapazarı volkaniti
	Arzulu dazit		Çobandede volkanik öyesi		Büyükdadağ volkaniti
	Taban Tuf düzeyi		Kök volkanik öyesi		Siyah ignimbrit
			Güngörmez volkaniti		Beyaz ignimbrit
			Taban Tuf düzeyi		Orta Tuf düzeyi
					Krafleren daziti
					Taban Tuf düzeyi
					Siyah andezit
					Eosen Narman formasyonu, Kışlacık volkanik öyesi
					Eosen Narman formasyonu

Sek. 2- Dumlu dağı ile Pasınler kuzeyi arasındaki alanın jeolojik haritası.

balardan geçen kesitler üzerinde ortaya konacaktır. Bu amaçla saha, altı ast alana ayrılarak incelenmektedir. Bunlar: (1) Dumlu dağı, (2) Kargapazarı dağı, (3) Pasinler, (4) Horasan, (5) Aladağ ve (6) Kağızman kuzevidir.

Erzurum-Kars Platosu volkanitlerinin temelinin niteliği

Erzurum-Kars Platosu volkanitleri temelde (1) Pontidler'in sedimanter ve volkanik ürünleri ve (2) Doğu Anadolu Yığılım Karmaşağı olmak üzere iki ana temel üzerinde diskordans ile otururlar.

(1) Pontid istifi, Liyas, Malm ve Kretase formasyonlarından meydana gelir. Özellikle Dumlu alanının batısında ve kuzeyindeki alanlarda çarpışma-kökenli volkanik istif, bu temel üzerinde diskordansla oturur.

(2) Şengör ve Yılmaz (1981) tarafından Doğu Anadolu Yığılım Karmaşağı olarak isimlendirilen birim, kıtasal çarpışma sonucunda kıta blokları arasına sıkışmış olan ve Neotetis Okyanusuna ait Üst Kretase yaşlı ofiyolitik ve sedimanter birimler içeren tektonik bir karmaşıktır. EKP'nun güneyindeki alanlarda, Pasinler güney alanlarından başlayarak doğuya doğru, Horasan ve Kağızman civarlarında görünür temeli hemen her yerde Doğu Anadolu Yığılım Karmaşağı oluşturur.

Erzurum-Kars Platosunun anatomisi

Dumlu dağı alanı.- Dumlu dağı alanı, EKP'nun en batı kesiminde bulunur. Söz konusu alan, 3000 m.yi aşan yükseklikleri ile yaklaşık kuzey-güney doğrultusunda bir sırt şeklinde uzanan bir dizi zirvenin meydana getirdiği Gavur dağları silsilesinin içinde yer almaktadır. Dumlu dağı, 3200 m. yüksekliği ile, Mescit dağından (3255 m.) sonra silsile içindeki en yüksek ikinci zirveyi oluşturur. Karahan ve Erinkar arasından geçen hattın batısında, Erzurum-Kars Platosu Volkanitleri (EKPV) tümüyle yok olurlar.

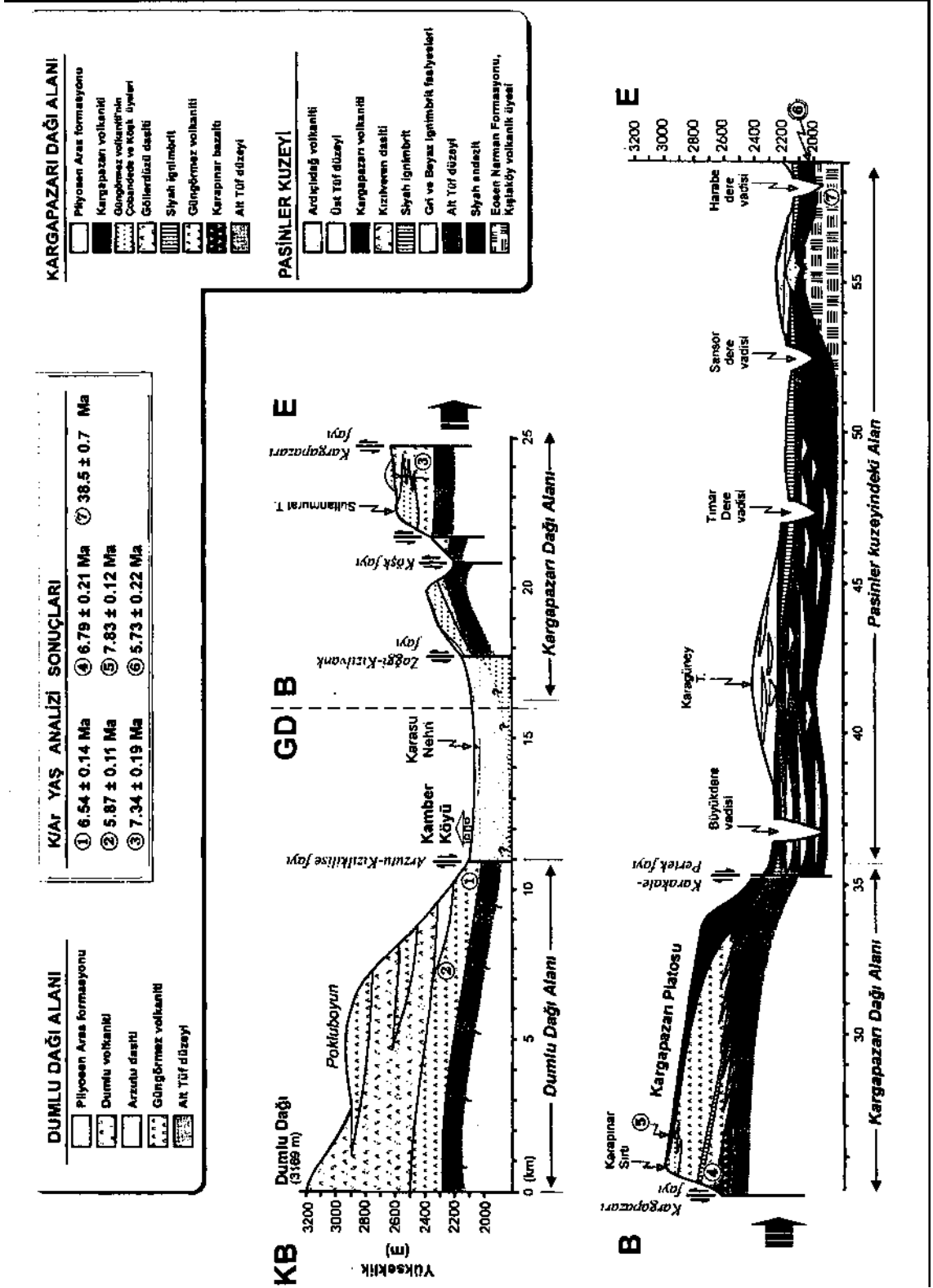
Çarpışma-kökenli volkanik istif, maksimum kalınlığına 1000 m. ile Dumlu alanında ulaşır. Dumlu alanında ortaç ve felsik lavlar, EKP'nun diğer kesimlerinden farklı olarak piroklastiklere oranla çok daha fazla hacim kaplarlar. Piroklastik ürünler, istifin taban kesimleri dışında hemen hemen hiç görülmez. Dumlu dağının çalışma sahası içinde kalan Erzurum ovasına komşu GD

yamacındaki istifin görünür tabanında riyodasitik-dasitik bileşimde bir tuf düzeyi mostra verir (Şek. 1). Taban Tuf düzeyi olarak isimlendirilen birim, krem ve beyaz renkler sunar ve ince külden lapilli boyutuna kadar değişen vitrik piroklastik kırıntılardan oluşur. Taban Tuf düzeyinin kalınlığı, yer yer 150-200 m.ye kadar ulaşır.

Taban Tuf düzeyinin üzerine Dumlu dağının GD yamacında Arzutu köyü ile Kızıldere arasında, başlıca plajiyoklaz (An_{38-64}), amfibol (magnezyo-edenit ve çermakit), çok az miktarda bronzit-hipersten ve ojit mikrokristalleri ve mikrolitleri içeren mikroporfiritik dokulu bir lav düzeyi gelir. Arzutu dasiti olarak isimlendirilen bu birim, çoğun gri, bazen pembemsi renkler sergileyen kalın ve masif lav akıntılarından oluşmaktadır ve toplam kalınlığı yaklaşık 50-70 m. civarındadır. Arzutu dasiti, üst dokanakta Güngörmez volkaniti adı verilen bir birim tarafından örtülür.

Güngörmez volkaniti, sahada çoğunlukla siyahtan açık griye dek değişen renkler ve afirik, yer yer devesiküler doku sergileyen masif genellikle homojen andezitik ve dasitik lav düzeylerinden oluşur. Kızıldere vadisinde, Güngörmez volkanitinin tabandaki Taban Tuf ile olan dokanağına yakın lav düzeyinden alınan bir numunenin K/Ar yaş tayini, 6.54 ± 0.14 milyon yıl vermiştir (Şek. 1). Hacimsel olarak Dumlu alanındaki en yaygın birim olan Güngörmez volkanitinin kalınlığı, genelde 300-400 m. civarında olmakla birlikte, Güngörmez köyü kuzeyinde 600 m.yi aşar. Birim bazı düzeylerde, örneğin Karaçağıldüzü mevki ve Şehitler tepe dolaylarında dış görünüşü itibarıyla bazaltı andıran dasitik bileşimde siyah, kompakt ve afirik lav düzeyleri de içerir. Vitrofirik dokulu bu kayalarda çok az miktarda bulunan plajiyoklaz mikrokristallerinin bileşimi An_{51-52} olup, klinopiroksen ojit ve endiyopsit, ortopiroksen ise bronzit ile temsil edilir. Güngörmez volkanitinde levhamsı eklem takımlarına da yaygınca rastlanır. Kimi yerde, eklemelerin birbirlerine çok yaklaşması sonucunda kaya yapraklanma benzeri bir yapı kazanır.

Güngörmez volkaniti, Dumlu volkaniti olarak isimlendirilen porfiritik ve masif bir lav istifi tarafından örtülür. Dumlu alanında en üstte yer alan bu birim, iri fenokristalli porfiritik dokusu ve bol amfibol fenokristalleri içermesiyle istifte tanıtilen bütün diğer birimlerden büyük farklılık sunar. Birim, Dumlu alanındaki en yüksek zirvelerde yaygınca mostra verir (Şek. 2). Andezitten dasite uzanan bir bileşim aralığına sahip olan Dumlu

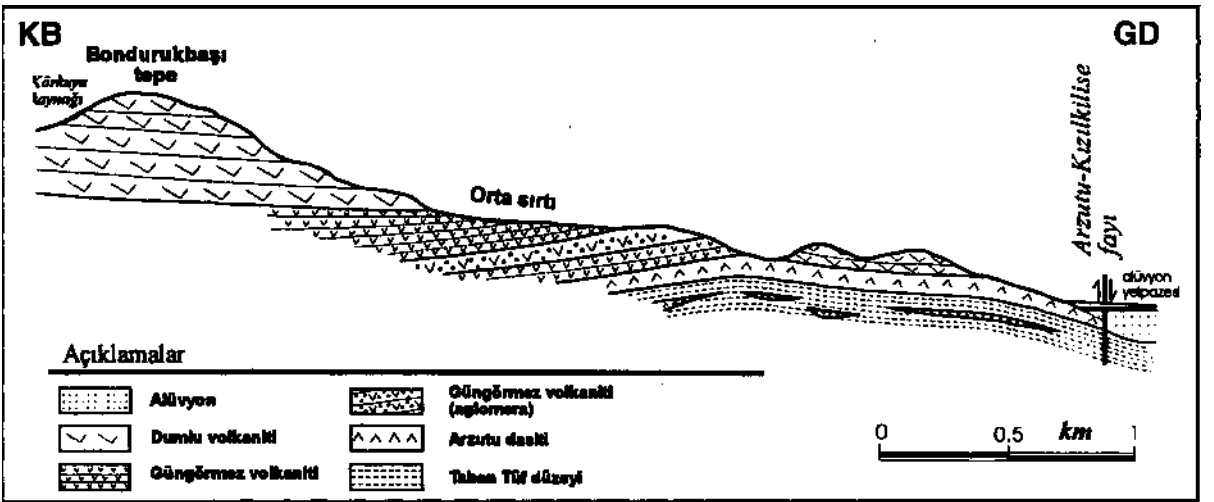


Şek. 3- D-B doğrultusunda haritalama alanını tümüyle kesen jeolojik sikeç enine kesit.

volkaniti, plajiyoklaz (An_{37-65}), amfibol (magnezyo-ferri-çermakit, magnezyo-edenit, bazen de magnezyo-alümino-kersutit ile magnezyo-ferri-taramit), ortopiroksen (çoğun bronzit ve az miktarda hipersten) fenokristalleri ve çok az miktarda klinopiroksen mikrokristalleri (genelde ojit, az miktarda endiopsit) içerir. Kalınlığı değişmekle birlikte, Dumlu dağı dolaylarında 400-450 m. ye ulaşır. Birim, Dumlu dağının güney yamacında, GD'ya doğru 10-15° lik bir eğim sunar (Şek. 4). Bu kesimde, Pokluboyun ve Mihrimat tepeleri ile Kızıldere arasındaki alanda Güngörmez volkanitine benzer bileşim ve dokuda ve yaklaşık 30-50 m. kalınlıkta merccek şeklinde iki lav düzeyi içerir (Şek. 2 ve 3).

Kargapazarı fayı; GD'da uzananı ise Karakale-Pertek fayı olarak isimlendirilmiştir (Şek. 2). Söz konusu faylar, Kargapazarı platosunun uzanımını denetlerler. Kargapazarı fayı boyunca GD bloğun yükselmesiyle, üzerinde lav düzeylerinin son derece güzel mostralral halinde izlenebildiği, 300-500 m. yüksekliğinde sarp bir eskarpment oluşmuştur.

Kargapazarı fayı ile Karasu nehri arasındaki alan da, yine Erzurum-Tiflis fay zonuna ait ve yukarıda tanıtilanlara paralel çok sayıda doğrultu atımlı faylar ile kesilmiştir. Dumlu dağı yamaçlarından D'ya, Kargapazarı dağına doğru bakıldığında, fayların volkanik istifi kese-



Şek. 4- Bondurukbaşı tepe (Dumlu dağı G yamacı) ile Erzurum ovası arasındaki jeolojik enine kesit.

Kargapazarı dağı alanı.- Erzurum'un kuzeyinde, Dumlu dağı yükselimi ile Doğudaki Pasinler platosu arasındaki alanda, KD-GB doğrultusunda 15-16 km. kadar uzanan ve 2800-3000 m. yüksekliğinde zirvelerden oluşan sırt şeklindeki yükselti, Kargapazarı dağı silsilesi olarak bilinmektedir. Erzurum ovasını Pasinler'den bir duvar gibi ayrılan bu sırt, aslında 15-16 km. uzunluğunda ve 3-5 km. eninde, 10-15° ile güneydoğuya eğimli, aşınmaya dayanım 11 olivinli bazaltik ve andezitik lavların en üst seviyesini oluşturduğu dar, uzun ve yüksek bir plato niteliğindedir. Bu çalışmada Kargapazarı platosu olarak isimlendirilen bu alan, Kargapazarı silsilesinin oluşturduğu sırtın hem KB ve hem de GD yamacında, KD-GB doğrultusunda uzanan ve önemli ölçüde normal atım bileşeni içeren doğrultu atımlı sol yönlü faylarla kesilmektedir. Faylardan KB'da olanı

rek, Erzurum ovasına doğru basamaklar şeklinde açtıkları jeomorfolojiden iyi görülür. Karasu nehri ve Köşk dere gibi akarsuların uzanımı da bu faylar tarafından denetlenmektedir. Doğudan batıya doğru bu faylardan en önemlileri: Zağgi-Kızılvank, Dumlu-Tafta ve Köşk faylarıdır (Şek. 2).

Kargapazarı alanında istifin görünür tabanında, krem-beyaz renkler sunan ve volkanoklastik kum ve silt arakatıkları içeren epiklastik bir tüf düzeyi mostra verir. Birim, Dumlu alanının tabanında görülen Taban Tüf düzeyinin eşdeğeridir. Taban Tüf düzeyi, üst dokanakta Güngörmez volkaniti ve Karapınar bazaltı olmak üzere başlıca iki birim tarafından örtülmektedir. Dumlu alanında homojen ve monoton afirik lav düzeyleri şeklinde izlenen Güngörmez volkaniti, Kargapazarı dağı

KD ANADOLU VOLKANİZMASININ VOLKANO-STRATİGRAFİSİ VE K/AR YAŞ BULGULARI

alanı civarında, birbirinden dokularının farklı olması ile ayrılan ancak benzeri bir bileşim sunan üç üye içermektedir: Girekösek, Köşk ve Çobandede üyeleri.

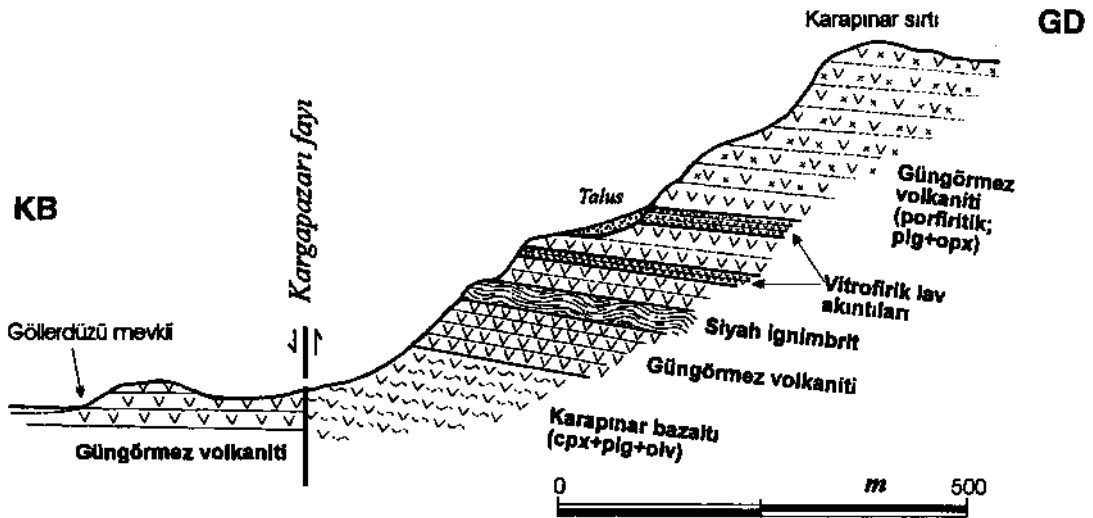
Girekösek üyesi, Karasu nehri vadisi içinde, Erzurum-Tortum yolu ile Girekösek köyü arasındaki alanda Karagöbek Tabya tepe ile Pertekligüney sırtı arasındaki 1 km.² civarında dar bir alanda mostra verir. Mercek şeklindedir ve maksimum kalınlığı 70-100 m. civarına erişir. Siyah camı bir hamur içinde iri, yuvarlak, magmatik korozyon gösteren kuvars ve öhedra / subhedral plajiyoklaz fenokristallerinden oluşur. Birimin diğer mostraları, Dumlu kasabasının 1 km. doğusunda, Zağgi-Kızılvanık fayına komşu 4-5 km.² lik bir alanda bulunur.

Köşk üyesi, Köşk köyünün hemen kuzeyinde, Zağgi-Kızılvanık ile Köşk fayları arasında uzanan bir sırt boyunca mostra verir. Tabanda 20-30 m. kalınlığında merceksi bir aglomera düzeyi ile başlar. Bu aglomera üstte, iri öhedral ojit fenokristalleri, az miktarda bronzit ve plajiyoklaz (An_{60-65}) mikrokristalleri içeren, hyaloplitik-vitrofirik dokulu andezitik-dasitik lav akıntıları ile örtülür. Zağgi-Kızılvanık fayına doğru KB'ya 15-20° ile eğim gösteren birimin kalınlığı 100-150 m. kadardır.

Çobandede üyesi, Köseahmet köyü doğusunda, üzerinde tarihi tabya harabelerinin bulunduğu Çobandede (2453 m.) tepesinden başlayarak KKD-GGB doğrultusunda Köşk yaylasına kadar uzanır. Dasitik-andezitik bileşimli ve kristalce zengin porfiritik dokulu lav akıntılarının oluşturduğu bir birimdir. Bol miktarda (%30-40'a varan oranda) Plajiyoklaz fenokristalleri ($An_{2g.53}$) ile bronzit ve ojit feno-ve mikrokristalleri içerir.

Köşk köyünün 2.5 km. kadar GD'sunda bulunan Çingeneyurdu tepenin kuzeyinde, yarım km.²den daha dar bir alanda, amfibol fenokristalleri içeren dasitik bir dom mostra verir. 40-60 m.ye kadar kalınlığa ulaşan birim, Güngörmez volkanitinin üzerinde yer alır. Dumlu volkaniti ile hemen hemen aynı mineralojik ve dokusal özellikler sergileyen bu birim, Göllerdüzü dasiti olarak isimlendirilmiş olup, Kargapazarı alanında gözlemlenmiş amfibol içeren tek lavdır.

Kargapazarı silsilesi içinde volkanik istifin en iyi görüldüğü kesitlerden birisi, Kargapazarı fayı ile Karapınar sırtı arasında kalan sarp yamaçtır (Şek. 5). Bu yamaçta, Taban Tüf düzeyinin üzerine gelen ilk birim, Karapınar bazaltı olarak bilinen ve plajiyoklaz (An_{37-38}), olivin (Fo_{84-85}) fenokristalleri ve bunları çevreleyen sa-



Şek. 5- Kargapazarı dağının Köşk köyü doğusunda, Göllerdüzü mevki ile Karapınar sırtı (zirve) arasından bulunan batı yamacını oluşturan volkanik birimler.

lit ve camsı hamurdan oluşan lav istifidir. Erzurum-Kars Platosu üzerindeki en bazik lavlardan birisi olan birim, karakteristik olarak subofitik ve intergranüle dokular sergiler. Birimin mostraları, Kargapazarı fayının yükselmiş olan GD bloğunun tabanında, faya paralel dar bir şerit şeklinde uzanır.

Karapınar bazaltı, Güngörmez volkanitine ait ortaç bileşimli afirik lavlarla örtülür. Karapınar sırtının zirvesine kadarki yaklaşık 300 m.lik kesitte Güngörmez volkanitine ait lavlar, kalın bir istif oluştururlar. Güngörmez volkanitinin Karapınar bazaltı ile olan dokanağı yakınında, birim içinde yaklaşık 3-5 m. kalınlıkta bir ignimbrit düzeyi yüzeylenir. Bu piroklastik akıntı, doğudaki Pasinler alanında anahtar bir düzey olarak izlenen Siyah ignimbrit ile aynı özellikleri sergiler, istifte üste doğru gitgide lavların fenokristal içeriği artar ve zirveye varıldığında Çobandede üyesine benzer dokuda, plajiyoklaz ve ortopirosen fenokristalleri içeren kalın lav akıntıları egemen olur.

Tanıtilan tüm bu lav istifi üzerine, zirvenin hemen arkasından başlayarak Kargapazarı Platosunun en üst seviyesini oluşturan, plajiyoklaz (An_{78-49}), olivin (Fe_{75-84}) ve indiyopsit/ojit feno- ve mikrofeno-kristallerinden oluşan ve porfiritik, hyaloplitik dokular sergileyen Kargapazarı volkaniti gelir. Kargapazarı volkanitinin kalınlığı, platonun eğimi yönünde GD'ya doğru artarak Acıköy kuzeyindeki heyelan aynası dolaylarında 300 m.ye ulaşır. Bu kesimde birim, 4-5 km.² lik sınırlı bir alanda Hawaii tipi erüptif karakterde olup lavlarla ardalanmış çoğun kırmızı okside skorya ve lapilliden volkan bombası boyuna ulaşan balistik parçaların (spatter) oluşturduğu piroklastik düzeyler içerir (Şek. 2).

Pasinler alanında ince ve yanal yönde daha devamsız yamalar şeklinde mostra dağılımı sergileyen Kargapazarı volkaniti, Kargapazarı ve Pasinler alanlarındaki istifler içinde olivin içeren tek birimdir. Kargapazarı dağıtımının Karakale-Pertek fayına komşu Doğu ve GD yamaçlarında, KB yamaçta görülen Güngörmez volkaniti ve üyelerine ait birimler hiç bir yerde görülmezler.

Pasinler alanı. - Bu çalışmada Pasinler alanı olarak isimlendirilen saha, Erzurum'un doğusunda, Kargapazarı dağıtımının GD eteklerinden başlayarak Pasinler ova-

sınının kuzeyinde uzanan arazi parçasıdır. Pasinler ovası, Doğu Anadolu'da Muş havzasından sonra en büyük ikinci dağlar arası havzadır. Sondaj verilerine göre, havza EKP volkanitlerinin, karbonat ve kırıntılı Sedi-ment arakatlıkları da içeren 2000 m.den kalın bir istifini içerir (Gedik, 1978; TPAO Arama Grubu elemanlarıyla sözlü görüşme). Söz konusu istifin içinde çokaldığı havza, pull-apart bir sistem içinde gelişmiştir. Pasinler alanının komşu Kargapazarı alanı ile sınırını, KD-GB doğrultusunda uzanan, sol yanal atımlı Karakale-Pertek fayı belirler (Şek. 2). Bu fay aynı zamanda birbirlerinden morfolojik ve istifsel olarak farklı iki alanı da bir araya getirir. Havzanın güneyinde ise, çarpışma kökenli volkanitler, GB'da Palandöken silsilesi dışında oldukça dar bir alanda mostra verirler.

Komşu Kargapazarı gibi Pasinler alanı da belirgin bir plato morfolojisine sahiptir. Pasinler platosu olarak isimlendirilen bu plato, denizden 2200-2300 m. yüksekliktedir ve batıdaki Kargapazarı platosuna nazaran ortalama 600-700 m. alçakta yer almaktadır. Platonun üst düzeylerinde bulunan daha dayanımlı Siyah ignimbrit ve Kargapazarı volkaniti gibi birimler, alttaki gevşek piroklastikleri koruyarak platonun dayanımlı üst kabuğunu oluştururlar ve morfolojiyi büyük ölçüde denetlerler. Platonu oluşturan volkanik birimler, yataya yakın konumda, güneye doğru 5-10° eğimlidirler. Ova-ya yakın bu eğim kısa bir mesafede 30-35°'ye ulaşır ve bu kesimde volkanik birimler monoklinal bir kıvrım yaparak ovayı örten Pliyosen Aras formasyonu ve Kuvarterner alüvyon örtüsü altında kaybolurlar.

Pasinler Platosu, kuzeyden güneye doğru uzanan, içlerinde volkanik istifin mükemmel mostralarnın ortaya çıkmış olduğu derin vadilerle kesilir. Pasinler ovasına dik olarak ovaya doğru uzanan bu vadilerde kuzeyden güneye akan dereler, ovadaki kalın Kuvaterner kırıntılı istiflerini besleyen ana drenaj kollarıdır. Batıdan doğuya doğru bunlar Büyükdere (Kumuç), Tımar, Samsor ve Harabe dereleridir (Şek. 2).

Batıdaki Kargapazarı ve Dumlu alanlarının aksine, Pasinler alanındaki volkanik istifin hacimsel olarak büyük kısmını piroklastik akıntı (pyroclastic flow: ignimbrit) ve döküntü (fall) birimleri oluşturur. Lav akıntıları ise çok daha az hacim kaplarlar, istifin alt kesimlerinde piroklastik ürünler egemenken, üst düzeylerine doğ-

KDANADOLU VOLKANİZMASININ VOLKANO-STRATİGRAFİSİ VE K/Ar YAŞ BULGULARI

ru lav katkılarında genel olarak artma görülür. Karakale-Pertek fayının hemen batısındaki Kargapazarı alanında ise, Taban Tüf düzeyinde sadece piroklastik döküntü ve tüf düzeyleri hâkimdir, ignimbritlere çok nadir rastlanır. Söz konusu fay istifin bu denli farklı iki kesimini bir araya getirebildiğine göre, önemli ölçüde sol yanal atıma sahip olmalıdır.

Aşağıda, Pasinler kuzeyinde yüzeyleyen çarpışma kökenli volkanitler, istifin tabanından başlayarak üste doğru sırasıyla tanıtılacaklardır.

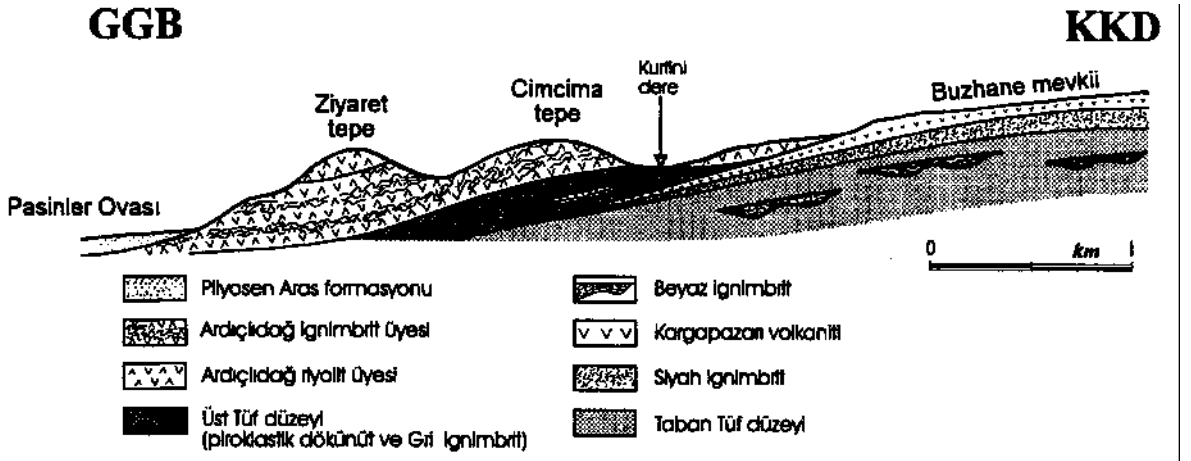
Pasinler ovası güneyinde, Pasinler alanının temelinde yer alan formasyonlar yaygınca mostra verirler. Bu kesimde bölgenin temelini, geniş alanlarda yüzeyleyen Üst Kretase yaşlı Doğu Anadolu Yığılım Karmaşığı oluşturur. Bu karmaşığı ilk üzerleyen birim, ofiyolit kökenli klastikler ve olistostromlara temsil edilen Eosen yaşlı Bulkasım formasyonudur. Bu formasyon, Eosen Narman grubu tarafından örtülür. Tüm bu formasyonlar, Alt-Orta Miyosen periyodunda çökelmiş olan ve evaporitik arakatlıklar içeren karasal kırıntılı istiflerden oluşan Güllüce formasyonu tarafından diskordans olarak örtülür. Stratigrafik istifte daha üstte, Üst Miyosen yaşlı resifal Hündül kireçtaşı bulunur. Dağınık ve küçük yamalar şeklinde izlenen EKP'nun çarpışma kökenli volkanik birimleri, yukarıda tanıtılan birimleri uyumsuz olarak örterler, istifin en genç kesimi ise, Pliyosen yaş-

lı kırıntılardan meydana gelen karasal Aras formasyonu ile temsil edilir.

Pasinler kuzeyindeki alanda ise istifin temeli, kuzeydoğuda bulunan 300-350 m. derinliğindeki Harabedere vadisi tabanında görülür (Şek. 2 ve 8). Bu kesimde, Eosen yaşlı Narman grubuna ait Kışlaköy volkanik üyesi vadi boyunca kuzeye doğru yaygınlık kazanarak mostra verir. Birim başlıca bazik ve ortaç bileşimde lavlar, aglomera ve az oranda fliš benzeri şeyil, marn ve silttaşı arakatlıklarından oluşur. Eosen volkanitlerinin, platoyu oluşturan EKP volkanitlerinden en büyük farkları; çok daha fazla alterasyonu olmaları, eklem takımlarıyla belirgin bir şekilde kesilmeleri ve ayrıca denizel Sediment arakatlıkları kapsamalıdır.

Eosen Kışlaköy volkaniti, bazaltik andezitten, bazaltik trakiandezit ve andezite kadar uzanan dar bir bileşim aralığına sahip, jeokimyasal olarak belirgin bir yay bileşeni içeren kalkalkalen lavlardan oluşmuştur. Lavlar plajiyoklaz fenokristalleri (An_{54-58}) ve ojit mikrofeno-kristallerinden oluşurlar ve porfiritik doku sunarlar. Kızılveren köyü doğusunda, Harabedere vadisi tabanından alınan bir numunenin K/Ar yaş tayini sonucunda 38.5 (± 0.7) milyon yıl yaşta elde edilmiştir.

Harabedere vadisinde Eosen volkanik istifi üzerine uyumsuz olarak gelen ilk birim, Siyah andezit olarak



Şek. 6- Pasinler KD'sunda bulunan Sansor köyü doğusunda, Pasinler ovası ile Buzhane mevkii arasından geçen enine kesit.

adlandırılan, her biri 5-15 m. kalınlıkta 4-5 andezitik lav akıntısından oluşan koyu renkli afirik lav istifidir (Şek. 1). Birim, vadinin her iki yamacında tabanda 3-4 km. uzunlukta bir şerit şeklinde mostra verir. Siyah andezitin tabanına yakın düzeyinden alınan bir numunenin K/Ar yaş tayini 7.83 (± 0.12) milyon yıl vermiştir.

Siyah andezit, üst dokanakta Taban Tüf düzeyi ile örtülür. Taban Tüf düzeyi, Pasinler Platosunun görünür tabanında en yaygın birimdir ve Plinian tipi güçlü patlamalı erüpsiyonlar sonucu yüzeye çıkmış olan riyolitik bileşimde piroklastik akıntı (flow), döküntü (fall) ve az miktarda surge istiflerinden oluşur. Birimin en belirgin özelliği, hemen hemen tümüyle camsı materyalden oluşması (vitrik) ve hiç kristal içermemesidir. Birimin görünür kalınlığı Pasinler ovasına yakın kesimlerde ve özellikle batıda 200-300 m. civarındadır. Doğuya ve kuzeye doğru bu kalınlık gitgide azalır. Doğuda, Harabedere vadisi boyunca kuzeydoğuya doğru gidildikçe, Taban Tüf düzeyi incelenerek kaybolur. Kuzey alanlarda ise, yer yer ince merccekler halinde görülür. Bu alanlarda birimin üzerine gelen Siyah ignimbrit, Eosen volkanitini doğrudan örter.

Batıda, Büyükdere (Kumuç) vadisi dolaylarında Taban Tüf düzeyinin hemen tümünü piroklastik akıntılar oluşturur, istif içinde piroklastik akıntı ürünlerinin döküntü ürünlerine oranı, Karakale-Pertek fayından doğuya, Harabedere vadisine doğru gidildikçe azalır. Büyükdere vadisi boyunca ve özellikle bu vadinin ovaya yakın 300-350 m. derinlikteki dik doğu yamacında, kalınlıkları 100 m.ye kadar ulaşan 3-4 adet piroklastik akıntı üniteleri mükemmel mostralar halinde izlenirler (Şek. 1). Piroklastik akıntı ünitelerinden her biri, kendi içinde rengi, kaynaklanma (welding) derecesi, iç yapısı ve dokusu ile birbirinden farklı "Beyaz" ve "Gri ignimbrit" fasiyesleri olmak üzere iki fasiyese ayrılabilir.

Beyaz ignimbrit, piroklastik akıntılarının esas malzemesini oluşturan bol vesiküllü pomzanın, üstteki yükün etkisiyle taban kesimlerde sıkışarak kaynaklanması sonucunda meydana gelmiştir. Birim, Taban Tüf düzeyinin kabaca %25-30'unu oluşturur. Beyaz ignimbrit içinde çok sayıda ve mm.den birkaç metreye kadar ulaşan boyutta akma kıvrımlanmaları ve 1 ilâ 10 cm. boyutunda yırtışım (accretionary) lapillileri vardır. Akma ünitelerinin tabanına yakın kesimler, kompaksiyonun en yo-

ğun olduğu yerlerdir ve bu düzeylerde obsidiyen bantları çok yaygındır. Beyaz ignimbrit, üste doğru tedricî olarak Gri ignimbrite geçiş gösterir. Gri ignimbrit, oldukça vesiküler, masif, tümüyle camsı gri renkli pomzadan oluşur. 1-2 mm.ye kadar çapta vesiküller içeren pomza, elde dağılacak derecede kırılıgandır, istifte daha az oranda bulunan piroklastik döküntü birimleri ise, genel olarak beyaz ve grimsi beyaz renklerde birkaç mm.den 2-3 cm.ye kadar ulaşan farklı tane boylarında ince vesiküllü pomzanın oluşturduğu düzeylerden meydana gelir. Bazı düzeylerde, tırmanan dün yapıları ve 50 cm.ye ulaşan boyutlarda iri, köşeli bloklar içeren surge düzeylerine de rastlanır. Büyükdere vadisinde görüldüğü gibi (Şek. 1), Taban Tüf düzeyi yer yer Kargapazarı volkanitine ait bazik daykılarla kesilir. Bu daykaların çoğu yaklaşık D-B doğrultusundadırlar.

Harabedere vadisi batısında Kızılveren köyü dolaylarında 2 km², lik dar bir alanda mostra veren Kızılveren dasiti (Şek. 8), Dumlu alanında istifin en üst kesiminde yer alan Dumlu volkanitine büyük benzerlik gösterir. Porfiritik doku gösteren birim, dasitik bileşimdedir ve plajiyoklaz ile kahverengi amfibol fenokristalleri ile az miktarda orto ve klinopiroksen içerir. Birimin maksimum kalınlığı 130 m.dir. Birim üst dokanakta önce ince bir tefra, daha sonra da Siyah ignimbrit ile örtülür.

Çoğun siyah, şarabî kırmızı, kiremit rengi, bordo, kahverengi ve bej renkler sergileyen Siyah ignimbrit, Pasinler Platosunun 1/3'den fazlasını kaplar. Bileşimi trakidasitten riyolite kadar değişir. Birimin kalınlığı birkaç metreden, 150-200 m.ye (ör. Tımar dere vadisinde görüldüğü gibi) kadar değişir. Çok iyi gelişmiş ötekstitik doku (eutaxitic texture) ve boyları 5-10 cm.ye ulaşan siyah renki fiammeler içeren birim, çoğunluğunu plajiyoklazların oluşturduğu %40'a ulaşan miktarda fenokristal içerir. Bazı düzeylerde Beyaz ve Gri ignimbritlere ait çok sayıda parçalar içerir. Harabesürbehan köyü civarındaki mostralarında görüldüğü gibi, birim içinde yer yer iyi gelişmiş sütun yapıları da vardır. Birimin tabanındaki Taban Tüf düzeyi ile dokanağı çoğun keskin ve düzlemseldir. Birim, üst dokanakta Kargapazarı volkaniti tarafından örtülür (Şek. 2 ve 8).

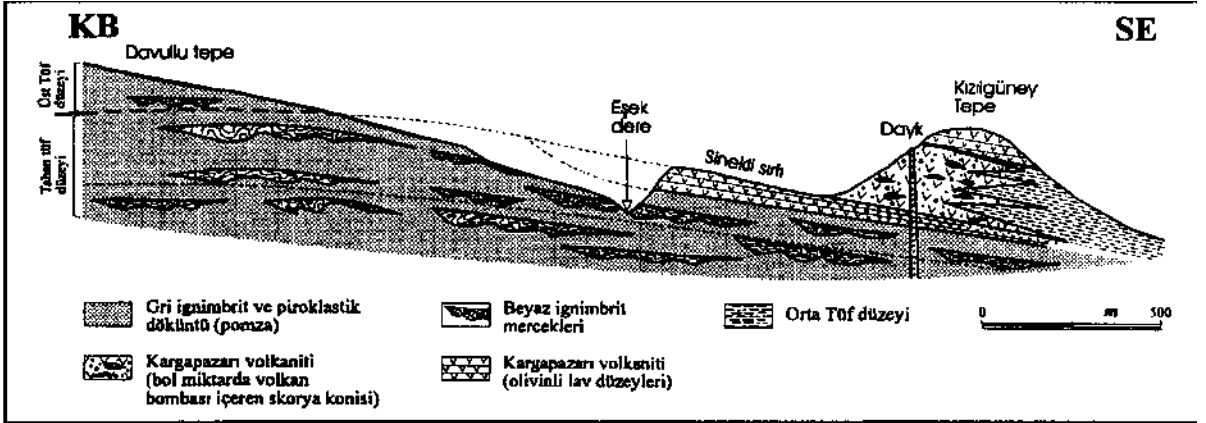
Komşu batı alanlarda kalın istifler oluşturmalarına karşın, Kargapazarı volkaniti Pasinler Platosu üzerinde ince (3-30 m.), yanal yönde devamsız, yer yer merccek

KD ANADOLU VOLKANİZMASININ VOLKANO-STRATİGRAFİSİ VE K/Ar YAŞ BULGULARI

biçimli lav akıntıları şeklindedir. Tımar köyü KB'sında Kızılgüney tepe dolaylarında 2 km², lik bir alanda birim, bol miktarda volkan bombası ve skoryadan oluşan bir spatter konisi içermektedir (Şek. 7).

Büyükdere vadisi ile Sansor dere arasındaki alanlarda Siyah ignimbrit ve Kargapazarı volkaniti, Taban Tüf düzeyi ile hemen hemen aynı özelliklere sahip afirik-riyolitik bir piroklastik istifile örtülür. Birim, Büyükdere köyü kuzeyinde Kotandüzü komu ile Karagüney ve Davullu tepelerini kapsayan geniş bir alanda ve ayrıca Sansor dere vadisi boyunca mostra verir (Şek 2 ve 7). Genel olarak birimin kalınlığı güneye, yani ovaya doğru artar. Üst Tüf düzeyi ise üst dokanakta Ardıçlıdağ riolyiti adlı porfiritik bir lav istifi ile örtülür.

sahip birimi besleyen bacalardan (conduit) birisi, Badıçivan köyü kuzeybatısında, Sarıtaş derenin yatağında görülür. Bu kesimde Eosen yaşlı Narman grubuna ait silttaş-şeyl istifini kesen birim, dokanakta yaklaşık 1 m.lik bir zonda yan kayaç renginin siyaha dönüştüğü bir pişme zonu oluşturmuştur (Şek. 8). Ardıçlıdağ volkanitine ait ignimbrit üyesi, Sansor dere vadisinin doğu yamacında yüzeylenir ve KKD-GGB doğrultusunda bir mostra paterni sergiler. Birimin lavları ile aynı mineralojik bileşime sahip olan ignimbrit, şiddetli kompaksiyona uğramış beyaz kaynaklı pomzadan oluşur ve ötekstitik (eutaxitic) doku gösterir. Platodaki diğer ignimbrit düzeylerinden bol feldispat ve kuvars fenokristalleri içermesiyle farklılık gösterir.

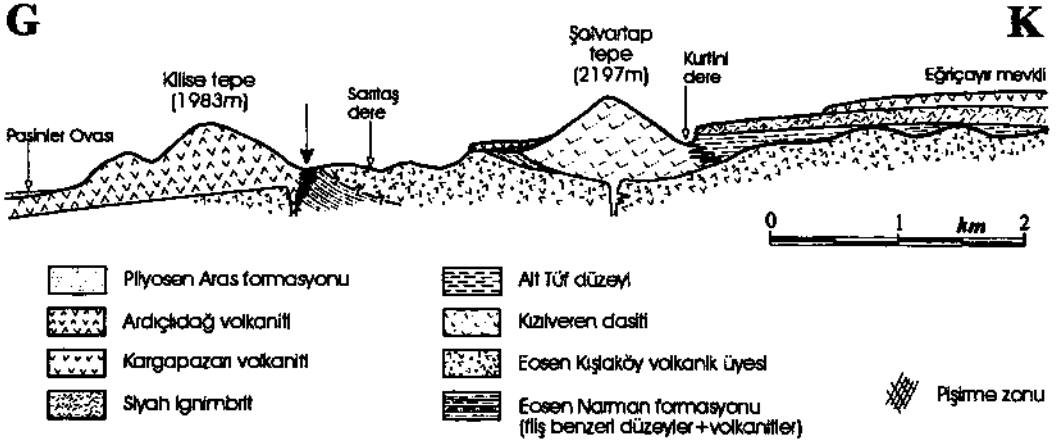


Şek. 7- Pasinler KD'sunda bulunan Tımar köyü batısında, Kızılgüney tepe ile Davullu tepe arasından geçen jeoloji enine kesiti.

Pasinler alanında volkanik istifin en üstünde yer alan Ardıçlıdağ volkaniti, porfiritik dokulu masif riolyolitik lav ve ignimbritten oluşur. Harabedere vadisinin her iki yanında platonun üst seviyelerinde, özellikle Sansor ile Badıçivan köyleri arasında Ardıçlıdağ dolaylarında, ayrıca Pasinler kasabası KW'sında Serçeboğazı ve Tizgi köyleri dolaylarında mostra verir. Ardıçlıdağ riolyolitik lav üyesinin Ardıçlıdağ tepe dolaylarında kalınlığı 200 m.ye kadar ulaşır ancak kuzeye ve doğuya gidildikçe bu kalınlık 30-50 m.ye düşer. Sarımsı beyaz, krem renkler sunan birim, iri sanidin, anortoklaz, plajiyoklaz, kuvars fenokristalleri ile az miktarda klinopiroksen mikrokristalleri içerir, camsı bir hamura sahiptir ve Vitrofirik doku gösterir. Çoğu yerde yaygınca altere olmuştur. Büyük oranda aşınmış bir dom geometrisine

Horasan kuzeyi. - Horasan kuzeyinde temel hemen hemen tümüyle Üst Kretase yaşlı Doğu Anadolu Yığılma Karmaşığı (DAYK) (Yılmaz ve diğerleri, 1988) tarafından temsil edilir. DAYK, içerdiği Triyastan Senomaniyene kadar yaşlara sahip kireştaşı olistolitleri, serpantinleşmiş peridotit, hazburjit, gabro, diyabaz ve yer yer yastık yapılı spilitik bazalt gibi ultrabazik ve bazik kaya blokları ile tipik bir ofiyolitik melanj niteliği sunar. DAYK- Karaurgan'ın batısında Kızılcadağ, Gökdağ ve Karataşdağ dolaylarında yaygınca mostra verir.

Horasan kuzeyinde DAYK üzerine uyumsuz olarak gelen ilk birim, ince tabakalı kumtaşı ve şeyl ardalanmasından oluşan Eosen yaşlı Narman grubudur. Ofiyolitik temeli uyumsuz olarak örten ilk volkanik birim



Şek. 8- Pasinler KD'sunda bulunan Badıcivan köyü kuzeyinde, Kilise tepe ile Kızıveren köyü kuzeyindeki Eğriçayırı mevki arasında geçen jeoloji enine kesiti.

ise, Akveren dasiti olarak adlandırılan ve öhedral/sub-hedral plajiyoklaz, aşırı altere hornblend ve yer yer biyotit fenokristalleri içeren ve pembemsi-bej renkler sunan masif bir porfiritik lav istifidir. Plato volkanitlerinin temelinde dağınık küçük mostralalar halinde yüzeylenen birim, Pasinler güneyinde K/Ar yöntemiyle yaşı saptanmış olan Tuzluyolları dasitine büyük benzerlik sunar. Bu nedenle EKP volkanitlerinden daha yaşlı (~ 23 milyon yıl) olduğu düşünülmektedir. Çerkezintaş tepe dolayında birim, 11 milyon yıl yaşındaki Kötek bazaltı ile örtülür.

Horasan kuzeyinde EKP volkanitlerine ilişkin volkanik istifin tabanı, Pasinler kuzeyinde tanımlanan Taban Tüf düzeyine çok benzer, aynı dönemde oluşmuştur ve dolayısıyla istifsel olarak onun yan al eşdeğeridir. Bu nedenle, bu çalışmada Horasan kuzeyindeki taban düzeyi için de aynı isim kullanılmıştır. Taban Tüf düzeyi, riyoilitik ve bazen riyo dasitik bileşimde afirik dokulu piroklastik akıntı, döküntü birimleri, surge üniteleri, epiklastik tüf düzeyleri ve ortalama 2-5 m. kalınlıkta bazik-ortaç lav ve aglomera arakatıkları içerir. Piroklastik taban düzeyinin maksimum toplam kalınlığı 200-250 civarındadır. Piroklastik materyal, birimin hacimce % 70-80'lik bir kesimini oluşturur.

Piroklastik döküntü birimleri, matriks destekli, ince vesiküler dokulu yuvarlak beyaz pomza parçalarının

oluşturduğu, tabakalı istiflerden oluşur. Piroklastik akıntı birimleri ise, Pasinler alanındaki ile aynı özellikler sunan Gri ve Beyaz ignimbrit düzeylerinden meydana gelir. Her iki fasiyese ait volkanik birimlerin mostralara, Büyükçay dere vadisi boyunca izlenir.

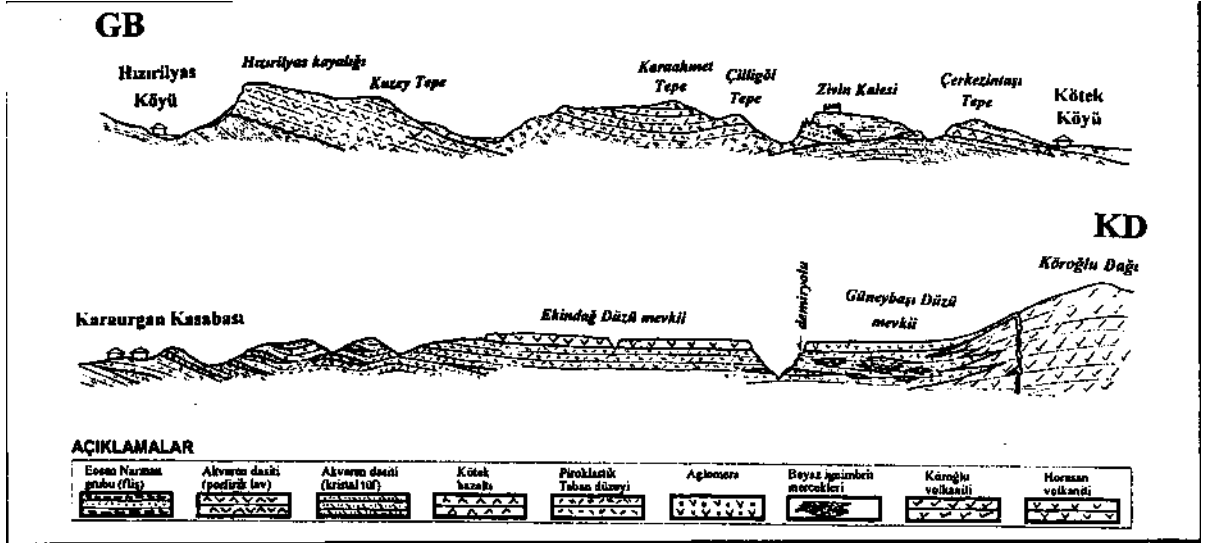
Piroklastik Taban düzeyinin görünür tabanında, Kötek köyü yakınlarında afirik dokulu ve siyah renkli bazik bir lav düzeyi mostra verir. Plajiyoklaz ve olivin mikrofeno kristalleri içeren, hiyalopilitik, intersertal ve bazen de amigdaloidal dokular sergileyen birim, 10-30 m. kalınlıktadır. Kötek bazaltı olarak isimlendirilen birimin (Şek.9) tabanından alınan bir numunenin K/Ar yaş tayini sonucunda 11.1 (± 0.5) milyon yıl bulunmuştur. Aynı birimin daha kuzeydeki mostralardan alınan diğer bir numune ise, 9.94 (± 0.40) milyon yıl yaşı vermiştir. Bu veriler, bu çalışmada EKP volkanitlerinden bulunan en eski K/Ar yaş sonuçlarıdır. Buna göre Kötek bazaltı, EKP üzerinde volkanik aktivitenin en erken merkezlerinden birini temsil etmektedir.

Piroklastik Taban düzeyi, amfibol içeren porfiritik dokulu lavlarla örtülür. Bu lavlar, bileşim ve dokuları bakımından batıda Dumlu dağı dolaylarında yüzeylenen Dumlu volkanitine çok benzerler. Söz konusu lavlar hemen hemen hiç piroklastik materyal içermezler ve plato üzerinde diğer birimlere nispetle yan al yönde az yayımlı ve yüzlerce metre kalınlığa ulaşan dom ben-

zeri yapılar şeklinde mostra verirler. Horasan kuzeyindeki alanlarda birimin en iyi mostraları, kuzeyde Köroğlu köyü civarındaki Köroğlu dağı dolaylarındadır ve bu nedenle birim Köroğlu volkaniti olarak isimlendirilmiştir. Köroğlu dağı dolaylarında birim, 400-500 m. kalınlığa kadar ulaşan porfiritik masif lav düzeylerinden oluşur (Şek.9). Fenokristallerin çoğunu plajiyoklaz (An_{40-57}), amfibol (magnezyo-ferri-çermakit, magnezyo-ferri-taramit ve magnezyo-edenit), ve az miktarda hipersten oluşturur. Ayrıca bazı lav düzeylerinde az miktarda korozyonlu kuvarsa da rastlanır.

K/Ar yaş tayinine göre birimin yaşı 4.14 milyon yıldır (± 0.21).

Süphan dağı dolaylarında ve Kağızman'a kadar Araş nehrinin kuzey ve güneyinde kalan yüzlerce km^2 .lik alanlarda, Horasan volkanitini oluşturan volkanik aktivite ile hemen hemen aynı zaman diliminde yüzeye çıkmış olan, aynı stratigrafik pozisyonu gösteren ve benzeri kimya ve petrografi sergileyen bazik lavlar, platonun en üst düzeylerinde yaygınca mostra verirler.



Şek. 9- Horasan kuzeyinde Hızırilyas köyü ile Köroğlu dağı arasından geçen jeoloji enine kesiti.

Horasan kuzeyinde EKP'nun en üst düzeyi, siyah-koyu gri renkli afirik lav akıntılarının oluşturduğu bir birimle temsil edilir. Horasan volkaniti olarak isimlendirilen birim, platonun yatay morfolojisini oluşturur (Şek. 9). Horasan volkaniti, bazaltdan bazaltik andezitike kadar dar bir bileşim aralığına sahip vitrofirik, hiyalopilitik, intersertal ve nadiren de mikroporfiritik ve kümülüüs dokular sergileyen lavlardan oluşur. Başlıca plajiyoklaz, olivin ve klinopiroksen fenokristalleri içerir. Birimin kalınlığı yerel olarak geniş bir aralıkta değişir. Örneğin Abulbart (Kurbançayırı) köyü doğusunda birim bir-iki metre kalınlıkta lav düzeyinden oluşurken, kuzeyde Sırbasan köyü kuzeyinde toplam 60-70 m. kalınlıkta bir istif oluşturan 7-8 adet benzeri doku ve bileşimde lavdan meydana gelir. Sırbasan köyü kuzeydoğusunda bulunan Karaderenin sırtı dolayından alınan bir numunenin

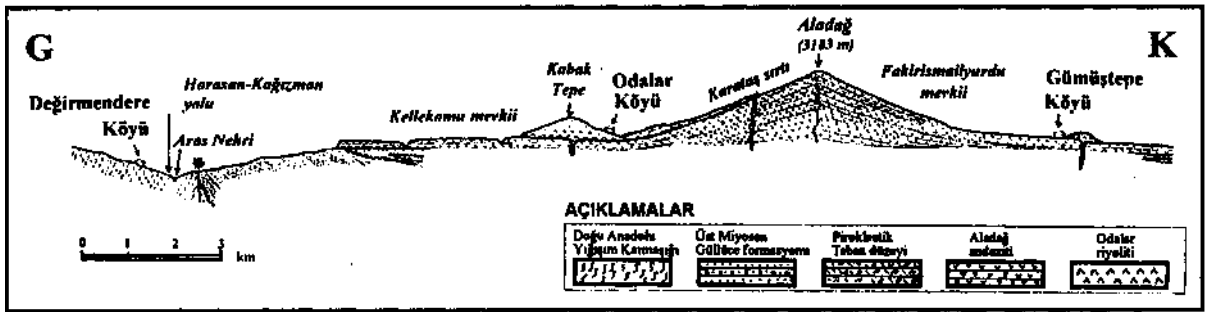
Horasan'ın güneyinde, Ağullu ve Yazılıtaş köyleri civarında Saçdağ ve Yazılıtaş tepeler dolaylarında dasitik bileşimli masif lavlar, bir iki km. çapında dom benzeri kitleler halinde Eosen Bulkasım ve Oligo-Miyosen Güllüce formasyonları üzerine diskordansla gelirler. Tipik porfiritik dokular gösteren ve iri Plajiyoklaz (An_{41-28}) yeşil amfibol (çermakit-edenit) ve öhedral biyotit fenokristallerinden oluşan bu lavlar, Saçdağ dasiti olarak isimlendirilmişlerdir. Besi ve Haydar komları arasında, Saçdağ dasiti bileşiminde ancak daha ince dokulu 5-15 m. kalınlıkta bir dayk, Güllüce formasyonunu keserek D-B doğrultusunda uzanır. Boyu 6-7 km. civarında olan bu sokulum, EKP, üzerinde bu çalışmada gözlenmiş olan en büyük dayktır.

Aladağ alanı. - Karakurt ile Kağızman arasında bulunan Aladağ, EKP üzerindeki orta büyüklükte volkan-

lardan biridir. Plato üzerinde yaklaşık 75-80 km² alan kaplar ve ortalama plato düzeyinden 950 m. daha yüksek (~ 3000 m.) bir zirveye ve radyal drenaj ağı ile kısmen aşındırılmış bir koni şekline sahiptir. Volkan konisinin kuzey yamacı, olasılıkla püskürmeler sırasında kraterin çökmesine bağlı olarak kısmen yok olmuştur. Aladağ volkanından çıkan lavlar, plato üzerinde yüzlerce km² alan kaplarlar. Aladağ'ın gövdesi, hemen tümüyle lavlardan oluşmuştur (Şek.10). Söz konusu koniyi ve çevre alanlarda platoyu oluşturan lavlar, çoğunlukla andezitik nadiren de dasitik bileşimlidirler. Mikroporfiritik, hyalopilitik ve zaman zaman da seriate dokuları gösteren lavlar, başlıca plajiyoklaz (An₃₇₋₅₈), ojit

doğuya doğru giderek derinleşir ve Çayarası ile Değirmendere köyleri arasında bölgenin temelini oluşturan DAYK'na ulaşır. Bu lokasyondan doğuda Kağızman'a kadar DAYK, Aras nehri güney alanlarında yaygınca mostra verir.

Aladağ alanında, EKP'na ilişkin volkanik istifin tabanında da, Horasan alanı için tanıtılmış olan Taban Tüf düzeyine benzer piroklastik akıntı, döküntü birimleri ve bunlarla ardalanmış bazik-ortaç lav akıntılarının yaygınca mostra verir. Bazı kesimlerde, örneğin Mescitti köyü dolaylarında, mesa biçimli obsidiyen akıntıları, coulee ve lensleri yaygınlık kazanır. Bu kesimlerde ob-



Şek. 10- Aras nehri ile Aladağ arasından geçen jeoloji kesiti.

(az oranda endiyopsit) ve çok az miktarda ortopiroksen (bronzit ve hipersten) mikrofeno kristalleri içerirler. Hamur hemen hemen tamamen volkanik camdan oluşur. Aladağ andeziti olarak isimlendirilen bu birimin Kalebaşı köyü civarındaki mostralardan alınan bir numunenin, K/Ar yöntemi ile 3.55 milyon yıl yaşında (± 0.13) olduğu saptanmıştır. Aladağ andezitinin EKP'nun en üst seviyesinde yer alan Horasan volkaniti gibi diğer birimlerden en büyük farkı, olivin içermemesi ve SiO₂'ce daha zengin olmasıdır.

EKP Aladağ güneyinde, batıdan doğuya doğru akan Aras nehri tarafından derince kesilir. Horasan ile doğusundaki Akkoz köyü arasında Aras nehri, ortalama derinliği 300 m. olan ve içinde EKP volkanitlerinin mükemmel bir kesitinin yüzeylendiği dik yamaçlı kanyon benzeri bir vadi oluşturur. Bu vadide EKP'nun temeli, doğudaki Kalebaşı köyü dolaylarına kadar yüzeylenmez. Kalebaşı köyünün doğusundaki alanlarda ise EKP volkanitlerinin Oligo-Miyosen Güllüce formasyonunun canlı kırmızı, sarı, beyaz, krem renkli kırıntılı düzeylerinin üzerine diskordansla geldiği görülür. Vadi

sidiyen siyah, gri, kahverengi, kırmızı, sarı renklerde, yer yer şeffaf yamalar içerir ve yer yer de kalem kılıvı gösterir. Karakurt-Sankamış yol yarmalarında bu tür obsidiyenlerin iyi mostralara rastlanır. Taban Tüf düzeyi, Horasan volkanitinin eşdeğeri plato oluşturan bir bazik lav düzeyi ile örtülür.

Plato üzerinde, Horasan volkanitinin üstünde bazı küçük, Hawaii tipi lav fiskiyelerinin oluşturduğu genç spatter konilerine de rastlanır. Bunlardan birisi, Karakurt'un 7 km. batısında, Uzungazi (Kızıl) köyü dolaylarında mostra vermektedir. 1/4 km² taban alanına ve 50-70 m. yüksekliğe sahip olan koni, kırmızı okside skorya, lapilli ve 30-40 cm.ye kadar varan boylarda iğ ve disk şeklinde çok miktarda balistik bombalar içerir. Piroklastik materyal yer yer kaynaklanmıştır (agglutinated). Volkan bombalarından alınan bir numunenin K/Ar yaş tayini, 4.59 milyon yıl (± 0.19) vermiştir.

Aladağ'ın güneyinde, Odalar köyüne yakın Kabak tepe dolaylarında, Aladağ andeziti üzerine porfiritik ve mikroporfiritik dokulu riyolitik ve diyodasitik bir lav do-

KDANADOLU VOLKANİZMASININ VOLKANO-STRATİGRAFİSİ VE K/Ar YAŞ BULGULARI

mu gelmektedir (Şek. 10). 200 m. kadar kalınlıkla 5 km² civarında alan kaplayan birim, açık gri renkli camsı bir hamur içinde sodik plajiyoklaz kristallerinden oluşur, porfiritik ve Vitrofirik doku sunar. Birim, Odalar riyodasiti olarak isimlendirilmiştir. Birime benzer konum ve bileşimde bir başka asitik dom, Aladağ'ın kuzeyinde, Gümüştepe köyü yakınındaki Gümüş tepede mostra vermektedir (Şek. 10).

Kağızman kuzeyi.- Kağızman alanının temelini, DAYK oluşturur (Şek.1). Aras nehri güneyinde geniş alanlar kaplayan birimi diskordansla örten en yaşlı formasyon, Kötek köyünün KD'sunda 15-20 km²'lik bir alanda mostra veren Üst Kretase yaşlı Kötek kireçtaşıdır (Şahintürk ve Erakman, 1978). İnce tabakalı mikritik karbonat düzeylerinden oluşan birim, *Globotruncana* sp. ve Globogeriinde fosilleri içerir. Kötek kireçtaşı, Camuşlu formasyonu adı verilen Eosen yaşlı sığ denizel fliş benzeri bir sedimanter birim ile diskordans olarak örtülür. Bazı düzeylerde *Nummulites* sp. içeren birim, başlıca kumtaşı, şeyl ve konglomera tabakalarından oluşur, tabana yakın düzeylerde ise karasal fasiyesler ve yer yer kömür tabakaları da kapsar.

Yukarıda tanımlanan tüm birimler, Üst Miyosen yaşlı Güllüce formasyonunun oluşturduğu kalın klastik sedimanter bir istif ile geniş alanlarda diskordans olarak örtülür. Tabanda kırmızı, bordo, kahverengi, sarı, bej, yeşilimsi gri ve beyaz gibi son derece renkli kalın tabakalı, konglomera hâkimken, birimde üste doğru çamurtaşı yaygınlık kazanır. Çamurtaşı, kötü boylanmalı kumtaşı ve konglomera arakatlıkları da içerir. Karasal bir ortamın ürünü olan bu formasyonun en üst düzeylerine yakın tuz ve jipsli evaporitik tabakalar da mostra verir. Aras nehrinin kuzeyindeki alanlarda, doğuda sınıra kadar EKP volkanitleri, Güllüce formasyonu üzerinde diskordans ile oturur.

Kağızman kuzeyinde EKP volkanitleri tabanda bir piroklastik düzey ile başlar. Piroklastik döküntülerin yoğun olduğu bu düzey içinde az miktarda piroklastik akıntı ve bazik/ortaç lav arakatlıkları da bulunur. Bu düzeyin kalınlığı 150-200 m. civarında değişir. Kuzeyde, Camuşlu köyü dolaylarından başlayarak Çukurayva ve Çilehane köylerine dek uzanan ve kalınlığı 50-150 m. ye kadar ulaşan bir piroklastik akıntı ünitesi, Taban Tüf düzeyinin en üst kesimine yakın düzeyde yer alır. Yoğun bir şekilde yataya yakın akma eklemleri içerir. Çu-

kurayva riyoliti olarak isimlendirilen birim, açık gri renkli camsı bir hamur içinde anortoklas, sanidin, andezin/oligoklaz ve kuvars fenokristalleri içerir. Boğaz Değirmeni mevki civarında, Çukurayva riyolitinin tabanında sütun yapıları sunan kesimden alınan bir numunenin K/Ar yaş tayini 5.15 (± 0.20) milyon yıl vermiştir.

Daha doğuda, Kağızman-Kars karayolunun platosunun güney yamacına tırandığı Paslı köyü dolaylarında, porfiritik dokulu, masif bir trakidasit birimi mostra verir. Açık gri-krem renkler gösteren birim, subhedral plajiyoklaz (An₃₆₋₄₅), kuvars, az miktarda amfibol ve biyotit fenokristalleri içerir. Paslı trakidasiti olarak isimlendirilen birim, piroklastik döküntü ve kül düzeylerine yanıl yönde geçiş gösterir.

Kağızman kuzeyinde volkanik istifin en üst düzeyi olivin içeren Kars Plato volkaniti ile temsil edilir. Birim, EKP'ndaki diğer birimlere göre daha bazik bazalt, bazaltik andezit ve bazaltik trakiandezitik (hawaiiite) bileşimler sergileyen lavlardan oluşur. Mikroporfiritik ve piroklastik dokuların yaygın olduğu birim, başlıca plajiyoklaz, klinopiroksen ve olivin feno ve mikrofenokristalleri içerir. Kars Plato volkanitinin alttaki birimlerle olan dokanağı çoğunlukla keskin ve düzlemseldir. Kars Plato volkaniti düzeyini oluşturan çok sayıda lav akıntıları, doğu ve kuzey alanlarda bölgenin önemli bir bölümünü kaplayarak, denizden 2 km. yüksekte bulunan Kars Platosunu oluştururlar.

Kars Plato volkaniti, doğuya doğru gidildikçe gençlesin Paslı köyünün 1 km. kuzeyinde birimden alınan numunenin K/Ar yöntemiyle saptanan yaşı 3.40 (± 0.10) milyon yıl iken, daha doğuda Yağlıca dağıının güney yamaçlarında platodan alınan numunenin yaşı ise 2.72 (± 0.10) milyon yıl olarak belirlenmiştir. Pearce ve diğerlerinin (1990) yaş bulguları, Kars Plato volkanitinin yaşının 1.5 my'a kadar gençleştiğini göstermektedir.

VOLKANİK İSTİFLERİN BÖLGESEL KORELASYONU

Yukarıda altı ast alanda tanımlanan volkanik istifler karşılaştırıldıklarında, Erzurum-Kars Platosu üzerinde erüptif karakterlerine ve mineralojik, petrografik ve kimyasal bileşimlerine göre temelde dört farklı düzeyin varolduğu görülmektedir. Tabandan üste doğru bu düzeyler (Çizelge 1):

Çizelge 1- Erzurum-Kars Platosunun çarpışma kökenli volkanitlerinin korelasyon çizelgesi.

Bölgelere göre formasyonların dağılımı							
Stratigrafik düzey	Alt tip	Dumlu Dağı Alanı	Kargapazarı Dağı Alanı	Pasinler Alanı	Horasan Alanı	Aladağ Alanı	Kağızman Alanı
Plato düzeyi üzerindeki felsik domlar	—	—	—	Ardıçdağ volkaniti	—	Odalar riyodasiti	—
	olivmalı	—	Kargapazarı volkaniti	Kargapazarı volkaniti	Horasan volkaniti	Horasan volkaniti	Kars Plato volkaniti
Plato oluşturan bazik/ortaç lav düzeyi	olivatsız	—	—	—	—	Aladağ andeziti	Aladağ andeziti
Amfibolitik, porfiritik lavlar	Dumlu volkanitli Arzuza dasiti	Göllerdağı lasiti	Kızılören dasiti	Köprü volkaniti	—	—	Yarı epiklastik
	Göğüşmen volkaniti Göğüşmen byeni Göğüşmen byeni	Göğüşmen volkaniti Uzunları Göğüşmen Köprü Çelmeçdağı	—	—	—	—	—
Taban Tüf düzeyi; piroklastik döküntü, akıntı (ignimbrit) surge, epiklastik tüf ve bunlarla arakatlı bazik/ortaç lav arakatlıları (bimodal volkanizma)	Taban Tüf düzeyi; (epiklastik tüf, tefra)	Siyah ignimbrit Taban Tüf düzeyi	Ust tüf düzeyi Siyah ignimbrit Taban Tüf düzeyi	Ust tüf düzeyi Siyah ignimbrit Taban Tüf düzeyi	Ust tüf düzeyi Siyah ignimbrit Taban Tüf düzeyi	Ust tüf düzeyi Siyah ignimbrit Taban Tüf düzeyi	Ust tüf düzeyi Siyah ignimbrit Taban Tüf düzeyi
	—	—	Gri ve Beyaz ignimbritler Piroklastik döküntüler (pomza)	Gri ve Beyaz ignimbritler Piroklastik döküntüler (pomza) Saçdağ dasiti	Gri ve Beyaz ignimbritler Piroklastik döküntüler (pomza) Saçdağ dasiti	Gri ve Beyaz ignimbritler Piroklastik döküntüler (pomza) Saçdağ dasiti	Gri ve Beyaz ignimbritler Piroklastik döküntüler (pomza) Çukurayva riyeliti,
Bazik-ortaç taban lav düzeyi	—	Karapınar bazaltı	Siyah andezit	Kötek bazaltı	—	—	—

B

D

KD ANADOLU VOLKANİZMASININ VOLKANO-STRATİGRAFİSİ VE K/Ar YAŞ BULGULARI

1. Taban Tüf düzeyi: Büyük hacmini riyoitik bileşimde piroklastik akıntı, döküntü ve surge birimlerinin oluşturduğu bu düzey, genel olarak platonun tabanını meydana getirir. Bu düzey içinde bileşimleri genelde riyoitik olup, yer yer de dasite kadar ulaşan küçük porfiritik domlar ve ayrıca bazik lav arakatıkları vardır, istifte andezitik bileşimli lavlar hemen hemen hiç yoktur. Taban Tüf düzeyi, bu özellikleriyle Bimodal bir karakter sunar.

Amfibol fraksiyasyonel kristalizasyonu gösteren düzey: Bu düzey (a) amfibol içeren porfiritik masif lav istifleri ve domlar ve (b) amfibol içermemelerine karşın yoğun bir amfibol kristalizasyonuna ilişkin jeokimyasal ve petrografik kanıtlar gösteren afirik veya mikroporfiritik lavlardan (düşük-Y serisi; Keskin, 1994) oluşur. Bu düzeyde yer alan birimlerin belirgin bir özelliği, hemen tümünün ortaç bileşimde olmaları, bazalt ve riyoitin hiç bulunmaması (unimodal) ve ayrıca piroklastik materyalin çok az olmasıdır.

2. Plato düzeyi: Bu düzey, Erzurum-Kars Platosunun karakteristik plato morfolojisini meydana getiren ve bazikten ortaca kadar değişen bileşimler sergileyen lavlardan oluşur. Çoğunlukla siyah, koyu gri renkler ve afirik, mikroporfiritik dokular sergileyen lavlar içeren bu düzey, olivinli ve olivinsiz olmak üzere iki alt tipe ayrılabilir. Kargapazarı, Horasan ve Kars Plato volkanitleri olivin içeren, Aladağ andeziti ise olivin içermeyen plato lavlarına örnek gösterilebilir. Çoğun Hawaii tipi çatlak erüpsiyonlar! ve bazen de merkezi erüpsiyonlar (Aladağ andeziti gibi) ile yüzeye çıkmış lavlardan meydana gelir. Bu düzeyde piroklastik materyal ya çok azdır ya da hiç bulunmaz.

3. Plato düzeyi üzerindeki felsik domlar: Taban Tüf düzeyindekilere benzer az sayıda felsik domlardan meydana gelirler. Platonun en üst seviyesinde bulunurlar.

VOLKANİZMANIN PLATO ÜZERİNDEKİ EVRİMİ

11-7 milyon yıl önce

Eldeki verilerin ışığında, Erzurum-Kars Platosunu oluşturan volkanik aktivite, çalışma alanı içinde yaklaşık 11 milyon yıl önce, bölgesel yükselmeden (uplift) kısa bir süre sonra Horasan kuzeyinde başlamıştır

(Şek.11a ve 12). Hawaii tipi çatlak erüpsiyonlarının oluşturduğu bazaltik lavlarla temsil edilen bu ilk volkanik örtü (Kötek bazaltı), fazla yaygınlık göstermemiş, yerel, ince lav istifleri şeklinde sınırlı alanlarda kalmıştır. Plato üzerinde en primitif lavlar, bu dönemde yüzeye ulaşmışlardır (Şek.11).

6-7 milyon yıl önce

K/Ar yaş verilerine göre, volkanik aktivite en şiddetli evresine 6-7 milyon yıl önce piroklastik taban düzeyini oluşturan erüpsiyonlar sırasında ulaşmıştır (Şek. 11 b). Volkanik aktivite özellikle EKP'nun batı alanlarında yaygınlık göstermiştir. Bu evre.yaygın riyoitik -dasitik piroklastik ürünler ve domların, bazik/ortaç lav arakatıkları ile ardalananak kalın istifler oluşturduğu "bimodal bir volkanizma" ile karakterize edilir. Bu evrede yüzeye ulaşmış olan ürünlerin hacimsel olarak % 70-80'i piroklastik akıntı, döküntü ve surge düzeyleridir. Piroklastik materyal yüzeye sub-Plinian ve Plinian türü yüksek enerjili patlamalarla çıkmış ve geniş alanlara piroklastik pomza/kül döküntüleri ve ignimbritler şeklinde yayılmıştır. Piroklastik malzeme, çoğunlukla tümüyle camsıdır; ya çok az oranda kristal içerir veya hiç içermez. Buna rağmen, bu birimlerin şiddetli feldispat (plajiyoklaz ve K-feldispat + klinopiroksen) fraksiyonel kristalizasyonu geçirdiklerine dair jeokimyasal kanıtlar bulunmaktadır (Keskin, 1994; Keskin, hazırlamada). Asit piroklastik birimlerin tersine, istif içinde birkaç yüz metreden km. mertebesine kadar değişen çaplarda gözlenen asitik bileşimli domların çoğu porfiritiktir ve önemli oranda feldispat (plajiyoklaz, anortoklaz, sanidin), çok az kuvars ve mafik mineral (çoğun klinopiroksen nadiren biyotit ve amfibol) fenokristalleri içerirler. Bu dönemde oluşan diğer birimler, Pasinler kuzeyinde yaygınca mostra veren Siyah ignimbrit gibi porfiritik trakidasitik-dasitik piroklastik akıntılar ve piroksen ve olivinli bazik-andezitik lavlardır.

Piroklastik taban düzeyi ile aynı zaman aralığında, ortaç bileşimli afirik lavlar (Güngörmez volkaniti) Dumlulu ve Kargapazarı alanlarında kalın istifler oluşturmuşlardır. Bunlar, amfibolün mafik fazda egemen olduğu bir fraksiyonel kristalizasyon evrimi geçirmiş olan lavlardır ve aynı dönem zarfında platoda yüzeye ulaşmış volkanik materyalden farklı bir kristalizasyon evrimi çizgisi izlenmiştir (Keskin, 1994).

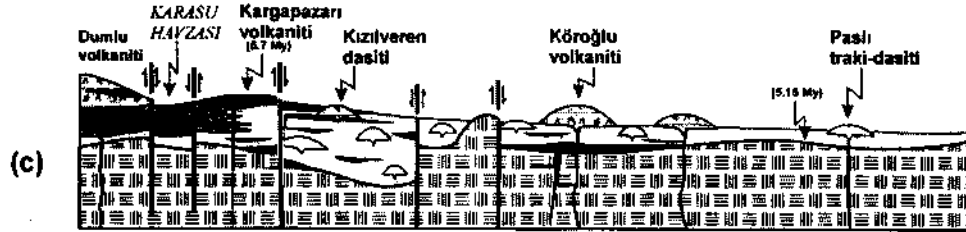
11-7 Milyon yıl önce: Platodaki ilk bazik lavların yüzeye çıkışı



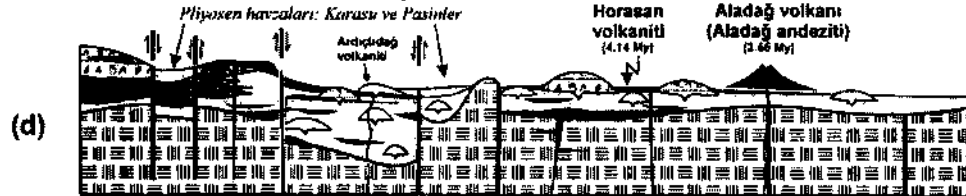
7-6 Milyon yıl önce: Piroklastik Taban düzeyini oluşturan bimodal volkanizma, Erzurum-Tiflis doğrultu atımlı fayna bağlı havza oluşumu



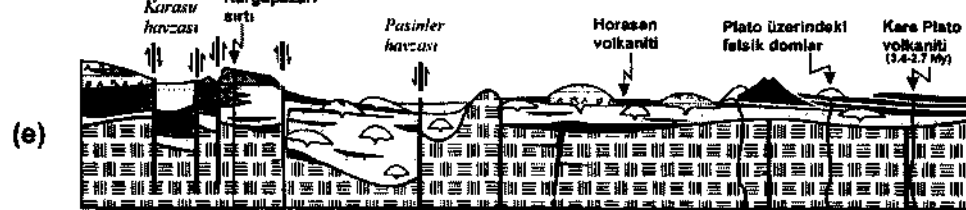
6-5 Milyon yıl önce: Amfibol içeren porfiritik domların oluşumu



5-3.5 Milyon yıl önce: Plato oluşturan lav düzeyinin ve Pliyosen çökellerinin oluşumu



3.5-2.5 Milyon yıl önce: Platonun doğusunda Plato oluşturan lav düzeyinin ve felsik domların oluşumu



Şek. 11- Erzurum-Kars Platosu üzerinde çarpışma kökenli volkanizmanın zaman ve mekândaki evrimini gösterir model. Kesit, yaklaşık 150 km. boyundadır.

KD ANADOLU VOLKANİZMASININ VOLKANO-STRATİGRAFİSİ VE K/Ar YAŞ BULGULARI

5-6 milyon yıl önce

Bu evrede plato üzerinde amfibol içeren andezitik porfiritik lavlar, yüzeye çıkarak domlar ve kalm-masif lav istifleri oluşturmuşlardır (Şek.11 c). Volkanik aktivite, özellikle batıda, Dumlu dağı dolaylarında etkin olmuş, daha doğuda ise irili ufaklı domlar oluşturmuştur. Bu evrede oluşan lavlar, 6-6.5 my önce Dumlu dağı alanında yaygınlık gösteren Güngörmüz volkanit! ile başlayan aktivitenin devamı niteliğindedirler. Bu evrede, 5.7 my önce olivini bazalt ve bazaltik andezitik lavlar Kargapazarı alanında yüzeye çıkarak, Kargapazarı platosunu oluşturmuşlardır.

3.5-5 milyon yıl önce

Bu evrede Horasan kuzeyindeki alanlardan, doğuya, Kağızman kuzeyine kadar uzanan geniş alanlarda, çoğunlukla olivini bazalttan bazaltik andezite kadar değişen bileşimde plato lav akıntıları platoyu kaplamışlardır (Şek.11 d). Horasan kuzeyinde geniş alan kaplayan Horasan volkaniti 4.1 my önce, daha doğudaki Aladağ volkanı ise 3.5 my önce oluşmuşlardır. Bu dönemde Karasu, Pasinler ve Horasan havzaları içinde Aras formasyonuna ilişkin karasal kırıntılılar çökelmiştir.

2.7-3.5 milyon yıl önce

Bu dönemde platonun en doğusunda Kağızman kuzeyi ile Kars arasındaki alanlarda Kars Plato volka-

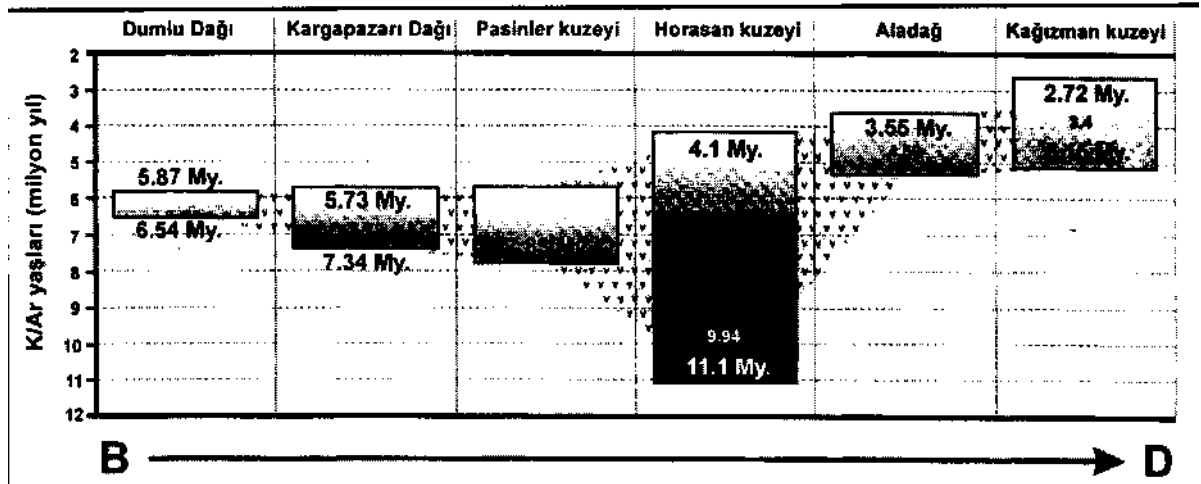
nit! olarak isimlendirilen bazalt ve bazaltik andezitlerin plato lav yaygıları şeklinde oluştuğunu görmekteyiz. Olivin ve klinopiroksenin esak mafik fazı temsil ettiği bu lav düzeyi üzerinde son evrede yüzeye ulaşmış birkaç küçük riolitik dom (Odalar riyodasit! gibi) da bulunmaktadır.

SONUÇLAR

1- Erzurum-Kars Platosu üzerindeki çarpışma-kökenli volkanizma, 11 my önce Horasan alanında bazik bileşimli lavlarla başlamıştır.

2- Volkanik aktivite 6-7 my önce doruğa ulaşmış ve asit piroklastik ve az oranda bazaltik lavların oluşturduğu bimodal bir karakter kazanmıştır. Bu evrede magma evrimi, piroksen ve plajiyoklaz (bazik üyelerde olivin) fraksiyonel kristalizasyonu tarafından denetlenmiştir. Aynı dönemde, mafik mineral olarak amfibol ve ortopiroksenin (\pm klinopiroksen) fraksiyonasyonu ile farklı bir evrim çizgisi izlemiş olan ortaç bileşimli afirik ve yer yer mikroporfiritik lavlar, Dumlu alanında yüzeye çıkmışlardır.

3- Erzurum-Kars Platosu volkanitleri, bölgeyi KD-GB doğrultusunda keserek geçen ve volkanizmanın gelişimi süresince aktif olan doğrultu atımlı fay sistemleri içindeki yerel gerilme alanları ve çatlaklar boyunca yüzeye çıkmıştır. Bu çatlaklardan çoğu, daha sonra çıkan volkanik ürünlerle örtülmüşlerdir. Söz konusu fay



Şek. 12- K/Ar yaş bulgularının batıdan doğuya plato üzerindeki dağılımları.

sistemleri aynı zamanda, Pasinler, Karasu gibi pull-apart havzaların oluşmasına neden olmuştur. Yüzeyle ulaşan volkanik ürünler, bu havzalar içinde kalın istifler halinde birikerek, kimi yerde kalınlıkça 2000 m.yi aşmışlardır (or. Pasinler havzası). Magmanın izlediği zayıflık düzlemlerini temsil eden dayklar, genel olarak D -B doğrultusunda uzanırlar ve doğrultu atımlı fay sistemlerinin oluşturduğu pull-apart sistemler üzerindeki bazı fayların gidişleri ile uyum gösterirler.

4- K/Ar yaş tayinlerinden görüleceği üzere volkanizma, genel olarak batıdan doğuya doğru gençleşmektedir. Buna göre, volkanik aktivite genel olarak zaman içinde doğuya doğru göç etmiş ve felsikten baziğe doğru bir evrim çizgisi izlemiştir.

5- Volkanizmanın zaman içinde giderek bazikleşmesinin nedeni, bölgede kabuğu derinlemesine kesen doğrultu atımlı sistemler içindeki gerilmelerin, volkanik etkinliğin son evresine doğru tedericen artmasıdır. Magma odalarında depolanan magma, yerel tektonik gerilmelerin serbestlendiği bir ortamda, magma pompalama sistemi aracılığıyla yüzeyle zaman içinde gittikçe daha kolay ve çabuk ulaşmıştır. Böylece magma, fraksiyonel kristalizasyon ile farklılaşmaya fazla uğramadan daha primitif lavlar şeklinde yüzeyle çıkmıştır.

KATKI BELİRTME

Bu makale, İngiltere'nin Durham Üniversitesi'ndeki doktora çalışmam sırasında yürütmüş olduğum saha incelemelerimin bir bölümünün sonuçlarını içermektedir. Doktora çalışmam süresince gerek saha çalışmaları ve gerekse laboratuvar ve tez yazım aşamasında eleştirileri ve yardımlarıyla çalışmamı zenginleştiren danışmanlarım Dr. Julian A. Pearce ve Dr. Dave Hirst'e teşekkürlerimi sunarım. Bu çalışma, yurtdışındaki doktora süresince maddi kaynak sağlayan Milli Eğitim Bakanlığı, Yurt Dışı Eğitimi Genel Müdürlüğü sayesinde mümkün olmuştur. Kendilerine teşekkürü bir borç bilirim. Çalışmamın saha kesimi, araç ve kamp imkânları açısından TPAO Arama Grubu Başkanlığı'nca desteklenmiştir. Arazi çalışmalarım sırasında sağladıkları olanaklar için Arama Grubu'ndaki tüm meslektaşlarıma ve özellikle 1991 Erzurum kampında görev alan Jeoloji Mühendisleri Ayhan Üngör ve Ömer Şahintürk'e teşekkür ederim. Arazi çalışmam sırasında, Dr. Evren

Yazgan, Dr. Jerf Asutay, Jeoloji Mühendisleri Ali Arbas, Latif Gök, Mehmet İmîk kamp imkânları konusunda destek vermişlerdir. Kendilerine içten teşekkürlerimi burada ifade etmek isterim.

Yayına verildiği tarih, 19 Şubat 1997

DEĞİNİLEN BELGELER

Ercan, T.; Fujitani, T.; Matsuda, J.L; Notsu, K.; Tokel, S. ve Di, T., 1990, Doğu ve Güneydoğu Anadolu Neojen-Kuvaterner volkanitlerine ilişkin yeni jeokimyasal, radyometrik ve izotopik verilerin yorumu; MTA Derg. 110, 143-164.

Gedik, A., 1978, Doğu Anadolu'da açılan stratigrafik inkişaf (açınsama) sondajları; Yeryuvarı ve insan, 31-35.

Gülen, L., 1980 a, Strontium isotope geochemistry of Mount Ararat and Mount Süphan Volcanics, Eastern Turkey; EOS, V. 61,17, 412.

———, 1980 b, Sr, Nd and Pb isotope systematics of Ararat and Süphan volcanoes, Eastern Turkey; EOS, V. 63, no. 45, p. 1145.

Innocenti, F.; Manetti, P.; Mazzuoli, R.; Pasquare, G. ve Villari, L., 1982 a, Anatolia and north-western Iran, in Andesites: (R.S. Thorpe ed.), John Wiley ve Sons.

———; Mazzuoli, R.; Pasquare, G.; Radicati di Brozola, F. ve Villari, L., 1976 Evolution of volcanism in the area of interaction between the Arabian, Anatolian, and Iranian plates (Lake Van, Eastern Turkey): Journal of Volcanology and Geothermal Research, V. 1, 103-112.

•;———; Pasquare, G.; Radicati di Brozola, F. ve Villari, L., 1982 a, Tertiary and Quaternary volcanism of the Erzurum-Kars area (Eastern Turkey): geochronological data and geodynamic evolution, Journal of Volcanology and Geothermal Research, V. 13, pp. 223-240.

KD ANADOLU VOLKANİZMASININ VOLKANO-STRATİGRAFİSİ VE K/Ar YAŞ BULGULARI

- inan, S., 1987, Erzurum-Tortum arasında Dumlu fay kuşağının sistematik ve yapısal özellikleri: C.Ü Mühendislik Fakültesi Derg. Seri A, Yerbilimleri- C.4, 3-11.
- Keskin, M., 1994, Genesis of collision-related volcanism on the Erzurum-Kars Plateau, Northeastern Turkey: Ph. D. Thesis (Doktora Tezi), University of Durham, U.K.
- Keskin, M., (incelemede), Partitioning of trace and REES between feldspars and melt: application to the modelling of fractional crystallisation history of Erzurum-Kars Plateau volcanics, NE Turkey.
- Koçyiğit, A., 1985, Muratbağı-Balabantaş (Horasan) arasında Çobandede fay kuşağının jeo-tektonik özellikleri ve Horasan-Narman depremi yüzey kırıkları: C.Ü. Mühendislik Fakültesi Yer Bilimleri Derg. C.2, S 1,17-33.
- ; Öztürk, A.; inan, S. ve Gürsoy, H., 1985, Karasu Havzası'nın (Erzurum) tektonomorfolojisi ve mekanik yorumu: C.Ü. Mühendislik Fakültesi Yer Bilimleri Derg. C.2, S 1, 4-15.
- Lambert, R.S.T.; Holland, J.G. ve Owen, P.F., 1974, Chemical Petrology of a suite of calc-alkaline lavas from Mount Ararat, Turkey: Journal of Geology, 82,419-438.
- Notsu, K.; Fujitani, T.; Ui, T.; Matsuda, J. ve Ercan, T., 1995, Geochemical features of collision-related volcanic rocks in Central and eastern Anatolia, Turkey: Journal of Volcanology and Geothermal Research, V. 64171-192.
- Pearce, J.A.; Bender, J.F.; De Long, S.E.; Kidd, W.S.F.; Low P.J.; Güner, Y.; Şaroğlu, F.; Yılmaz, Y.; Moorbath, S. ve Mitchell, J.G., 1990, Genesis of collision volcanism in Eastern Anatolia, Turkey: Journal of Volcanology and Geothermal Research, 44, 189-229.
- Sungurlu, O., 1971, Kuzeydoğu Anadolu'nun 1/50.000 ölçekli Jeolojik Haritaları: TPAO arşivi, (yayımlanmamış).
- Şaroğlu, F.; Güner, Y.; Kidd, W.S.F. ve Şengör, A.M.C., 1980, Neotectonics of Eastern Turkey: new evidence for Crustal shortening and thickening in a collision zone, EOS, Transactions of American Geophysical Union, V. 61 360 (Abstract).
- ve Güner, Y., 1981, Doğu Anadolu'nun jeomorfolojik gelişimine etki eden öğeler, jeomorfoloji, tektonik, volkanizma ilişkileri: Türkiye Jeoloji Kurumu Bülteni, 24, 39-52.
- ve Yılmaz, Y., 1986, Doğu Anadolu'da Neotektonik dönemdeki jeolojik evrim ve havza modelleri: MTA Derg. 107,73-93.
- ve———, 1987, Geological evolution and basin models during neotectonic episode in Eastern Anatolia: MTA Derg. 107, 62-83, Ankara-Turkey.
- Şengör, A.M.C., 1980, Türkiye'nin neotektoniğinin esasları: Türkiye Jeoloji Kurumu, Konferans Serisi, 2, 40.
- Tokel, S., 1984, Doğu Anadolu'da kabuk deformasyonu mekanizması ve genç volkanitlerin petrojenezi: Türkiye Jeoloji Kurumu, Ketin Sempozyumu, 121-130.
- Yılmaz, Y., 1984, Magmatic activity in the geological history of Turkey and its relation to tectonic evolution: special Publication of Türkiye jeoloji Kurumu, Ketin Symposium, (T. Ercan and M.A. Çağlayan eds.) 63-81, Ankara-Turkey.
- ; Şaroğlu, F. ve Güner, Y., 1987, Initiation of the neomagmatism in East Anatolia: Tectonophysics, 134, 117-199.

EARLY DEVONIAN CONODONTS FROM LIMESTONE OLISTOLITHS WITHIN THE KARASENİR FORMATION OF THE KARAKAYA COMPLEX

Şenol ÇAPKINOĞLU* and Osman BEKTAŞ*

ABSTRACT.- Limestone olistoliths of different size are commonly observed in the elastics of Karasenir formation (Amasya) which is unconformably overlain by the Liassic deposits. In two of these olistoliths, conodont faunas belonging to eurekaensis, delta and Pesavis zones of early Devonian (Lochkovian) were determined. Typical Permian algaees (Gymnocodiacea) were described in thin sections of a dark gray limestone olistolith. Since it contains early Devonian and Permian olistoliths and unconformably covered with the Liassic units, the age of Karasenir formation is believed to be Triassic. Including of underlying metamorphic rocks to the Karakaya complex necessities also including of Karasenir formation as their stratigraphic continuation.

GEOLOGY OF THE GÜZELSU CORRIDOR AND ITS NORTHERN PART IN THE CENTRAL TAURIDES

Mustafa ŞENEL*; Halil DALKILIÇ*; İbrahim GEDİK*; Mualla SERDAROĞLU*; Sait METİN*; Kadri ESENTÜRK*;
A. Sait BÖLÜKBAŞI**; Necdet ÖZGÜL***

ABSTRACT.- Anamas-Akseki autochthon, Antalya nappes and Alanya nappe are observed in the study area which is situated to the southwest of Central Taurus mountains. The Anamas-Akseki autochthon, in the region, is represented by outcrops of dolomites and limestones of Upper Norian?-Rhaetian age (Menteşe dolomite, Leylek limestone), conglomerate, sandstone and mudstones of Rhaetian-Lower Liasic age (Üzümdere fm), limestones of Middle Liassic-Cenomanian age (Kurucaova fm) + dolomite and limestones of Liassic-Dogger? age (Hendos dolomite, Alıçbeleni fm.), limestones of Dogger-Malm age (Çamkuşağı fm), limestone of Malm age (Akkuyu fm, Karlığın fm.), limestones of Malm-Lower Cretaceous age (Belalan fm.), limestones of Lower Cretaceous age (Akseki limestone), limestones of Berriasian age (Susuzkır fm.), limestones of Campanian-Maasrichtian age (Seyrandağı fm., Dumanlı fm), Danian age olisthostrome of Upper Paleocene-Lower Eocene age (Çetmi limestone) and sandstones and conglomerates of Middle Eocene age (Gümüştamla fm). The Antalya nappes, cropping out in a narrow approximately east-west trending corridor between Anamas-Akseki autochthon and Alanya nappe, according to its structural and stratigraphic features are subdivided into nappes as given below: Çataltepe nappe represented by Aygırdere (Kasımlar formation, Karasay limestone, Kepezbeleni formation) and Güzelsu (Kasımlar formation, Kayabükü formation, Gören formation, Keçili formation) sequences; Alakırçay nappe represented by rocks of Lower Triassic-Upper Cretaceous age, Alakırçay (Akıncıbeli formation, Çandır formation, Keçili formation) and Hocaköy (Halobia bearing limestone, Hocaköy radiolarite, Keçili formation) sequences; and Tahtalıdağ nappe represented by rocks of Upper Cambrian-Upper Cretaceous age, Katrandağı (Çukurköy formation, Akıncıbeli formation, Günlük formation, Katrandağı kireçtaşı, Keçili formation), Kavzandağı (Seydişehir formation, Güneyyaka formation, Çukurköy formation, Akıncıbeli formation, Günlük formation, Kavzandağı formation, Keçili formation) and Gündoğmuş (Seydişehir formation, Bozşehir formation, Güneyyaka formation, Kızılbaş formation, Akıncıbeli formation, Sinektepe formation) sequences. In general, during Mesozoic, Çataltepe nappe represented passive continental margin, whereas Alakırçay nappe and Tahtalıdağ nappe represented basin and offshore platform, respectively.

FEATURES OF THE TERTIARY VOLCANISM AROUND SEA OF MARMARA

Tuncay ERCAN*; Ahmet TÜRKECAN*; Herve GUILLOU"; Muharrem SATIR""; Dilek SEVİN*** and Fuat SAROĞLU*****

ABSTRACT.- In the region around the sea of Marmara, limited by the boundaries of the 1:500 000 scale Istanbul Quadrangle, the volcanism starting in Upper Cretaceous and intermittently continuing through the end of Upper Miocene has been differentiated into five different stages, namely Upper Cretaceous, Eocene, Oligocene, Lower-Middle Miocene and Upper Miocene, and the volcanic outcrops situated in the region have been dated. Together with the detailed petrographic studies, nine samples from different areas and stages have been dated by K/Ar method, resulting in that the oldest and the youngest lava is of 74.3 ± 1.0 million years old (Upper Cretaceous) and 8.9 ± 0.2 years old (Upper Miocene), respectively. Of these, belonging to the first four stages are mostly calcalkaline (some of the Eocene aged samples are tholeiitic) and are of basalt, basaltic andesite, trachyandesite, andesite, dacite, rhyolite type, whereas that of belonging to the fifth stage are alkaline and of basanite, basalt and trachybasalt types. The pyroclastics of various size and the tufts of the first four volcanism stages crop out in a wide area. The Upper Cretaceous volcanics have completely formed beneath the sea. On the other hand, some of Eocene volcanics have formed beneath the sea which are seen intercalated with sediments while the others have formed on land. The lavas of Oligocene, Lower-Middle Miocene and Upper Miocene age have formed on land and are observed to be intercalated with lacustrine sediments, in places. Of the lavas stranded along the Black sea coast, the Upper Cretaceous aged ones have formed in a group of island arc volcanics and have been produced in a subduction zone and the Eocene, Oligocene and Lower-Middle Miocene aged ones have formed in an environment of compression during and after the collision and have been produced from a material of crust and mantle mixture. It is proposed that the Upper Miocene aged alkaline basaltic volcanics have formed in an environment of extension by the uplift of mantle after the change of tectonic regime in Middle Miocene.

INTRODUCTION

In the area around sea of (Marmara region, an intense volcanism has been effective starting from Upper Cretaceous to the beginning of Pliocene displaying various stages and forming widespread lavas and pyroclastics having different petrographic and geochemical features. Although there have been many geological studies in the region, there are no special and sufficient studies to reveal the Tertiary volcanism, the regional extension of the volcanic rocks, their ages, stages, petrochemical features and genetic explanations. This study intends to shed light on these questions together with their relations with the adjacent sedimentary rocks and their datings. For this reason, samples from the Upper Cretaceous, Eocene, Oligocene, Lower-Middle Miocene and Upper Miocene were taken and dated by K/Ar method.

THE FEATURES OF THE TERTIARY VOLCANISM

The Tertiary volcanics around the sea of Marmara, limited by the boundaries of the 1:500000 scale Istanbul Quadrangle, and the Upper Cretaceous volcanics cropping out along the Black sea coast have all together been studied and differentiated into five different groups:

Upper Cretaceous volcanics

Upper Cretaceous volcanics in the study area are situated in the north, along the Black sea coast in vicinity of Istanbul and in Igneada, close to Bulgarian-Turkish State Boundary (Fig. 1). They generally are observed to intercalate with the sedimentary rocks of the same age. Upper Cretaceous aged sedimentary and volcanic rocks are widespread in the east of Istanbul, aro-

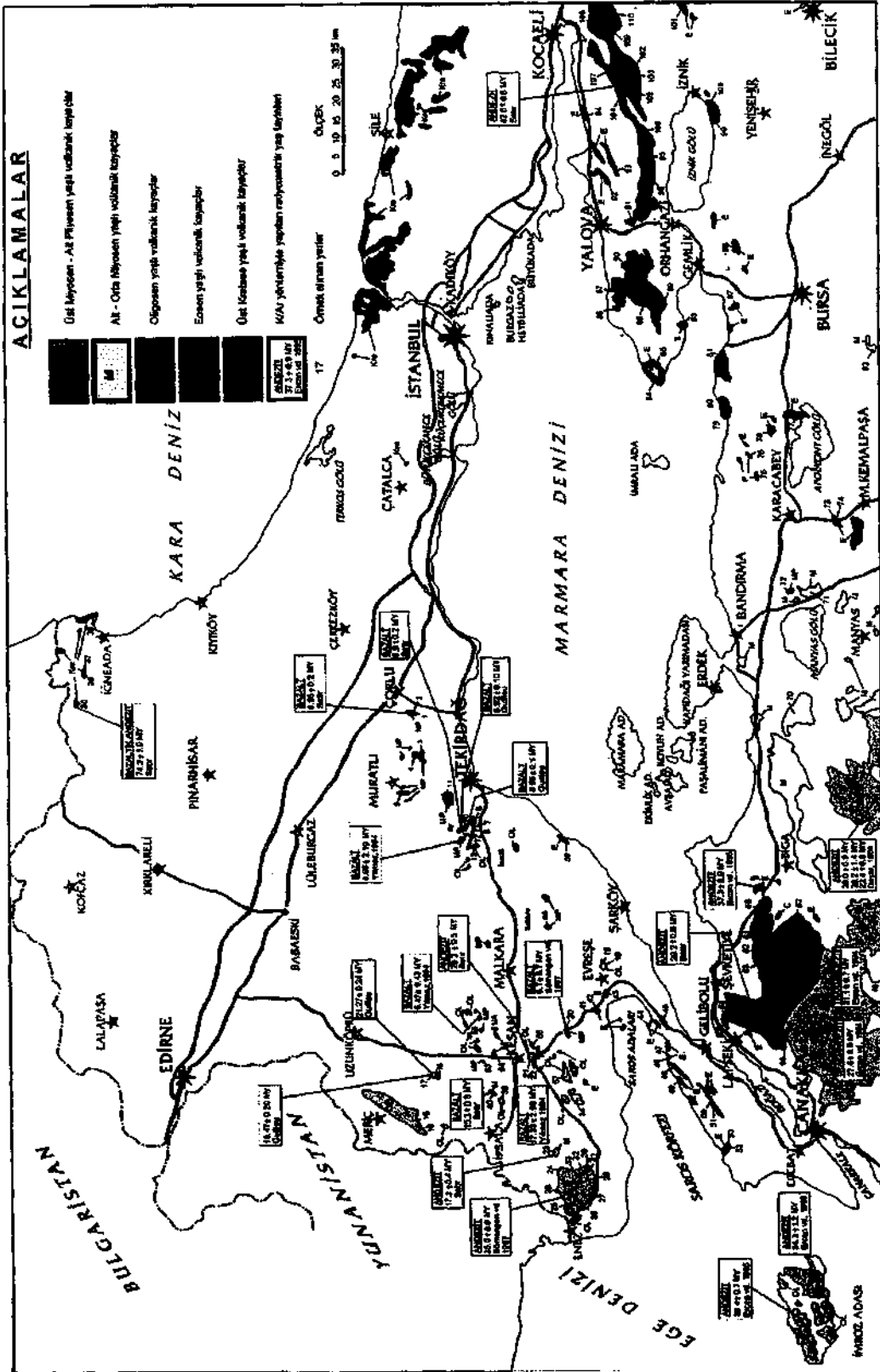


Fig. 1- The distribution of Upper Cretaceous and Tertiary volcanics around sea of Marmara.

und Şile. Flysch type sediments, comprising an alternation of conglomerate, sandstone, siltstone, marl, claystone and limestone, bear various kinds of pyroclastics and lava flows in rather lesser amounts. These are spilitic basalts, basalts, andesites, basaltic andesites, trachyandesites, dacites rhyolitic lavas, agglomerates and tuffs, displaying typical submarine volcanism. The most widespread of these is highly altered andesitic lava which contains plagioclase, rather less hornblende, biotite, augite and opaque minerals. The argillization observed in these rocks is of large scale and significant in industrial point of view. Besides, sericitization, chloritization, carbonatization and zeolitization are observed. Andesitic lavas are of porphyritic, hyaloporphyritic, partly pylotaxitic texture. Plagioclase phenocrysts are hypidiomorph in places and its types such as albite showing polysynthetic twinning and zonal structure, andesine, oligoclase and labrador were determined (Yeniyoğlu and Ercan, 1989/1990). Augites are partly idiomorphic and have uralitized and epidotized in places. Generally biotites have undergone magmatic corrosion. In dacites and rare rhyolites, additional to the minerals listed above quartz crystals in various amounts can be seen. In trachyandesitic lavas sanidine crystals are clearly visible. Spilitic lavas are in lesser amounts than intermediate lavas. Spilites comprise albite, augite and opaque minerals. Serpentinization, chloritization and carbonatization are seen in places. Basaltic lavas display porphyritic, pylotaxitic, hyaloporphyritic and vitrophyric textures. They comprise mainly of plagioclase and augite microliths together with plagioclase, augite, opaque mineral and olivine phenocrysts in a matrix of volcanic glass. Plagioclases display polysynthetic twinning and zonal structure and are of andesine and labradorite type. Augites are observed to be partly twinned and altered. Basaltic lavas also show chloritization, zeolitization, carbonatization and argillization. Upper Cretaceous volcanism, in vicinity of Istanbul, around Anadolu-kavağı and Rumelikavağı at the northern end of the Bosphorus and Şile, is represented by agglomerates, sinerite, tuffs and lavas. Baykal (1943 and 1971) Baykal and Kaya (1966), Baykal and Önalın (1979), Okay (1948), Akartuna (1953) and Yeniyoğlu and Ercan (1989/1990) who studied fossiliferous sedimentary rocks intercalated with the volcanic rocks representing the submarine volcanism have concluded that both volcanic and sedimentary

rocks have completely formed during Upper Cretaceous (Santonian - Campanian - Maastrichtian).

In the study area, the Upper Cretaceous volcanism having small outcrops towards west (Akartuna 1953; Erentöz, 1953) is observed again in vicinity of Iğneada. These are basalts, basaltic andesites, spilitic basalts, andesites, rhyodacites and rhyolitic lavas, tuffs and andesites and are intercalated with Upper Cretaceous marine sediments. Pillow lavas are locally observed. They are mostly andesites and basaltic andesites. Andesites are called "pyroxene andesites" since the samples displaying porphyritic texture includes plagioclase and pyroxene crystals. The plagioclases (andesine and oligoclase), crystallized as macro and microphenocrysts in hypidiomorph form, are generally sericitized, chloritized and epidotized. Some display glomeroporphyritic texture. Pyroxenes (clinopyroxene-augite) form assemblages of glomeroporphyritic texture as in xenomorph crystals. Some change into chlorite pseudomorphs including carbonates and carbonatization. The matrix has intersertal texture and is formed by the interfingering plagioclase microliths and the altered pyroxene granules, chlorite and interstitial silica filling the space between. In the matrix, locally, concentric carbonatization, silicification and epidotization is observed. The andesitic lavas which are close to basalts in texture, have been called as pyroxene andesite or basaltic andesite in andesite-basalt transition. Tuffs are in many places have the appearance of lavas and are called as lapilli tuff and crystal tuff. Lapilli tuffs have a silicified, epidotized and prehydrated matrix including volcanic rock fragments of andesitic nature and pyroxene andesite fragments, feldspat, amphibole (green hornblende) and pyroxene fragments. The fragments forming the samples are of angular, between 0.36 mm (coarse grained tuff) to 5.5 mm (lapilli) in length. Crystal tuffs include fragments of plagioclase, quartz, amphibole (green hornblende), devitrified glass and chloritized volcanic rocks, and epidotized, carbonatized and argillized fragments, sericite flakes and organic fragments. All these compounds mostly have been bound with material changed into chlorite and/or clay minerals (most probably volcanic glass ashes and dusts). Crystal tuffs generally are composed of fine grained materials of 0.01 mm grain size.

In order to clarify the age problem of the Upper Cretaceous volcanics around the sea of Marmara a sample was taken from a basaltic andesite lava in vicinity of İğneada which yielded 74.3 ± 3.1 million years (Campanian-Upper Cretaceous) by K/Ar method.

Eocene volcanics

In the region around sea of Marmara Eocene volcanism has widespread outcrops in three different areas:

a) Eocene volcanics in Biga peninsula : Between Lapseki and Biga, to the north of Biga peninsula, mostly andesitic and locally dacitic lavas and tuffs which are the first products of Eocene volcanism are observed. They are underlain by the "Soğucak limestone" determined to be of Middle Eocene age by Siyako et al., (1989). Lavas and tuffs are observed to be intercalated with conglomerates having thin coal seams, sandstones and shales, called "Fıçitepe formation", which is defined to be delta plain -fluvial sediments (Siyako et al., 1989). These volcanics are supposed to be of Lower-Middle Eocene age. On the other hand, there are some opinions about the volcanism to start in Paleocene (Siyako et al., 1989; Ertürk et al., 1990). There is a significant transgression in Middle Eocene resulting in the deposition of shallow marine "Soğucak limestone" in the region while the Eocene volcanism was still effective, forming lavas and tuffs of 1000 m in thickness. Later on, the southern shelf of the basin has gradually deepened and Ceylan formation (Ünal,1967; Siyako et al.,1989) comprising mainly of turbidites was deposited. Two dacitic tuff levels (10-30 m thick), blue and green in color, which forms a marker bed in Ceylan formation (500 m thick) comprising turbiditic sandstone, shale and marls in Biga peninsula, proves that the Eocene volcanism was continuing in Upper Eocene. Together with the lavas and tuffs of andesitic and dacitic nature, there are ignimbritic tuffs that formed close to the land. Despite the presence of all these data, it is very difficult to differentiate and to map the members of the Eocene volcanism. Ercan et al., (1995) have named all the Eocene volcanics in the Biga peninsula as

"Balıklıçeşme volcanics" and dated the unit as 37.3 ± 0.9 million years (Uppermost Eocene) based on the K/Ar dating of the sample of andesitic lava with biotite taken from the Balıklıçeşme village. The petrographic studies on the Eocene volcanics situated in Biga peninsula result in that the andesitic lavas contain chloritized and argillized plagioclase microliths with porphyritic texture, plagioclase phenocrystals in a matrix containing pyroxene and opaque minerals and also diopside augite crystals whereas the dacitic lavas locally include quartz phenocrystals. Tuffs generally are of vitric and lithic but sometimes appear as ignimbritic in the field. They are composed of, generally, sericitized, argillized plagioclase fragments, quartz fragments and volcanic rock fragments (andesite and dacite) and devitrified glass fragments. These are bound with a matrix composed of sericitized volcanic glass, ash and dust. Grain sizes are varying between 3.2 mm (lapilli) and 0.02 mm (fine grained tuff).

b) Eocene volcanics in Gelibolu peninsula and southern thrace : Eocene volcanism in Gelibolu peninsula and in southern Thrace has outcrops same as that seen in Biga peninsula. For example, in vicinity of Gelibolu town, mostly green and wine colored andesitic and dacitic tuffs are observed as alternating with Middle-Upper Eocene sediments and lavas are seen as small sills in places. Kopp (1964) has differentiated the Gelibolu volcanics as "Kömürtepe Andesite and tuffs", "Kavaklı Andesite", "Uçaktepe tuffite" and "Kocakuş tuffite". Onal and Yılmaz (1983) stating that the volcanics are of Upper Eocene, "Karaağaç member" of flysch type "Burgaz formation" includes tuff levels alternating with the other sedimentary units. Önal (1986) indicates that the Upper Eocene volcanic rocks, "Gelibolu volcanics" in his terminology, are andesites and dacites. Sumengen et al., (1987) have observed tuff levels of Middle Eocene age in "Burgaz formation" which is a 600 m thick flysch unit. The same researchers have indicated the presence of tuff levels in the "Gaziköy formation" which is of shale-sandstone unit situated in the upper levels. These thin bedded, light green colored silicified tuffs are determined to be of Middle-Upper Eocene age. Ceylan formation, observed in Gelibolu pe-

ninsula, is a turbiditic sequence reaching up to 500 m in thickness and is an alternation of sandstone, conglomerate and limestone displaying Bouma sequences also includes tuff levels (Siyako et al., 1989) It is of Upper Eocene age (Toker and Erkan, 1985). This formation can be seen in the inner sections of the Thrace basin with increasing acidic tuff levels reaching up to 500 m. The tuffs, observed as silicified locally, are quite widespread and can be correlated in well logs (Siyako et al., 1989). Burkan (1995) studied the distribution of these tuffs in Thrace basin making use of 11 different tuff levels observed in 52 well logs and concluded that especially along the Çorlu-Edirne line there lies a tuff layer of 450 m in thickness. They are of rhyolite, rhyodacite and dacite types and locally zeolitized (Özkanlı and Sonel, 1995).

In Gelibolu peninsula, at the thalweg of the dam near Tayfurköy, the green ignimbritic tuffs placed on the Eocene sandstones and the tuffs in vicinity of the Bakla burun to the west of Bolayır are typical outcrops. To the north, on the Keşan-Gelibolu roadcut near Evreşe, Eocene sandstones include volcanic materials and are cut by andesitic lavas. The small islands in gulf of Saros were formed by Eocene lavas (Ercan and Günay, 1984). In vicinity of U9makdere village, to the south of Tekirdağ, the siliceous tuffs of Eocene age are observed together with the flysch of the same age. These tuffs, called "vitric tuffs", include devitrified glass fragments, lesser plagioclase, biotite, sanidine, quartz in very few amount and volcanic rock fragments. They have undergone intense chloritization and the traces of glass chips are visible in them. Grain sizes are between rarely 4 mm (lapilli) and 0.08 mm (coarse grained tuff) but the average grain size can be said to be 0.3 mm (coarse grained tuff). Ertürk and Uygur (1994) studying on the tuffs have differentiated products of two different lithofacies formed in the marine environment. These are well bedded, laminated green tuffs and locally carbonatized, siliceous white tuffs. They also state that the tuffs are mostly vitric and crystalline in places. Lavas, on the other hand, are of andesitic type with porphyritic texture and include plagioclase and amphibole phenocrystals, Plagioclases range from

macrophenocrystals to fine grained and microphenocrystals in size and were crystallized in zonal structure as hypidiomorph. Some of them display antiperthite formation. They have changed into chlorite and/or clay minerals due to alteration. Amphiboles (green hornblende) were crystallized as idiomorphs in forms of medium to thin in size microphenocrystals. Some of them form assemblages in glomeroporphyritic texture while some others display carbonatization. Together with hornblende, sphene is also seen as secondary mineral. The matrix is probably formed by devitrification of volcanic glass and is of cryptocrystalline-felsitic texture. Along the fractures carbonate fillings are seen.

c) The Eocene volcanics in Armutlu peninsula and around the the lake Apolyont : In Armutlu peninsula mostly andesitic lavas, tuffs and agglomerates of Middle-Upper Eocene age spread over wide areas and are in primary relation with the sedimentary rocks of the same age. Akartuna (1968) who studied in the region in detail for the first time, states that the volcanism starts on the flysch with tuffs which is overlain by lava tuffs and agglomerates of Paleocene-Eocene age which are later on called as "Sarısu volcanics" by Erendil et al., (1991). They stated that this formation, comprising pyroclastic and epiclastic rocks of 1000 m. thick, overlies the sedimentary units made up of conglomerate, sandstone, mudstone and limestone of 5-10 m situated over the basement, metamorphic rocks. Pyroclastics levels comprise fine or coarse grained tuffs displaying normal, reverse or symmetrical grading and andesitic tuffs and lava fragments of various size in lapilli. Pyroclastic flow deposits are alternated with lahar deposits of generally symmetric graded and ill sorted. At some levels epiclastic deposits comprising large andesite blocks and pebbles, most probably of shore conglomerate type are situated. In this sequence, lava flows at the upper levels, as 5 m thick layers, are alternated with pyroclastic rocks. Lava flows are andesitic volcanics with plagioclase, pyroxene (augite) and hornblende phenocrysts. Tuffs include plagioclase, glass and volcanic rock fragments having fluidal texture in a glassy matrix. All of this sequence, especially in the upper levels is cut by basaltic dykes. Basalts, with com-

pounds such as olivine, augite and plagioclase, are more fresh than andesites. In the limestones and sandstones situated at the lowest levels of the volcanic sequence fossils of Lutetian age were found (Erendil et al., 1991) and it was concluded that the sequence started since then. The andesitic lava flow sample taken from the north of İznik, between the villages Osmaniye-Sansu yields 42.0 ± 0.8 million years (Lutetian-Bartonian) by K/Ar method and therefore the whole volcanism can be said to be of Middle-Upper Eocene age.

Bargu and Sakiñç (1987; 1989/1990) called the lavas "Kızderbent andesite" and differentiated the pyroclastics as "Taşlıtepe formation" and "Geyikdere tuff member", "Tavşanlı tuff member" and "Handere tuff member". They proposed that the depositional environment is a gradually deepening shallow marine environment and the region emerged in Oligocene.

The pyroclastic rocks which locally gets thicker of this volcano- sedimentary sequence defined in Armutlu peninsula have in some places undergone intense alteration. As a result of the diagenetic alteration of these andesitic, dacitic and rhyodacitic tuffs, hauylendite-clinoptilolite group minerals from zeolites, mica, clay mixed layered minerals (seladonite, glokonite), opal-CT from silica group and calcite from carbonates have authigenically formed (Uz et al., 1992; 1995). The tuffs which are seen in white, dirty white, yellow-green in color in the field display crystalline-glassy and lithic transitions. Dusty tuff transitions as bands with binding material which is in ash size can also be seen. The phenocrystals are quartz, plagioclase (albite-orthoclase), sanidine and biotite in the acidic tuffs in which the alteration is higher. Intermediate (andesitic) tuffs include hornblende crystals. Lavas are mostly of andesitic, and in places are of basaltic which cuts the andesitic lavas. Flow breccia structure and concentric alterations in agglomerates are seen in places. Agglomerates are observed from large block (a few meters) to lapilli size. All these coarse clastic volcanic materials are bound loosely with fine grained clay and tuff of volcanic origin.

The Eocene volcanics cropping out in Armutlu pe-

ninsula, continue to appear southwestward, in the north of lake Apolyont, along the ranges parallel to the sjiore and in vicinity of Kemalpaşa displaying the same features. Lavas are hard, green in color, mostly andesitic and basic and pillowed. Pyroxene andesitic lavas are of porphyritic and comprise plagioclase, pyroxene, less hornblende and quartz as trace minerals. Plagioclases are of various type and are crystallized as hypidiomorph showing zonal structure. Pyroxenes (clinopyroxene-pidgeonite, augite and orthopyroxene-hypersthene) are generally as hypidiomorph crystals. Matrix is intergranular in places and pyroclastic and includes primary silica. Carbonatization and chloritization can be seen locally. Brown and green hornblende crystals are idiomorph with their surroundings opacitized. Basaltic andesite lavas contain idiomorph olivine crystals which are chloritized due to alteration. Basaltic lavas are called "olivine basalt", they are porphyritic and comprise plagioclase, olivine and pyroxene phenocrysts. They are generally hypidiomorph. They are as macro and microphenocrystals, some of them show zonal structure. Mostly they form glomeroporphyritic assemblages. Some of them are poikilitic and have pyroxene inclusions. Olivines are chloritized, carbonated due to alteration and their fractures are filled with iron oxide. Pyroxenes (clinopyroxene-augite) are hypidiomorph and are in forms of macro and microphenocrystals. The matrix is intergranular and rather coarse grained and they are formed by the plagioclase microliths and microcrystals and by the granulated opaque minerals and chloritized and carbonated mafic mineral traces in between them. They have amygdaloidal structure in places, filled by chlorite (at the sides) and calcite (in the center).

Oligocene volcanics

The Oligocene volcanics situated around the sea of Marmara crop out at three different areas:

a) Oligocene volcanics in Biga peninsula : Biga peninsula, starting from Lower Oligocene uplifted and emerged (Ercan et al., 1995) and first of all, the area between Çan and Çanakkale and the region around

Manyas were effected from a volcanic stage expressed by widespread lavas and tuffs of andesite, dacite, rhyodacite type. Many of them have been altered and silicified. These are observed in white, yellow, red, brown, green and blue colors and in different situations. Silicified tuffs are hard and conchoidal. Unaltered lavas, which are quite rare, are mostly dark colored and include brown plagioclase crystals, gray-black biotite and dark gray pyroxene phenocrystals. Andesitic lavas are porphyritic and include plagioclase, amphibole and pyroxene phenocrystals. Plagioclases (oligoclase-andesine-labrador) are hypidiomorph and display zonal structure. Sometimes they show antiperthite formation and have poecilitic texture. They have changed into clay minerals in places due to alteration.

Amphiboles (oxyhornblende) are as hypidiomorph macro and microphenocrystals. Some of them are opacitized. Pyroxenes (clinopyroxene-augite) are as hypidiomorph thin microphenocrystals. Dacitic lavas have the same features. The quartz minerals they include are as subautomorph crystals. The components of the tuffs are sericitized, argillitized plagioclase fragments, quartz fragments, volcanic rock fragments (andesite, quartz andesite and dacite) and devitrified glass fragments. These are bound with a matrix of volcanic glass, ash and dust. Grain size is varying between 3.2 mm (lapilli) and 0.04 mm (fine grained tuff) but generally considered as 0.30 mm (coarse tuff). Ignimbrites are observed with tuffs in places. Great part of the lavas are silicified, argillitized and pyritized locally. There are some hydrothermal quartz veins in tuffs. In general, all of the mineral deposits in the region have formed in relation with the Oligocene volcanism. The alteration of tuffs have resulted in formation of rich kaoline deposits.

The Oligocene volcanics are called "Çan volcanics" by Ercan et al., (1995) during their study in which they showed the distribution of the volcanics. An andesite sample taken from, Lapseki-Umurbey village yielded 29.2 ± 0.6 million years (between Chattian-Rupelian) based on K/Ar dating method. Dayal (1984) reached almost the same result during his study in the area* with the samples taken from the east of Çan: 28.2 ± 2 ,

28.0 ± 0.9 and 22.4 ± 0.8 million years. The first stages of Oligocene volcanism in Biga peninsula which is known as "Çan volcanics" is very important in NW Anatolia from the rich metallic mining point of view. Hydrothermal alteration is very intense, in such areas, in silicified zones Au, Ag, Pb, Cu, As, Fe, Mo, Zn and Hg deposition are seen which have been exploited since thousands of years.

In the last stages of the Oligocene volcanism producing outcrops of andesitic and locally dacitic lavas, tuffs and agglomerates the nature of the volcanism was changed and instead the above listed generally black dykes and black, small outcrops of trachyandesitic and basaltic lava flows were produced. These which are called "Kirazlı volcanics" by Ercan et al., (1995) have yielded 27.6 ± 0.6 and 31.1 ± 0.7 million years by K/Ar dating method. The texture of these trachyandesitic lavas are microlitic porphyritic and hyalomicroclitic porphyritic and they bear plagioclase (labrador and andesine), augite and lesser biotite and hornblende crystals in a glassy microcrystalline matrix. Plagioclases which appear as phenocrystals and microliths have been altered in places and have turned into minerals like sericite and zeolite. Basaltic lavas have intergranular and microlitic porphyritic texture and bear plagioclase (labrador and andesine), augite and olivine minerals in matrix of plagioclases and microliths of mafic minerals.

b) Oligocene volcanism in Gökçeada (Imroz) island : Gökçeada island is entirely made up of Tertiary rocks. At the basement there are two flysch deposits of Eocene and Oligocene age (Akartuna, 1950; Okut, 1975). Lavas, tuffs and agglomerates of andesitic and dacitic nature cut and overlie these rocks. Ercan et al., (1995) obtained 30.4 ± 0.7 and 34.3 ± 1.2 million years of age from the K/Ar dating of two different samples.

c) Oligocene volcanism in Thrace : The Oligocene volcanism in Biga peninsula and in Gökçeada island spreads in Thrace and westward, in Greece and Bulgaria. Ternek (1949) and Kopp et al., (1969) have stated that the volcanism was effective during the whole Oligocene. They also stated that andesitic and dacitic lavas during both two volcanic stages and in Lower Oli-

gocene and towards Upper Oligocene intense andesitic and dacitic and in places trachytic lavas were produced. An andesitic sample collected near a quarry around Keşan yielded 26.2 ± 0.5 million years (Upper Oligocene-Chattian) by K/Ar dating method. The phenocrystals of the dated sample are mainly plagioclase and lesser amphibole (hornblende) and pyroxene. Opaque minerals and apatite are secondary minerals. Plagioclases have turned into sericite and/or clay minerals and they appear as hypidiomorph crystals in zonal structure. Some of them form glomeroporphyritic assemblages. Amphiboles (green hornblende) mostly observed as idiomorph crystals. Pyroxenes (augite) are seen in lesser amounts as microphenocrystals. The matrix, having cryptocrystalline felsitic texture, is made up of crystalites.

Oligocene volcanism in Hisarlıdağ, in vicinity of Enez, is being represented by lavas, tuffs and agglomerates of mostly andesitic and dacitic nature. They, which are called "Hisarlıdağ volcanics" by Saner (1985) reach up to a thickness of 800 m. The same name was used for the volcanics in the region by Sümençen et al., (1987). A sample from this region yielded 35.0 ± 0.9 million years (Lower Oligocene) by K/Ar dating method. There are ignimbrites and tuffs in different colors with large fiammes in Hisarlıdağ which formed at different stages, agglomerate levels and andesitic lavas in places. The summit was formed by black and pink colored ignimbrites. The components of the ignimbrites are plagioclase, biotite, devitrified glass fragments and volcanic rock fragments. They are stained by ironoxide hydroxides and volcanic glass flakes are lined up in flow structures. Andesitic lavas include plagioclase, pyroxene and biotite phenocrystals. Plagioclases (andesine) are hypidiomorph in zonal structure. They range in a series from macrocrystals to microliths. Generally they are crystallized in zonal structures as hypidiomorphs. Biotites are observed as hypidiomorph and xenomorph crystals whereas pyroxenes (clinopyroxene-augite) are crystallized as hypidiomorphs. They are stained by the ironoxide hydroxides and due to intense corrosion around they are rounded. The matrix is of cryptocrystalline felsitic texture and margarite and globulite structures due to devitrication of volcanic glass can be observed. In Hisarlıdağ volca-

nic rocks start with, at the bottom, rhyodacitic tuffs, andesite, altered andesitic tuffs and reddish green tuffs formed by the lahar flow. In the upper levels white rhyolitic tuffs, rhyodacites, andesites, agglomerates and ignimbrites are seen. Between Ipsala and Meriç andesitic and dacitic rocks of Oligocene age crops out. Tuffs generally form thin layers between syndimentary deposits. Especially around Büyükaltağaç village ignimbritic tuffs with small obsidian fragments are observed. Altered small dacitic lava outcrops in places can also be seen.

In Central Thrace, on the other hand, tuff horizons that have formed in a couple of stages having various thicknesses in between Oligo- Miocene deposits can be seen spread in wide areas. These are the products of Oligocene volcanism (Lebküchner, 1974). These are generally weathered and kaolinized andesitic and dacitic glassy tuffs and are difficult to differentiate from the sedimentary units (Ercan, 1979). Some of them are reworked and some are air-fallen during the formation of deposits. For example, the Oligocene aged tuffs in vicinity of the Seğmenli and Selçuk villages to the west of Tekirdağ are observed have formed in lacustrine environment and are intercalated with the siltstone-claystone units. There are very thin coal seams in between. The tuffs have come from a volcanic center in the vicinity, Kale tepe, and fallen into a lacustrine environment to form layers. Gök (1990) named the tuffs as the "Ferhadanlı tuff member" of the "Danışmen formation" of Middle Oligocene age. They are white, dirty white, light gray in color and bear agglomerate levels with a thickness of maximum 25-30 m. They are processed and used as trass in cement factories. They include abundant quartz, biotite, amphibole (green hornblende), plagioclase and volcanic rock fragments. Cement is made up of volcanic glass, dust, ash, carbonate and clay. The lava samples taken from the Kale tepe are silicified, carbonatized dacitic lavas and have amygdaloids and totally chloritized mafic minerals, quartz and plagioclases turned into clay minerals.

The Oligo-Miocene aged deposits spreading over wide areas in Thrace overlies, in places, volcanic rocks of Oligocene age. Ercan and Gedik (1986) studied the core samples of Maltepe-1 well opened by Deilmann-

Shell Oil Company in the north of Keşan (41° 01' 17" latitude and 26° 42' 3" longitude) and found out dacitic and rhyodacitic lavas of Oligocene age at 1850-1860 m depth. The same researchers also studied the core samples taken from incek-1 well opened by Gulf Oil Company in the east of Malkara (40° 55' 44" latitude and 27° 17' 16" longitude) and observed the existence of dacitic lavas of Oligocene age at 1488-1492 m depth.

The Oligocene volcanism in Thrace is observed in wide areas both in Greece and Bulgaria.

Lower-Middle Miocene volcanics

Lower-Middle Miocene volcanics around the sea of Marmara takes place mainly in two places:

a) Lower-Middle Miocene volcanics in Biga peninsula and in Manyas : During Lower-Middle Miocene an intense volcanism took place in Biga peninsula in different stages and produced andesitic, dacitic, rhyodacitic, trachyandesitic and basaltic lavas, tuffs, agglomerates and ignimbrites. These rocks are well known and well studied with detailed investigations and the datings have yielded 21.5-16.8 million years (Ercan et al., 1990; 1995). The volcanic rocks of Lower-Middle Miocene age in Biga peninsula and around Manyas have formed at the same time with deposits of Neogene age in a terrestrial environment. In places volcanic products have formed and sometimes in depositional environments volcanic rocks and sedimentary rocks have mixed and formed volcano-sedimentary units. Lavas are mainly of andesitic and in places of dacitic and rarely rhyodacitic, trachyandesitic and basaltic. Andesitic lavas are generally pink, purple, dark gray or beige in color, with irregular and angular breaks and rarely show flow structure. They mostly have hyalocrystalline porphyric texture and include plagioclase, biotite, amphibole (hornblende) and pyroxene (augite) phenocrystals. Plagioclases are andesine and oligoclase and crystallized as hypidiomorph in forms macro and microphenocrystals and display zonal structure. Amphiboles (brown hornblende) are generally hypidiomorph and opacitized mostly. Biotites are as lar-

ge, medium to small sized phenocrystals as hypidiomorphs and their outer boundaries are opacitized. Pyroxenes (clinopyroxenes-augite) are as hypidiomorph and idiomorph microphenocrystals and their outer boundaries are stained with ironoxide hydroxides. They are observed either as single crystals or as glomeroporphyritic textured assemblages. The matrix is pylotaxitic and in places in cryptocrystalline felsitic texture and made up of plagioclase microliths and crystals and cryptocrystalline mesostases in between them. Dacitic lavas, pinkish white, dirty white in color, includes quartz and coarse plagioclase (andesine-oligoclase), biotite and hornblende phenocrystals. The matrix is in spheroidal texture. This matrix, generally seen in acidic rocks has obtained this feature by the recrystallization of the glass already present. Rhyodacitic lavas have more quartz phenocrystals than dacitic lavas and these phenocrystals are embedded in the matrix. As another difference from dacites, sanidine in less amount is also observed. Tuffs are generally inter-fingered with andesitic lavas and agglomerates and include epidotized, chloritized and partly carbonatized mostly hornblende (idiomorph), biotite (hypidiomorph), epidot group minerals (pistacite), chlorite fragments, and argillized-sauritized feldspat fragments. The matrix is generally made up of biotite as microliths, less hornblende, plagioclase microliths (albite), pyroxene and quartz in lesser amounts.

b) Lower-Middle Miocene volcanism in Thrace : Although there are widespread outcrops of Lower-Middle Miocene volcanism in Biga peninsula, in Thrace, the outcrops of this volcanism is observed in five small locations:

/- Koyuntepe, to the east of Hisarlıdağ. - Lavas of pyroxene andesite type are very hard, black in color and have the appearance of basalt. Koyuntepe mountain is made up of these lavas. They have plagioclase and pyroxene phenocrystals and amphibole (brown hornblende) in lesser amounts. Plagioclases (andesine) display zonal structure and are generally hypidiomorph. They include glassy matrix as inclusions and are in various sizes as macro and microphenocrystals. Pyroxenes (clinopyroxene-augite and orthopyroxene-

hypersthene) have crystallized as hypidiomorph. Clinopyroxenes are much more in amount whereas there are very few amphiboles (brown hornblende), they are opacitized in their surroundings. The matrix is in pylo-taxitic texture, the space between the crystals are filled with volcanic glass. The samples yielded 17.3 ± 0.4 million years (Burdigalian-Lower Miocene) by K/Ar method.

//- Asar tepe, in the north of Korucuköy. - Asar tepe is composed of basaltic lavas. The lavas are in porphyritic texture and include abundant olivine and pyroxene and less plagioclase. Olivines are the most abundant phenocrystals and generally crystallized in hypidiomorph form as macro and microphenocrystals. Some of them form assemblages in glomeroporphyritic texture. Pyroxenes (basaltic augite) display zonal structure and are observed as xenomorph crystals, as thin phenocrystals forming assemblages in glomeroporphyritic texture and microphenocrystals seen as hypidiomorph-single crystals. In these basaltic lavas having coarse grains, the matrix is intergranular in places (the space between plagioclase-labrador microliths filled with pyroxenes and opaque minerals) and intersertal in some places (chloritized mezostaz fill the space between plagioclase microliths). The lavas building Asar tepe are similar with the Upper Miocene basaltic lavas. The samples taken yielded 15.0 ± 0.3 million years by K/Ar method (Lower-Middle Miocene, Burdigalian-Langhian). These are the first products of the alkali basaltic volcanism in Thrace.

III-Kale tepe and Kartal tepe near Harala village. - The volcanics forming the Kale tepe and Kartal tepe near Harala (Altinyazı) village are similar with the other Lower-Middle Miocene aged basalts in their appearance. On the other hand, the detailed petrographic and geochemical studies have shown that these are subvolcanic rocks crystallized in depth rather than the basaltic lavas crystallized at the surface. The samples generally have poikilitic texture. They are composed of mainly pyroxene (clinopyroxene-augite) and plagioclase (oligoclase-andesine) in decreasing amount, biotite, olivine, opaque minerals and apatite as secondary mineral and all of them are in alkali feldspaths (orthocla-

se and sanidine) displaying perthitic structure. Augites are generally hypidiomorph and in glomeroporphyritic texture. Plagioclases are seen as thin spikes and microliths. They change into chlorite and/or clay minerals in places. Biotites are crystallized as hypidiomorphs and opacitized. The trace minerals that changed into chlorite + carbonate + opaque minerals are most probably olivines. The samples, according to Streckeisen 1976 classification, may be micromonzonites in syenite-monzonite transition. The two samples collected in the area have yielded $21.27 + -0.24$ and $18.47 + -0.20$ million years (Lower Miocene) by K/Ar method. Thus, by this work subvolcanic rocks of Miocene age in Thrace was found for the first time.

IV- Karakaya tepe near Yenimuhacir village northeast of Keşan. - At the basement marl of Oligocene age, sandstone, coal seams and tuffs are situated and the magmatic rocks cutting these are similar to those subvolcanic hypabyssal rocks seen both in Kale tepe and Kartal tepe. They are of porphyritic texture, generally. The main minerals are alkali feldspat, analcime, pyroxene, biotite and olivine. Alkali feldspaths (orthoclase and less sanidine) are observed to include biotite and pyroxene minerals as xenomorph crystals both in interstitial and in poikilitic texture. Change into analcime and clay minerals, in places, are seen. Analcimes are mostly idiomorph and interstitial as xenomorphs and in places found together with zeolite minerals. Pyroxenes (clinopyroxene-diopside) are crystallized as idiomorph and hypidiomorph. Some of them are surrounded with a slight dark mantle (possibly a transition to aegirin augite). They are observed as medium and thin microphenocrystals. Biotites are generally crystallized as hypidiomorph and are in reddish brown color (probably Ti biotite). They are observed as coarse phenocrystals. As secondary minerals apatite and opaque minerals are seen. The samples are named "analcime syenite porphyry", a vein rock, as attached to fold syenides according to Streckeisen I.U.G.S.-1979 classification.

V-Karamaden tepe, in the north of Keşan. - This is a small andesitic dyke. The phenocrystals of the samples are plagioclase, amphibole and pyroxene. The texture of the samples are porphyritic. Plagioclases (oli-

goclase-andesine) have undergone magmatic corrosion, they are seen as hypidiomorph crystals with zonal structures. Some of them are changed into chlorite and/or clay minerals. Amphiboles (green hornblende) are mostly hypidiomorph as macro and microphenocrystals. Some of them are in glomeroporphyritic texture. Pyroxenes (augite) are crystallized as hypidiomorph. They are seen as macro and microphenocrystals and are lesser than amphiboles. The primary texture of the matrix is hyalopilitic and as a result of alteration chloritization and the formation of secondary silica can be seen.

Upper Miocene volcanics

The Upper Miocene volcanic rocks around the sea of Marmara are seen as cutting the Tertiary sedimentary rocks and forming single volcanic cones. They are seen in Thrace but now here else in the region, except for a small outcrop situated to east of lake Manyas. They are completely of alkali olivine basalt type. They have used the young opening fissures to reach to the surface and have spread around them forming small flow outcrops and volcanic cones. In Thrace, some young basaltic volcanics crop but as scattered in between Çorlu and Tekirdağ (Kara tepe, Çevrimkaya köyü, Balabanlı köyü, Muratlı, Karakaya tepeleri, Osmanlı köyü, Beşik tepe), in vicinity of Malkara (Karademir köyü, south of Ballıköy) and in vicinity of Keşan (Mahmutköy, Kartal tepe, Sivri tepe, Küçükdoğanca köyü, Beğendik köyü). The samples defined as olivine basalt are in porphyritic texture and bear abundant olivine, less plagioclase, and lesser pyroxene as thin phenocrystals. In some samples very few biotite is found. The matrix is of intergranular texture, the space between interfingering plagioclase microliths are filled with granulated pyroxene, less olivine and lesser opaque minerals. In a very small area intersertal texture is seen. Olivines are the most abundant minerals and they are mostly crystallized as idiomorph. Some of them are observed as relicts changed into chlorite and calcite while the others are as less altered. They are surrounded by secondary, granulated opaque minerals (magnetite?). Pyroxenes (clinopyroxene-augite) are seen in zonal structure as hypidiomorph crystals. The texture

is generally glomeroporphyritic. Plagioclases are generally seen in the matrix rather than as phenocrystals.

The age of the young alkali basaltic volcanism in Thrace has been under debate for long years. For example, Umut et al., (1984) and Umut (1988) proposes that they can be divided into two groups of Upper Miocene-Pliocene age and of Pliocene-Quaternary age while Ercan (1992) states that the latest stage of the basalts was effective towards the end of the Pliocene. Tapırdamaz and Yalıtırak (1997) proposes that a part of these basalts may be of Pliocene-Quaternary age. Sümmengen et al., (1987), depending upon a radiometric dating of a sample taken from Mahmutköy to the south of Keşan, states that the basalts are 6.7 ± 0.7 million years old (Upper Miocene). Besides, there are some other dating results from some outcrops such as 4.88 ± 2.19 million years and 6.47 ± 0.43 million years (Upper Miocene) (Yücel Yılmaz, personal communication). In order to shed light to the problem, during this research, four different sample was dated by K/Ar method. The sample taken from Kara tepe (the basaltic cone appearing the youngest in the region) in vicinity of Çorlu yielded 8.95 ± 0.2 million years (Upper Miocene) and the samples taken from Karakaya tepe in the north of Tekirdağ yielded 8.9 ± 0.2 , 8.96 ± 0.1 , 8.92 ± 0.1 million years (Upper Miocene). Therefore the age of the youngest volcanism is determined as Upper Miocene. No volcanic rocks of Pliocene and Quaternary were found.

GEOCHEMICAL FEATURES OF THE TERTIARY VOLCANISM AROUND THE SEA OF MARMARA

During this study carried out around the sea of Marmara, other than the petrographic and geochronologic studies on the volcanic rocks differentiated into five groups according to their ages, chemical analyses on the representative samples were done and some geochemical results were also obtained. Four samples from Upper Cretaceous volcanics, 27 samples from Eocene volcanics, 21 samples from Oligocene volcanics, 9 samples from Lower-Middle Miocene volcanics and 13 samples from Upper Miocene volcanics (Fig.1) were collected and the total 74 samples were analyzed in MTA Chemical Laboratories to determine the major elements (Tables 1-2-3-4-5). Besides, 9 samples used

Table 1- Chemical analyses related with Upper Miocene volcanics.

SAMPLE NO	T-1	T-2	T-3	T-4	T-5	T-9	T-10	T-11	T-14	T-20	T-55	T-58	T-60
SiO ₂	47,60	46,93	49,04	50,14	50,67	46,62	47,00	46,49	46,72	47,36	49,37	54,55	45,32
TiO ₂	2,61	2,47	2,55	2,53	2,74	2,38	2,32	2,89	2,07	2,33	2,10	1,25	2,14
Al ₂ O ₃	12,53	12,76	13,79	14,18	14,49	12,02	12,13	12,08	11,89	13,99	13,44	13,30	11,71
Fe ₂ O ₃	3,34	2,59	4,62	8,58	6,00	1,73	2,47	5,10	2,52	4,70	3,48	2,54	2,24
FeO	7,52	8,59	6,69	2,58	4,81	9,17	8,69	6,95	8,89	6,83	7,46	4,26	10,08
MnO	0,10	0,21	0,10	0,20	0,10	0,10	0,20	0,11	0,21	0,11	0,11	0,10	0,20
MgO	11,48	12,35	7,15	6,08	5,37	13,47	12,13	11,76	14,47	9,22	9,66	9,56	12,22
CaO	9,60	8,85	10,01	9,52	10,34	9,32	9,10	10,26	8,48	10,81	9,03	6,55	9,57
Na ₂ O	2,82	2,68	3,68	3,75	2,84	2,38	3,13	2,78	2,58	2,33	2,42	1,56	4,18
K ₂ O	1,67	1,85	1,74	1,82	1,93	2,07	2,02	0,75	1,55	1,70	2,31	5,51	1,32
P ₂ O ₅	0,73	0,72	0,61	0,61	0,71	0,73	0,81	0,85	0,62	0,64	0,63	0,83	1,02

Table 2- Chemical analyses related with Lower-Middle Miocene volcanics.

SAMPLE NO	T-17	T-23	T-40	T-54	T-68	T-69	T-70	T-71	T-82
SiO ₂	53,46	58,23	48,96	62,54	62,03	61,78	67,49	61,25	74,88
TiO ₂	1,15	0,62	2,19	0,62	0,61	0,72	0,60	0,70	0,57
Al ₂ O ₃	16,25	16,70	13,13	16,40	16,57	16,48	16,12	17,07	8,51
Fe ₂ O ₃	2,72	3,84	1,19	3,42	3,50	3,57	3,30	3,60	2,21
FeO	5,66	4,43	9,43	3,38	1,42	2,63	1,11	2,81	1,59
MnO	0,21	0,10	0,10	0,10	0,10	0,10	0,10	1,00	0,11
MgO	5,35	4,33	8,96	2,77	2,03	1,96	0,60	2,21	2,27
CaO	7,55	8,45	9,38	6,66	4,58	5,97	3,22	5,52	4,65
Na ₂ O	2,52	2,47	3,65	2,87	3,66	3,19	3,53	3,41	2,04
K ₂ O	4,19	0,72	2,40	1,03	5,08	3,90	3,73	2,11	2,95
P ₂ O ₅	0,94	0,10	0,63	0,21	0,41	0,31	0,20	0,30	0,23

Table 3- Chemical analyses related with Oligocene volcanics.

SAMPLE NO	T-8	T-13	T-18	T-19	T-21	T-22	T-24
SiO ₂	69,88	72,74	86,33	71,95	58,79	62,91	59,31
TiO ₂	0,54	0,31	0,64	0,53	0,58	0,52	0,62
Al ₂ O ₃	14,19	17,38	7,95	16,93	18,67	15,73	16,99
Fe ₂ O ₃	2,76	0,57	3,07	3,55	2,65	3,44	3,41
FeO	0,81	0,52	0,48	0,42	4,67	3,04	4,53
MnO	0,11	0,10	0,11	0,11	0,12	0,31	0,10
MgO	1,72	0,10	0,05	0,74	1,96	2,10	2,99
CaO	5,05	1,47	0,21	0,21	4,38	4,72	7,11
Na ₂ O	1,94	1,99	0,21	0,26	5,30	4,51	2,78
K ₂ O	2,80	4,71	0,74	5,08	2,77	2,62	1,96
P ₂ O ₅	0,22	0,10	0,21	0,21	0,12	0,10	0,21

Table 3- (Continued)

SAMPLE NO	T-26	T-27	T-28	T-29	T-30	T-31	T-32
SiO ₂	61,58	64,01	65,71	62,21	60,81	60,26	67,01
TiO ₂	0,72	0,62	0,61	0,82	0,62	0,71	0,51
Al ₂ O ₃	18,47	18,27	17,79	18,36	17,58	17,51	15,96
Fe ₂ O ₃	5,63	1,81	2,45	5,26	4,14	2,74	5,16
FeO	0,10	2,27	0,71	0,41	2,79	5,14	0,51
MnO	0,10	0,10	0,10	0,10	0,10	0,10	0,10
MgO	0,46	1,03	0,40	0,51	1,34	2,34	0,51
CaO	2,05	2,79	1,42	3,47	7,03	6,31	3,07
Na ₂ O	3,90	3,61	3,44	3,37	3,21	2,75	2,66
K ₂ O	6,67	5,16	7,08	5,10	2,17	1,93	4,30
P ₂ O ₅	0,31	0,31	0,30	0,41	0,21	0,20	0,20

Table 3- (Continued)

SAMPLE NO	T-33	T-34	T-39	T-56	T-57	T-66
SiO ₂	66,64	71,24	57,89	76,70	65,11	66,80
TiO ₂	0,50	0,31	1,13	0,32	0,52	0,53
Al ₂ O ₃	16,64	16,69	13,60	16,81	16,36	15,43
Fe ₂ O ₃	4,90	2,00	1,62	1,03	2,02	2,02
FeO	1,00	1,22	4,84	0,21	2,15	2,75
MnO	0,10	0,20	0,10	0,11	0,10	0,11
MgO	0,40	0,31	5,77	0,11	1,78	1,48
CaO	3,11	1,83	5,67	0,21	7,55	2,85
Na ₂ O	2,61	3,05	2,78	0,63	2,31	3,59
K ₂ O	3,91	2,95	5,77	3,68	1,99	4,23
P ₂ O ₅	0,20	0,20	0,82	0,21	0,10	0,21

Table 4- Chemical analyses related with Eocene volcanics.

SAMPLE NO	T-43	T-44	T-45	T-46	T-47	T-49	T-50	T-51	T-52	T-53	T-59	T-61	T-62
SiO ₂	57,89	70,42	57,33	71,96	73,15	78,95	73,38	73,70	60,78	56,33	70,32	74,54	62,37
TiO ₂	0,71	0,22	0,83	0,42	0,41	0,30	0,21	0,31	0,63	0,64	0,41	0,32	0,61
Al ₂ O ₃	18,28	15,95	16,68	14,56	14,63	12,75	14,36	15,05	17,82	19,31	14,48	14,69	17,24
Fe ₂ O ₃	4,38	0,92	5,87	1,39	0,89	0,40	0,39	0,57	2,85	4,23	1,03	1,12	4,06
FeO	3,10	1,16	2,50	1,21	1,24	0,91	1,75	0,87	2,62	2,95	1,86	0,65	1,83
MnO	0,10	0,11	0,10	0,11	0,10	0,10	0,11	0,10	0,10	0,11	0,10	0,11	0,10
MgO	2,44	1,65	3,13	1,37	1,34	0,51	0,55	0,30	2,93	4,83	0,62	1,30	1,52
CaO	5,38	2,97	6,78	1,90	0,72	0,10	0,96	0,51	5,03	5,90	3,10	3,24	3,55
Na ₂ O	4,06	2,09	3,65	3,80	3,91	2,83	5,00	5,83	4,93	4,83	3,93	0,25	6,09
K ₂ O	3,25	4,40	2,71	3,17	3,50	3,04	3,19	2,66	2,10	0,64	3,93	3,67	1,72
P ₂ O ₅	0,41	0,11	0,42	0,11	0,10	0,10	0,11	0,10	0,21	0,21	0,21	0,11	0,91

Table 4- (Continued)

SAMPLE NO	T-63	T-64	T-66	T-67	T-73	T-74	T-75	T-76	T-77	T-78	T-79	T-80	T-81
SiO ₂	56,97	63,45	66,80	49,60	62,11	61,69	49,71	48,06	58,30	60,39	67,38	56,50	49,99
TiO ₂	0,82	0,52	0,53	0,99	0,52	0,61	1,76	1,60	0,83	0,75	0,52	0,82	1,65
Al ₂ O ₃	20,02	17,15	15,43	16,75	18,63	17,19	16,05	17,09	17,70	18,98	17,42	17,98	19,78
Fe ₂ O ₃	5,97	5,40	2,02	8,68	4,75	5,44	4,97	6,50	4,93	5,20	3,05	3,99	5,75
FeO	2,16	0,77	2,75	3,69	1,78	1,02	7,83	4,53	3,25	1,63	1,92	5,10	7,68
MnO	0,10	0,10	0,11	0,22	0,10	0,10	0,21	0,11	0,10	0,11	0,21	0,21	0,11
MgO	1,13	1,55	1,48	4,85	2,28	1,42	7,25	6,84	4,16	1,73	0,49	3,90	3,74
CaO	6,16	5,99	2,85	10,69	5,59	5,66	9,11	13,03	7,81	6,04	4,35	8,22	9,23
Na ₂ O	3,39	3,00	3,59	3,20	1,76	3,54	1,55	0,96	1,56	3,02	2,38	2,36	1,54
K ₂ O	2,98	1,86	4,23	1,21	2,26	3,03	1,24	0,85	1,15	1,94	1,97	0,72	0,33
P ₂ O ₅	0,31	0,21	0,21	0,11	0,21	0,30	0,31	0,43	0,21	0,22	0,31	0,21	0,22

Table 4- (Continued)

SAMPLE NO	T-83	T-84	T-85	T-86	T-87	T-88	T-89	T-90	T-91	T-92	T-93	T-94	T-95	T-96
SiO ₂	55,72	56,75	52,91	51,06	57,91	58,92	55,70	58,07	58,33	72,94	66,41	69,92	59,14	63,05
TiO ₂	0,82	0,62	1,45	8,01	0,68	0,64	1,05	1,10	0,85	0,55	0,51	0,43	0,71	0,72
Al ₂ O ₃	20,75	12,90	14,52	16,02	17,94	19,11	18,92	18,08	17,50	14,96	17,16	15,53	17,84	16,92
Fe ₂ O ₃	2,67	0,89	3,06	2,35	6,16	2,88	3,19	5,00	6,26	2,62	1,94	2,46	6,22	6,12
FeO	4,50	10,90	7,51	2,84	2,43	4,77	6,12	4,17	2,86	0,83	1,10	1,16	1,10	0,58
MnO	0,10	0,21	0,10	0,20	0,11	0,21	0,21	0,11	0,11	0,11	0,10	0,11	0,10	0,10
MgO	2,66	7,84	8,30	2,40	3,63	2,12	4,52	3,72	3,92	1,00	0,51	1,29	1,53	0,82
CaO	9,41	9,29	9,34	14,42	7,72	7,22	4,73	6,57	6,36	4,88	5,41	4,82	6,53	3,79
Na ₂ O	2,86	0,41	2,49	1,30	1,48	2,55	5,36	1,53	1,70	0,78	5,52	3,11	5,51	7,07
K ₂ O	0,31	0,10	0,10	1,20	1,70	1,27	0,11	1,42	1,91	1,22	1,23	1,07	1,12	0,62
P ₂ O ₅	0,20	0,10	0,21	0,20	0,23	0,32	0,11	0,22	0,21	0,11	0,10	0,11	0,20	0,21

Table 4- (Continued)

SAMPLE NO	T-97	T-98	T-99	T-100	T-101	T-102	T-103	T-104	T-105	T-106	T-107	T-108	T-109	T-110
SiO ₂	51,89	48,98	64,68	55,95	70,29	58,26	60,79	59,21	63,27	64,34	57,77	57,60	57,31	52,23
TiO ₂	1,14	1,38	0,63	1,04	0,42	0,95	0,94	0,82	0,74	0,51	1,03	0,82	0,92	1,15
Al ₂ O ₃	18,23	19,38	16,17	19,17	14,16	16,95	16,77	16,96	17,40	17,87	17,02	16,51	17,40	19,85
Fe ₂ O ₃	6,51	7,20	3,65	3,90	3,36	3,24	3,53	3,28	3,05	5,21	4,77	2,22	3,90	5,08
FeO	3,27	3,67	2,25	3,57	0,76	4,71	3,62	4,73	4,09	0,74	3,41	5,32	4,41	4,36
MnO	0,10	0,21	0,10	0,10	0,10	0,11	0,10	0,21	0,11	0,10	0,10	0,10	0,10	0,21
MgO	4,66	2,13	1,46	2,80	0,63	3,71	2,41	3,29	0,27	0,61	2,27	2,57	3,48	4,28
CaO	9,53	11,71	4,69	7,46	4,41	6,36	4,93	6,37	4,43	4,49	7,02	7,10	6,96	6,58
Na ₂ O	3,52	4,15	4,49	5,49	4,41	3,50	4,51	3,70	4,64	4,29	4,33	4,53	4,09	4,70
K ₂ O	0,93	0,85	1,67	0,31	1,26	2,01	2,20	1,23	1,69	1,63	1,96	1,03	1,23	1,36
P ₂ O ₅	0,21	0,32	0,21	0,21	0,21	0,21	0,21	0,21	0,32	0,20	0,31	0,21	0,20	0,21

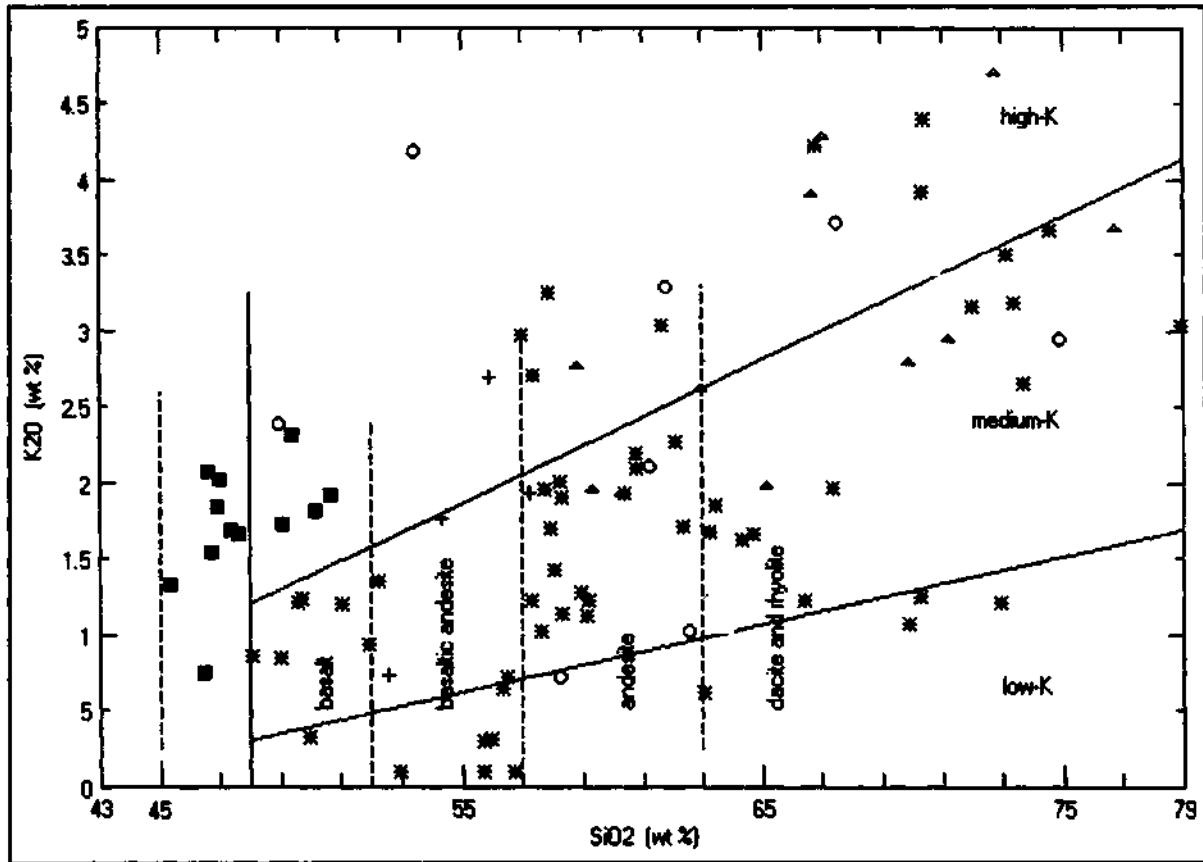


Fig. 3- K₂O-SiO₂ diagram of volcanics (legend same as in Fig. 2).

of calcalkaline and high potassium nature, and Eocene volcanics have tholeiitic character. The same situation was observed on the FeO-(Na₂O+K₂O)-MgO diagram, too (Fig.4).

According to their chemical composition, when the (Na₂O+K₂O) and SiO₂ contents of the samples were plotted on the diagram prepared by Le Maitre et al., (1989), it can be said that the Upper Cretaceous volcanics are basaltic andesite, and trachyandesite, Eocene volcanics are basalt, trachybasalt, trachyandesite, basaltic andesite, andesite, trachyandesite, trachyte, dacite and rhyolite, Lower-Middle Miocene volcanics are trachyandesite, trachybasalt, andesite, dacite and rhyolite, Upper Miocene volcanics are basanite, basalt, trachybasalt and trachyandesite (Fig. 5). This result is concordant with the petrographic determinations.

RESULTS

By this research, the post-Upper Cretaceous volcanic rocks around the sea of Marmara were differentiated in five groups and through detailed petrographic and radiometric studies the "age" problem was clarified and some undated volcanics were dated.

Especially in Thrace, some alkali basalts which were claimed to be of Plio-Quaternary age by some previous researchers by field observations were sampled and dated -some of them were dated two times- to be of Upper Miocene age. Besides that, the existence of Miocene aged subvolcanic rocks, which had not been observed before this study, was put forward. This study aims only the dating, distribution and the petrographic features of the volcanic rocks around the sea of Mar-

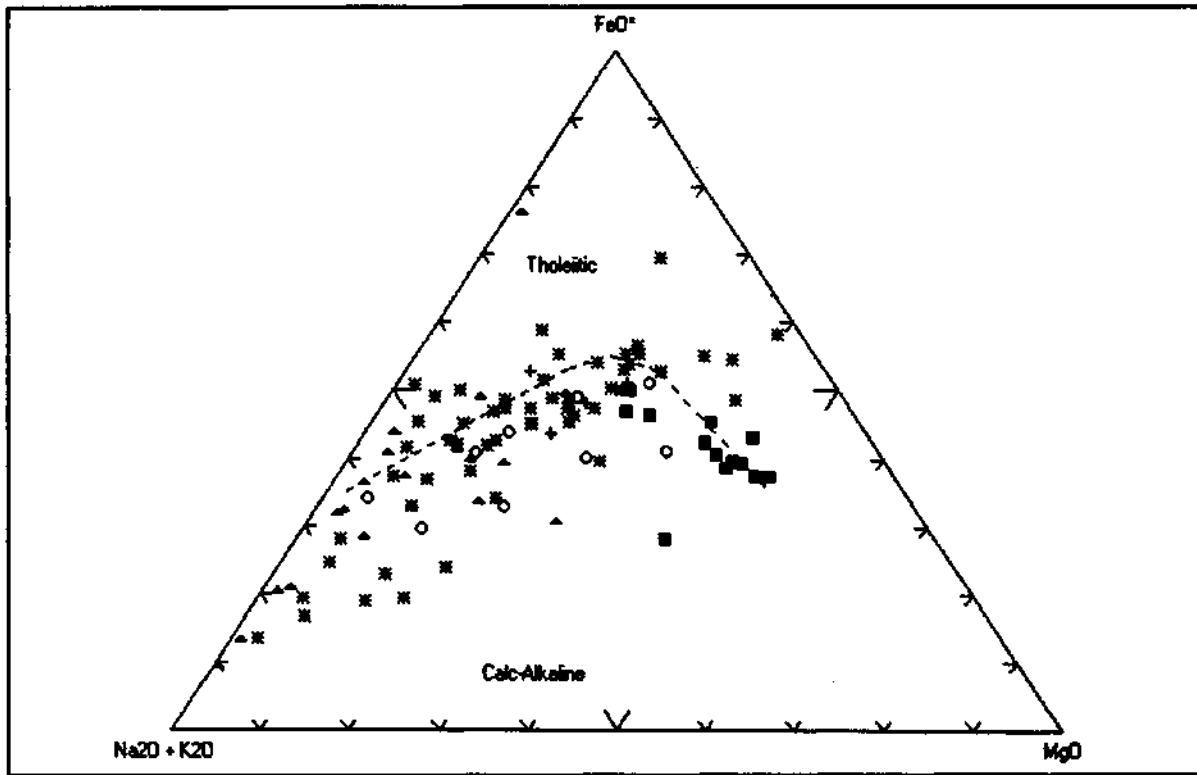


Fig. 4- FAM triangle diagram of volcanics (legend same as in Fig. 2).

mara but not the genesis of them. In fact, there are many research on the volcanic rocks in the region including the major, trace and rare earth elements and the genesis of the volcanic rocks. For example, it was concluded that the Upper Cretaceous volcanic rocks are generally produced from the crust and they belong to a group of island arc volcanics produced from a subduction zone developed in a compressional regime due to the converging plates (Yeniyo and Ercan, 1989/1990).

The major and trace element contents of the granitic rocks situated around İğneada together with the volcanics in Thrace and known to be of Upper Cretaceous age by K/Ar (Moore et al., 1980; Ohta et al., 1988) imply that they were formed in an island arc type subduction zone (Tokel and Akyol, 1987). It is stated that after the subduction of Sakarya continent and Rhodopontide block, the continent to continent collision star-

ted in Upper Cretaceous and ended in Lower Tertiary (Şengör and Yılmaz, 1981; Yılmaz, 1995) but after the consumption of the oceanic material the convergence continued in Eocene. This convergence was taken up with the shortening and thickening of the crust and lithosphere which possibly continued until Middle Miocene (Yılmaz, 1989). Therefore, post-Upper Cretaceous Eocene, Oligocene, Lower-Middle Miocene volcanics are the last products of the subduction and collision, post-collision type volcanics (Ercan et al., 1995; Ercan, 1992). Polat et al., (1997) studying the Thrace volcanics in detail from the point of view of geochemistry proposes that andesitic volcanics of Eocene and Oligocene age are from subcontinental lithospheric mantle whereas alkali basalts of Upper Miocene age from asthenospheric mantle. The alkali basalts of Upper Miocene age must have formed due to the uplift of mantle arising from an extensional system created by a new tectonic regime in the region after Middle Miocene.

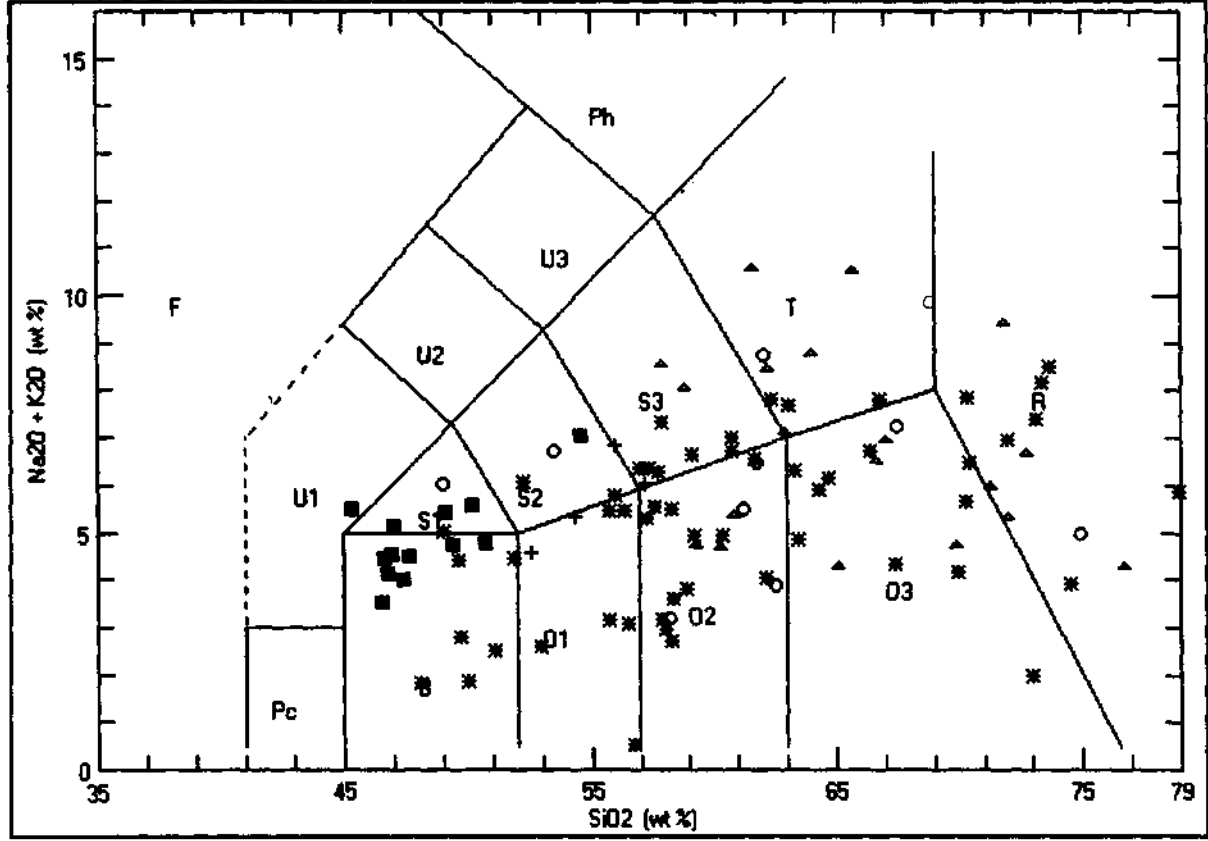


Fig. 5- Naming of the volcanics in the diagram prepared by Le Maitre et al., (1989) (legend same as in Fig. 2).

ACKNOWLEDGEMENTS

The writers would like to thank İrfan Özcan and Kemal Yenigün for their invaluable help during the fieldwork of this study which was realized in context of the project "Map of Tertiary-Quaternary Volcanics of Turkey" of MTA General Directorate Geological Research Department.

Manuscript received July 28, 1997

REFERENCES

- Akartuna, M., 1950, İmroz adasında bazı jeolojik müşahadelere: Türkiye Jeol. Kur. Bül., 2/2, 8-17.
- , 1953, Çatalca-Karacaköy bölgesinin jeolojisi: İst. Üniv. Fen. Fak. Monog. 13, 86 s.
- Akartuna, M., 1953, Şile Şaryajının İstanbul Boğazı kuzey yakalarında devamı: MTA Derg., 61, 14-20.
- , 1968, Armutlu yarımadasının jeolojisi: İst. Üniv. Fen Fak. Monog. 20, 12 s.
- Bargu, S. and Sakıncı, M., 1987, Armutlu yarımadasında Kretase-Paleosen ilişkisi: Türkiye Jeol. Bül., 30, 41-48.
- and ——, 1989/1990, İzmit Körfezi ile İznik Gölü arasında kalan bölgenin jeolojisi ve yapısal özellikleri: İstanbul Üniv. Müh. Fak. Yerbilimleri Derg., 6/1-2, 45-76.
- Baykal, F., 1943, Şile mıntkasının jeolojisi: İst. Üniv. Fen. Fak. Mecm., B, VII/3, 166-233.
- , 1971, Historik jeoloji: KTÜ Yayını No:38, 436 sayfa, Trabzon.

- Baykal, F. and Kaya, O., 1966, İstanbul Boğazı kuzey kesiminin jeolojisi: Türkiye Jeol. Kur. Bült., 10, 31-43.
- and Önalan, M., 1979, Şile sedimanter karışığı (Şile Olistostromu): Türkiye Jeol. Kur. Altın Semp. Bildiriler Kitabı, 15-26.
- Bürkan, K., 1955, Trakya Havzasındaki tüflerin stratigrafik konumu, yayılımı ve hidrokarbon potansiyeli: Trakya havzası Jeolojisi Sempozyumu Bildiri Özleri Kitabı 48.
- Dayal, A., 1984, Yenice (Çanakkale) granitinin petrografisi ve buna bağlı cevherleşmeler: Doktora tezi, Dokuz Eylül Üniv. Fen Bilimleri Enst., (unpublished), İzmir.
- Ercan, T., 1979, Batı Anadolu, Trakya ve Ege adalarındaki Senozoyik volkanizması: Jeoloji Mühendisliği Derg., 9, 23-46.
- , 1992, Trakya'daki Senozoyik volkanizması ve Bölgesel Yayılımı: Jeoloji Müh. Derg., 41, 37-50.
- and Günay, E., 1984, Kuzeybatı Anadolu, Trakya ve Ege adalarındaki Oligo-Miyosen yaşlı volkanizmanın gözden geçirilmesi: Türkiye Jeoloji Kurultayı Bült., 5, 119-139.
- and Gedik, A., 1986, Karadeniz ve Trakya'da yapılan derin sondajlardan alınan karotlardaki volkanik kayaların petrolojisi ve volkanizmanın bölgesel yayılımı: Jeomorfoloji Derg., 14, 39-48.
- ; Ergül, E.; Akçaören, F.; Çetin, A.; Granit, S. and Asutay, J., 1990, Balıkesir-Bandırma arasında jeolojisi, Tersiyer volkanizmasının petrolojisi ve bölgesel yayılımı: MTA Derg., 110, 113-130.
- ; Satır, M.; Steinitz, G.; Dora, A.; Sarfakioğlu, E.; Adis, C.; Walter, H.J. and Yıldırım, T., 1995, Biga Yarımadası ile Gökçeada Bozcaada ve Tavşalı adalarındaki (KB Anadolu) Tersiyer Volkanizmasının özellikleri: MTA Derg., 117, 55-86.
- Erendil, M.; Göncüoğlu, M.C.; Tekeli, O.; Aksay, A.; Kuşçu, I.; Ürgün, B.; Tunay, G. and Temren, A., 1991, Armutlu yarımadasının jeolojisi: MTA Rap., 9165, (unpublished), Ankara.
- Erentöz, C., 1953, Çatalca bölgesinde Jeoloji tetkikleri: MTA Yayl., B 17, 94s.
- Ertürk, O.; Dinçöz, E. and Alaygut, D., 1990, Petrology of the Cenozoic Volcanics in the Biga Peninsula, NW Turkey: International Earth Sciences Congress on Aegean Region Proceedings, II, 368-384.
- and Uygur, E., 1994, Petrographical, Sedimentological and diagenetic characteristics of the Ceylan tuffs and their reservoir potential, Thrace basin, Turkey: IAVCEI International Volcanology Congress, Abstracts, Ankara.
- Gök, L., 1990, Tekirdağ-Malkara (Tekirdağ ili) Keşan-Ipsala (Edirne ili) arasının jeolojisi: MTA Rap., 9710 (unpublished), Ankara.
- Irvine, T.N. and Baragar, W.R.A., 1971, A guide to the chemical classification of the common volcanic rocks: Can. Jour. Earth. Scien., 8, 523-548.
- Kopp, K.O., 1964, Geologie Thrakiens it: Die Insel und der chersones: N. Jb. Geol. Pae. Abh. 119, 172-214.
- , Pavoni, N. and Schindler, C., 1969, Das Ergene Becken: Beihefte Geol. Jahrbuch., 76, 136 s.
- Le Maitre, R.W.; Bateman, P.; Dudek, A.; Keller, J.; Lameyre, J.; Le Bas, M.J.; Sabine, P.A.; Schmid, R.; Serenson, H.; Streckeissen, A.; Wooley, A.R. and Zanettin, B., 1989, A classification of igneous rocks and glossary of terms: Blackwell Scientific Publications, 208 p, Oxford.
- Lebkücher, R.F., 1974, Orta Trakya Oligoseninin Jeolojisi hakkında: MTA Derg., 83, 1-29.
- Moore, W.J.; McKee, E.H. and Akıncı, Ö., 1980, Chemistry and chronology of plutonic rocks in the Pontide mountains, Northern Turkey: European Copper Deposits- Belgrade, 209-216.
- Ohta, E.; Doğan, R.; Batık, H. and Abe, M., 1988, Geology and mineralization of Dereköy porphyry Copper Deposit, Northern Thrace, Turkey: Bull. Geol. Surv. Japan, 39/2, 115-134.
- Okay, A.C., 1948, Şile, Mudarlı, Kartal ve Riva arasındaki bölgenin jeolojik etüdü: İst. Üniv. Fen Fak. Mecm., XIII/4, 311-335.

- Okut, M., 1975, Çanakkale ili, Gökçeada ilçesi Hammadde Prospeksiyon Raporu: MTA Kuzeybatı Anadolu Bölge Müdürlüğü Rap., 297 (unpublished).
- Önal, M., 1986, Gelibolu yarımadasındaki iki ana kayanın organik jeokimyası ve kil mineralleri ile incelenmesi: Türkiye Jeol. Kur. Bül., 29/1, 97-104.
- and Yılmaz, H., 1983, Gelibolu yarımadasında iki ana farklı yaşta fliş fasiyesindeki kil mineralleri ve gömülme derinliğine ait bazı ipuçları: Jeoloji Müh. Derg., 18, 23-30.
- Özkanlı, M. and Sonel, N., 1995, Trakya Havzası Geç Eosen yaşlı tuf seviyelerinin rezervuar potansiyeli: Trakya Havzası Jeolojisi Sempozyumu Bildiri Özetleri Kitabı, 49.
- Peccerillo, A. and Taylor, S.R., 1976, Geochemistry of Eocene calcalkaline volcanic rocks from Kastamonu area, Northern Turkey: Contrib. Mineral. Petrol., 58, 63-81.
- Polat, A.; Korrich, R.; Yılmaz, Y.; Yaltırak, C. and Tapırdamaz, C., 1997, Trace element Systematics of Cenozoic Calc-alkaline to Alkaline volcanism in NW Turkey; Implications for Magma sources in a Collisional Tectonic Setting: Tectonophysics (Inpress).
- Saner, S., 1985, Saros körfezi dolayının çökeltme istifleri ve tektonik yerleşimi, Ege denizi, Türkiye: Türkiye Jeol. Kur. Bül., 28, 1-10.
- Siyako, M.; Bürkan, K.A. and Okay, A.I., 1989, Biga ve Gelibolu yarımadalarının Tersiyer Jeolojisi ve hidrokarbon olanakları: TPJD Bül., 1/3, 183-199.
- Sümengen, M.; Terlemez, İ.; Şentürk, K. and Karaköse, C., 1987, Gelibolu yarımadası ve güneybatı Trakya Havzasının stratigrafisi, sedimentolojisi ve tektoniği: MTA Rap., 8128 (unpublished), Ankara.
- Şengör, A.M.C. and Yılmaz, Y., 1981, Tethyan evolution of Turkey: A plate tectonic approach; Tectonophysics, 75, 181-241.
- Tapırdamaz, C. and Yaltırak, C., 1997, Trakya'da Senozoyik Volkaniklerinin Paleomanyetik özellikleri ve Bölgenin tektonik evrimi: MTA Derg., 119, 27-42.
- Ternek, Z., 1949, Geological study of the region Keşan-Korudağ: Doktora tezi, İstanbul Üniv. Fen Fak. 78 s., (unpublished), İstanbul.
- Tokel, S. and Aykol, A., 1987, Kırklareli-Demirköy granitoidinin jeokimyası: Kuzey Tetis Ada yayı sisteminde Srednogorie-Istranca bölümünün evrimi: Türkiye Jeoloji Kurultayı, 1987 Bildiri Özetleri Kitabı, 17-18.
- Toker, V. and Erkan, E., 1983, Gelibolu yarımadası Eosen formasyonları nannoplankton biyostratigrafisi: MTA Derg., -101/102, 72-91.
- Umut, M., 1988, Kırklareli C-4 paftası izahnamesi: MTA Genel Müdürlüğü 1/100.000 ölçekli Açınama nitelikli Türkiye Jeoloji Haritaları Serisi, Ankara.
- ; İmlik, M.; Kurt, Z.; Özcan, İ.; Ateş, M.; Karabıykoğlu, M. and Saraç, G., 1984, Edirne ili-Kırklareli ili-Lüleburgaz (Kırklareli ili)-Uzunköprü (Edirne ili) civarının Jeolojisi: MTA Rap., 7604 (unpublished), Ankara.
- Uz, B.; Esenli, F.; Manav, H. and Aydos, Z., 1995, Karamürsel-Yalova arasındaki (Kuzeybatı Anadolu) piroklastik kayalarda oijen mineral oluşumları: Yerbilimleri (Geosound), 27, 135-147.
- ; ——— and ———, 1992, Yalova-Karamürsel arası bölgede Eosen yaşlı tüflerde Zeolitleşmenin etüt ve değerlendirilmesi: A.Ü. Isparta Müh. Haftası-VIII Bildiri Özetleri Kitabı, 11.
- Ünal, D., 1967, Trakya Jeolojisi ve Petrol imkanları: TPAO Arama Grubu Rap., 391 (unpublished).
- Yeniyoğlu, M. and Ercan, T., 1989/1990, İstanbul Kuzeyinin Jeolojisi ve Üst Kretase Volkanizmasının Petrokimyasal özellikleri ve Pontit'lerdeki Bölgesel yayılımı: İst. Üniv. Fak. Yerbilimleri Derg., 7/1-2, 125-147.
- Yılmaz, Y., 1989, An approach to the origin of young volcanic rocks of Western Turkey: In: A.M.C. Şengör (ed); Tectonic Evolution of the Tethyan region, Kluwer, The Hague, 159-189.
- , 1995, Ege Bölgesindeki Genç Magmatizmanın oluşumu ile Litosferin Evrimi arasındaki ilişki üzerine düşünceler: Jeofizik, 9, 107-110.

BENTHIC FORAMINIFERA (HOLOCENE) PALEOBIOFACIES OF BOSPHORUS (GOLDEN HORN - SARAYBURNU - ÜSKÜDAR): A NEW APPROACH TO MEDITERRANEAN-BLACK SEA WATERWAY

Mehmet SAKINÇ**

ABSTRACT.- Young sediments in the shelf areas in the sea of Marmara have some faunal signs of Mediterranean transgression, Flandrian, developed following the Würm period. The evolution of locally tectonic-controlled foraminifera paleobiofacies formed as a result of this transgression 7.5-3.5 thousand years before present in the triple junction between entrance of Bosphorus in Northern Marmara Shelf-Mouth of Golden Horn-Üsküdar indicates that Mediterranean-Black Sea connection in late Quaternary was accomplished over Bosphorus as a result of tectonic-transgression association.

NEOGENE-QUATERNARY EVOLUTION OF THE EASTERN MARMARA REGION, NORTHWEST TURKEY

Ömer EMRE*, Tevfik ERKAL*, Andrey TCHEPALYGA**, Nizamettin KAZANCI***, Mustafa KEÇER* and Engin ÜNAY*

ABSTRACT.- Three main stages have been distinguished in the Neogene-Quaternary morphotectonic evolution in the East Marmara region. They are Early-middle Miocene, Late Miocene-Pliocene and Latest Pliocene-Present. Three different sedimentary sequences, each overlies the other with an angular unconformity, have been formed in these stages. Early-middle Miocene sedimentary sequence is characterised by continental detritics whereas the Late Miocene-Pliocene rocks are represented by continental to marine transitional sediments. Terrestrial-marine sediments have been deposited since the latest Pliocene till Present. The region was transformed to denudational area by the closure of the Intra-Pontid Ocean in the end of the Oligocene and it was under the effect of paleotectonic events during the early-middle Miocene. In the end of this erosional period which lasted until the end of middle Miocene, a peneplain morphology covering large area was formed and terrestrial sediments were deposited. Neotectonics which has affected actual geology in the region, initiated in the beginning of late Miocene and occurred in two stages which differ tectonic styles. In the late Miocene-Pliocene time, the region was affected by N-S directed compressional regime and it was uplifted by NE-SW and NW-SE trending strike-slip faults with E-W lying folds as a result of this compression. During this stage, a Late Miocene-Pliocene sedimentary sequence which starts with fluvial sediments at the bottom and passes into lacustrine to marine at the top, was deposited. In the end of the period, depressions in which late Miocene-Pliocene sediments were deposited, were spread out and the region was formed as a denudational area in the late Pliocene. The second stage of the neotectonic period covers a time interval from the Latest Pliocene to Present and it begun with the occurrence of the North Anatolian Fault. Actual morphology and active tectonic frame of the Eastern Marmara region were developed in this time interval which is known with the transform character of the North Anatolian Fault. However, structural evolution of actual Marmara sea region which is related to North Anatolian Fault, initiated in Latest Pliocene.

INTRODUCTION

Many investigations related to structural and paleogeographic evolution of the sea of Marmara and its surrounding region in Neogene and Quaternary times were done (e.g. Şengör, 1979, 1980, 1982; Şengör et al., 1985; Crampin and Evans, 1986; Barka and Kadinsky-Cade, 1988; Wong et al., 1990, 1995; Görür et al., 1995, 1997; Erol and Çetin, 1995). In these studies it was thought that regional paleogeographic changes were linked and identified with the structural evolution of the North Anatolian Fault (NAF) supposed that there has been since Late Miocene (Görür et al., 1995, 1997). It was pointed out that, as proposed by Şengör et al. (1985), the geography of sea of Marmara and the surrounding region has been formed with the emergence of the NAF in Late Miocene, the whole region being under the effect of a N-S oriented extensional regime in between Western Anatolia and the NAF, and the NAF itself undergoing a structural evolution process based on its displacement and younging southward. In many research, it was agreed that, in the region the

rocks of Neogene - Quaternary age including marine units were deposited in the basins developed accordingly this model of evolution (Şengör et al., 1985; Siyako et al., 1989; Erol and Çetin, 1995; Görür et al., 1995, 1997).

In this paper, the widely exposed Neogene-Quaternary sediments in the Eastern Marmara region are discussed (Fig.1). For this purpose, sedimentary basins considering the rocks and their stratigraphic positions, their actual morphology and the their deformations in neotectonic period were studied to provide a new perspective on the paleogeographic evolution of the region in Neogene - Quaternary based on the interrelation between tectonics, morphology and sedimentation.

STRATIGRAPHY

The pre-Neogene basement of the region consists of rock assemblages of Istanbul and Sakarya zones developed in the paleotectonic period (Şengör and

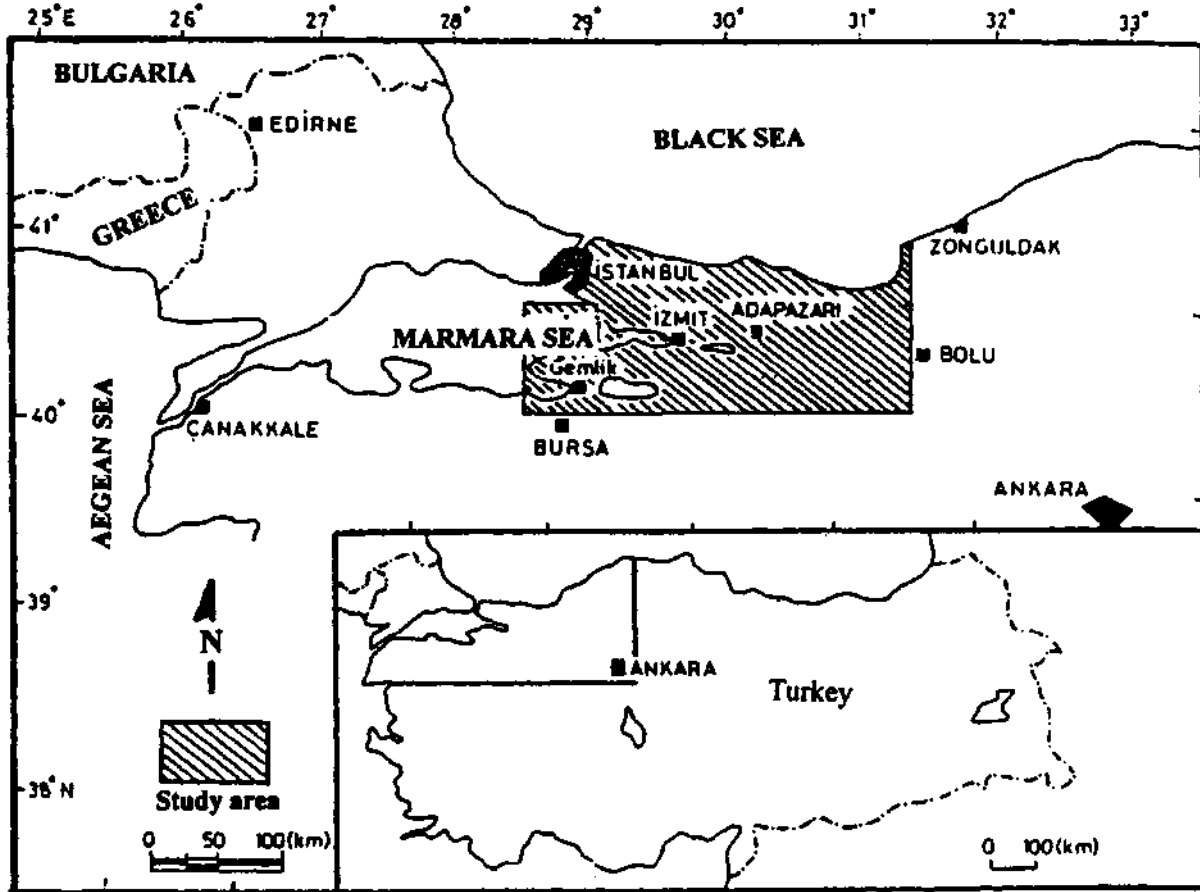


Fig. 1- Location Map of the studied area.

Yılmaz, 1981; Okay, 1989; Okay and Görür, 1995; Yılmaz et al., 1995) (Fig.2). These two zones juxtapose along the suture which formed as a result of the closure of the Intra-Pontide Ocean in Early Eocene-Oligocene where the NAF is present now (Şengör and Yılmaz, 1981; Okay, 1989; Okay and Görür, 1995). Of these, the Istanbul zone comprises the sedimentary rocks of Ordovician-Lower Tertiary age and whereas the Sakarya zone is made up of a metamorphic basement and a sedimentary cover of Jurassic - Cretaceous age (Okay, 1989; Okay and Görür, 1995; Yılmaz et al., 1995).

The Neogene-Quaternary aged rock assemblages in the region make up three different sedimentary sequence developed in different time and facies (Figs. 3 and 4). They can clearly be distinguished by angular unconformities. Of these, the oldest ones, Early - Midd-

le Miocene aged rocks are seen in Kocaeli peninsula, the Late Miocene- Pliocene aged ones are observed in Armutlu peninsula and in Bilecik-Bursa regions, and the Latest Pliocene-Recent aged ones are seen in the basins/corridors situated along the NAF zone (Figs. 3 and 5). The recent distribution of the sediments are conformable with the age and character of the neotectonic structures in the region, and with the morphotectonic structure they formed. The above mentioned conformity is the main support of the evolution proposed in this paper. Therefore, the stratigraphy of the region is given in sub-regions each corresponding to a different morphotectonic unit. In the wide study area, the related geological units are simplified and the names of the small settlements have not been indicated (Figs. 1-6). To provide easy comprehension the stratigraphy of each region are separately emphasized. Since the

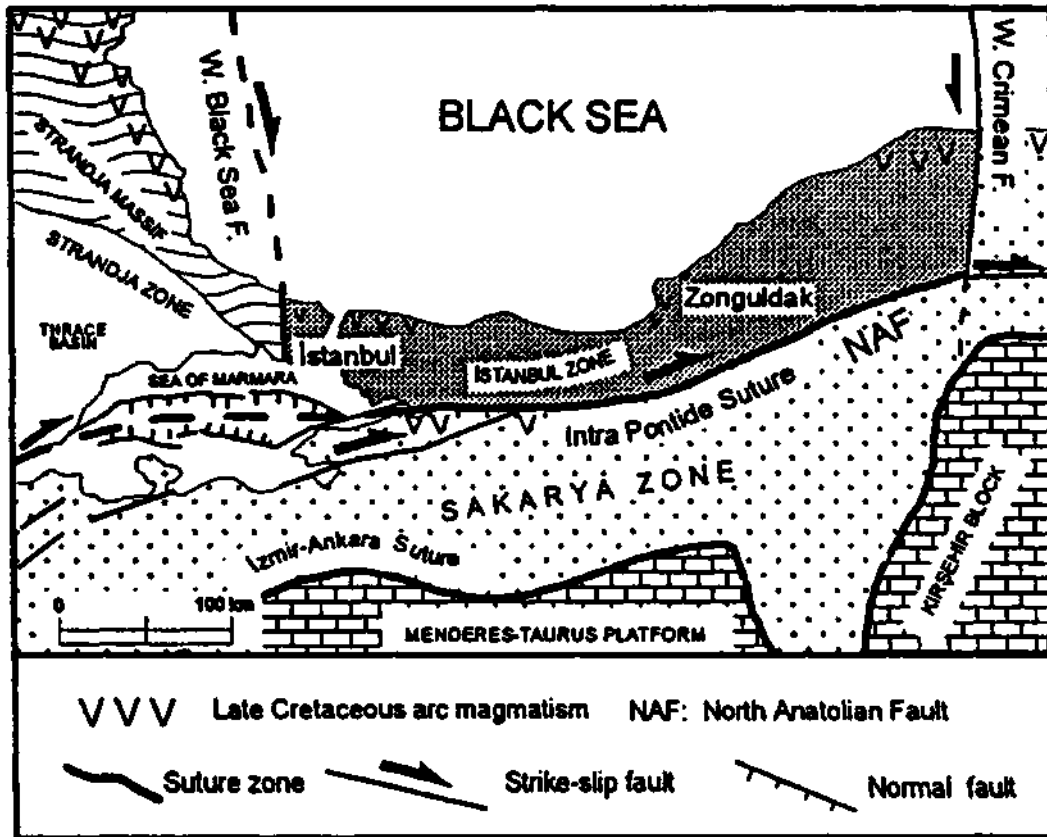


Fig. 2- Tectonic setting of the studied area (from Görür et al., 1997).

stratigraphic details are stated good enough to explain the morphotectonic evolution no stratigraphic descriptions are given.

BLACK SEA REGION

The region bounded by the NAF, sea of Marmara and the Black sea is defined under this heading. In this region the distribution of the Neogene-Quaternary sediments are limited and comprises of two rock assemblages (Figs. 3 and 4).

EARLY MIDDLE MIOCENE

Karasu formation

Crops out along the Black sea coast in Karasu-Kefken and in the Istanbul section of the Kocaeli peninsu-

la (Fig.3). It was defined in 1: 500 000 scale geological map of Turkey (MTA, 1964) as of Plio-Quaternary age, in Aydın et al. (1987) as Örencik formation of Pliocene age and both in Baykal and Önalán (1979) and Seymen (1995) as Belgrat ormanı formation of Plio-Quaternary age. The red, yellow and brown colored formation is made up of sandstone, pebbles, siltstone and mudstone. Typical locality is Karasu region (Fig.3) where the thickness of the unit is 30-40 m cropping with angular unconformity on the pre-Neogene basement (Fig.4). At the lowermost levels, on the basement rocks, a red and brown colored paleosol layer up to 10m thick is observed overlain by an alternation of sandstone, pebbles, siltstone and mudstone. Sandstones mostly include quartz grains. Pebbles have undergone severe weathering. In these detritic levels weathering crust up to 1 m thick can be observed.

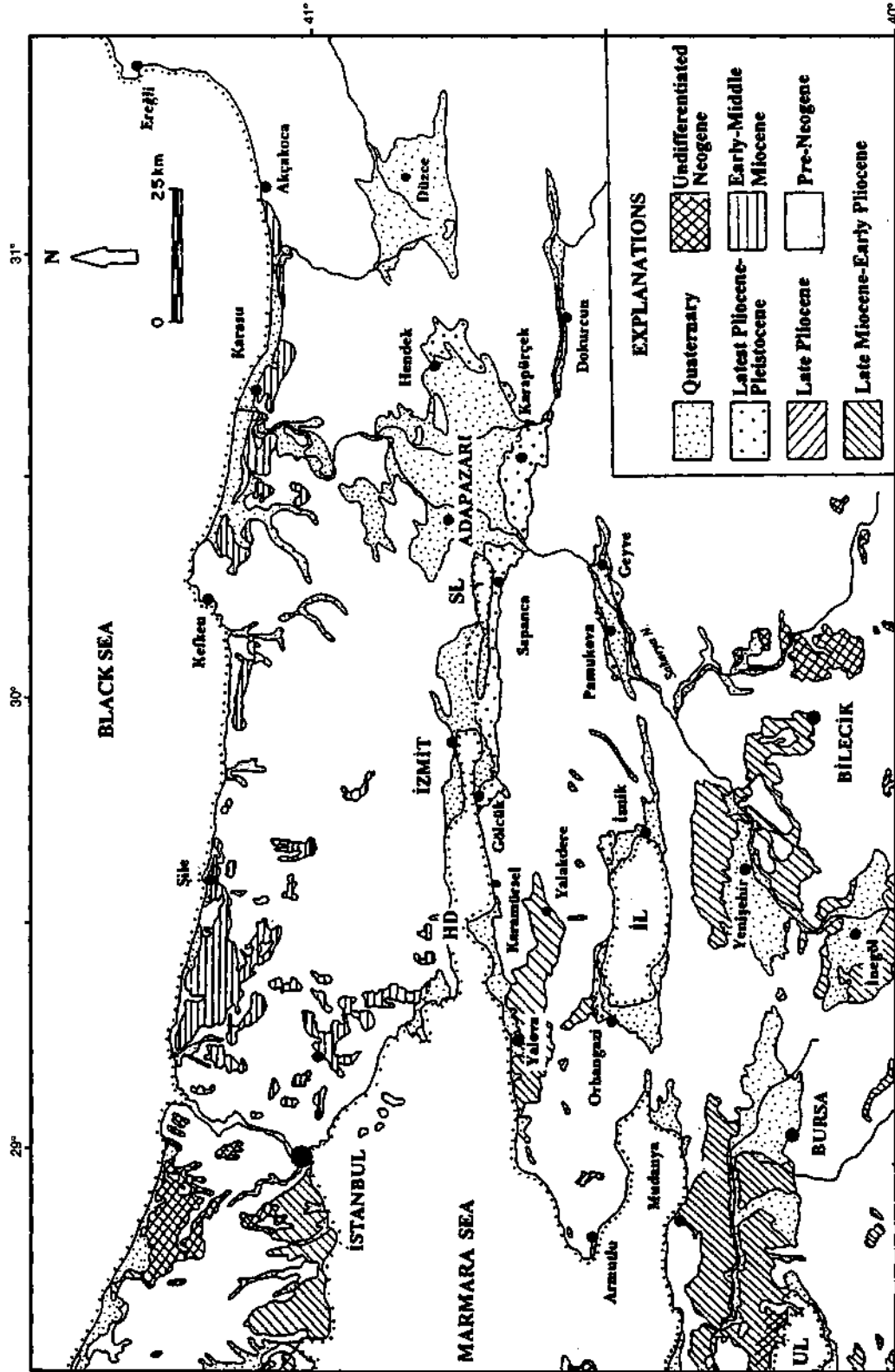


Fig. 3- Map showing the distribution of Neogene and Quaternary sediments in the eastern Marmara region. HD: Hersek Delta, SL: Sapanca Lake, IL: Iznik Lake, UL: Ulubat Lake (modified from MTA, 1964).

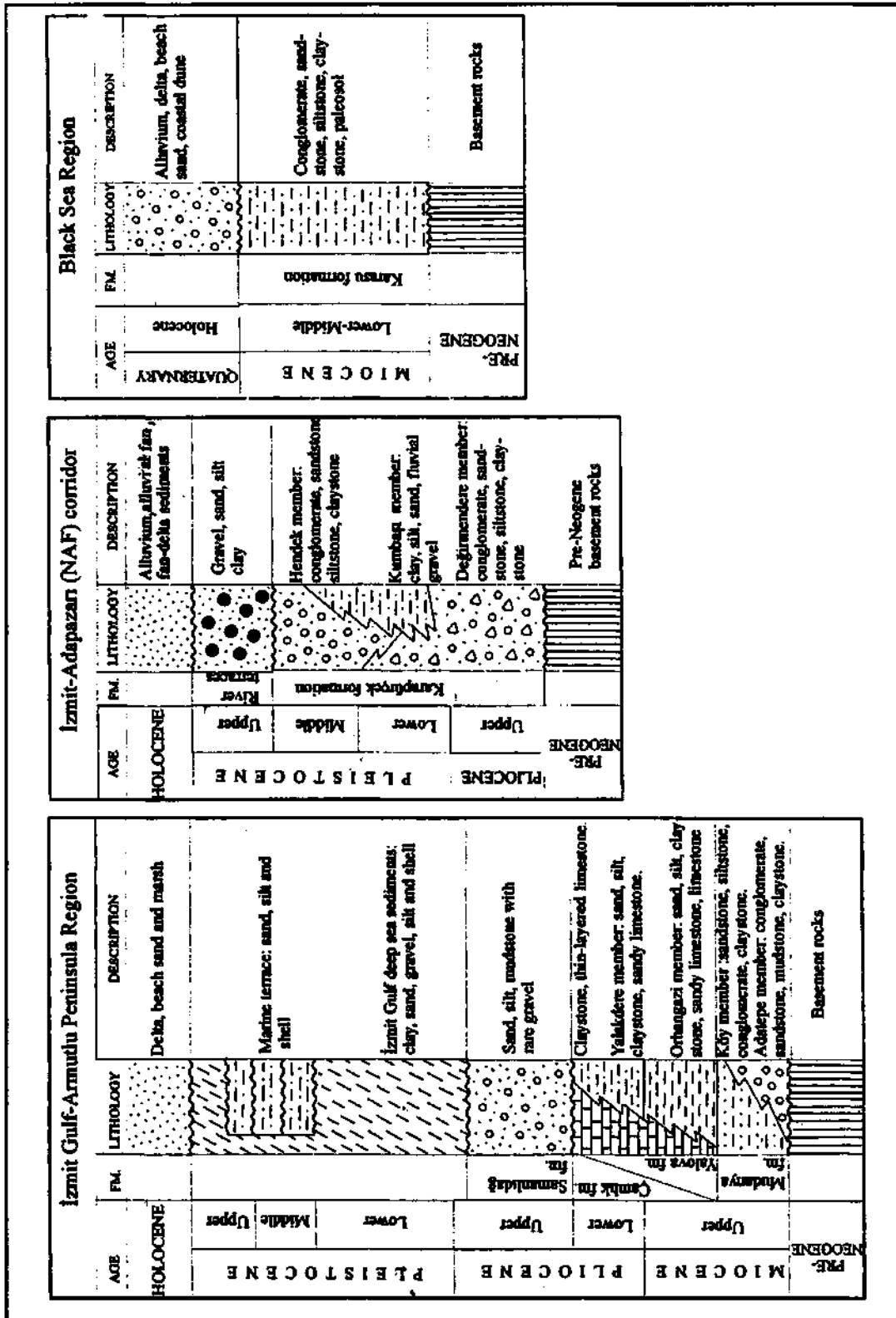


Fig. 4- Columnar stratigraphic sections of the studied area (not in scale).

No dating information was provided for this formation. It is overlain by Holocene shore sediments in Karasu area. The thick paleosol at the base, the severe weathering in pebbles and the weathering crust included indicate the unit is deposited in humid and warm climatic conditions (Wright, 1992a, 1992b; Mack et al., 1993). In Mudanya formation of Upper Miocene age in Armutlu peninsula weathered pebbles of this formation can be seen. Erol (1981) states that the regional geomorphological data indicates that the formation was deposited as terrestrial sediments of a peneplanation process took place under humid and warm climatic conditions in Early - Middle Miocene. The age of the formation, therefore, is assumed to be of Early - Middle Miocene age.

HOLOCENE

Quaternary in Black sea region is made up of Holocene aged deposits. The Holocene sediments on land comprise alluviums. On the Black sea coast, on the other hand, delta of Sakarya river, actual beach, old and new coastal dunes and back- swamp deposits were formed (Fig.4).

ARMUTLU PENINSULA - İZMİT BAY

The Neogene-Quaternary sediments in the region crops out in Mudanya-Nilüfer creek valley, in Armutlu peninsula and in the surroundings of İzmit Bay (Fig.3). The sediments here with respect to the ones in the other regions include much more time intervals stratigraphically (Fig.4). The distribution of the sediments, when examined in morphological point of view, are as follows: The Neogene aged ones are situated at the morphologic heights whereas those of Quaternary aged are observed along the depressions along the NAF zone. Except for the ones surrounding İzmit Bay, there are no data on the distribution and on the character of those take place in the eastern part of the sea of Marmara.

LATE MIOCENE

Mudanya formation

This formation cropping out in vicinity of Yalova-Yalakdere and Mudanya-Nilüfer Creek, forms the base of

the Neogene sediments in Armutlu peninsula (Fig.4). The lithology of the unit is an alternation of conglomerate, sandstone, siltstone, mudstone and claystone and it is deposited in an environment of fluvial and fan-delta. The formation was named by Görmüş et al. (1997) and were divided into two members: Adatepe and Köy. In Yalova region, this unit is same as Yalakdere formation defined by Bargu and Sakınç (1989). It rests on pre-Neogene rocks with angular unconformity and its thickness varies between 100-300 m. It is transitive at the top with Yalova formation, a brackish water-marine unit.

Adatepe member. - It crops out widely in the vicinity of Mudanya-Nilüfer creek. Its relation with the basement rocks are clearly visible on the roadcuts of Yalova-Bursa road. It is red, green and brown colored and made up of conglomerate, sandstone, mudstone with pebbles and claystone (Fig.4). At the base of the unit, on the basement rocks, a pedogenic zone rich in caliche is observed. Caliche forms interbeds and concretions inside the unit which is a characteristic feature of the formation. At the base of the formation debris flow sediments, and at the top fluvial and alluvium fan deposits are seen (Şahbaz et al., 1997). The thickness of the unit is approximately 100 m. It is laterally gradational with the Köy member which is paleontologically determined to be of Late Miocene (Sichenberg et al., 1997), therefore assumed to be of the same age (Görmüş et al., 1997).

Köy member. - This member, cropping out to the south of Yalova, Karamürsel and Bursa-Mudanya regions is made up of gray, yellow, beige colored sandstone, siltstone, conglomerate and grayish green claystone (Fig.4). It was deposited in fan delta environment and is vertically and horizontally gradational with Adatepe member at the lower contact. To the southwest of Mudanya, it is observed to have gradational transition with Çamlık formation at the upper contact (Şahbaz et al., 1997; Görmüş et al., 1997). At a roadcut outcrop at 10th km of Mudanya-Bursa road, marine siltstone and carbonates of Yalova formation observed to conformably overlie the unit. It bears the pebbles of Karasu formation in vicinity of Yalova. Near Yörükali village, Mudanya, *Amebeledon* sp. ("frincki" typ), a mammal fossil of Upper Miocene age was found in this unit (Sic-

enberg et al., 1975). These data indicate that Köy member and Mudanya formation were deposited in Late Miocene.

LATEST MIOCENE-EARLY PLIOCENE

Yalova formation

The Neogene sediments widespread in Eastern Marmara and deposited in brackish water - fresh water, brackish water and open sea fades in different localities are called Yalova formation in this paper. The different levels of the formation were called Kılınç and Yalakdere formations in previous papers (Bargu and Sakiñ, 1989). However, the Yalakdere formation made up of fluvial and fan delta sediments described by Bargu and Sakiñ (1989) is as equivalent of the Mudanya formation in vicinity of Yalova. The formation forming a transgressive sedimentary sequence is transitive with the Mudanya formation at the bottom (Görmüş et al., 1997). The formation in the research area is made up of siltstone, claystone, carbonate sandstone, marl and limestone (Fig.4). In the areas where the Mudanya formation can not be observed at its bottom, it overlaps the pre-Neogene rock assemblages. In Yalova-Karamürsel region it is overlain with angular unconformity by Altınova and Kaytazdere marine terrace sediments of Pleistocene age (Bargu and Sakiñ, 1989). Its thickness reaches up to 400 m and has two members, Orhangazi and Yalakdere.

Orhangazi member. - It crops out in Orhangazi region to the northwest of lake İznik. It is made up of silt, sand, sandy limestone and limestone. It is thin to medium bedded and dirty white, white, gray and yellowish in color. It rests on pre- Neogene basement rocks with angular unconformity in Orhangazi region. On the other hand, at a roadcut outcrop at 10th km on Mudanya-Bursa road it conformably overlies the deltaic deposits of Mudanya formation. On the section here, the unit with a 10 m thickness passes upwards into the clays bearing coal seams and deposited in lagoon environment. These clay levels bearing coal seams were observed on the roadcuts along Orhangazi-Yalova road. However, here, the lower levels of the clays bearing gastropoda shells and alternating with limestones cannot be observed.

This member is the first marine unit deposited in eastern Marmara in Neogene. Its typical section is seen at Orhangazi-Yeniköy roadcut. It bears mollusk shells characterizing brackish water environment. *Pseudocatillus pseudocatillus* Sinzov, *Pseudocatillus* sp., *Dreissena* cf. *tenussima* Sinzov, *Dreissina* sp. were found in the samples taken from this fauna. This assemblage is similar with the Pontian fauna of Paratethys. The same fauna was met in Serres and Chalkidiki basins in North Aegean (Jacobshagen, 1986). The Latest Miocene-Early Pliocene fauna in the North Aegean is of Mediterranean origin and takes place in a transgressive sedimentary assemblage (Jacobshagen, 1986). This similarity results in deducing that the first marine water entrance may be from Mediterranean Sea.

Yalakdere member. - Crops out in vicinity of Yalakdere (Fig.3). Its typical locality is the roadcut at the 2nd km of the Yalakdere-İznik road. This member, named by Bargu and Sakiñ (1989) corresponds to the Karasu limy sandstone member of Yalakdere formation. On the other hand, the Yalakdere formation defined by these authors corresponds to Mudanya formation. It is yellow, beige, white and gray in color. It is made up of sand, claystone alternated with silt, limestone and carbonate sandstone. The bottom of the unit was not observed. However, in Yalakdere region, because of the colluvium cover the contact can not be clearly traced and in a short distance fan delta sediments of the Mudanya formation starts. This member where the E-W folds have developed is overlain with angular unconformity by marine terrace deposits of Pleistocene age in Karamürsel region (Bargu and Sakiñ, 1989).

Some levels of the Yalakdere member includes abundant large shells. *Pontalmyra* sp., *Dreissena* ex. gr. *rostriformis* Deshayes, *Dreissena* sp. which indicate brackish water environment are found in between them. This mollusk fauna shows similarity with Cymmerian in Paratethys. This stage covering 5.3-3.5 million years corresponds Early Pliocene in Mediterranean chronology.

Çamlık formation

Widely crops out on Bursa-Karacabey road and in Nilüfer creek valley. The dominant rock type is white,

beige colored, thin to medium bedded limestone and gray-green colored claystone alternating with it. In limestones there are two facies determined: at the bottom dolomitic and developed in deep brackish water environment, and at the top shallow and reflecting fresh water environment (Varol et al., 1997). It is gradually transitive with Mudanya formation at the bottom (Görmüş et al., 1997). In some places it onlaps the basement rocks. In Armutlu Peninsula, on the roadcuts of Yalova-Orhangazi road the unit alternates with gastropoda bearing claystone and limestone.

No paleontologic dating was obtained from the unit. However, its lower levels reflecting deep brackish environment is transitive with Late Miocene aged Mudanya formation (Görmüş et al., 1997). Considering the contact relations, Çamlık member assumed to be of Late Miocene-Early Pliocene age.

Samanlıdağ formation

This formation comprises the old alluviums (Fig.3) situated on top of Samanlıdağları (Armutlu Peninsula) mass (Fig.6) which is bounded in the north and south by the NAF. The lithology of the brown, yellowish and reddish unit is mudstone with scarce pebbles, silt and sand (Fig.4). In places it includes debris and its thickness is 30-40 m. It is typically observed in Adliye, west of Pamukova and in Sultaniye, west of Armutlu Peninsula, on the old valley floors. It rests on pre-Neogene rock assemblages with angular unconformity and no unit overlying the formation has been observed.

No dating information is available for the unit. The old valley forms in which the unit was deposited in Yalakdere region were observed to have formed on the Yalova formation of Late Miocene-Early Pliocene age. In the İzmit-Adapazarı corridor, the oldest rock assemblage deposited along the NAF zone cutting the drainage pattern in which these deposits were developed is Karapürçek formation of Latest Pliocene-Pleistocene age. Therefore, it is assumed that the formation is of Late Pliocene.

Marine terraces

In the area surrounding İzmit bay marine terraces of Pleistocene age crops out (Chaput, 1936; Erinç,

1956; Göney, 1964; Akartuna, 1968; Bargu and Sakiç, 1989; Sakiç and Bargu, 1989; Paluska et al., 1989). These sediments which are widespread between Karamürsel-Yalova, to the south of the bay, are found at three different morphometric levels. The sequence is called as Altınova formation in vicinity of Karamürsel (Bargu and Sakiç, 1989). Their being at different morphologic levels and being tilted, at some places have led the interpretation that they took that step-like position because of tectonic movements (Erinç, 1956; Sakiç and Bargu, 1989).

Faunal content and radiometric datings indicate that these three terrace fillings have deposited during different sea levels. The oldest terrace deposits are seen in southwest of Karamürsel, 60-90 m above the present sea level (Paluska et al., 1989). They rest on the Mudanya formation of Late Miocene age with angular unconformity. The fauna of this deposit developed in lagoon environment includes *Mytilus galloprovincialis* Lamark, *Ostrea lamellosa* Brocchi, *Chlamys opercularis* Linne, *Venerupis calverti* Newton, *Cerastoderma edule* Linne, *Loripes lacteus* Linne and *Cerithium* spp. the dating result, 260 000 years B.P., obtained with Tl method corresponds to Early Tyrrhenian (Paluska et al., 1989).

The other two terrace deposits crop out along Bursa - İzmit road, in the immediate east of Karamürsel (Sakiç and Bargu, 1989). Here, the terrace surface situated morphologically, upper is 20-25 m higher above the sea level and rests on the Eocene rocks with angular unconformity. Its bottom is 10 m high above the sea level. It includes sand bearing shell fragments and Mediterranean fauna, silt and pebbles and also includes ostrea banks (Sakiç and Bargu, 1989). The U/Th dating by Paluska et al. (1989) has yielded 130.000 years from the samples collected from these banks.

The morphologic surface of the lowermost terrace is 10-15 m high above the sea level. The bottom of this terrace was not observed. Its typical outcrops are seen in Kaytazdere region. This terrace bears richer mollusk fauna than the upper one.

Bottom sediments in İzmit bay

The deep drillings have shown the existence of a thick sediment sequence in the bay (Meriç, 1995). The

deepest of these drillings was made in Hersek delta, south of the bay and samples were taken from 118m. Yet, the bottom of the sequence was not reached but levels bearing clay, sand, pebbles, silt and shell fragments were cut. This sequence was investigated in many different ways (Meriç, 1995; Meriç et al., 1995; Çetin et al., 1995; Ediger and Ergin, 1995; Gülen et al., 1995; Toker and Şengüler, 1995; Taner, 1995). The source area of the sediments is of terrestrial origin. The most apparent of these is Hersek delta.

İzmit bay is a tectonic corridor developed upon the formation of the NAF (Emre et al., 1997d). Therefore, the sediments situated at its base have the same age with the NAF. During the Hersek drilling it was observed that the sedimentation was continuous under different conditions since Latest Pliocene (Meriç, 1995). At the bottom of the sequence *Discoater brouweri* zone was determined which indicates the most Latest Pliocene (Toker and Şengüler, 1995). Meriç et al., (1995) state that the sediment assemblage was deposited at four different environments in four different stages. Accordingly, during Latest Pliocene anoxic marine, in Lower-Middle Pleistocene deep and brackish water, in the beginning of Upper Pleistocene brackish water, delta and terrestrial, and in the end of Upper Pleistocene - Holocene marine conditions were dominant (Meriç, 1995).

The Latest Pliocene- Middle Pleistocene section of the sediments are the marine equivalent of the Karapürçek formation situated to the eastern part of the NAF corridor (Fig.4). The marine terraces around the bay corresponds to the Middle Pleistocene section of the sequence.

Holocene

Holocene sediments are observed in the beach, swamp and delta areas around the bay. The deltas having sources from the south have greater fans. Hersek delta is the largest sedimentary body developed in the bay (Fig.3). There are lagoons on the delta. To the west of the bay swamps are widespreadly situated.

İZMİT - ADAPAZARI (NAF) CORRIDOR

This region includes the NAF segment in between the İzmit bay and Karapürçek. The Neogene-Quater-

nary sediments here are divided into three stratigraphic units (Figs. 3 and 4).

Karapürçek formation

In Sapanca-Karapürçek-Hendek area, this formation bounds the Adapazarı plain in the south, and also observed in between Sapanca-İzmit bay (Fig.3). It comprises alluvial fan and fluvial fillings. Its bottom is not observed but in NAF zone, it rests on the pre-Neogene rocks with angular unconformity. Its apparent thickness is 150 m and is unconformably overlain by Late Pleistocene aged terraces and Holocene fillings of the Sakarya river. It is divided into three members having vertical and horizontal transitions (Fig.4).

Değirmendere member. - Forms the base of the formation. It crops out in between Sapanca and Karapürçek, south of Adapazarı plain, and in the south of G61-ciik. It comprises alluvial fan deposits. Rock types are poorly sorted gray, beige yellowish pebblestone, gray, blackish, yellow and brown colored sandstone, siltstone and dark gray, black, green and bluish claystone (Fig.4).

These are transitive with each other. Pebblestones and sandstones have well exposed outcrops in Akçay creek valley. Here the sandstones and pebblestones include levels cemented with carbonates. Siltstones and claystones taking place in the distal sections of the fans are typically observed in Değirmendere valley. There are levels among them bearing gastropoda fragments and vertebrate fossils. Its bottom can not be observed. This member is the oldest unit deposited in NAF morphology. The alluvial fans forming the depositional environment for the unit have their source areas in the heights situated to the south of the NAF. However, the layers have tilted up to 25° towards south and southwest because of the normal faults of the Adapazarı pull-apart basin. It is transitive with the Kumbaşı member of the formation and is unconformably overlain by the Hendek member at the top.

In the member, in Şükriye and Değirmendere locations small mammal fauna is found. In Değirmendere large mammal fauna are found, too. The small mammals are *Microtus* sp. and *Kalymnomys* sp. which indi-

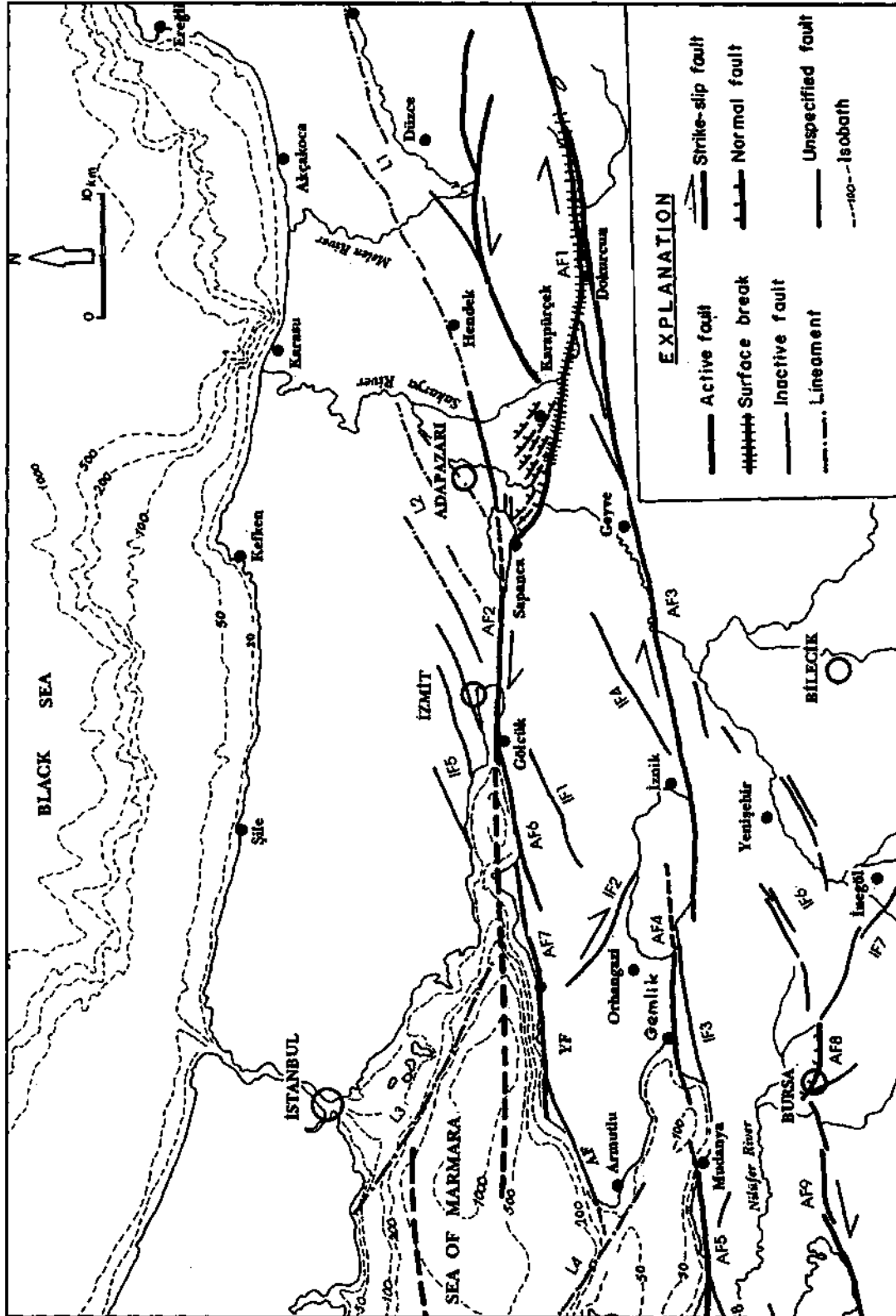


Fig. 5- Neotectonic period faults in the eastern Marmara region. Key: 1. Active faults: NAF Zone. AF 1, Dokurcun segment, AF 2, Izmit-Adapazarı segment, AF 3, Izmit-Geyve segment, AF 4, Gemlik segment, AF 5, Zeytinbağı segment, AF 6, Gölcük fault (probably active), AF 7, Yalova fault (probably active), AF 8, Bursa fault, AF 9, Ulubat fault, AF 10, Düzce fault; 2. Inactive faults: IF 1, Yalakdere fault, IF 2, Orhangazi fault, IF 3, Gençali fault, IF 4, Adliye fault, IF 5, Izmit fault zone, IF 6, Yenişehir fault zone, IF 7, İneğöl fault, IF 8, Karacabey fault; 3. Lineaments: L 1, Hendek-Yığılca lineament, L 2, Izmit-Karasu lineament L 4, İmralı lineament.

cates Late Villanian and Early Biharian. Therefore, the age of the Değirmendere member is Latest Pliocene-Early Pleistocene. This member may be assumed to be the terrestrial equivalent of the Latest Pliocene-Early Pleistocene aged unit which is found at the base of the drilling in İzmit bay (Toker and Şengüler, 1995) and of the sediments dated $817\ 000 \pm 105\ 000$ years by Çetin et al. (1995).

Kumbaşı member. - The river bed and flood plain deposits seen along the Sakarya river to the south of Adapazarı plain are called as Kumbaşı member. Its typical section can be seen in the quarry next to Kumbaşı village. It is made up of gray, beige colored pebblestone, dark gray, black and greenish claystone alternation. The thickness of the pebbles dominant at the top reaches up to 30 m. The thickness of the beds are between 0.5-4 m. Erosional based and lenticular pebblestones are of river bed, silt and clays are of flood plain origin.

The thickness of this member reaches up to 60 m. Its base can not be observed. It is transitive with the Değirmendere formation which is evaluated as the old sediments of the Sakarya river and also overlain by Hendek member. *Kalymnomys* sp. was found in the typical locality of the member and it is assumed that the age of the Kumbaşı member is Early Pleistocene.

Hendek member. - It crops out between Sapanca-Karapürçek-Hendek region and İzmit bay-lake Sapanca. It has 80 m thickness in Balıklıdere valley where it is well observed. It is made up of alluvial fan deposits. It has a very distinctive color: red, brown and yellowish. Its lithology is poorly sorted, loose pebblestone, sandstone, mudstone and siltstone. This member is less affected by the tectonics created by the Adapazarı pull-apart basin than the other units in the south. It rests on Değirmendere and Kumbaşı members with erosive contact and is overlain by river terraces of Late Pleistocene and Holocene with angular unconformity. According to these contact relations, the unit is assumed to be of Middle Pleistocene age.

Terraces of Sakarya river

The river terraces cropping out to the west of Sakarya river, south of Adapazarı (Bilgin, 1984) forms two

morphometric levels. The upper levels of the terraces are made up of brown, yellowish colored flood deposits whereas the lower levels comprise sand and well rounded pebbles. These terrace fillings are not observed along the Sakarya river in the north of the line between Adapazarı and Hendek. They overlie the Karapürçek formation with angular unconformity and are overlain by Holocene aged flood plain deposits. According to these relations the terrace fillings are of Late Pleistocene age.

HOLOCENE

The actual river bed fillings of the Sakarya river comprise flood plain deposits and alluvium fans. The bottom sediments of the lake Sapanca are included in this category (Figs. 3 and 4). On the southern shores of the lake Sapanca fan delta forms are observed. The thickness of the Holocene at the base of the Adapazarı plain exceeds 100 m.

MORPHOLOGY

The study area is one of the rare places in Anatolia where paleotectonic and neotectonic morphology can be observed. Paleotectonic relief group, where the primary morphology is preserved, forms the lowest topography except for the tectonic depression areas. The morphology of this period, in the north of the sea of Marmara and along the shores of Black sea, corresponds to the underwater shelf areas (Fig.6). The relief of the neotectonic period, on the other hand, are as high mountain belts, depressions along the fault zones, tectonic depression basins in between the faults and as hollows (Figs. 5 and 6).

Neotectonic landscape reflects two different stages of tectonics (Fig.7). The morphotectonic prolongations not affected or dissected by the NAF are aligned in NE-SW or in NW-SE directions. The landscape groups developed in NAF zone, on the other hand, cut them in E-W direction and form morphologic discordance which are reflected in distribution of Upper Miocene-Quaternary deposits. The Upper Miocene-Pliocene deposits, except for along the NAF zone, can also be observed on high morphologies. On the contrary, Quaternary sediments are bounded with the basin-corridor shaped

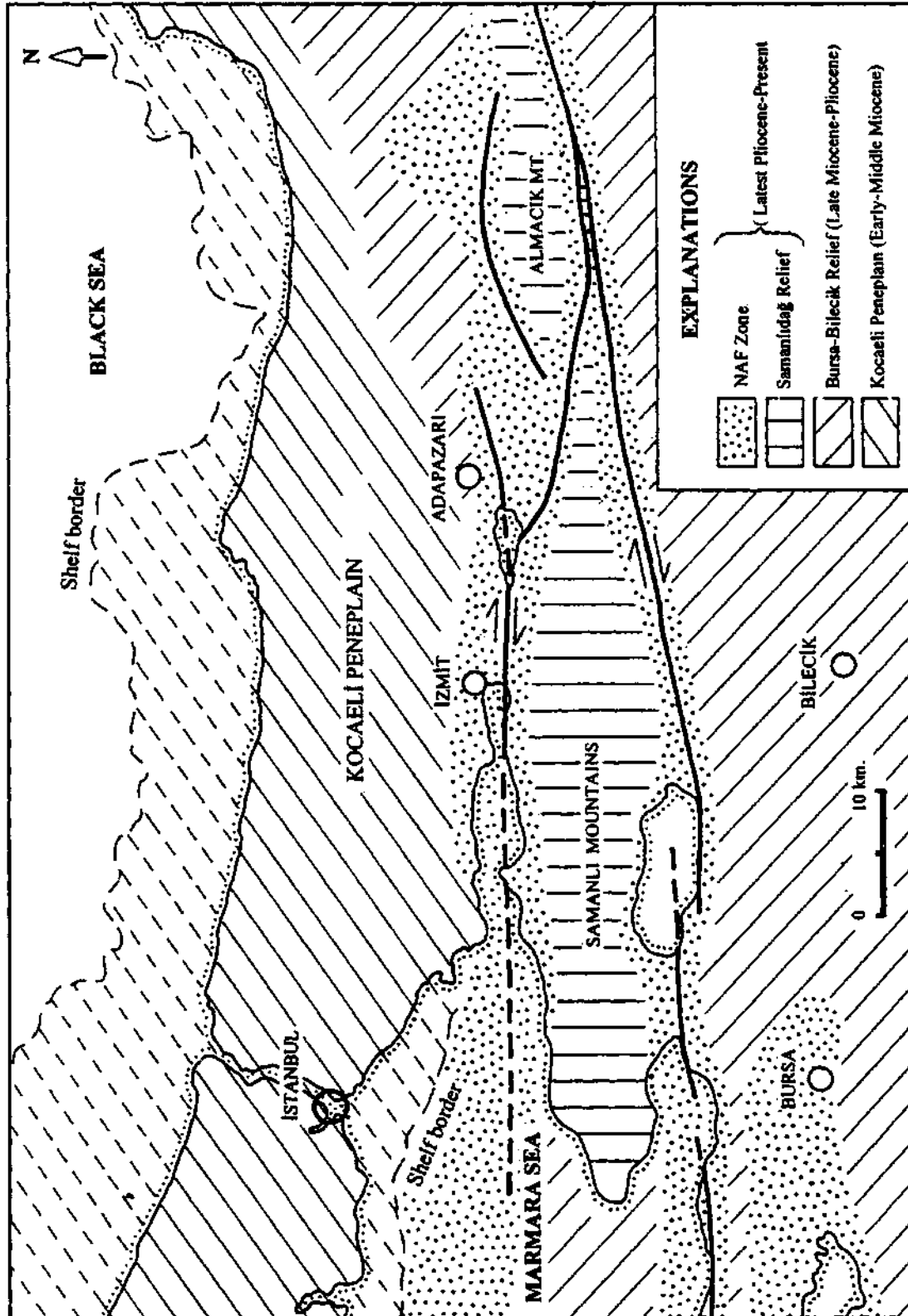


Fig. 6- Morphotectonic units of the eastern Marmara region.

depressions and with the base of the depressions eroded and emptied (Figs. 3 and 5).

MORPHOTECTONIC UNITS

Four different morphotectonic belts having different relief characteristics were observed in the investigation area (Fig.6). These, from north to south, are Kocaeli peneplain, Samanlıdağ and Bursa-Bilecik reliefs and NAF zone (Fig.6). The three relief groups displaying uplift morphology have been separated from each other with a sharp morphologic discordance, E-W trending depressions and hollows developed on the northern and southern branches of the NAF. Kocaeli peneplain reflects the morphology of paleotectonic era while the others have developed in neotectonic era (Fig.7).

Kocaeli peneplain

This is the relief group of the Kocaeli peninsula situated in the west of Sakarya valley. There is a peneplain surface on the peninsula with an average elevation of 150-200 m (Fig.6). Monadnocks are typical landforms on this north inclined surface. The inclination between İzmit and Karasu is higher because of tilting. Sea bottom topography makes one think that Black sea shelf is the prolongation of the peneplain under the water. Northern shelf of the sea of Marmara on which the Prince Islands are situated reflect the same characteristic features with the peneplain (Fig.6). The present watershed-line is very close to the sea of Marmara and NAF zone. In the watershed, along north oriented old drainage forms, hanging valleys and captured streams can be observed.

On the peneplain, Karasu formation is situated (Figs. 3 and 6) which is deposited during the process of peneplanation. The paleosol at the base and the weathering zones included are the indicators for humid and warm climatic conditions of the time of peneplanation. This climatic condition is known to prevail during Lower-Middle Miocene in Anatolia (Erol, 1981). On the other hand, in Armutlu peninsula and in Bursa region the pebbles of Karasu formation were observed in Mudanya formation of Late Miocene age. The rock assemblages of Latest Miocene-Early Pliocene are known to situate on a paleotopography having pene-

plain character (Emre et al.,1997c). This discordance surface which appears locally by the unveiling of the sediment cover most probably corresponds to Kocaeli peneplain. All these data indicate that Kocaeli peneplain was formed in Early-Middle Miocene and covered widespread areas before the neotectonic period in sea of Marmara region.

Except for tilting northward, Kocaeli peninsula is the only place where the peneplain preserves its shape very close to its original situation. Basement geology of the area corresponds to the Istanbul zone which belongs to paleotectonic era (Okay and Görür, 1995) (Fig.2). Peneplain morphology is preserved on the west of the Adapazarı-Karasu line. Istanbul zone, in the east of the line, displays a high mountain morphology where folds and thrusts are seen (Aydın et al., 1987) (Fig. 6). The southern boundary of the peneplain is marked by the NAF which in paleotectonics corresponds to Intra-Pontide suture (Şengör and Yılmaz, 1981; Okay and Görür, 1995) (Figs. 2 and 6).

These data show that Kocaeli peninsula (western sector of Istanbul zone) bounded by the NAF zone and Adapazarı-Karasu line (Fig. 5) reacted against the deformations arising from neotectonic period as a rigid mass, and these deformations could only happen as doming and tilting/warping and therefore the peneplain morphology that developed in Early-Middle Miocene could be preserved until present time (Fig.7).

Bursa-Bilecik relief

It comprises the landscape between east of Bursa and Sakarya valley (Figs. 3 and 6). The main elements of this landscape are İnegöl and Bursa depressions, plateaus and mass-like blocks in the region. All these high terrain has been dissected by the Sakarya river and its drainage.

İnegöl and Yenişehir depressions lie in NW-SE and NE-SW directions, skew to each other. Their bases are filled with Quaternary alluviums. Around them, Upper Miocene-Pliocene aged sediments, their base corresponding to Mudanya formation and in the upper levels changing into lacustrine sediments crop out (Genç, 1986; Erendil et al., 1991). These sediments can also

be observed in the SE slopes of Uludağ and on the Bilecik plateau. The directions of paleocurrents in the old alluvial fan deposits here show that their source area is on the north of the NAF (Emre et al., 1997c). A watershed line separates the NAF zone and Yenişehir depression at present.

Upper Miocene-Pliocene aged sediments on the Bilecik plateau are observed in paleo-karst depressions as relicts of denudation. Here, the plateau surface is tilted towards the Yenişehir and İnegöl depressions. The surface of the plateau corresponds to the paleotopography (surface of unconformity) which unveils from the sediment cover. It also corresponds to Kocaeli peneplain in the region.

In the plateaus surrounding the depressions valley forms as relicts from an old drainage are observed. In the bases of these valleys Samanlıdağ formation crops out. In the north of the NAF, in Armutlu peninsula, the same valley forms are also seen. They are hanging valleys between the peninsula and the NAF zone dividing Bursa-Bilecik relief. Quaternary incisions of Sakarya river are buried in this valley system. However, along the NAF zone between Gemlik and Geyve this system is cut off and deformed.

Bursa-Bilecik relief is made up of lineations in NE-SW and NW-SE directions in the same direction with the faults of neotectonic period. The data show that the region displayed peneplain morphology in Early-Middle Miocene which later on, in Late Miocene, underwent tectonic deformation and in the basins formed fluvial and lacustrine sediments were deposited. In the later stages of the deformation the region was uplifted and the faults in NE-SW and NW-SE directions became dominant. During the uplift, sedimentary basins also were deformed and some parts of them reached up to the elevation of the present day mountains. On the high relief developed in this way, in Late Pliocene, the drainage system of Sakarya river was set and along the valley Samanlıdağ formation was deposited. Together with the emerge of the NAF, between Gemlik and Geyve the morphologic relation between the Armutlu peninsula and Bursa-Bilecik relief was cut off. As a result of the rapid dissection in Pleistocene the Sakarya river drainage was deepened and along the river canyon-

like valleys were formed. The Upper Miocene-Pliocene deposits taking place along the NW-SE and NE-SW directions were transferred with erosion giving birth to Yenişehir and İnegöl erosive depressions. In Holocene the bases of these depressions were filled again and formed present days plains.

Samanlıdağ unit

This unit comprises the Samanlıdağ relief between the northern and southern strands of the NAF (Fig.6). The section of Samanlıdağ between Gemlik and İzmit bays, prolonging towards sea of Marmara forms Armutlu peninsula. It lies between Dokurcun valley and Armutlu in E-W direction and approximately is 165 km in length. In the eastern and western terminations it gets narrower, and appears in form of a shuttle (Fig. 6). This high relief has been isolated by the corridors of the NAF in the north from Kocaeli peneplain and in the south from Bursa-Bilecik relief. The mass is cut in east by Geyve gorge in which Sakarya river flows and in the west by Orhangazi-Yalova trough in N-S direction. Except for the steps to the south of Yalova, Samanlıdağ displays a massive height and has plateau character with an average elevation of 700-1000 m.

The high relief comprises generally the pre-Neogene rocks (Akartuna, 1968; Bargu and Sakinç, 1989; Erendil et al., 1991; Yılmaz et al., 1995). In its central parts, in Yalova - Yalakdere - Orhangazi regions, sediments of Late Miocene-Early Pliocene (Mudanya and Yalova formations) crop out (Figs. 3 and 4). In the old valley floors fluvial deposits of Late Pliocene (Samanlıdağ formation) take place.

There are two different drainage systems with different characteristic features on the mass. On the plateau, a northward flowing drainage pattern in wide valley floors and with less energy and bearing sediments of Late Pliocene (Samanlıdağ formation) is dominant. In places this drainage system is deformed. On the other hand, in parts close to the NAF zone, the second drainage system with short streams and "V" shaped valleys is seen. This drainage which developed in Quaternary is linked with the older drainage system through backward erosion and in places, has changed

AGE		TECTONISM		MORPHOTECTONIC REGIONS					
				NAF ZONE			BURSA BİLECİK	BLACK SEA	
MIOCENE Early-Middle	PLIOCENE Early Late	QUATERNARY Pleistocene Holocene	NEOTECTONIC PERIOD N-S Compressional Stage	İzmit-Sapanca Trough	Adapazarı Basin	Samanlı Mountains	EROSION	Tilting to the North	
				NAF					Regional (en-block) uplift due to folding and strike-slip faulting
PALEOTECTONIC PERIOD Stabil			PENEPLAINATION					PROCESSES	
NEOTECTONIC PERIOD N-S Compressional Stage			Regional (en-block) uplift due to folding and strike-slip faulting						
NEOTECTONIC PERIOD NAF Stage			Strike-slip deformation					EROSION	Tilting to the North
NEOTECTONIC PERIOD NAF Stage			Subsidence (Pull-apart mechanism)						
NEOTECTONIC PERIOD NAF Stage			Uplift (positive flower structure)					EROSION	Tilting to the North

Fig. 7- Table showing the stages of morphotectonic evolution.

the course of the older system by abstractions. The mature drainage systems on the mass are observed as hanging valleys along the NAF zone both on the northern and southern strands. They indicate Samanlı mountains were in the same drainage system with Kocaeli peneplain and Bursa-Bilecik region. In the watershed line between Kocaeli peneplain and the NAF zone in İzmit-Adapazarı area, the northward directed old val-

ley troughs show that the Samanlıdağ drainage, in pre-NAF period, was towards the Black sea.

Samanlı mountains is an E-W trending, active fault bounded morphotectonic unit. Contrarily, in the physiographic structure of the surface of the mass NE-SW and NW-SE trending lineations are dominant and the surface morphology displays a blocky structure which

is consistent with the conjugate fault systems lying in the same direction. These are inactive faults and the physiographic structure controlled by them were cut by the NAF in E-W direction (Fig. 5). Of these conjugate faults, the NW-SE trending Orhangazi fault is a right lateral strike-slip fault (Erendil et al., 1991). Some of the others in NE-SW direction give clues of being left lateral strike-slip fault (Bargu and Sakinç, 1989). In Mudanya and Yalova formations cut by these faults roughly E-W trending folds were developed (Bargu and Sakinç, 1989). These data indicate that, Samanlı mountains, in pre-NAF periods, were under N-S compressional tectonic regime.

The data on pre-Late Miocene morphology of the Samanlı mountains are limited. The morphology of the region in post-Upper Miocene was determined with tectonic processes. On the other hand, in the surface morphology of the mass there is an erosional plain inconsistent with these tectonic processes. The above mentioned older drainage forms were buried in this erosional surface which is cut by NW-SE and NE-SW trending faults and possibly corresponds to Kocaeli peninsular plain.

Samanlıdağ height forms a positive flower structure displaying a fault wedge geometry between the northern and southern strands of the NAF. The data indicate that, in the first stage of the neotectonic period this region had the same morphotectonic features with Bursa-Bilecik region. Together with the emerge of the NAF, in Latest Pliocene, Samanlı mountains have uplifted as pressure ridge and isolated from Kocaeli peninsula and Bursa-Bilecik relief and formed a different morphotectonic unit. Samanlı mountains, when compared with Kocaeli peninsula in morphometric terms, can be said to be uplifted averagely 700-800 m from the beginning of the neotectonic period.

NAF zone

In the research area, consistent with the structural prolongation of the NAF, there are two morphologic troughs as corridors in E-W direction along the northern and southern strands (Figs. 5 and 6). Of these, the northern one can be called İzmit-Adapazarı whereas the southern one can be as Gemlik-Geyve. These two

corridors in the east gets closer to each other but in the west they fall apart. In İzmit and Gemlik Bays the corridors are invaded by the sea of Marmara. Westward, at the bottom of the sea, they lie apart from each other. The northern corridor, on which the deep depressions were formed at the bottom of the sea, joins the Saros-Gaziköy fault making a concave turn southward. The southern one terminates in Bandırma bay (Emre et al., 1997c).

These corridors lying along the NAF zone separates the other morphotectonic units from each other (Fig.6). The floors of the corridors in which İznik and Sapanca lakes are situated were filled with Latest Pliocene-Recent sediments. The morphology observed in them reflects the active tectonics of the region. The development process of the erosive landforms in both zones are similar with each other. These landforms are known with deep valleys with steep morphology intruded into the other morphotectonic units. On the other hand, the landforms having depositional origins are different in both corridors from the formation processes point of view. For example, although marine terraces were developed along the shores of the İzmit bay (Erinç, 1956; Göney, 1964; Akartuna, 1968; Bargu and Sakinç, 1989; Sakinç and Bargu, 1989; Erol and Çetin, 1995), in Gemlik bay they are not present. The situation is vice versa when comparing the lakes. It is known that there are terraces of Pleistocene age on the shores of the lake İznik (Ardel, 1954; Bilgin, 1968; Akartuna, 1968; Ikeda et al., 1991) whereas none on the shores of Sapanca lake. This example shows the difference in between the morphotectonic development in northern and southern corridors of the NAF. The characteristic localities of the fault is briefly given below:

- The NAF zone forms an approximately 150 km long morphologic corridor between Geyve and Gemlik (Figs. 3 and 6). The western continuation of this corridor corresponds to the bottom topography of the sea of Marmara in Gemlik and Bandırma bays. Between Geyve and Bandırma the segments of the NAF are İznik-Geyve, Gemlik, Zeytinbağ and Bandırma (Emre et al., 1997c). These are en echelon and transtensional segments complementing each other. Where the en echelon structures are seen, pull-apart basins have formed corresponding to lake İznik, Gemlik and Ban-

dirma depressions in sea of Marmara (Barka,1992; Barka and Kuşcu,1996).

- The depositional surfaces observed around lake İznik are lined up as terraces (Fig. 3). The terraces, mostly seen on the north and west parts of the lake as four levels (Bilgin,1968) and mostly comprise fan delta deposits. The lowest terrace filling has yielded 18 000 years by C_{14} method (Ikeda et al.,1991). Fan deltas to the north were deposited in front of the young valleys capturing the Late Pliocene valleys on the Samanlıdağ mass. These data indicate that lake İznik was formed in Pleistocene.

- The NAF is a single line between İznik-Geyve (Fig. 5). Right lateral strike-slip fault morphology is dominant at the depression developed along the fault. This depression divides Bursa-Bilecik relief and Samanlıdağ mass (Fig.6). Along the zone, the Late Pliocene drainage on the heights have been preserved as hanging valleys. The Pamukova depression situated in the east, was opened on the NAF, in the beginning due to erosive processes of Sakarya river, but later on was filled with the alluviums of the same river. Around the basin, fluvial-lacustrine sediments of Pleistocene are observed as terraces. In the western end where the river enters to the depression terrace deposits include deltaic sections. On the floor of the depression flood plain deposits of Holocene age are seen. The sediments imply that Pamukova depression from time to time gained a lacustrine basin character. The 22 km right lateral offset the river at the floor of the depression (Fig. 5), at the first glance, may be interpreted as the movement of the NAF (Şaroğlu et al., 1987; Koçyi- (Jit, 1989), but, since the southern strand of the fault corresponds to a fault of paleotectonic period (Yılmaz et al., 1995) it is difficult to argue that the offset is totally because of the NAF.

- İzmit-Adapazarı corridor lying between the sea of Marmara and Dokurcun valley separates the Kocaeli penepain and the Samanlıdağ height (Fig. 6). On this trough there are sedimentary basins having different features such as Adapazarı plain, lake Sapanca and İzmit bay (Fig. 3). Adapazarı plain which is situated in a transtensional region in between the Dokurcun and İzmit-Adapazarı segments of the NAF was developed

as a pull-apart basin (Fig. 5). Düzce fault also effects the morphology of the basin. Pull-apart morphology is quite apparent in the south of the basin. Between Dokurcun valley and Sapanca, this basin is separated from the Samanlıdağ mass by a morphologic discordance corresponding to the NAF. Starting from Karapürçek region where the fault enters the basin, together with its right lateral strike-slip character, the fault also displays normal slip component and in between Sakarya river and Sapanca it totally becomes a normal fault (Fig. 5). Between the NAF and the floor of the basin, in Karapürçek-Sapanca region, there many normal faults in NW-SE direction (Fig. 5) displaying step-like morphology. On the surfaces of the blocks between the faults cutting the Karapürçek formation of Latest Pliocene-Pleistocene age, southward tiltings of 20° - 25° can be seen. The amount of tilting and the offset of the faults decrease in NE direction. The younging of the fans here is also in the same direction. Besides, the bed migration in Sakarya river is from west to east. No normal faults in the NE of the basin were observed. These data indicate that Sakarya plain is a pull-apart basin developed as a half graben and younged in NE direction.

- The morphology of the corridor between lake Sapanca and İzmit bay is controlled by strike-slip movement. The floor is filled with Pleistocene and Holocene aged sediments. The youngings at the fans are in vertical direction in Sapanca region, whereas in the bay region they are as lateral onlaps. This difference indicates that the offset of the fault increases from west to east. As a matter of fact, on the Pleistocene fans to the west of lake Sapanca, right lateral offsets reaching up to 10 km can be seen (Emre et al., 1997d). Lake Sapanca is situated just on the trace of the NAF. No terrace is observed around it. The floor of the lake, most probably formed as erosional fault valley during the last glacial age. Due to the alluvium accumulation in Sakarya plain in Holocene the east end of this valley was blocked and the basin of the lake was formed.

- Western termination of the corridor is under the waters of İzmit bay (Fig. 6). Shore morphology of the bay is jagged with two depressions at the bottom (Fig. 5). Because of the structural features of the NAF, this morphology was intended to be explained with

pull-apart basin models (Barka and Kadinsky-Cade, 1988; Barka, 1992; Barka and Kuşcu, 1996). At present, the fault comprises only one single trace in the bay (Fig. 5). The NE-SW trending faults on land represent the structures in the first formation stage of the NAF and now are inactive. They are responsible from the jagged appearance of the shore. The closed depression situated to the east of the bay is due to Hersek delta. The fan of this delta has divided the NAF corridor into two, morphologically, and has caused the formation of the closed eastern depression (Figs. 3 and 5).

- The first sediments deposited in the İzmit-Adapazarı corridor in NAF morphology are of Latest Pliocene and Early Pliocene aged. On the other hand, Late Pliocene drainage situated on the Samanlıdağ mass and draining towards Black sea via Kocaeli penneplain was cut and deformed by the fault. In Geyve-Gemlik corridor there are no deposits older than Pleistocene in NAF morphology. All these data indicate that the NAF emerged in Latest Pliocene.

DISCUSSION AND RESULTS

THE STAGES OF NEOTECTONICS

The neotectonics in Anatolia begins with the continent to continent collision between African and Anatolian plates in the end Middle Miocene-Upper Miocene (McKenzie, 1972; Şengör, 1979, 1980, 1982; Şengör and Kidd, 1979; Şengör and Yılmaz, 1981; Jackson and McKenzie, 1984). Through this process took place under N-S compression tectonic regime, since the continental crust thickening in East Anatolia was not taken up by folding, thrusting and strike-slip faulting exceedingly, two long transform faults, the NAF and EAF (Eastern Anatolian Fault) was formed and the western escape of the Anatolian plate, the neotectonic framework of Turkey was set (Şengör, 1979, 1980; Şengör et al., 1985; Şaroğlu, 1985). The authors mostly have emphasized that the emergence of the NAF and the EAF and therefore the western escape of Anatolian plate started in Upper Miocene.

In the beginning of the neotectonic period, the eastern part of Anatolia was inundated and the western part was displaying penneplain morphology (Erinç,

1953,1955; Şengör, 1980; Şengör et al., 1985; Şengör and Yılmaz, 1981; Erol, 1981; Şaroğlu and Güner, 1981; Şaroğlu, 1985). This paleomorphology, through the structural processes in neotectonic period has undergone changes by inversions in E-W and N-S profiles and the hypsographic curve of the land has shown tendency to increase from west to east (Erinç, 1953, 1955, 1973; Şengör, 1980; Şengör et al., 1985; Erol, 1981; Şaroğlu and Güner, 1981; Şaroğlu et al., 1983, 1987). In this process of change East Anatolia was uplifted, Central Anatolia was turned into inner depressions and in West Anatolia, horst and graben structures were developed. Tauride and Pontide belts have changed into border fold mountains by uplifting.

In papers about Marmara region, it is mostly accepted that the neotectonism started in Middle-Upper Miocene with the emergence of the NAF, and the region took place in between the NAF zone and West Anatolian graben system and the Neogene-Quaternary sediments were deposited in the structures developed under these conditions (Şengör, 1979, 1980, 1982; Şengör et al., 1985; Barka and Kadinsky-Cade, 1988; Barka, 1992; Wong et al., 1990, 1995; Taymaz et al., 1991; Straub, 1995; Görür et al., 1995, 1997).

The data collected during this study is roughly parallel with the above outlined structural evolution model of neotectonics of Anatolia. However, the character of neotectonic events, timing and the geochronologic order of the morphotectonic changes do not match with the proposed models.

The neotectonic structures of the Marmara can be grouped into two (Fig. 5). The faults showing the large scale morphotectonic prolongations are in E-W direction in east Marmara, whereas in NE-SW in west Marmara and Biga peninsula (Şaroğlu et al., 1987, 1992; Emre et al., 1997c). These are active neotectonic structures (Fig. 5). The second group faults are in NW-SE and NE-SW directions and are conjugate with each other (Fig. 5). Most of these are inactive. The NAF zone lies in E-W direction, incompatible to them. The morphotectonic prolongations developed by these conjugate systems are cut by the NAF.

The findings have revealed that the neotectonic framework of the Marmara (Fig. 5) developed in two stages which reflect different tectonic styles. These stages are divided into two: Late Miocene-Pliocene and Latest Pliocene-Recent. Of these the first one is of compressional tectonic regime, and the second is, represented by the NAF, the stage of vertical tectonic movements with transform character.

North-South compression stage

The first neotectonic deformations in the region were started in Upper Miocene (Fig. 7). They were as large scale undulations and the peneplain morphology resting on the basement rocks were deformed and undulated due to. Mudanya formation which is transitive with the Yalova formation at the top and is the first deposit of neotectonic period was deposited in the basins developed due to these deformations. The first depositional basins correspond to wide synclines, in structural sense.

Late Miocene-Early Pliocene sediments, recently are observed at the floor of the depressions bounded by the faults in NE-SW and NW-SE directions and on the surrounding high topography. In these sediments folds in E-W directions are seen. In fault zones, more deformation on these can be observed. Findings indicate that the NE-SW and NW-SE trending faults have developed after the deposition of Mudanya and Yalova formations and these depositional basins were cut by them. These units in present day geology are observed as erosive relicts in the troughs in between the faults (Figs. 3 and 5).

Both the deformational structures in the fault zones and their morphologic features, show that the faults complementing each other in NE-SW and NW-SE directions are of strike-slip nature. Of these, the ones in NW-SE, as in the case of Orhangazi fault (Erendil et al., 1991), are right lateral (Fig. 5). However, the faults in Yalakdere region the faults in NE-SW direction are of left lateral (Bargu and Sakiç, 1989) which are being accompanied by folds and reverse faults in E-W direction. These structural data show that the region in Late Miocene-Pliocene was under N-S compression and was deformed due to. The peneplain morphology

developed in Early-Middle Miocene is observed in high mountainous and plateau areas and are tilted, blocked and domed due to compression and uplift. Another data for rising morphology is the presence of Mudanya and Yalova formations in morphometrically high areas as seen in Bilecik and Yalakdere regions.

Most of the conjugate faults developed under the N-S compressional tectonic regime in Late Miocene are inactive. The active faults of the Marmara are seen in the NAF zone lying in E-W direction (Fig. 5). This relation with the strike and the activity of the faults show that the tectonic regime in which the above mentioned strike-slip faults developed ended in Latest Pliocene with the emergence of the NAF.

The N-S trending compression may be defined as the first stage of the neotectonics in Marmara (Fig. 7). The faultings related to this tectonics can not be observed in Kocaeli peninsula, situated in the north of the Intra-Pontide suture belt where presently the NAF takes place (Figs. 2 and 5). The deformations here are as warping and doming (Fig. 7). Contrarily, all the structural elements related to compressional regime were developed in the south of the suture belt. The morphotectonic character of the Armutlu peninsula, in the compressional stage, shows that it had the same behaviour with the Bilecik-Bursa region situated in the of this rise (Fig. 7).

The NAF stage

The neotectonic regime effective in the area has changed style in the Latest Pliocene with the emergence of the NAF. The N-S compressional tectonics in Late Miocene-Pliocene has left its place with the formation of this fault to the lateral shears and displacements (Fig. 7). The structures of this stage is well marked with the faults forming the transform NAF in east Marmara (Fig. 5). The same process is valid for the Biga peninsula and west Marmara. In these regions, the fault, changing its general trace of E-W starting from Bandırma to westward, has caused the formation of new faults (Şaroğlu et al., 1987, 1992; Emre et al., 1997c). The structures of this period forms the NAF between sea of Marmara and Saros bay (Şengör,

1979; Şengör et al., 1985). Biga peninsula, in this period, has been dissected by the NE-SW trending faults (Şaroğlu et al., 1987, 1992; Emre et al., 1997a, b, c).

The NAF, between Karlıova and Dokurcun valley is made generally up of linear faults (Şengör, 1979; Şengör et al., 1985; Şaroğlu et al., 1987, 1992; Barka and Kadinsky-Cade, 1998; Barka, 1992). This structure of the NAF changes starting with Dokurcun valley and towards west, it is made up of two strands diverging each other (Fig. 5). The prolongation of the southern strand between Bandırma and Dokurcun is concordant with that of east of Dokurcun (Fig. 5). This zone comprises of short, single fault segments, shortening more westward, such as İznik-Geyve, Gemlik, Zeytinbağı and Bandırma (Emre et al., 1997c). In this section the fault has replaced an old fault zone of Cretaceous (Yılmaz et al., 1995). Between the segments where transtensional overlaps are seen pull-apart basins have formed (Barka, 1992; Barka and Kuşçu, 1996).

Northern strand of the NAF developed in Intra-Pontide belt (Şengör and Yılmaz, 1981) displays a more complex structure than the southern strand (Figs. 2 and 5). Here the fault has two segments, Dokurcun and İzmit-Adapazarı. Dokurcun segment, which in its eastern termination lies in NE-SW direction, changes its trace towards Adapazarı plain and runs in NW-SE direction (Fig. 5). In vicinity of Karapürçek where it enters Adapazarı depression it gains normal component. Between Sakarya river and Sapanca, it totally displays normal fault features (Fig. 5). On the other hand, Adapazarı segment, starts in the east as a continuation of Hendek-Yığılca lineation, a former paleotectonic period fault which later on moved in the first stages of the neotectonic period (Aydın et al., 1987) (Fig. 5). It changes its direction to E-W in the west of Sapanca which is NE-SW in the east. Along this zone, between Adapazarı and Yalova, there are inactive faults in NE-SW direction (Fig. 5). These en echelon faults, defining the border morphology of İzmit bay in the north and south are cut by the NAF (Fig. 5). These structures accompanying the active trace of the NAF most probably represent the shear zone in the first stages of the formation of the fault. The right lateral offset on the fault reaches up to 10 km (Emre et al., 1997d).

Between the segments in the northern strand Adapazarı pull-apart was developed. The normal faults responsible for the formation of this basin lie in NW-SE direction diagonal to the main trace of the fault (Fig. 5). Its offset is verified by the fault plane solution of the after shocks of the 30.7.1967 earthquake (McKenzie, 1978; Jackson and McKenzie, 1984).

At this stage, due to the NAF, two large pressure ridges were formed where the fault bifurcates. These ridges, reaching mountain scales morphologically, form Samanlıdağı and Almacıkdağı masses (Fig. 6). The downcutting of the Sakarya river bed in an antecedent gorge implies the Samanlıdağ ridge is uplifting.

PALEOGEOGRAPHIC DEVELOPMENT PERIODS

Three distinctive periods of structural processes in the geomorphologic evolution of the East Marmara region in Neogene-Quaternary were differentiated (Fig. 7). These periods are also defined with three sedimentary sequences with angular unconformity (Fig. 4). Of these, the first one corresponding to Early-Middle Miocene represents a technically quiescent period and reflects the morphology of the paleotectonic period. Neotectonic period is represented by Late Miocene-Recent. The morphologic structure reflects two different tectonic styles (Fig. 7). The following paleogeographic evolution is based on the events in these three morphotectonic periods.

Early-Middle Miocene: Paleotectonic period

Istanbul and Sakarya zones, in the end of the Oligocene, have joined along the suture zone as a result of the closure of Intra-Pontide ocean (Fig. 2) and emerged. The region therefore has turned into terrestrial erosion area (Okay and Görür, 1996; Görür et al., 1995, 1997).

During the Early-Middle Miocene, a peneplanation period was observed under warm and humid climatic conditions on this land mass (Fig. 7). By the end of Middle Miocene, the area covering today's sea of Marmara and the shelf of Black sea has gained a mature peneplain morphology. The relief today observed on Kocaeli peninsula is a relict of that. The presence of a

thick paleosol cover indicates the long period of peneplanation and the lack of tectonic effect on the formation of this landscape (Brown and Kraus, 1987; Retalack, 1990; Wright, 1992a, b; Kraus and Asian, 1993; Mack et al., 1993). The Early-Middle Miocene peneplain, except for Marmara, has developed in whole Western Anatolia and in Strandja (Pamir, 1938; Erinç, 1955; Erol, 1981; Erol and Çetin, 1995).

The fluvial, lacustrine deposits of the peneplanation period are observed both in Biga peninsula and in Thrace basin (Sümengen et al., 1987; Siyako et al., 1989; Yalıtırak, 1995; Görür et al., 1995, 1997). On the other hand, in SE Marmara they are not seen. This situation explains the increasing height of the peneplain morphology from west and north to SE Marmara and this section was an erosional area.

Late Miocene-Pliocene: N-S compression stage of Neotectonic period

Great morphological changes happened in Marmara region as seen in whole Anatolia together with the initiation of neotectonics in the end of Middle Miocene-Early Late Miocene (Şengör 1979,1980,1982; Şengör and Yılmaz, 1981; Şengör et al., 1985; Barka and Kadinsky-Cade, 1988; Barka, 1992; Görür et al., 1995, 1997; Erol and Çetin, 1995; Emre et al., 1997a,b,c). The region together with the neotectonism started compressing in N-S direction and uplifting and the peneplain morphology got deformed. The first deformations took place as great undulations. As a result of this change in the relief, the first deposit of the neotectonic period, Mudanya formation, began depositing. The caliche zones in and at the base of the formation reflect the dry climatic conditions of Late Miocene. The reddish mudstone at the base were deposited as pediment deposits. These mudstones, most likely represent the accretion of thick soil cover at the floor of the basins situated at the surface of the deformed and uplifted Early-Middle Miocene peneplain. They upwards pass into the alluvium fan deposits bearing pebbles of basement rock which indicates the tectonic originated uplifting is increasingly continuing.

Together with the neotectonics initiated in Late Miocene the region began morphologically uplifting

(Fig. 7). The negative uplifting areas corresponding to synclines have formed the depositional basins. Deformations have taken place mostly as folds and the faults have not had any important role in the formation of the development of the basins.

Towards the end of the Late Miocene fluvial-lacustrine environments in the region have spread over, and the alluvial fans and the fan deltas of Mudanya formation began developing. In vicinity of Mudanya the paleocurrent directions indicate that their source area was in the north (Şahbaz et al., 1997) and therefore some parts of the sea of Marmara were erosional areas.

The first marine water entrance to the East Marmara was in the end of Late Miocene. This sea has transgressed over the fluvial, lacustrine basins and the other morphologic depressions where Mudanya formation deposited and therefore has led the deposition of Yalova formation. The marine conditions in the area continued by the end of the Early Pliocene (Cymmerian). As a result of the above mentioned transgression, the morphologic depressions developed as intermontane basins (Şaroğlu and Güner, 1981) under the effect of N-S oriented compressional tectonic regime have gained marine basin character. The paleogeographic extension of this marine basin is not concordant with the NE-SW and NW-SE trending faults developed in neotectonic period and with the direction of the NAF (Figs. 3 and 5).

As a result of the continuing N-S compression and therefore the regional narrowing and uplifting, towards the end of the Early Pliocene, the marine areas began to spread out and close and underwent the effect of terrestrial processes. The transition of the dolomites of Çamlık formation defining the deep brackish water environment to the limestones reflecting the shallow fresh water environment (Varol, 1997) may be explained by spread of seas and change into lakes.

The morphologic change resulting with the closure of marine basins was provided by the NE-SW and NW-SE trending faults apart from the folds (Fig. 5). This deformational stage under the dominance of strike-slip faulting is the maximum uplifting stage of East Marmara-

ra. As a result of the relief inversion occurred by this deformation, as in Mudanya and Yalakdere regions, the floors of marine basins of Late Miocene-Early Pliocene have reached up the peaks of mountains.

The Late Pliocene morphology including east part of the present day sea of Marmara where terrestrial erosional conditions were effective have led an increasing trend from Black sea to south. On this morphology which was technically controlled except for the Kocaeli peninsula a drainage pattern which could be assumed to be the ancestor of the present day Sakarya river was set and the whole region began to drain towards Black sea (Figs. 3 and 5).

The Latest Pliocene-Recent: The NAF stage

This time interval is a period of large scale morphologic changes due to style changes in neotectonics. The present day morphotectonic framework was mainly set in this interval with the emergence of the NAF. To the north of the Dokurcun, the fault has bifurcated into two independent faults with different structural developments. The southern strand has placed on an old fault developed in the paleotectonic period (Yılmaz et al., 1995) and the faults here has developed as single traces. In the en echelon regions between the segments forming the zone subsidence areas of pull-apart nature was formed and lake İznik and in Gemlik and Bandırma bays sea of Marmara has invaded these structures.

The faults on the northern strand of the NAF were developed in the second stage of the neotectonics. Here, the NAF has appeared as a shear zone in the beginning, as seen in the east (Şaroğlu, 1988) and in this first stage en echelon NE-SW trending shear faults were developed (Fig. 5). In the later stages of this break up, the main fault breaks representing the active tectonics today appeared and the fault gained its transform character.

In the east of the NAF zone, the depression between İzmit-Adapazarı and Dokurcun segments was formed as a pull-apart basin and Sapanca-İzmit bay sec-

tion has gained a corridor morphology. In this context, in the east terrestrial, and in the west marine sediments began depositing. The sediments in the bay indicate that there are four major level changes in sea of Marmara in Late Pliocene-Holocene (Meriç, 1995). The fauna and the features of the environment show a very intense tectonics in Middle Pleistocene (Meriç, 1995). The same findings were met in the east of the corridor. The deformational structures in the Karapürçek formation deposited in Adapazarı basin are mostly of Middle Pleistocene-age. Therefore it can be said that the maximum activity of the NAF was in Middle Pleistocene.

With the emergence of the NAF, in Late Pleistocene, the uplifting morphologic structure from Black sea towards Samanlıdağ mass was deformed and the mass in between the two strands of the fault was heaved as a positive flower structure (pressure ridge) and isolated from the surrounding morphology. The surface of the Kocaeli peninsula, on the north of the NAF was tilted northward (Fig. 7). The absence of marine terraces on the shores of the Black sea, opening of Sakarya river into a deep submarine canyon (Fig. 5) indicate that the shore areas of the present day shelf, in that period, was not invaded by water. In the south, in vicinity of Bilecik, together with the initiation of the NAF regime erosional processes increased and the region was dissected by the drainage of Sakarya river.

By the end of the Late Pleistocene (the latest glacial age) the erosional processes reached a maximum in the area during the sea level decrease in Black sea and sea of Marmara, and together with tectonics some other processes controlling the morphologic development prevailed. As a result of that the rivers dissected their beds and the morphologic dissection in the region was reached its maximum. İnegöl and Yenişehir basins in the south, Pamukovası, Sapanca trough and Adapazarı plain shaped as erosive depressions. After the sea level increase in Holocene these erosive morphologies were filled with sediments and present day's alluvium plains were formed. During the process of filling with alluvium, Sapanca trough which opened on the NAF as a fault valley was blocked and the basin of the Sapanca lake was formed. The earthquakes indicate that today's landscape forming is due to the NAF.

ACKNOWLEDGEMENTS

This research, supported by TÜBİTAK, was carried out in context of "National Marine Geology and Geophysics Programme" prepared by TÜBİTAK, MTA General Directorate and universities and coordinated by Prof. Dr. Naci Görür and Mr. Murat Erendil, Deputy General Director of MTA General Directorate. The authors would like to extend their sincere thanks to the above institutions and persons. Thanks also go to Mr. İsmail Kuşçu, of MTA, for making corrections in English.

Manuscript received December 30, 1997

REFERENCES

- Akartuna, M., 1968, Armutlu yarımadasının jeolojisi. İst. Üniv. Fen Fak. Monog., 20, 105 p.
- Ardel, A., 1954, İznik depresyonu ve Gölü. İst. Üniv. Coğr. Enst. Derg., 5-6, 225-229.
- Aydın, M.; Serdar, H.S.; Şahintürk, Ö.; Yazman, M.; Çokuğraş, R.; Demir, O. and Özçelik, Y., 1987, Camdag (Sakarya)-Sünnicedağ (Bolu) yöresinin jeolojisi. Türkiye Jeol. Kur. Bült., 30, 1-14.
- Bargu, S. and Sakıncı, M., 1989, İznik Körfezi-İznik Gölü arasında kalan bölgenin jeolojisi ve yapısal özellikleri. İst. Üniv. Müh. Fak. Yerbilimleri Dergisi, 6, 45-76.
- Barka, A. A., 1992, The North Anatolian fault. Annales Tectonicae, 6, 174-195.
- and Kadinsky-Cade, K., 1988, Strike-slip fault geometry in Turkey and its influence on earthquake activity. Tectonics, 7, 663-684.
- and Kuşçu, İ., 1996, Extents of the North Anatolian fault in the İzmit, Gemlik and Bandırma bays. Turkish J. Marine Sci., 2, 93-106.
- Baykal, F. and Önalın, M., 1979, Şile Sedimanter Karşığı (Şile Olitostromu). Türkiye Jeol. Kur. Altın Simpozyumu, Ankara, 15-25.
- Bilgin, T., 1968, Samanlı Dağları. Pub. İst. Üniv. Coğ. Enst., 50, 196 p.
- , 1984, Adapazarı Ovası ve Sapanca oluğunun alüvyal morfolojisi ve Kuvaterner'deki jeomorfolojik tekamülü. Pub. İst. Üniv. Ed. Fak., 2572, 199 p.
- Brown, T.M. and Kraus, M. J., 1987, Integration of channel and flood-plain suites, I. Developmental sequences and lateral relations of alluvial paleosols. J. Sedim. Petrol., 57, 587-601.
- Chaput, E., 1936, Voyages d'etudes geologiques et geomorphogeniques en Turquie. Paris. (Türkiye'de Jeolojik ve Jeomorfojenik Tetkik Seyahatleri). Çev. A. Tanoğlu. Pub. İst. Üniv. Ed. Fak., 11, 1947.
- Crampin, S. and Evans, R., 1986, Neotectonics of the Marmara Sea Region of Turkey. J. geol. Soc. Lond., 143,343-346.
- Çetin, O.; Çetin, T. and Ukav, İ., 1995, İzmit Körfezi (Hersek Burnu-Kaba Burun) Kuvaterner istifinde gözlenen mollusk kavrıklarının Elektron Spin Rezonans (ESR) yöntemi ile tarihlendirilmesi (Electron Spin Resonance (ESR) dating of fossil mollusc shells observed in Quaternary sequence in the Gulf of İzmit (Hersek Burnu-Kaba Burun). In: İzmit Körfezi Kuvaterner İstifi (Quaternary Sequence in the Gulf of İzmit) (Ed. E. Meriç), 269-276.
- Ediger, V. and Ergin, M., 1995, İzmit Körfezi (Hersek Burnu-Kaba Burun) Kuvaterner istifinin sedimentolojisi (Sedimentology of the Quaternary sequence in the Gulf of İzmit, Hersek Burnu-Kaba Burun). In: İzmit Körfezi Kuvaterner İstifi (Quaternary Sequence in the Gulf of İzmit) (Ed. E. Meriç), 241-250.
- Emre, Ö.; Erkal, T.; Kazancı, N.; Görmüş, S.; Görür, N.; Kuşçu, İ. and Keçer, M., 1997a, Güney Marmara'nın Neojen-Kuvaterner tektoniği ve jeomorfolojisi (Tectonics and geomorphology of the southern Marmara Region during the Neogene and Quaternary). In: Marmara Denizi Araştırmaları Workshop III, 2-3 Haziran 1997. Genişletilmiş Bildiri Özleri, Ankara, 55-60.

- Emre, Ö.; Erkal, T.; Kazancı, N.; Kuşçu, I. and Keçer, M., 1997b, Güney Marmara'nın Neojen ve Kuvaterner Morfotektoniği (Morphotectonics of the southern Marmara Region during the Neogene and Quaternary). In: Kuzey Ege, Marmara Denizi ve Dolayının Jeolojisi, Deniz Yapılanmalarındaki Önemi Kollokuyumu. Genişletilmiş Bildiri Özleri, İstanbul, 7-17.
- ; ———; ———; Görmüş, S.; Görür, N.; Kuşçu, İ. and Keçer, M., 1997c, Güney Marmara'nın Neojen ve Kuvaterner'deki morfotektoniği (Morphotectonics of the southern Marmara Region during the Neogene and Quaternary). In: Güney Marmara Bölgesinin Neojen ve Kuvaterner Evrimi. TÜBİTAK YDABÇAG-426/G Proje Raporu, 36-68.
- ; ———; Ünay, E.; Keçer, M. and Tchepalyga, A., 1997d, İzmit Körfezi-Sapanca oluşunun tektonik yapısı ve Kuzey Anadolu Fayı'nın yaşı hakkında ön bulgular. In: Aktif Tektonik Araştırma Grubu 1. Toplantısı Bildiri Özleri. 8-9 Aralık 1997. İstanbul, p.17.
- Erendil, M.; Göncüoğlu, M.C.; Tekeli, O.; Aksay, A.; Kuşçu, I.; Ürgün, M. B.; Temren, A. and Tunay, G., 1991, Armutlu yarımadasının jeolojisi. MTA Rep. No: 9165 (unpublished), Ankara.
- Eriñ, S., 1953, Doğu Anadolu Coğrafyası. Pub. İst. Üniv. Coğr. Enst. 15, 124 p.
- , 1955, Orta Ege bölgesinin jeomorfolojisi. MTA Rep. No: 2217, (unpublished), Ankara.
- , 1956, Yalova civarında bahri Pleyistosen depoları ve taraçaları. Türk Coğ. Derg., 15-16, 188-190.
- , 1973, Türkiye'nin şekillenmesinde neotektoniğin rolü ve jeomorfoloji jeodinamik ilişkileri (Geomorphological Evidences of Neotectonics in Turkey). Jeomorfoloji Dergisi, 5, 11-26.
- Erol, O., 1981, Neotectonic and Geomorphological Evolution of Turkey. Z. Geomorph. N.F. Suppl. Bd, 40, 193-211.
- Erol, O. and Çetin, O., 1995, Marmara Denizi'nin Geç Mi-yosen-Holosen'deki evrimi (Evolution of the Marmara Sea from late Miocene to Holocene). In: İzmit Körfezi Kuvaterner İstifi (Quaternary Sequence in the Gulf of İzmit) (Ed. E. Meriç), 313-342.
- Genç, Ş., 1986, Uludağ-İznik Gölü arasının jeolojisi. MTA Rep. No: 7853, (unpublished), Ankara.
- Göney, S., 1964, Karamürsel civarında Pleyistosen'e ait bazı eski kıyı izleri. İst. Üniv. Coğ. Enst. Derg., 14, 200-208.
- Görmüş, S.; Şahbaz, A.; Varol, B.; Kazancı, N.; Bayhan, E.; Emre, Ö. and Özdoğan, M., 1997, Güney Marmara (Bursa-Karacabey) bölgesinin stratigrafisi ve yapısal özellikleri (Stratigraphy and Structural properties of the south Marmara area, Bursa-Karacabey). In: Güney Marmara Bölgesinin Neojen ve Kuvaterner evrimi. TÜBİTAK YDABÇAG-426/G Proje Raporu, 22-35.
- Görür, N.; Sakıncı, M.; Barka, A.; Akkök, A. and Ersoy, S., 1995, Miocene to Pliocene Palaeo-geographic evolution of Turkey and its surroundings. J. Human Evol., 28, 309-324.
- ; Çağatay, N.M.; Sümengen, M.; Şentürk, K.; Yaltırak, C. and Tchepalyga, A., 1997, Origin of the Sea of Marmara as deduced from the Neogene to Quaternary palaeogeographic evolution of its frame. Intern. Geology Review, 39, 342-352.
- Gülen, L.; Kubanç, C. and Altınsoçlı, S., 1995, İzmit Körfezi (Hersek Burnu-Kaba Burun) Kuvaterner istifinin ostrakod faunası (Ostracoda fauna of the Quaternary sequence in the Gulf of İzmit, Hersek Burnu-Kaba Burun). In: İzmit Körfezi Kuvaterner İstifi (Quaternary Sequence in the Gulf of İzmit) (Ed. E. Meriç), 153-172.
- Ikeda, Y.; Herece, E.; Svgai, T. and Işıkara, A.M., 1991, Post glacial crustal deformation associated with slip on the western part of the North Anatolian fault zone in the İznik Lake basin, Turkey. Bull. Dept. Geog. Univ. Tokyo, 13-23.
- Jackson, J. and McKenzie, D., 1984, Active tectonics of the Alpine-Himalayan Belt between western Turkey and Pakistan. Geoph. J. Roy. Astro. Soc., 77, 185-264.

- Jacobshagen, V., 1986, Geologie von Griechenland gebürder Bomtraeger. Berlin, Stuttgart, 363 p.
- Koçyiğit, A., 1989, Suşehri basin: an active fault-wedge basin on the North Anatolian Fault Zone, Turkey. *Tectonophysics*, 167, 13-29.
- Kraus, M.J. and Asian, A., 1993, Eocene hydromorphic paleosols: significance for interpreting ancient floodplain processes. *J. Sedim. Petrol.*, 63, 453-463.
- Mack, G.H., James, W.C. and Monger, H.C., 1993, Classification of paleosols. *Bull. geol. Soc. Amer.*, 105, 129-136.
- McKenzie, D., 1972, Active tectonics of the Mediterranean region. *Geophys. J. Roy. Astro. Soc.*, 30, 109-185.
- , 1978, Active tectonics of the Alpine-Himalayan Belt: The Aegean Sea and Surrounding regions. *Geoph. J. Roy. Astro. Soc.*, 55, 217-254.
- Meriç, E., 1995, İzmit Körfezi (Hersek Burnu-Kaba Burun) Kuvaterner'inin stratigrafisi ve ortamsal özellikleri (Stratigraphy and positional Features of the Quaternary Sequence in the Gulf of İzmit, Hersek Burnu-Kaba Burun). In: İzmit Körfezi Kuvaterner İstifi (Quaternary Sequence in the Gulf of İzmit) (Ed. E. Meriç), 251-258.
- ; Yanko, V.; Avşar, N.; Nazik, A. and Koral, H., 1991, Kuvaterner döneminde Akdeniz ile Marmara Denizi arasındaki deniz bağlantıları (On the Marine interactions between the Mediterranean Sea and the Sea of Marmara during Quaternary time). In: İzmit Körfezi Kuvaterner İstifi (Quaternary Sequence in the Gulf of İzmit) (Ed. E. Meriç), 285-294.
- MTA, 1964, 1:500 000 Ölçekli Türkiye Jeoloji Haritası İstanbul Paftası (1:500 000 Scale Geological Map of Turkey, İstanbul Sheet), Ankara.
- Okay, A. I., 1989, Tectonic Units and sutures in the Pontides, northern Turkey. Tectonic evolution of the Tethyan Region (Ed. A.M.C. Şengör) Dordrecht / Boston / London. Kluwer Academic Publishers, 109-116.
- Okay, A.I. and Görür, N., 1995, Batı Karadeniz ve Trakya Havzaları'nın kökenleri arasında zaman ve mekan ilişkisi. Symposium on Geology of Thrace Basin, Ankara, 9-11.
- Pamir, H.N., 1938, İstanbul Boğazı'nın teşekkülü meselesi, MTA Mecmuası, 3-4, 61-68.
- Paluska, A., Poetsch, S. and Bargu, S., 1989, Tectonics, paleoseismic activity and recent deformation Mechanism in the Sapanca-Abant region (NW Turkey, North Anatolian Fault Zone). Turkish-German Earthquake Research Project. Earth Research Institute, Ankara, Turkey, University of Kiel, West Germany, 18-33.
- Retallack, G. J., 1990, Soils of the Past: an introduction to Paleopedology. Unwin Hyman, Boston, 520 p.
- Sakıncı, M. and Bargu, S., 1989, İzmit Körfezi güneyindeki Geç Pleystosen (Tireniyen) çökel stratigrafisi ve bölgenin neotektonik özellikleri. *Türkiye Jeol. Kur. Bült.*, 32, 51-64.
- Seymen, I., 1995, İzmit Körfezi ve çevresinin jeolojisi (Geology of the İzmit Gulf Region, NW Turkey). In: İzmit Körfezi Kuvaterner İstifi (Quaternary Sequence in the Gulf of İzmit) (Ed. E. Meriç), 1-22.
- Sichenberg, O.; Becker-Platen, D.J.; Benda, L.; Berg, Detrich; Engesser, B.; Gaziry, W.; Heissig, K.; Hinermann, A.K.; Staesche, V.; Steffens, P. and Tobelin, H., 1975, Die Gliederung des - Höheren Jungtertiars und Altquartars in der Turkey nach Vertebreten und ihre Bedeutung für die Internationale Neogen-stratigraphie. *Geologisches Jahrbuch Reihe B, Heft 15*, 167 p.
- Siyako, M., Burkan, A.K. and Okay, A. I., 1989, Biga ve Gelibolu yarımadasının Tersiyer jeolojisi ve hidrokarbon olanakları (Tertiary Geology and Hydrocarbon Potential of the Biga and Gelibolu Peninsulas). *TPJD Bült.*, 1/3, 183-199.
- Straub, C., 1996, Recent crustal deformation and strain accumulation in the Marmara Sea region, NW Anatolia inferred from GPS measurements. Ph.D. Thesis, ETH, 122 p.

- Sümengen, M.; Terlemez, İ.; Şentürk, K.; Karaköse, C.; Erkan, E.N.; Ünay, E.; Gürbüz, M. and Atalay, Z., 1987, Gelibolu yarımadası ve Güneybatı Trakya Havzası'nın stratigrafisi, sedimantolojisi ve tektoniği. MTA Rep. No: 8128, (unpublished), Ankara.
- Şahbaz, A., Özdoğan, M. and Görmüş, S., 1997, Mudanya (Marmara Denizi Güneyi) Orta-Geç Miyosen istifinin sedimantolojik özellikleri (Sedimentological Properties of Middle-Late Miocene Mudanya Sequence, S. of the Marmara Sea). In: Güney Marmara bölgesinin Neojen ve Kuvaterner evrimi. TÜBİTAK YDABÇAG-426/G Proje Raporu, 69-86.
- Şaroğlu, F., 1985, Doğu Anadolu'nun neotektonik dönemde jeolojik ve yapısal evrimi. İstanbul Üniv., Fen Bilimleri Enst., Jeoloji Müh. Böl., Doktora tezi, (unpublished), İstanbul.
- , 1988, Age and offset of the North Anatolian fault. METU Jour. Pure and Appl. Sci., 21/1-3, 65-79.
- and Güner, Y., 1981, Doğu Anadolu'nun jeomorfolojik gelişimine etki eden öğeler: jeomorfoloji, tektonik, volkanizma ilişkileri. Türkiye Jeol. Kur. Bül., 24/1, 39-50.
- ; Boray, A.; Özer, S. and Kuşçu, I., 1983, Orta Toroslar-Orta Anadolu'nun güneyinin neotektoniği ile ilgili görüşler. Jeomorfoloji Dergisi, 11, 45-52.
- , Emre, Ö. and Boray, A., 1987, Türkiye'nin aktif fayları ve depremsellikleri: MTA Rep. No: 8174, (unpublished), Ankara.
- , ——— and Kuşçu, I., 1992, Türkiye Diri Fay Haritası. Publ. MTA, Ankara.
- Şengör, A.M.C., 1979, The North Anatolian transform fault: its age, offset and tectonic significance. J. geol. Soc. Lond., 136, 269-282.
- , 1980, Türkiye'nin neotektoniğinin esasları. Publ. Türkiye Jeol. Kur., 40 p.
- , 1982, Ege'nin neotektonik evrimini yöneten etkenler. Batı Anadolu'nun genç tektoniği ve volkanizması paneli (Eds. O. Erol ve V. Oygür). Publ. Türkiye Jeol. Kur. Ankara, 59-72.
- Şengör, A.M.C. and Kidd, W.S.F., 1979, Post-collisional tectonics of the Turkish-Iranian Plateau and a comparison with Tibet. Tectonophysics, 55, 361-376.
- and Yılmaz, Y., 1981, Tethyan evolution of Turkey: a plate tectonic approach. Tectonophysics, 75, 181-241.
- , Görür, N. and Şaroğlu, F., 1985, Strike-slip faulting and related basin formation in zones of tectonic escape: Turkey as a case study. In: Strike-slip Deformation, Basin Formation and Sedimentation (Eds. K.T. Biddle and N. Christie-Blick). Soc. Econ. Paleont. Min. Spec. Pub., 37, 227-264.
- Taner, G., 1995, İzmit Körfezi (Hersek Burnu-Kaba Burnu) Kuvaterner istifinin pelesipod ve gastropoda faunası (Pelecypoda and Gastropoda fauna of the Quaternary sequence in the Gulf of İzmit, Hersek Burnu Kaba Burnu) In İzmit Körfezi Kuvaterner İstifi (Quaternary Sequence in the Gulf of İzmit) (Ed. E. Meriç), 219-239.
- Taymaz, T.; Jackson, J. and McKenzie, D., 1991, Active tectonics of the north and central Aegean Sea. Geoph. J. Int., 106, 433-490.
- Toker, V. and Şengüler, İ., 1995, İzmit Körfezi (Hersek Burnu-Kaba Burnu) Kuvaterner istifinin nannoplankton florası (Nannoplankton flora of the Quaternary sequence in the Gulf of İzmit, Hersek Burnu-Kaba Burnu). In: İzmit Körfezi Kuvaterner İstifi (Quaternary Sequence in the Gulf of İzmit) (Ed. E. Meriç), 173-178.
- Varol, B.; Şahbaz, A.; Görmüş, S.; Bayhan, E.; Özdoğan, M. and Emre, Ö., 1997, Karacabey- Mudanya B61gesi Üst Miyosen-Pliyosen Karbonatlarının Sedimantolojisi ve İzotop Jeokimyası (Sedimentology and Isotope Geochemistry of the Upper Miocene-Pliocene Carbonates in the Karacabey-Mudanya Region). In: Güney Marmara Bölgesinin Neojen ve Kuvaterner Evrimi. TÜBİTAK YDABÇAG-426/G Proje Raporu, 87-99.
- Wong, H.K.; Uluğ, A.; Özel, E. and Luddmann, T., 1990, Neotectonic structure of the Sea of Marmara. Mitt. Geol.-Palaontol. Inst. Univ. Hamburg, Degens Mem., 69, 99-116.

- Wong, H.K., Lüddmann, T., Uluğ, A. and Görür, N., 1995, The Sea of Marmara: a plate boundary sea in a tectonic escape regime. *Tectonophysics*, 244, 231-250.
- Wright, V.P., 1992 a, Paleosol recognition: a guide to early diagenesis in terrestrial settings. *Diagenesis III* (Eds. K.H. Wolf and G.V. Chilingarian). *Developments in Sedimentology*, 47, Elsevier, Amsterdam. 591-619.
- , 1992 b, Paleopedology: stratigraphic relationships and empirical models. *Weathering, Soil and Paleosols* (Eds. I.P. Martini and W. Chesworth). Elsevier, Amsterdam, 475-499.
- Yaltırak, C., 1995, Gelibolu yarımadasında Pliyo-Kuvaterner sedimantasyonunu denetleyen tektonik mekanizması. *Nezihi Canitez Sempozyumu, İstanbul. Jeofizik*, 10, 103-106.5
- Yılmaz, Y.; Genç, Ş.C.; Yiğitbaş, E.; Bozcu, M. and Yılmaz, K., 1995, Geological evolution of the late Mesozoic continental margin of Northwestern Anatolia, *Tectonophysics*, 243, 155-171.

RESERVOIR ROCK PROPERTIES OF MIDDLE EOCENE SANDSTONES IN NORTHERN THRACE BASIN

Nurettin SONEL**** and Aynur (Geçer) BÜYÜKUTKU****

ABSTRACT.- Değirmencilik and Yeniköy formations at north of Thrace basin were examined by means of detailed sedimentologic and petrographic studies. In this study, reservoir rock features of sandstones were studied with thin section, sonic well log, core, and scanning electron microscope (SEM) works. Results of laboratory analysis yield that sandstones of Değirmencilik and Yeniköy formations have a reservoir rock potential for oil. Petrographic studies indicate that dissolution of carbonate and feldspars together with pressure dissolutions facilitate widening of secondary pores in sandstones providing development of diagenetic traps.

DETECTION OF POTENTIAL AQUIFER USING REMOTE SENSING DATA AND DIGITAL ELEVATION MODEL,
SADRAZAMKÖY, THE TURKISH REPUBLIC OF NORTHERN CYPRUS

Kenan TÜFEKÇİ***

ABSTRACT.- The Turkish Republic of Northern Cyprus (T.R.N.C.) is under the Mediterranean climatic conditions and there is fairly water trouble due to insufficient rainfall and incorrect irrigation methods. For this reason, the investigations have been carrying out by The General Directorate of Mineral Research and Exploration (MTA) and also have been supporting by remote sensing methods. In this application, Landsat 5 TM's thermal IR band, which is the date 28.06.1994, 176/35-36 path/row and 30x30 m resolution, was evaluated and the temperature analysis of the sea surface along the T.R.N.C. shorelines was processed and the cold areas which can be interpreted as ground water outputs were detected in the surrounding of the Cape Koruçam (NW of Cyprus). The relation between these data from the satellite image and the land was researched by both aerial photographs and field observations. It is found that the paleokarstification was developed on the Upper Pliocene-Pleistocene aged bioclastic limestones and also a probably calcerous crust covering this formation in the surrounding of Sadrazamköy. It is understood that the bioclastic limestones and the karstic areas formed under the humid climatic conditions and morphometrically located at same levels as the sea terrace levels can be thought as a potential aquifer area.